Characterization of HIV-1 Integrase Nuclear Translocation and Chemokine Receptor Internalization for Development of New Class of Anti-AIDS Drugs

GU, Wangang

A Thesis Submitted in Partial Fulfillment

of the Requirements for the Degree of

Doctor of Philosophy

in

Biochemistry(Medicine)

The Chinese University of Hong Kong

August 2011

Thesis/Assessment Committee

Professor Pang Chui Shaw (Chair)

Professor David Chi Cheong Wan (Thesis Supervisor)

Professor Tzi Bun Ng (Committee Member)

Professor Yongtang Zheng (External Examiner)

Acknowledgements

I would like to express my deepest gratitude to my supervisor Prof. David C.C. Wan for his continuous support and also for his kind guidance, advice and preparation of this thesis.

I am grateful to Prof. Zheng Yongtang for his guidance in my study in KIZ, CAS. I would like to thank Denis Ip for his invaluable technical support and advice in this project. Thanks are also given to all my colleagues Joe, Lin Huangquan, Leo, Lisa, Winston from SC193 in CUHK and Zhang Xuan, Wang Ruirui, Liu Yajuan, Liu Fengliang, Zhangxingjie and all members in Room 618 (KIZ) for their technical support and fruitful discussion. Finally I would like to thank my family for their understanding, support and encouragement.

Abstract

Translocation of viral integrase into nucleus is a critical precondition of integration during the life cycle of HIV, a causative agent of Acquired Immunodeficiency Syndromes (AIDS). It has been considered as an important target for the drug development to treat AIDS. In order to understand the detailed mechanisms of integrase-host cell protein complex interactions, we cloned HIV-1 integrase-EGFP into pTRE2hyg as visible tag to monitor the translocation process. When transiently transfected this vector into Tet-off ready HeLa cells, the EGFP: integrase is mainly localized in the nucleus. It has been hypothesized that any drugs that can inhibit the translocation process are novel class of drugs for AIDS treatment. More than 30000 synthetic compounds and 80000 natural products were screened by virtual screening. A total of 34 compounds were obtained and screened for their ability to block the nuclear entry of HIV-1 integrase by monitoring the EGFP fluorescence in the cells by high-throughput live cell imaging. Eight synthetic compounds (DW-IN4, DW-IN5, DW-IN6, DW-IN9, DW-IN15, DW-IN16, DW-IN17, DW-IN21) and one natural product (DW-IN719) were found to block integrase translocation significantly. According to our screening result, six compounds (INNB-1, INNB-2, INNB-3, INNB-4, INNB-5, INNB-6) were designed and synthesized. INNB-1 and INNB-2 had significant inhibition on integrase nuclear translocation. DW-IN6, DWIN719, INNB-1, INNB-2, INNB-3 and INNB-4, showed significant inhibition on P24 production in live virus assay. DW-IN6, INNB-1, INNB-2, INNB-3 and INNB-4 showed significant syncitia formation inhibition in live virus assay. Six compounds (KM7, KM8, KM14, KM30, KM37, KM79) from Kunming were screened as integrase nuclear translocation inhibitors. Using similar cell imaging techniques, we have cloned the GFP-tagged chemokine receptor CXCR4 using the lentivirus transfection system. CXCR4 receptor is a critical co-receptor in CD4 positive lymphocytes mediating the fusion of HIV into the CD4 positive cells. CXCR4-GFP

was over-expressed in 293T cells and the results showed that GFP:CXCR4 receptor is expressed at the plasma membrane of the cells. These cells have been used to monitor the blockage of CXCR4 receptor internalization for drug development. Four compounds (KX128, KX166, KX171, KX180) from Kunming showed CXCR4 internalization blockage in imaging assay. The interaction of these compounds with CXCR4 was predicted by molecular docking. KX128 showed significant HIV inhibition in live virus assays.

論文摘要

艾滋病毒整合酶的核轉位是艾滋病毒複制周期整合步驟的關鍵先決條件。已經被作爲抗艾滋病藥物開發的重要靶點。爲了研究整合酶與宿主複雜相互作用的機制，EGFP 標記的整合酶被克隆進表達載體 pTRE2hyg 以便對整合酶核轉位進行操作。瞬時轉染 Tet-off ready HeLa 細胞，整合酶主要定位在細胞核。我們假設任何藥物能阻止整合酶的核轉位過程可能是艾滋病治療的潛在新藥。經過對 3 萬個合成化合物和 8 萬個天然產物進行虛擬篩選，34 個化合物被選擇進行細胞平台的測試。8 個 SPECS 來源的化合物(DW-IN4, DW-IN5, DW-IN6, DW-IN9, DW-IN15, DW-IN16, DW-IN17, DW-IN21)和一個天然產物(DW-IN719)顯示出顯著的整合酶核轉位抑制作用。基于上述結果，我們合成了 6 個新化合物(INNB-1, INNB-2, INNB-3, INNB-4, INNB-5, INNB-6)。INNB-1, INNB-2 顯示出顯著的抑制整合酶核轉位的作用。DW-IN6, DWIN719, INNB-1, INNB-2, INNB-3 和 INNB-4 顯著抑制 P24 抗原合成。DW-IN6, INNB-1, INNB-2, INNB-3 和 INNB-4 顯著抑制合胞體形成。昆明動物所來源的 6 個化合物（KM7, KM8, KM14, KM30, KM37, KM79）也對整合酶核轉位有顯著的抑制作用。我們將 GFP 標記的 CXCR4 克隆進慢病毒表達系統，CXCR4 是 HIV 侵入細胞的關鍵輔助受體之一。實驗顯示 CXCR4 主要表達在 293T 細胞的膜上。通過操作 CXCR4 的細胞內化現象，可以篩選 CXCR4 拮抗劑。4 個昆明動物所來源的化合物（KX128, KX166, KX171, KX180）顯示出 CXCR4 內化的抑制作用。通過分子對接，我們對這些化合物和 CXCR4 的相互作用進行了研究。在隨後進行的活病毒實驗中，KX128 有顯著的抗 HIV-1 活性。

Content

Abbreviations

AIDS	Acquired Immunodeficiency Syndrome
ARV	AIDS related virus
A-MuLV	Amphotropic murine leukemia virus
AZT	3'-azido-2',3'-dideoxyctidine
ADT	AutodockTools
CDC	Centers for Disease Control and Prevention
CTS	Central termination signal
CC50	50% cytotoxicity concentration
CPE	Cytopathic effect
CCD	Catalytic core domain
CAPE	Caffeic acid phenethyl este
CADA	Cyclotriazadisulfonamide
CCR5	CC chemokine receptor 5
CXCR4	CXC Chemokine Receptor 4
ddI	2',3'-dideoxyinosine
ddC	2',3' -dideoxycytidine
d4T	2'-3'-didehydydro-2',3'- dedeoxythymidine
DMSO	Dimethyl sulfoxide
DMEM	Dulbecco's modified Eagle's medium
DHICA	5,6-dihydroxyindole-2-carboxylic acid
EC50	50% effective concentration
ETOH	Post-source dissociation
EGFP	Enhanced green fluorescent protein
Env	Envelope
ELISA	Enzyme-Linked Immunosorbnent Assay
FIV	Feline immunodeficiency virus
FBS	Fetal bovine serum
GA	Genetic algorithms

GPCR	G protein coupled receptor
HAART	highly active antirerociral therapy
HIV	Human Immunodeficiency Virus
HTLV-III	Human T lymphotropic virus type III
HRP	Horseradish peroxiase
HAART	Highly active antirerociral therapy
HEK	Human embryo kidney
IC(50)	50% Inhibitory concentration
IBD	Integrase binding domain
IN	Integrase
LEDGF	Lens epithelium-derived growth factor
LTR	Long terminal repeats
LiCl	Lithium chloride
LAV	Lymphadenopathy associated virus
MTT	3-(4,5)-dimethylthiahiazo (-z-y1)-3,5-diphenytetrazoliumromide
NRTIs	Nucleoside reverse transcriptase inhibitors
NNRTIs	Non-nucleoside reverse transcriptase inhibitors
NMR	Nuclear Magnetic Resonance
PDB	Protein data bank
PCR	Polymerase chain reaction
PBMC	Peripheral blood mononuclear cells
PCP	Pneumocystis carinii pneumonia
PIC	Preintegration complex
RTC	Reverse transcription complex
RT-PCR	Reverse transcription polymerase chain reaction
RT-PCR	Reverse transcription polymerase chain reaction
RSV	Alpharetrovirus Rous sarcoma virus
RT	Reverse transcriptase
SIV	Simian immunodefciency virus

SU	Subunit
TRIM	Tripartite motif
TCID50	Tissue culture infectious dose
TM	Transmembrane
TFIID	Transcription factor IID
TAR	Transactivation response region
TCL	T-cell-line
VSV-G	Vesicular stomatitis virus G glycoprotein
3TC	2',3'-dideoxy-3'-thaicytidine

Lists of figures

Chapter 1

Chapter 3

Chapter 4

Chapter 5

Lists of tables

Chapter 3

Chapter 5

Chapter 1
Introduction

1.1 History of HIV (Human Immunodeficiency Virus)

On June 5 of 1981, some researchers from US CDC (Centers for Disease Control and Prevention) reported a disease. This disease came out from report of five cases of Pneumocystis carinii pneumonia (PCP) among previously healthy gay young men in Los Angeles. Shortly after this report, some more cases were reported from other places such as New York City, San Francisco, and other cities (MMWR, June 5, 1981 / Vol. 30/ No. 21, http://fohn.net/history-of-aids/).

On November 5 of 1981, although the pathogen was not identified, it was thought to transmit through intimate, direct contact involving mucosal surfaces, such as sexual contact among homosexual males, or through parenteral spread, such as occurred among intravenous drug abusers and possibly hemophilia patients using Factor VIII products. The cause of Acquired Immunodeficiency Syndrome (AIDS) was still unknown at that time (MMWR, November 05, 1982 / 31(43);577-80, http://www.cdc.gov/hiv/resources/reports/mmwr/1981.htm).

In 1983, two French scientists, Barre-Sinoussi and L. Montagnier, isolated a new retrovirus from the blood of patient with AIDS (Barre-Sinoussi et al., 1983; Montagnier, 1988). As we know, this virus is human immunodeficiency virus type 1 (HIV-1)(Barre-Sinoussi et al., 1983).

Where does HIV come from? In fact, new study has shown that the oldest HIV-1 sequence that we knew was the ZR59, which was isolated from an adult male from Kinshasa, Democratic Republic of Congo (DRC) in 1959(Zhu et al., 1998). Sequencing study has identified that this HIV sequence was assigned as M group. Study showed that the genetic distance between ZR59 and the M-root is nearly half of the sequences of today. This means that the HIV existed a long time before 1959, and a molecular clock dating studies showed that HIV was originated around 1920-1930(Korber et al., 2000; Salemi et al., 2001; Sousa, 2009).

1.2 What is AIDS

The infection of HIV leads to the disease of AIDS, which is the result of suppression of human immune system(Lee, 1993; Seligmann, 1990; Taube and Goldberg, 1983) (Pivel et al., 1987). In January 1993, the US CDC made a definition on AIDS. It included all identified AIDS defining illness and CD4 lymphocyte counts, all patients with CD4 counts less than 200 cells/mm^3 (or CD4 percentage <14), and three AIDS defining condition namely, pulmonary tuberculosis, invasive cervical cancer and recurrent bacterial pneumonia [US Center of Disease Control, 1993].

HIV was transmitted through three ways(Brown et al., 1997; Titti et al., 1987). Firstly, the virus can be transmitted through body fluid exchange, such as semen, vaginal fluids and blood, during sexual contact in all heterosexual, homosexual, and bisexual relationships(Lyons, 1994; Solomon and DeJong, 1986; Tindall et al., 1992). The second transmission way is through transfusion of virus contaminated blood and blood products, needles sharing among injection drug user, needle sticks, open cut and mucous membrane exposure in healthcare worker and the use of HIV-contaminated skin-piercing instruments(Cleary et al., 1986; Ingold and Ingold, 1989; Mhalu, 1990; Takamatsu, 1997). Thirdly, the virus carrying mother can transmit the virus to their babies through intrauterine, peripartum and breast feeding(Casals et al., 1991; Ledesma-lujan et al., 1989; Teasdale et al., 2011).

The progress of AIDS can be divided into three stages according to the process of disease development: early acute stage, chronic/latent stage and AIDS stage(Justice et al., 1989). Acute stage lasts for 1-2 weeks where CD4 cell count range is 1000-5000 cells/mm^3. It is characterized by fever, headache, nausea, anorexia, fatigue, sweaters sore throat and dry cough(Kaplan et al., 1989; Venet et al., 1990). Chronic/latent stage lasts for 8-10 years. CD4 cell count range is 750-500 cell/mm(Rosenberg and Fauci, 1989). No obvious symptom can be found in this stage. Finally, AIDS stage lasts for 1-2 years and CD4 cell count range drop from 500-0 cells/mm^3. Several clinical signs

can be found such as tuberculosis, lymphadenopathy, Kaposi's sarcoma, mouth and esophageus pain and odynophagia and CNS lymphoma, etc(Fouret et al., 1987; Saag, 1994; Saxinger et al., 1987).

HIV causes immunodeficiency after infection but not immediately, this usually occurs in HIV infected but untreated persons after as long as to 10-15 years(Huang et al., 1995b). Since first reported in the United States in 1981(Curran et al., 1985; Smith and Walker, 1992; Waskin et al., 1986), the AIDS has caused about 25 million people lives while there are still more than 33 million infected persons living with virus(http://pathmicro.med.sc.edu/lecture/hiv2000.htm)(Little and Rhodus, 2007; Pinheiro Edos et al., 2008). According to scientists' estimation, about 2.5 million people were newly infected with HIV-1, and 2.1 million people die of AIDS or AIDS-related diseases every year (http://www.irishaid.gov.ie).

1.3 Types of HIV

Just after two years when the AIDS case was reported among young homosexually active men, the virus was isolated in 1983 (Barre-Sinoussi et al., 1983); it had been named other names. Such as lymphadenopathy associated virus (LAV), human T lymphotropic virus type III (HTLV-III) and other names such as AIDS related virus (ARV)(Gostin, 1990; Volsky et al., 1986; Wain-Hobson et al., 1991). HIV is a member of the lentiviruses from the retrovirus family. Lentiviruses are prevalent in many mammalian species such as horse (equine infectious anaemia virus), sheep (visna maedi virus), cattle (bovine immunodeficiency virus), cat (feline immunodeficiency virus), and in almost all monkey species (simian immunodefciency virus, SIV)(Fanales-Belasio et al., 2010; Gonda, 1988).

There are two types of HIV, HIV-1 and HIV-2. The HIV-1 is the popular type. HIV-2 was discovered in 1986 from the patient in West Africa(Clavel et al., 1986). HIV-2 is mainly in the region of Western and Central Africa(Ng, 2000). HIV-1 consisted of the

groups M, N and O, in which M is most prevalent in the world. HIV-2 was consisted of the groups A to G, which were formerly named subtypes(Sarker et al., 2008; Sarrami-Forooshani et al., 2006)(HIV sequence database, http://www.hiv.lanl.gov). On the molecular basis, HIV-1 group M was nearly identical to SIVcpz, virus clades that were found in chimpanzees (*Pan troglodytes*) in Central Africa, and HIV-1 group O viruses had been detected in the faeces of three wild living gorillas in Cameroon, while HIV-2 was identical to SIV from sooty mangabey monkeys (*Cercopithecus atys*—SIV smm)(Heeney et al., 2006; Lemey et al., 2004; Ondoa et al., 2002; Ondoa et al., 2003).

1.4 Structure of HIV

The HIV genome is made up of two copies of single-stranded RNA. HIV-1 genome is consisted of 9181 nucleotides, and HIV-2 genome is consisted of 10359 nucleotides (NCBI database). There are some difference between the genomes of HIV-1 and HIV -1 although the whole backbone is similar. HIV genome is mainly made up with nine genes. Among them, there are three structural genes: gag, pol and env(Allan et al., 1987; Bruce et al., 1993; Candotti et al., 1994). Another six genes are regulatory and accessory genes: Vif, Vpr, Vpu, Tat, Rev, Nef (Figure 1.1)(Graeble et al., 1993; Michael et al., 1995; Strebel et al., 1987).

The structure of the viral particle is similar for HIV-1 and HIV-2 as shown in figure 1.2. The diameter of the virus particle is about 100nm. The virus particle is surrounded by a lipoprotein-rich membrane(Barklis et al., 1998; Gelderblom et al., 1987). The viral capsid has the three important HIV enzymes: transcriptase (RT), integrase (IN) and protease. Reverse transcriptase became the first target in AIDS treatment.

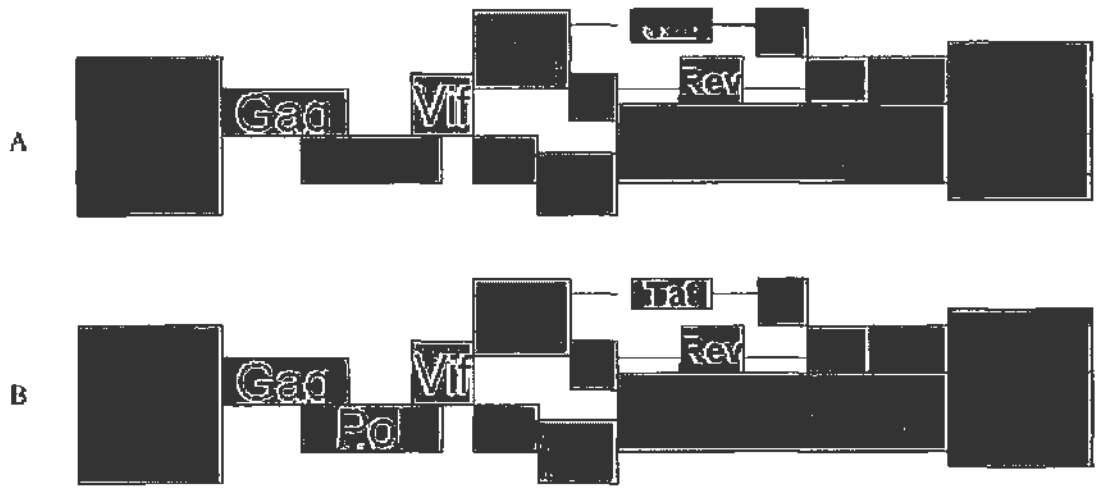

Figure 1.1 Organization of the HIV genome(Fanales-Belasio et al., 2010)
A) HIV-1 genome
B) HIV-2 genome
Both HIV-1 and HIV-2 genomes are consisted of Gag, Pol, Env, Vif, Vpr, Vpu/Vpx, Tat, Rev and Nef totally nine genes. At both terminals of the viral genome is a LTR(Long Terminal Repeat) region.

1.5 HIV replication cycle

From the binding of the virus to cell to the virus particle release from cell is the complete process of infection. It is also called replication cycle. Though many kinds of cells can be infected by HIV, CD4 positive T cells are first to be found as the target in human body(Elhaggar, 1993). For all cell types, the replication cycle of HIV is similar. The HIV replication cycle can be divided into six steps: 1) binding and entry; 2) uncoating; 3) reverse transcription 4) provirus integration 5) virus protein synthesis and assembly 6) budding(Minoli and Grossi, 1994).

1.5.1 Binding and entry

For any virus infection, binding to host cell is the first step. Binding initiates the infection to host. Binding is the interaction process of virus and host. During this process, viral envelope proteins and host receptors play important role. First, the virus bind to the host cell, then an interaction of viral envelope protein and host receptor and co-receptors happens to complete the binding and entry of virus (Figure 1.3). The heterodimer proteins gp120 and gp41 composed a viral envelope trimeric complex, which is essential for viral recognition and entry into target cell(Este et al., 1998; Weissenhorn et al., 1996).

Gp120 binds to target cell, interacts with coreceptor, and induces conformational changes in gp41. Several domains in both gp120 and gp41 were involved in CD4/coreceptor binding or the membrane fusion process. Ectodomain of gp41 contained a highly hydrophobic N-terminus and two heptad repeat motifs, referred to as the N-helix and the C-helix(Chan et al., 1997; Weissenhorn et al., 1997).

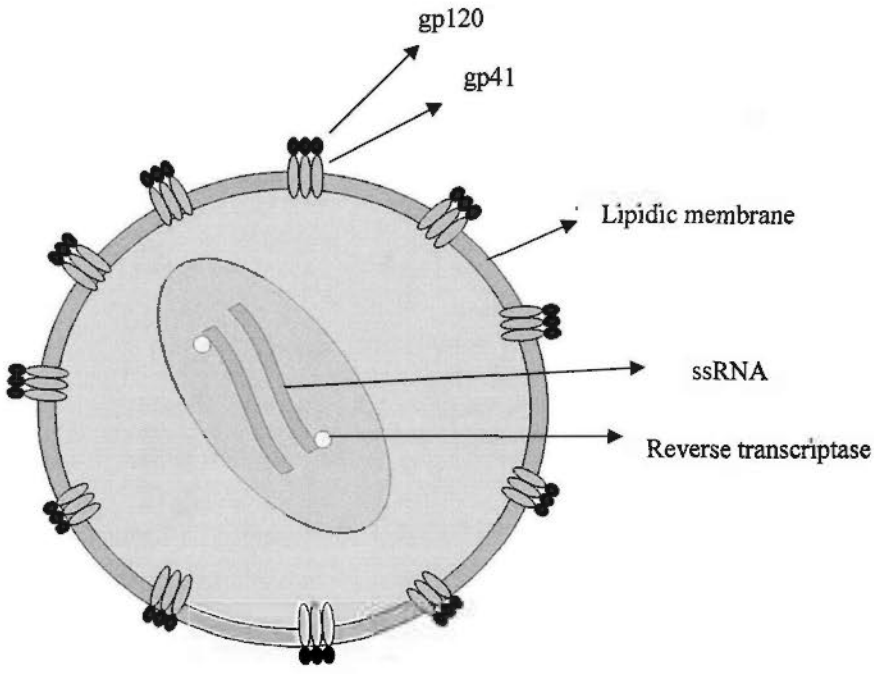

Figure 1.2 Structure of the HIV-1 particle(Fanales-Belasio et al., 2010).
ssRNA: single strand RNA
HIV is an enveloped virus. The virus particle has a diameter of 100nm, which is surrounded by a lipoprotein-rich membrane. Inside the viral particle are two copies of viral ssRNA.

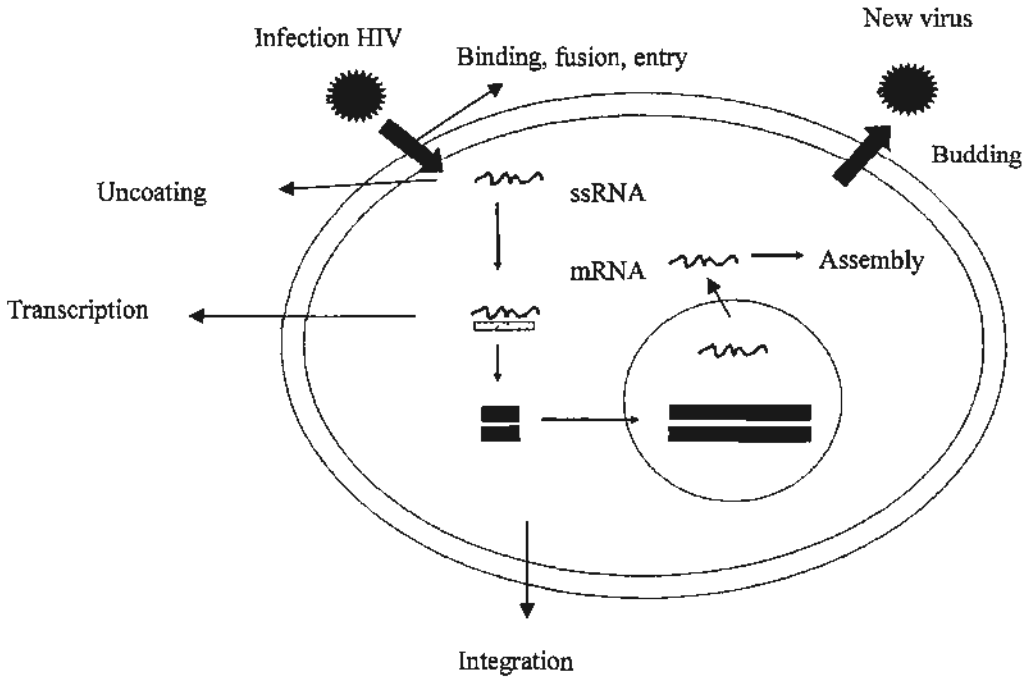

Figure 1.3 HIV replication cycle(Fanales-Belasio et al., 2010)
RT: reverse transcriptase; dsDNA: double strand DNA.
The HIV replication cycle includes six steps: 1) binding and entry; 2) uncoating; 3) reverse transcription 4) provirus integration 5) virus protein synthesis and assembly 6) budding.

The virus was found to attack CD4 positive cells specifically. Then CD4 was identified as the receptor of HIV. Later study discovered that CD4 was not sufficient for HIV Env-mediated membrane fusion and virus entry. This leads to the discovery of co-receptors for HIV infection(Callahan et al., 1991; Deng et al., 1996; Martin et al., 1998).

Some members of the G protein-coupled receptor superfamily of seven transmembrane domain proteins were found to serve as co-receptors for HIV entry(Unutmaz et al., 1998). These proteins served as receptors for their natural ligands (alpha and beta chemokines)(Doms and Peiper, 1997). Chemokine receptors are small proteins expressed on cell membrane which are recognized by chemotactic cytokines and mediated the homing and recruitment of immune cells during the process of inflammation(Doms, 2001). Chemokine receptors are classified on the basis of the position of disulfide like cysteine residues as well as their angiogenic effects. Many members of GPCRs are reported to serve as co-receptors for some HIV strains, but CXCR4 and CCR5 are two major and most important coreceptors (Deng et al., 1996; Endres et al., 1996; He et al., 1997) (Figure 1.4).

Gp 120 has five hyper-variable regions, V1-V5. V3 loop is important for the troposim choice of HIV. Changing the V3 region between isolates leaded to co-receptor usage switching(O'Brien et al., 1990). After binding of gp120 to CD4, the HIV envelope undergoes a structural change that leads to the exposing the specific domain in the gp120 which is able to bind the chemokine receptors on the cell membrane(Berger et al., 1999).

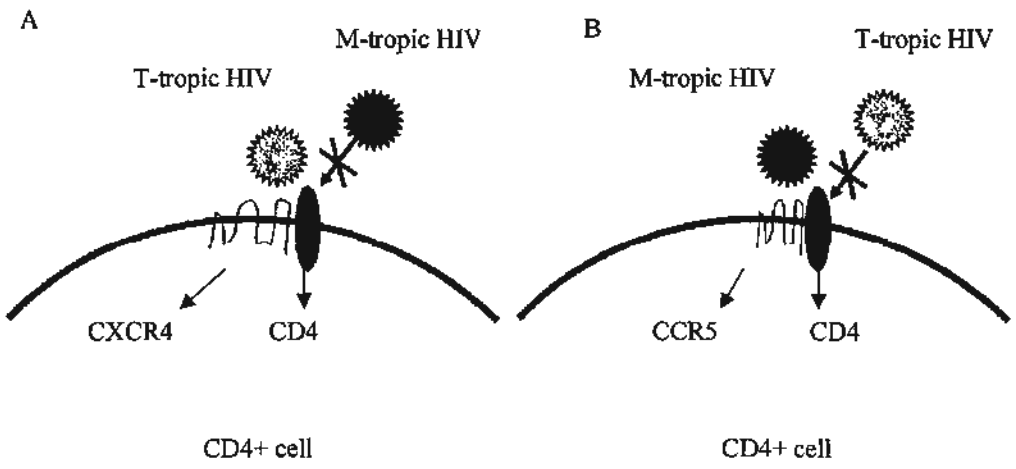

Figure 1.4 HIV tropism(Fanales-Belasio et al., 2010)
M-tropic HIV: monocyte/macrophage-tropic HIV;
T-tropic HIV: T-lymphocyte-tropic HIV.

1.5.2 Uncoating

The fusion of HIV envelope protein with host cell membrane leads to the completion of HIV entry. Through entry, the HIV core goes into the host cytoplasm.The uncoating process is not well known in the HIV infection process. It remains to be approached in details. After uncoating, HIV particle (without envelope) was converted to a complex referred to as the reverse transcription complex (RTC)(Carr et al., 2006; Fassati and Goff, 2001). After transcription, the newly synthesized viral DNA was made into a complex called preintegration complex (PIC)(Li and Craigie, 2009; Raghavendra et al., 2010).

1.5.3 Reverse transcription

As other retroviruses, HIV has the ability to convert their RNA genomes into double-stranded DNA in host cells. This reaction is catalyzed by the reverse transcriptase (RT). HIV-1 RT is a heterodimer of two subunits, one of which is 66 kDa (p66), the other 51 kDa (p51)(Tasara et al., 1999). The two subunits are derived from the same region of the Pr160GagPol precursor protein. According to a number of groups' studies on RT crystallization, the p66 and p51 domains, while largely overlapping in protein sequence, adopt quite different conformations(Arnold et al., 1992; Ding et al., 1995).

The result of reverse transcription leads to the production of viral DNA. As it is well known, DNA is a more popular type of genetic vector than RNA. What is more, DNA is more stable than RNA in physiological environment, such as in host cells and animal body.

1.5.4 Provirus integration

After reverse transcription, the HIV genome exists in the host cells in the form of DNA. The viral DNA will be transported to the host nucleus in the complex of preintegration complex (PIC). PIC is a complex of HIV DNA and many different kinds of host factors(Raghavendra et al., 2010). LEDGF, also is called p75, is the well

known host factor involved in this process. It is also the first one to be found(Busschots et al., 2005). After nuclear import of reverse transcribed DNA, the 31 kDa HIV IN protein catalyzes the insertion of the linear, double-stranded viral DNA into the host cell genome. The integrated DNA is called "provirus". It behaves just as a human gene(Engelman, 2009; Engelman et al., 2009).

Integration is the critical event in the whole HIV infection process. Like reverse transcription, HIV integration involves in several steps which are also seen in other lentivirus (Van Maele and Debyser, 2005). Usually, the integration is completed in three events: 3'-terminal processing, strand transfer and integration gap repair. The final gap repair is completed by the host factors.

1.5.5 Virus protein synthesis and assembly

On completion of integration, the viral DNA was used as template for viral mRNA synthesis and transcription. The viral RNA encodes all the HIV proteins.

HIV-1 LTR (long terminal repeats) is used as the site of transcriptional initiation and harbors *cis*-acting elements required for RNA synthesis(Nishitsuji et al., 2001; Reed-Inderbitzin and Maury, 2003; Reynolds et al., 2003). The TATA element, to which transcription factor IID (TFIID) binds in transcription, locating approximately 25 nucleotides upstream of the transcription start site. At the 5' of the TATA box there are three Sp1 and two NF-κB binding sites(Garza and Carr, 1995; Kashanchi et al., 1994; Ross et al., 1991; Song et al., 1995; Varin et al., 2003).

1.5.6 Budding

The final step of infectious virus production is virus budding. For HIV-1, the L domain is present in p6. Deletion of mutation of p6 within the highly conserved Pro-Thr/Ser-Ala-Pro (P-T/S-A-P) motif, which located near the N-terminus of p6, significantly impairs particle release(Gottlinger et al., 1991; Huang et al., 1995a).

1.6 AIDS therapy and anti-HIV drugs

Since first reported in the United States in 1981, the AIDS has caused about 25 million people died while there are still more than 33 million infected persons living with virus(Pinheiro Edos et al., 2008). It is estimated that, about 2.5 million people are newly infected with HIV-1, and 2.1 million people die of AIDS or AIDS-related diseases every year(Little and Rhodus, 2007). Shortly after the virus was identified, some scientists had claimed that AIDS could be cured in 10 year. However, AIDS is still a deadly disease and there is still a continued effort to find an effective treatment to cure AIDS and eliminate the virus from infected bodies thoroughly.

Before 1996, AIDS is still untreatable and patients infected with HIV are literally sentenced to death. In1996, highly active antiretroviral therapy (HAART) was introduced into clinical practice subsequently(Williams, 1997). The principle impetus behind the development of combination therapies for HIV HAART was a combination of anti-virus drugs targeting usually reverse transcriptase and protease(Hirschel and Francioli, 1998).

1.6.1 Drugs targeting HIV entry

The HIV receptor CD4 and two major co-receptors CXCR4 and CCR5 are all important targets for drug development.

As the first step in the HIV infection, virus binding and entry is naturally the first target for virus prevention. Many drug candidates have been developed targeting this step. The virus binding through nonspecific interactions and CD4 binding can be blocked by inhibitors such as cyanovirin-N, cyclotriazadisulfonamide（CADA） analogues, PRO 2000, TNX 355 and PRO 542. BMS 806 was reported to block CD4-induced conformational changes(Allaway et al., 1995; Barrientos et al., 2002; Botos et al., 2002; Esser et al., 1999; Reeves et al., 2005; Reimann et al., 1997;

Rusconi et al., 1996; Vermeire et al., 2003; Vermeire and Schols, 2003; Vermeire et al., 2002).

Fusion is the early step in the HIV-host cell interaction process which leads to successful infection, this makes fusion an important target go stop virus from entry into target cells. In 2003, the first HIV entry inhibitor was approved for clinical use(Greenberg et al., 2004). T20 (enfurviride) is the first approved fusion inhibitor which is composed by 36 amino acids and derived from GP41. T-20 has a substitutive effect for the gp41 trimmer formation so as to blocking the conformational change of viral spike after binding of gp120 to target cells(Baldwin et al., 2004; Champagne et al., 2009; Kitchen et al., 2008).

According to previous study, Δ32 CCR5 individuals showed some resistance to HIV infection compared with non-mutant(Eugen-Olsen et al., 1997; Husain et al., 1998; Meyer et al., 1997; van Rij et al., 1999). CCR5 is a considered a potential target for anti-HIV drug development. In 2007, maraviroc (developed by Pfizer) was approved in U.S. for clinical treatment of HIV infection and AIDS patients. This is the first and the only FDA approved drug targeting CCR5 against HIV(Jones et al., 2007).

The success of maraviroc sheds light on development of chemokine receptor antagonists as novel class of anti-HIV drugs. Maraviroc has validated co-receptor as a target for inhibition of HIV-1(De Clercq, 2009; Lalezari et al., 2003).

CXCR4 is also considered an important target for anti-HIV drug development. Previous studies showed that SDF-1 or CXCR4 knock-out mice have developmental defects and are non-viable. In fact, the knockout of SDF-1 and CXCR4 leaded to physiological defects in systematic development, such as abnormal B-cell development, impaired colonization of BM by hematopoietic progenitors, defects in blood vessel formation and the gastrointestinal tract, abnormal cardiac ventricular septum formation and cerebellar development, and embryonic lethality(Tachibana et

al., 1998; Zou et al., 1998). During the course of this study, researchers from The Scripps Research Institute and University of California at San Diego reported the structures of the CXCR4 chemokine GPCR with small-molecule and cyclic peptide antagonists(Wu et al., 2010). In that study, the crystal structures of human CXCR4 in complex with a small-molecule antagonist at 2.5 Å resolution and with a cyclic peptide inhibitor at 2.9 Å resolution were reported(Wu et al., 2010).

AMD3100 was the first compound found to inhibit the CXCR4-HIV interaction. It is a bicyclam compound(De Clercq et al., 1994). Based on the significant effect of AMD3100 on HIV infection, a lot of work has been conducted on the research of AMD3100(Donzella et al., 1998; Schols et al., 1997a; Schols et al., 1997b). However, researchers found that the use of AMD3100 can cause a dose dependent eukocytosis(Hendrix et al., 2000). This side effect together with other adverse effects finally leaded to the stop of development of AMD3100.

Although AMD3100 was proved to be not suitable for clinical usage, it shed light on the significance of CXCR4 as HIV entry inhibitors. It also demonstrated that CXCR4 was a plausible target for anti-HIV drugs. The structural and experimental information that AMD3100 provides us lead to the discovery of better CXCR4 antagonists.

Subsequently, a follow-up compounds of AMD3100, AMD070 (AMD11070; AnorMED, Inc.) was reported. In 2004, AMD070 was put into clinical trials. The clinical phase I trial results showed that AMD is well tolerated (Schols, 2004; Schols D, 2003).

1.6.2 Drugs targeting HIV reverse transcriptase

HIV is an RNA virus whose genome is composed of two identical RNA copies. To complete replication, HIV performs a reverse transcription of RNA into DNA after entry of target cells. HIV reverse transcriptase is the viral enzyme to catalyze this event. Therefore RT inhibitors are the first group of drugs in anti-HIV treatment to be

used in the US as early as 1987 when approved by food and drugs administration (FDA)(Herzyk et al., 1987; St Clair et al., 1987). There are two types of reverse transcriptase inhibitors at present, nucleoside reverse transcriptase inhibitors (NRTIs) and non-nucleoside reverse transcriptase inhibitors (NNRTIs)(Ghani et al., 2003).

The NRTIs are first class of anti-HIV drugs in clinical practice since 1987 which are a wide family of 2', 3'-dideoxynucleosides. The members of this family are 3'-azido-2',3'-dideoxyctidine (AZT), 2',3'-dideoxyinosine (ddI) 2',3' -dideoxycytidine (ddC) , 2'-3'-didehydydro-2',3'- dedeoxythymidine (d4T) and 2',3'-dideoxy-3'-thaicytidine (3TC)(Boyle et al., 2005; Broder, 1990).

NRTIs act at the reverse transcription step. They are synthesized into the viral DNA instead of the natural nucleotides, the purine nucleosides adenosine (A) and guanosine (G), and the pyrimidine nucleosides thymidine (T) and cytidine (C)(Vrang et al., 1987). Nucleotide annlogues are triphorylated or undergo further modifications in the cells. Nucleotide analogues resemble monophosphorylated nucleosides, and therefore require only two additional phosphorylations to become active inhibitors in the DNA synthesis. Reverse transcriptase fails to distinguish the phosphorylated NRTIs from the natural counterparts, and use the drugs in the synthesis of viral DNA by mistake. This causes stop of viral DNA synthesis(Gao et al., 1994; Herzyk et al., 1987; Vrang et al., 1987).

Different from NRTIs, NNRTIs directly target the viral reverse transcriptase for inhibition. There are two members of this class of drugs in present AIDS treatment Efavirenz and nevirapine. Nevirapine binds to the hydrophobic pocket amino acid Tyr^{181} and Tyr^{188} near the polymerization active sites to cause a conformational change and therefore inhibits enzyme activity. The group of inhibitors was approved in 1996(Bowersox, 1996; Dong, 1998; Kelly et al., 1997; Vazquez, 1997; Wiese, 1997).

1.6.3 Drugs targeting HIV protease

Proteins are the main component of the virus particle such as formation of viral envelop. The virus needs protease to cleavage the precursor polyprotein into structural and functional active viral proteins. Protease inhibitors such as amprenavir, atazanavir, indinavir and nelfinavir, are the third kind of anti-HIV drugs in the market(Busti et al., 2004; James, 1995; Partaledis et al., 1995; Vacca et al., 1994). They act as peptidomimetic inhibitors to be tailed after the target peptide linkage in the gag and gag-pol polyproteins at the position Phe^{167}-Pro^{168} that are cleaved by the protease. This leads to the stop of polyprotein cleavage so as to stop the normal virus life cycle(Cheng, 1995; Lu et al., 2010).

1.6.4 Drugs targeting HIV integrase

Since integration is the key step in HIV infection process, integrase naturally is one important target for drug development. Integrase was encoded by *pol* gene of the human immunodeficiency virus (HIV)(Holler et al., 1993). This gene is required for HIV-1 replication by encoding viral enzymes. HIV-1 integrase is derived from the translated protein precursor of *pol* together with reverse transcriptase and protease(Netzer et al., 1993). The polyprotein precursor is called Pr160gag-pol. It encodes PR (p10), RT(p61/p52) and IN (p31). IN (p31) is the encoding gene for integrase. HIV-1 integrase is a key enzyme for HIV infection. This enzyme enables the virus to incorporate its genome into host genome efficiently. This leads to the result of permanent infection. Structurally HIV-1 integrase is composed of three functional domains. The zinc fnger, catalytic core domain and DNA binding domain. HIV-1 integrase was consisted of 288 amino acids, in which a 13 amino acid region spanning residues 161-173 conferred nuclear localization and was defined nuclear localization signal. Valine at position 165 and arginine at position 166 are essential for translocation of integrase(Bouyac-Bertoia et al., 2001; Bukrinsky and Haffar, 1997; Bukrinsky et al., 1993).

Integrase is a target with many advantages. First, integrase catalyzes the critical step of intergration in HIV infection. Without integration, HIV cannot cause permanent infection. Second, at present, there is only one integrase inhibitor approved by FDA targeting the strand transferred step. It is raltegravir from Merck. Raltegravir (MK0518) is a pyrimidine carboxamide integrase inhibitor. Its name is *N*-[(4-fluorophenyl)methyl]-1,6-dihydro-5-hydroxy-1-methyl-2-[1-methyl-1-[[(5-met hyl-1,3,4-oxadiazol-2-yl)carbonyl]amino]ethyl]-6-oxo-4-pyrimidinecarboxamide monopotassium salt (C20H20FKN6O5)(Anker and Corales, 2008; Buzon et al., 2008).

Since integrase has no cellular counterpart in human body, it has become an important target for anti-HIV drug development. Many studies have been conducted on HIV integrase in order to illustrate its structure and function. In 1996, HIV-1 integrase was expressed with a yeast expression system in order to investigate its potential lethal effect mediated by DNA damage(Caumont et al., 1996). Some integrase mutants were found fail to interact with LEDGF and proved to be essential for integrase function in HIV-1 replication(Emiliani et al., 2005). The crystal structure of integrase is important for understanding the function of this enzyme in HIV-1 infection process. It is also a key factor for drug development. The catalytic core domain of HIV-1 integrase in complex with an inhibitor (5CITEP) was reported in 1999. The inhibitor was found to bind centrally in the active site of the integrase and made a number of close contacts with the protein(Goldgur et al., 1999).

The LEDGF is the first identified cellular factor which involved in the interaction with HIV-1 integrase. HIV-1 integrase is transported into nucleus as a part of PIC together with LEDGF. Scientists have realized that the interaction between integrase and LEDGF is critical for HIV-1 replication. The interaction between HIV-1 integrase and LEDGF has become a new target in integrase inhibitors development. The crystal structure of HIV-1 integrase catalytic core domain dimer in complex with LEDGF

integrase binding domain was reported in 2005(Cherepanov et al., 2005). The crystal structure is collected in Protein Data Bank (PDB ID: 2B4J).

The crystal structure of HIV-1 integrase contains dimeric catalytic core domain of HIV-1 integrase complexed to the IN-binding domain of LEDGF was reported in 2005(Cherepanov et al., 2005). The principal structural features of integrase that were recognized by the LEDGF were the backbone confirmation of residues 168-171 from one monomer and a hydrophobic patch that is primarily comprised of alpha-helices 1 and 3 of the second integrase monomer(Cherepanov et al., 2005).

The discovery of beta-diketo acids was a crucial event in the validation of IN as a legitimate target in drug discovery against HIV infection(Dayam et al., 2005; Nair et al., 2006). In 2005, Dayam and coworkers discovered a novel class of IN inhibitors using a 3D pharmacophore guided database search(Dayam et al., 2005). They used S-1360 (Shionogi-GlaxoSmithKline Pharmaceuticals), the IN inhibitor which was undergoing clinical trials, and three other analogues to develop a common feature pharmacophore hypothesis(Dayam et al., 2005). 1700 compounds were yielded from a multiconformational database of 150,000 structurally diverse small molecules testing with the above four featured pharmacophore(Dayam et al., 2005). All 1700 compounds docked into the active site of integrase in subsequent molecular docking(Dayam et al., 2005). Then 110 compounds were selected for biological screening on the basis of docking results, Lipinski's rule-of-five, and structural novelty(Dayam et al., 2005). Researchers found that compounds that contained both salicylic acid and a 2-thioxo-4-thiazolidinone (rhodanine) group showed significant inhibitory potency against IN, while the presence of either salicylic acid or a rhodanine group alone did not(Dayam et al., 2005). Though some compounds containing only a salicylic acid showed inhibitory potency against IN, none of the compounds containing only rhodanine exhibited considerable potency(Dayam et al., 2005). Researchers reported 52 compounds in that study, and 11 compounds inhibited 3'-processing or strand transfer activities of IN with IC(50) < or = 25μM(Dayam et al.,

2005). That was the first reported use of S-1360 and its analogues as leads in developing a pharmacophore hypothesis for IN inhibition and for identification of new compounds with potent inhibition of this enzyme(Dayam et al., 2005).

The discovery of salicylic acid containing compound as HIV-1 inhibitor is really interesting(Dayam et al., 2005; Rinaldi et al., 2011; Woloschak et al., 1995). Rinaldi and coworkers synthesized three novel series of salicylic acid derivatives using three versatile and practical synthetic strategies and were assayed for their capacity to inhibit the catalytic activity of HIV-1 integrase(Rinaldi et al., 2011). Biological experiments showed that some of the synthesized compounds possess good inhibitory potency in enzymatic assays and inhibited viral replication in MT-4 cells at low micromolar concentrations(Rinaldi et al., 2011). Finally, docking studies were conducted to analyze the binding mode of the synthesized compounds within the DNA binding site of integrase, providing information to refine their structure-activity relationships(Rinaldi et al., 2011).

Lens epithelium-derived growth factor (LEDGF/p75) is the first discovered cellular cofactor of HIV-1 integrase that promotes viral integration by tethering the preintegration complex to the chromatin(Botbol et al., 2008; Christ et al., 2010; Llano et al., 2006; Maertens et al., 2003). Because of its crucial role in the early steps of HIV replication, the interaction between LEDGF/p75 and HIV-1 integrase represents an attractive target for antiviral therapy(Christ et al., 2010; De Luca et al., 2010; Du et al., 2008; Hayouka et al., 2010a). Christ and coworkers had rationally designed a series of 2-(quinolin-3-yl) acetic acid derivatives (LEDGINs) that acted as potent inhibitors of the LEDGF/p75-integrase interaction and HIV-1 replication at submicromolar concentration by blocking the integration step(Christ et al., 2010). In their study, a 1.84-A resolution crystal structure corroborated the binding of the inhibitor in the LEDGF/p75-binding pocket of integrase(Christ et al., 2010).

In research of effective HIV-1 integrase inhibitors, not only natural compounds were screened, new derivatives were synthesized on the basis of screened effective

compounds, but also inhibitors composed of short peptides were approached for their ability to inhibitor virus infection and replication through this enzyme.

Hayouka and coworkers also had developed a new approach for inhibiting IN by "shiftides": peptides derived from its cellular binding protein LEDGF/p75 that inhibit IN by shifting its oligomerization equilibrium from the active dimer to an inactive tetramer(Hayouka et al., 2008). In addition, they described two peptides derived from the HIV-1 Rev protein that interacted with IN and inhibit its activity *in vitro* and in cells(Hayouka et al., 2008). In their study, results showed that the Rev-derived peptides also act as shiftides(Hayouka et al., 2008). They demonstrated that IN was dimeric when bound to the viral DNA, but tetrameric in the presence of the rev-derived peptides through analytical gel filtration and cross-linking experiments(Hayouka et al., 2008). Rev-derived peptides inhibited the DNA binding of IN in fluorescence anisotropy studies(Hayouka et al., 2008).

After described a peptide derived from residues 361-370 of the IN cellular partner protein LEDGF/p75, which inhibited IN catalytic activity *in vitro* and HIV-1 replication in cells(Hayouka et al., 2007; Hayouka et al., 2008), Hayouka and coworkers performed a comprehensive study of the LEDGF 361-370 mechanism of action in vitro, in cells and in vivo(Hayouka et al., 2010b). They demonstrated that all residues in LEDGF 361-370 contribute to IN binding and inhibition through alanine scan, fluorescence anisotropy binding studies, homology modeling and NMR studies(Hayouka et al., 2010b). They also demonstrated that LEDGF 361-370 specifically inhibited integration of viral cDNA through kinetic studies in cells(Hayouka et al., 2010b).

Hayouka and coworkers used a cyclic peptide library with conformational diversity for selecting an active and stable peptide that mimicked the structure and activity of the HIV-1 integrase (IN) binding loop from its cellular cofactor LEDGF/p75 (residues 361-370)(Hayouka et al., 2010a). All the peptides used in the library had the same primary sequence, differing only in their conformation(Hayouka et al., 2010a). Finally,

the cyclic peptide, c(MZ 4-1), was found to be a potent and stable inhibitor of IN activity *in vitro* and in cells even after 8 days(Hayouka et al., 2010a). The peptide, c(MZ 4-1), obtained a bioactive conformation that was similar to the parent site in LEDGF/p75 revealed by NMR structure(Hayouka et al., 2010a).

Phage display technique was also applied in an attempt to search for peptides *in vitro* selection procedure that specifically interact with integrase (IN) and inhibit its function. Desjobert and coworkers used a phage display library of random heptapeptides to screen for potential peptide ligands of HIV-1 IN(Desjobert et al., 2004). Several phage clones were identified that specifically bound IN by researchers. Two peptides (FHNHGKQ and HLEHLLF) exhibited a high affinity for IN and were chemically synthesized(Desjobert et al., 2004). High affinity was confirmed by a displacement assay(Desjobert et al., 2004). Displacement assay showed that FHNHGKQ and HLEHLLF were able to compete with the phages expressing the corresponding peptide(Desjobert et al., 2004). None of them inhibited the 3'-processing reaction when assayed on the *in vitro* IN activities(Desjobert et al., 2004). The FHNHGKQ peptide was found to be an inhibitor of the strand transfer reaction(Desjobert et al., 2004).

Drug design and synthesis on the basis of IN structural information is always a promising direction in IN inhibitors development(Kong et al., 2005). The peptides derived from the helix of IN were reported to have the potency of inhibition(Kong et al., 2005). Kong and coworkers designed a series of peptides based on interface with the aim of increasing their inhibitory activity. Researchers claimed that the helix-forming tendency and the affinity with IN were essential for interfacial peptide inhibitors(Kong et al., 2005). Favorable results for the designed peptides were got through MD simulation and AGADIR prediction(Kong et al., 2005). Then the designed peptides were tested for binding mode and binding free energy of peptide with IN(Kong et al., 2005). Researchers found that improvement in binding free energy compared with that of interfacial alpha1 and alpha5 of the integrase dimer

indicated that some of the designed peptides may have a higher potency for inhibiting the dimerization of IN(Kong et al., 2005). Their study provided some useful information for rational design of IN peptide inhibitor(Kong et al., 2005).

Although plenty of trials have been made in HIV-1 integrase inhibitors searching, and many kinds of different substances such as STI(Marchand et al., 2009), recently developed hydroxylated aromatics, natural products, peptide, antibody and oligonucleotide inhibitors have been demonstrated as potential anti-HIV integrase drug candidates with promising effects, small molecules may be the most feasible and effective candidates for HIV-1 IN inhibitors development(Dayam and Neamati, 2003; Marchand et al., 2009; Tramontano et al., 2004; Yang et al., 2010).

1.7 Vaccine development

Vaccine is the most effective way in preventing virus from widely transmission. Vaccine is successful and effective in controlling many virus causing diseases such as HBV, Measles, Mumps & Rubella Virus. For some RNA viruses with high frequently mutation, vaccine proven to be effective as it does in flu control. But for HIV, all available vaccines failed in the past decades.

There are three main challenges in development of HIV vaccine. First, because of thermostability concealed conserved target, highly variable exposed targets and heavy glycosylation, HIV is difficult to induce long-lasting neutralizing antibodies. Second, HIV integrates viral DNA into host genome to cause a permanent infection. Third, the HIV reverse transcriptase is an enzyme of high error rate, this leads to the high variability in HIV replication.

HIV vaccine development is mainly focused on cellular immunity induction at present. Living viral vector technologies and DNA vaccines are introduced into HIV vaccine development. HIV-1 envelop proteins are also important targets in HIV vaccine development in recent years(Charles-Nino et al., 2011; Ndirangu et al., 2011). The

first HIV vaccine which was demonstrated modest protective efficacy was RV144 trial conducted in Thailand. Although waned considerably over time, the estimated initial efficacy was □74%(Rerks-Ngarm et al., 2009; Schneider et al., 2011). Recently Karen Schneider and coworkers developed a mathematical model to reflect historical and current HIV trends across different at-risk populations in Thailand(Schneider et al., 2011). A study conducted with this model denmonstrated that an RV144-like vaccine with coverage of 30% of the population would lead to a 3% reduction in HIV incidence during the next 10 years while 30% coverage of annual or biannual re-vaccination with the vaccine was found to result in 14% and 23% reductions in incidence, respectively; Also, coverage of 60% without re-vaccination resulted in a 7% reduction(Schneider et al., 2011).

1.8 Question and hypothesis

According to the World Health Organization's estimates in 2007, close to 33 million people worldwide are living with HIV/AIDS. AIDS is becoming a major healthcare threat to many countries, particularly the developing countries like China. There are more than 740 thousand cases have been reported to be infected with HIV up to now. In the past two decades, significant progress has been made in understanding HIV pathogenesis and AIDS progression, which has allowed the identification of a multitude of drugs and vaccine targets.

Since there is no effective vaccine for the prevention and treatment of HIV infection, the HAART is still the most effective way in AIDS treatment. HAART requires a combination of different drugs targeting different steps in virus infection. Althought more than 20 kinds of drugs have been approved in the past 2 decades, some AIDS patients still cannot find suitable drugs for therapy. Why? This is probably due to the high mutation rates of HIV. Another factor, emerging of drug resistant viruses is also an important reason.

The anti-HIV drugs are mainly targeting the reverse transcriptase and protease of HIV. Besides, many drugs have been developed aiming at several steps in virus infection, including the drugs directly or indirectly targeting the HIV envelope, the drugs targeting the fusion of virus and the cell membrane, the drugs targeting the HIV integration, the drugs targeting the virus proteins synthesis and transportation, finally the drugs targeting the virus budding.

In the history of AIDS drug development, zidovudine (NRTI), is the first anti-HIV drug that is approved for AIDS treatment(Vrang et al., 1987). This is a drug targeting the reverse transcriptase. After that, another six NRTIs were approved. More reverse transcriptase inhibitors including three non-nucleoside reverse transcriptase inhibitors (NNRTIs) and one nucleotide reverse transcriptase inhibitor have been approved(De Clercq, 2009) in the past decades. For HIV-1 protease, totally eight inhibitors have been approved(Rodriguez-Barrios and Gago, 2004).

Although currently available drugs have greatly decreased the mortality rate of AIDS, drug resistance is an inevitable consequence that limits the duration of successful treatment(Baldwin et al., 2004). Thus, a preventative vaccine remains the top priority; however, no vaccine trial performed up to now is successful. Therefore, we must strive to develop new drugs to reduce the viral loads after HIV infection.

In this study, a cell-based assays is established to examine the nuclear translocation of HIV-1 IN. In principle, the translocation of HIV-1 IN from cytoplasm into the nuclei is a critical step to mediate incorporation of viral DNA into host DNA(Desfarges et al., 2009). Therefore, compounds that are able to block the translocation of HIV-1 IN into nucleus should be potential inhibitors of viral integration. The natural compounds isolated from exotic herbs should provide a good resource for the screening of blockers of HIV-1 integrase into the nucleus. It was hypothesized that if any chemical or natural product that can inhibit the HIV-1 integrase nuclear translocation, these compounds maybe new types of HIV-1 integrase inhibitor candidates.

CXCR4 and CCR5 are the two common receptors of HIV, expressing respectively on human T cells and macrophages. In November 2010, some researchers from The Scripps Research Institute and University of California at San Diego reported the structures of the CXCR4 chemokine GPCR with small-molecule and cyclic peptide antagonists. In that study, the crystal structures of human CXCR4 in complex with a small-molecule antagonist at 2.5 Å resolution and with a cyclic peptide inhibitor at 2.9 Å resolution were repoted(Wu et al., 2010). As natural ligand of CXCR4, SDF-1α, inhibits cell fusion and infection by HIV strains of the syncytium-inducing (SI) phenotype (Bleul et al., 1996). So SDF-1α interact with CXCR4 and induce internalization of CXCR4 is a good target for anti-HIV drugs development(Jenkinson et al., 2010). Any chemical or natural products that can inhibit the SDF-1α induced CXCR4 internalization maybe important anti-HIV drug candidate!

Chapter 2 Materials and Methods

2.1 Materials

2.1.1 Chemicals

DNA primers, 100bp marker, 1kb marker, agarose (electrophoresis grade) and phosphate-buffered saline (PBS) were purchased from Invitrogen (Invitrogen Corporation, CA, USA). The compounds were purchased from SPECS bank. The structure and purity were confirmed by NMR (dissolved in DMSO-D6). 2−ME, 2-Mercaptoethanol were purchased from Bio-Rad. Natural product DW-IN719 was purchased from ChemBridge. KM and KX compounds screened for integrase inhibitors and CXCR4 internalization antagonists were provided by Kunming Institute of Zoology, the Chinese Academy of Sciences. AZT (3'-Azido-3'-deoxythymidine), HEPES, MTT, Penicillin, Streptomycin sulfate, Glutamine, DMSO-D6 (Dimethyl sulfoxide-D6) and AMD3100 were purchased from Sigma Chemicals (Sigma-Aldrich, MO, USA). All other chemical and reagent were of molecular grade or higher grade.

2.1.2 Enymes, proteins and virus

T4 DNA ligase and restriction enzymes were purchased from New England BioLabs (New England BioLabs Inc. MA, USA). Ampli Taq Golden polymerase was purchased from Roche. Superscript II reverse transcriptase and RNaseH were purchased from Invitrogen (Invitrogen Corporation, CA, USA). SDF-1α was purchased from R & D Systems. The laboratory-derived viruses HIV-1IIIB and human T cell line C8166 was obtained from MRC, AIDS Reagent Project, UK.

2.2 Methods

2.2.1 Cell based HIV-1 integrase inhibitors screening platform construction

2.2.1.1 PCR for HIV-1 Integrase-EGFP amplification

The PCR mixture was set up in a 50μl reaction containing 2μl of the integrase containing plasmid(pT7-7 His(Tx) HIV-IN plasmid, gift from Dr. S.A. Chow from School of Medicine, UCLA), as the template, 5μl 10X PCR Golden buffer (Roche);

3µl 25mM $MgCl_2$ (Roche); 1µl of 10mM dNTP mix (Invitrogen), 1µl of each 10mM forward primer and 10µM reverse primer and 1µl of Ampli Taq Golden polymerase (Roche) (5U/µl) and adjusted the volume by autoclaved distilled water. The PCR reaction was carried out at denaturation temperature at 94°C for 3 minutes. Then the amplification was performed at 94°C for 30 seconds, 55°C for 30 seconds, 72°C for 30 seconds for 30 cycles. A final extension step was given at 72°C for 7 minutes. The thermal cycling reaction was carried out in the thermal cycler (Eppendrof Matercycle gradient).

Forward primer: 5'-CAATCGGGATCCATGTTTTTAGATGGAATAGATAAGGC (Bam HI)

Reverse primer: 5'-CTTTTCGCGGCCGCTTAATCCTCATCCTGTCTACTTGC (Not I)

2.2.1.2 Gel Analysis of PCR Product

After the PCR amplification, 5µl of PCR product was examined by 1% agarose gel in presence of 0.5µg/ml ethidium bromide with 100bp marker.

2.2.1.3. Purification of PCR product

The PCR product was purified by using the High Pure™ PCR Product Purification Kit (Boehringer Mannhem) following the manufacturer's guide. Briefly, 50µl of PCR product after PCR was mixed with binding buffer. The mixture was loaded in the upper reservoir of *High Pure* filter tube and centrifuged at 13,000 rpm for 30 seconds. The flow through was discarded and 500µl of wash buffer was added to the upper reservoir and centrifuged at 13,000 rpm for 30 seconds. The washing step was repeated one more time by using 200ul washing buffer. The PCR product was eluted out by 50µl elution buffer by centrifugation in 13,000 rpm for 30 seconds. The purified PCR product was stored in -20°C.

2.2.1.4 Restriction enzyme digestion

The Tet-off expression vector pTRE2hyg (Clontech) and the PCR product were digested with BamHI/NotI. Vector was digested with 0.5µl of both PmeI (20,000U/ml,

NEB) and MluI (20,000U/ml, NEB), in 1X NEB buffer 4 and 1X NEB BSA in 37°C overnight. Integrase-EGFP PCR product was digested with 0.5µl of MluI (20,000U/ml, NEB), in 1X NEB buffer 4 and 1X NEB BSA in 37°C overnight. All the reaction mixtures were then incubated in 65°C for 20 minutes for restriction enzyme inactivating.

2.2.1.5 Gene Clean

The digested vector and insert were purified by the QIAquick gel extraction kit (QIAGEN). Briefly, the digested products were undergoing electrophoresis in 1% agarose gel. The gel containing vectors/inserts was slicing by clean scalpel. The gel was weighted and 3 volume of QG buffer (100mg added 100µl) was added and incubated in 50°C for 10 minutes for completely dissolved. The QG buffer was then passed through QIAquick spin column by centrifugation in 13,000 rpm for 1 minute. DNA was washed by 0.75ml PE buffer by centrifugation in 13,000 rpm for 1 minute. The trace amount of washing buffer was removed by centrifugation in 13,000 rpm for 1 minute one more time. Finally, DNA was eluted in 50ul elution buffer in 1.5 ml centrifuge tube and stored in -20°C.

2.2.1.6 Ligation

The ligation was performed in 1:5 of vector to insert ratio. 10ul ligation mixture was set up: 10ng linearized expression vector, 1µl 10X T4 ligase buffer (NEB) and 50ug digested integrase-EGFP DNA was mixed with 1X NEB T4 ligation buffer. 1µl of NEB T4 ligase (5U/µl) was added and incubated in 16°C overnight.

2.2. 1.7 Preparation of competent bacterial cells (*E.coli* strain DH5α)

Single colony of *E.coli* cell, DH5α, was inoculated into 50ml LB medium at 37°C with 250 rpm shaking overnight (<16 hours). The next day, 4 ml of overnight culture was inoculated into 400ml LB medium in 2-liter flask and grown at 37°C with 250rpm shaking for about 3-4 hours until its absorbance at wavelength 600nm (OD_{600}) reach 0.5 for mid-log phase. The bacterial cells were aliquoted in 50 ml pre-chilled,

sterile polypropylene tube (totally 8 tubes) for 10 minutes on ice cooling and harvested by centrifugation at 4,000 rpm for 10 minutes at 4°C. The medium was decant from cells pellet and the traces amount of medium was removed by standing the tube in an inverted position on a pad of paper towels for 1 minute. Each of the cell pellets was resuspended in 10ml ice-cold $CaCl_2$ solution (60mM $CaCl_2$) in gently and centrifuged at 4,000 rpm for 10 minutes at 4°C. The medium then was removed as mention before and resuspended in 10ml cold $CaCl_2$ solution again and incubated in ice for 30 minutes. Each of the cell pellets then resuspended in 2ml cold $CaCl_2$ solution with 10% glycerol (w/v). 50ul of resuspended competent cells was aliquoted into per-chilled 1.5ml eppendorf and stored in -80°C.

2.2.1.8 Transformation into DH5α

The ligation product was transformed into DH5α *E.coli* competent cell by heat-shocking. Frozen competent bacterial cells, DH5α, were thawed on ice for 10 minutes. 1μl of plasmid was mixed gently with 50μl thawed competent cell and incubated in ice for 10 minutes. The mixture was incubated in 42°C for 90 seconds, and then chilling in ice for 5 minutes. 200μl LB medium was added in transformed competent cells and incubated in 37°C for 1 hour with shaking at 250 rpm. 50μl of incubated product was spread on agar plate with 100μg/ml ampicillin and incubated in 37°C overnight.

2.2.1.9 Selection of positive colony

Ten different single colonies of different sets of transformation were inoculated in 1ml LB medium with 100 μl/ml ampicillin at 37°C for overnight (<16 hours) with 250 rpm shaking. 100μl of the cell was spun down at 13,000 rpm for 1 minute. Cell pellet was resuspended by autoclaved distillated water and boiled in 100°C for 2 minutes. Cell pellet was removed spun down at 13,000 rpm for 1 minute. 1μl of the supernatant was used as the template for PRC as mentioned in section 2.2.2.3. The PCR product was analyzed with 1% agarose gel.

2.2.1.10 Small scale plasmid purification

The positive clone remained culture was used on plasmid preparation by using the QIAprep Spin Miniprep kit. Briefly, remained over night culture was collected by centrifugation in 13,000 rpm for 1 minutes. The pellet was resuspended in 250μl Buffer P1 with RNaseA by vortex. 250μl Buffer P2 was added and mixed gently by inverting the tube 10 times and incubated in room temperature for 2 minutes. 250μl Buffer N3 was added and mixed the tube by inverting 10 times immediately. The precipitation was spun down at 13,000 rpm for 10 minutes. The supernatant containing plasmid was loaded on the QIAperp colmum and centrifuged in 13,000 rpm for 1 minute. 0.75ml Buffer PE was loaded in the column and centrifuged in 13,000 rpm for 1 minute to wash the plasmid. The trace amount of PE was further removed centrifuged in 13,000 rpm for 1 minute again. The plasmid was eluted out by 50 μl Buffer EB (10mM Tris-Cl, pH 8.5). The plasmid was stored in -20oC.

The plasmid for pTRE2hyg with IN-EGFP DNA was named pTRE2hyg-IN-EGFP. The concentration of plasmid was measured under OD_{260} 1μg of plasmid was taken for sequencing analysis by Tech Dragon Limited.

2.2.1.11 Large scale plasmid preparation by alkaline lysis and phenol/chloroform extraction

Tet off vector pTRE2hyg-IN-EGFP and control vector pTRE2hyg-EGFP were transformed into DH5α competent cells respectively according to the protocol mentioned before. Single clones were picked and positive clones were selected as mentioned in before. For each vector, single clone was picked and inoculated in 20 ml LB medium with 100μg/ml ampicillin in 37oC with 250rpm shaking for overnight (<16 hours). Overnight culture was centrifuged down at 5000rpm at 25°C for 15 minutes. Cell pellet was resuspended in 2ml Solution 1 (25mM Tris-Cl, pH 8.0, 10mM EDTA, 50mM glucose 100μg/ml RNaseA) by vortex. 2ml fresh prepared Solution 2 (0.2M NaOH and 1%SDS) was added and mix by inverting the tube 10 times. The mixture was kept at room temperature for 5 minutes. 2ml Solution 3 (5M potassium acetate, pH 4.8) was added and mixed by inverting the tube 10 times. The

mixture was kept at room temperature for 10 minutes. The mixture was centrifuged at 11,000rpm at 25°C for 15 minutes. The supernatant was transferred to new tube. 0.6v/w isopropanol was added and incubated at room temperature for 5 minutes for DNA precipitation. DNA pellet was centrifuged down at 11,000rpm for 15 minutes at 25 °C. DNA pellet was washed with 2ml 75% ethanol. The DNA was then dry in room temperature for 5-10 minutes and dissolved in 0.5ml autoclaved distilled water.

The plasmid was further purified by phenol/chloroform extraction. 0.5ml phenol/chloroform was mixed with DNA prepared above and vortex vigorously for 5 minutes. Milky mixture was centrifuged at 15,000rpm for 10minutes. The upper aqueous layer was transferred to new tube.1/10 volume of 3M sodium acetate (NaAc), pH 5.2, was added and mixed well by vortex. 2 volume of absolute (100%) ethanol was added and mixed by vortex to precipitate the plasmid. DNA pellet was centrifuged at 15,000rpm for 10 minutes and washed with 1ml 75% ethanol. The pellet was dried for 5-10 minutes. The plasmid was dissolved in 50µl autoclaved water for 15 minutes. The concentration of plasmid was measured under OD_{260} The plasmid was diluted to final concentration 0.5µg/µl and stored in -20°C.

2.2.1.12 HeLa Tet-Off Advanced Cells culture and passage

HeLa Tet-Off Advanced Cells (Clontech) were cultured in 100 mm2 culture plates with Dulbecco's Modified Eagle Medium with 25mM HEPES and 10% Tet-System Approved Fetal bovine serum (FBS) (Clontech #8630-1), geneticin (G418. 100 µg/ml) hygromycin (100µg/ml) were used for the keeping of Tet-off cell line. This was the whole medium for normal keeping of cells. For every 3-4 days, the medium was removed and the cells were washed with 10 ml PBS, followed by trypsinization by adding 1ml of trypsin/EDTA solution. The cells were agitated for the dissociation of cells from the surface of the culture plate for 5 minutes at room temperature. 1 ml DMEM was added to stop the trypsin reaction. The suspension was transferred into a snap-cap and centrifuged at 1800 rpm for 4 minutes at room temperature. The cell pellet was resuspended in 1 ml DMEM. After counting the cells, cells were seeded at

a density of 2 x 10^6 cells into a new culture plate with 10 ml medium. The cells were incubated in a 5 % CO2 incubator at 37 °C.

2.2.1.13 Transfection of pTRE2hyg-IN-EGFP into HeLa Tet-Off Advanced cells

Twenty-four hours before transfection, 2 x 10^5 HeLa Tet-Off Advanced cells were seeded onto a flamed glass plate in 24-well plate (BD) in DMEM whole culture medium. EGFP-C-IN expression vector was transfected into HeLa Tet-Off Advanced cells using Lipofectamine 2000 reagent (Invitrogen) in accordance with the following description. For each well of cells, dilute 1μg of DNA into 25 μl medium without serum (e.g., OptiMEM® I Medium) in 24-well, sterile micro titer plates. For each well of cells, dilute 5 μl of Lipofectamine™ 2000 into 100 μl OptiMEM® Medium and incubate for 5 min at room temperature. Once the Lipofectamine™ 2000 is diluted, combine it with the DNA within 30 min. Longer incubation times may result in decreased activity. This dilution can be prepared in bulk for multiple wells. Add 100 μl of the diluted Lipofectamine™ 2000 to each well containing diluted DNA, mix gently, and incubate at room temperature for 20 min to allow DNA- Lipofectamine™ 2000 complexes to form. Add the DNA- Lipofectamine™ 2000 complexes (200μl) directly to each well of the plates containing cells and mix gently. The medium was removed five hours after transfection. Twenty-four hours after transfection, cells were fixed with 4% paraformaldehyde in PBS for 15 min at RT. EGFP expression vector was transfected into HeLa Tet-Off Advanced cells using the same protocol as control.

2.2.1.14 Fluorescence microscopy analysis

The cells that seeded on the flamed glass plate in the 24 well-plate were washed with 1ml PBS to remove the death cell after 24 hours post-transfection. The glass plate was mounted on the stage adaptor (Model: SA-20L/Z) with growing medium. Fluorescent imaging was carried out to monitor EGFP expression. Images were collected using Leica SP5 confocal microscope.

2.2.2 Virtual screening of integrase inhibitors

Based on the crystal structure of the IN CCD-LEDGF IBD complex (PDB ID: 2B4J), a small-molecule database that contained about 30000 drug-like compounds from the library of the SPECS company was searched by using the program AutoDock 4.2. First, IBD part of the crystal structure was removed. Second, AutoDockTools 1.5.4 was employed to add hydrogen atoms, remove water molecules, and optimize the grid box according to the IBD binding site. Last, small molecules were docked into the binding pocket of IN CCD with the aid of the AutoDock program, and were ranked according to the scores that were calculated by using the energy scoring function in the AutoDock 4.2 software.

The whole docking operation in this study could be stated as follows. A grid map with 40×40×40 points and a spacing of 0.375 Å was generated by using the AutoGrid 4.2 program. The grid centre was set at the active-site position (-14.685, 4.189, -7.387), and the affinity and electrostatic potential grids were calculated for each type of atom in the inhibitors. The Lamarckian genetic algorithm (LGA) was applied to deal with the protein–ligand interactions. The number of generation, energy evaluation, and docking runs were set to 500 000, 2 500 000 and 20, respectively. The evaluation with the lowest binding energy was used to analyze ligand pose. Twenty-three candidate molecules were selected for further study; all these compounds were purchased from the SPECS.NET (http://www.specs.net/). Finally, the interaction model of IN CCD with ligand was produced by using the LIGPLOT program, and was based on the docked complex structure.

2.2.3 Cell based screening of integrase inhibitors

2.2.3.1 SPECS compounds' test of integrase nuclear translocation inhibition

HeLa Tet-Off Advanced Cells (Clontech) were cultured and maintained in Dulbecco's modified Eagle's medium (DMEM) supplemented with 10% fetal bovine serum (FBS), 100μg/ml G418 and 100 U/ml of streptomycin–penicillin (Invitrogen) at 37 °C in a 5% CO2 incubator. Twenty-four hours before transfection, 5×10^4 HeLa Tet-Off

Advanced cells were seeded onto a black/clear 96-well plate (BD) in DMEM containing 10% FBS. EGFP-C-IN expression vector was transfected into HeLa Tet-Off Advanced cells using Lipofectamine 2000 reagent (Invitrogen) in accordance with the protocol mentioned above. The medium was removed five hours after transfection. Fresh medium containing compound solution was added at final concentrations of 1μM, 5μM and 10μM separately. Corresponding concentrations of DMSO were used as control. Twenty-four hours after transfection, cells were fixed with 4% paraformaldehyde in PBS for 15 min at RT and stained with Hoechst 33342(2μg/ml) for 15 min. The well was washed with 400μl PBS for twice. Fluorescent imaging was carried out to monitor EGFP expression and Hoechst staining. Images were collected using GE IN cell analyzer 1000 cell imaging system.

2.2.3.2 Cloning of HIV-1 integrase into pcDNA6/V5-HisA

The HIV-1 integrase was amplified from the IN-C-EGFP expression vector with the following primers:

Forward Primer: 5'-CAGCGTAAGCTTATGTTTTTAGATGGAATAGATAAG (Hind III)

Reverse Primer: 5'-GTGGATCTCGAGTTAATCCTCATCCTGTCTACTTGC (Xho I)

PCR product was purified as mentioned in 2.2.1.3, then the PCR purified PCR product and pcDNA6/V5-HisA was digested with restriction enzymes as mentioned in 2.2.1.4, DNA insert and linearized Vector was performed gene clean as mentioned in 2.2.1.5, insert and vector was ligased as mentioned in 2.2.1.6; Recombinant plasmid was transformed into DH5α competent cells as mentioned in 2.2.1.8; Positive clone was selected as mentioned in 2.2.1.9; Large scale plasmid was prepared as mentioned in 2.2.1.11. The concentration of plasmid was measured under OD_{260} 1μg of plasmid was taken for sequencing analysis by Tech Dragon Limited. The recombinant plasmid containing HIV-1 integrase was named as pcDNA6/V5-HisA-IN.

2.2.3.3 Immunofluorescence

Transfection procedure and concentration of compounds were as mentioned above. Twenty-four hours after transfection, cells were fixed in 4% paraformaldehyde in PBS for 15 min at RT. The cells were rinsed in PBS, post fixed, and made permeable in 0.5% Triton X-100 at RT for 15 min. After rinsing with PBS, the cells were incubated in 3% BSA for 1 hour, washed in PBS, and incubated in anti-integrase-1 antibody (Santa Cruz Biotechnology) diluted with PBS containing 1% BSA for 1 hr at 37°C in a humid chamber. Then cells were washed for 30 min in three changes of PBS at RT and then incubated in FITC-conjugated antibody (Santa Cruz Biotechnology) diluted with PBS containing 1% BSA for 1 hr at 37°C in a humid chamber Then cells were washed as before. Cells were stained with PI (0.3 μg/ml) for 20 min. Fluorescent imaging was carried out to monitor integrase expression. Images were collected using Leica SP5 confocal microscope.

2.2.4 Screening of integrase inhibitors from drug database in Kunming institute of Zoology, CAS

2.2.4.1 Human embryo kidney (HEK) 293T cell culture and passage

Human embryo kidney 293T cell line was purchased from ATCC. 293T cells were cultured in 100 mm2 culture plates with Dulbecco's Modified Eagle Medium with 25mM HEPES and 10% Fetal bovine serum (FBS) (Invitrogen Cat # 10099-141), 1% of streptomycin–penicillin (Invitrogen Cat# 15140-122) was supplemented. This was the whole medium for normal keeping of cells. For every 2-3 days, the medium was removed and the cells were washed with 10 ml PBS. Then add 1ml 0.25% Trypsin and kept for 5minutes for digestion. Wash the cells with 10 ml PBS after centrifuged at 1000rpm for 10 min, the cell pellet was resuspended in 1 ml DMEM medium. After counting the cells, cells were seeded at a density of 2 x 10^6 cells into a new culture plate with 10 ml full culture medium. The cells were incubated in a 5 % CO2 incubator at 37 °C.

2.2.4.2 Screening of drug candidates by transfection of pEGFP-C1-IN into 293T cell line

Twenty-four hours before transfection, 5×10^4 293T cells were seeded onto a 96-well plate (BD) in DMEM containing 10% FBS. pEGFP-C1-IN expression vector was transfected into 293T cells using Lipofectamine 2000 reagent (Invitrogen) in accordance with the protocol mentioned above. The medium was removed five hours after transfection. Fresh medium containing compound solution was added at final concentrations of 1μM, 5μM and 10μM or 200μg/ml according to concentration of different samples. Corresponding concentrations of DMSO were used as control. Twenty-four hours after transfection, cells were fixed with 4% paraformaldehyde in PBS for 15 min at RT. The well was washed with 400μl PBS for twice. Fluorescent imaging was carried out to monitor IN-EGFP expression. Images were collected using Leica DMI6000B fluorescent microscopy.

2.2.5 Synthesis of Novel HIV-1 integrase inhibitors

Based on the structural information of DW-IN6, DW-IN15 and DW-IN-16 provided by NMR, one new compound was designed and synthesized. The principle concerns of new compounds were to reinforce the anti-HIV activity as well as to reduce the cytotoxicity to human cells and human body. Newly synthesized compound was designated INNE-1. After synthesis, INNE-1 was dissolved in DMSO-D6 and analyzed by NMR. Following the synthesis route of INNE-1, another five compounds, INNE-2, INNE-3, INNE-4, INNE-5 and INNE-6 were synthesized later. INNE-1, INNE-2, INNE-3, INNE-4, INNE-5 and INNE-6 were synthesized in corporation with Dr. Joseph Chan.

2.2.5.1 Inhibition assay of INNE-1 on HIV-1 integrase nuclear translocation

Twenty-four hours before transfection, 2 x 10^5 HeLa Tet-Off Advanced cells were seeded onto a flamed glass plate in 24-well plate (BD) in DMEM whole culture medium. EGFP-C-IN expression vector was transfected into HeLa Tet-Off Advanced cells using Lipofectamine 2000 reagent (Invitrogen) in accordance with the following description. For each well of cells, dilute 1μg of DNA into 25 μl medium without serum (e.g., OptiMEM® I Medium) in 24-well, sterile micro titer plates. For each

well of cells, dilute 5 μl of Lipofectamine™ 2000 into 100 μl OptiMEM® Medium and incubate for 5 min at room temperature. Once the Lipofectamine™ 2000 is diluted, combine it with the DNA within 30 min. Longer incubation times may result in decreased activity. This dilution can be prepared in bulk for multiple wells. Add 100 μl of the diluted Lipofectamine™ 2000 to each well containing diluted DNA, mix gently, and incubate at room temperature for 20 min to allow DNA- Lipofectamine™ 2000 complexes to form. Add the DNA- Lipofectamine™ 2000 complexes (200μl) directly to each well of the plates containing cells and mix gently. The medium was removed five hours after transfection. Fresh medium containing compound solution was added at final concentrations of 1μM, 5μM and 10μM separately. Corresponding concentrations of DMSO were used as control. Twenty-four hours after transfection, cells were fixed with 4% paraformaldehyde in PBS for 15 min at RT. EGFP expression vector was transfected into HeLa Tet-Off Advanced cells using the same protocol as control.

2.2.5.2 Inhibition assay of INNE-2, INNE-3, INNE-4, INNE-5, INNE-6 on HIV-1 integrase nuclear translocation

Twenty-four hours before transfection, 2 x 10^5 HeLa Tet-Off Advanced cells were seeded onto a flamed glass plate in 24-well plate (BD) in DMEM whole culture medium. EGFP-C-IN expression vector was transfected into HeLa Tet-Off Advanced cells using Lipofectamine 2000 reagent (Invitrogen) in accordance with the following description. For each well of cells, dilute 1μg of DNA into 25 μl medium without serum (e.g., OptiMEM® I Medium) in 24-well, sterile micro titer plates. For each well of cells, dilute 5 μl of Lipofectamine™ 2000 into 100 μl OptiMEM® Medium and incubate for 5 min at room temperature. Once the Lipofectamine™ 2000 is diluted, combine it with the DNA within 30 min. Longer incubation times may result in decreased activity. This dilution can be prepared in bulk for multiple wells. Add 100 μl of the diluted Lipofectamine™ 2000 to each well containing diluted DNA, mix gently, and incubate at room temperature for 20 min to allow DNA- Lipofectamine™ 2000 complexes to form. Add the DNA- Lipofectamine™ 2000 complexes (200μl)

directly to each well of the plates containing cells and mix gently. The medium was removed five hours after transfection. Fresh medium containing compound solution was added at final concentrations of 1μM, 5μM and 10μM separately. Corresponding concentrations of DMSO were used as control. Twenty-four hours after transfection, cells were fixed with 4% paraformaldehyde in PBS for 15 min at RT. EGFP expression vector was transfected into HeLa Tet-Off Advanced cells using the same protocol as control.

2.2.6 Cloning of human CXCR4 gene into lentivirus vector

2.2.6.1 Preparation of competent bacterial cell (*E.coli* strain DH5α)

Single colony of *E.coli* cell, DH5α, was recovered from -80°C for competent cell preparation. The experiment protocol was as mentioned in section 2.2.1.7. After preparation, 50μl of resuspension competent cell was aliquoted into per-chilled 1.5ml eppendorf and stored in -80°C for use.

2.2.6.2 H9 cell culture and passage

H9 cell line was purchased from ATCC. H9 cells were cultured in 100 mm^2 culture plates with RPMI1640 with 25mM HEPES (Invitrogen Cat# 72400-120) and 10% Fetal bovine serum (FBS) (Invitrogen Cat # 10099-141), 1% of streptomycin–penicillin (Invitrogen Cat# 15140-122) was supplemented. This was the whole medium for normal keeping of cells. For every 3-4 days, the medium was removed and the cells were washed with 10 ml PBS after centrifuged at 1000rpm for 10 min, the cell pellet was resuspended in 1 ml PRMI1640. After counting the cells, cells were seeded at a density of 2 x 10^6 cells into a new culture plate with 10 ml full culture medium. The cells were incubated in a 5 % CO2 incubator at 37 ℃.

2.2.6.3. Reverse transcription polymerase chain reaction (RT-PCR)

RNA was extracted by adding 1 ml Trizol reagent (Invitrogen) into the culture dish, and incubated at room temperature for 5 minutes. The Trizol solution was transferred to a 1.5 ml tube and 0.2 ml chloroform was added, vortexed the tube vigorously for 15

seconds and incubated for 3 minutes. The tubes were centrifuged at 15000 rpm for 15 minutes at 4 °C. The aqueous phase was transferred to a fresh tube; the RNA was precipitated by mixing with isopropanol at room temperature for 10 minutes and centrifuged at 15000 rpm for 10 minutes at 4 °C. The pellet was washed with 1ml 75 % ethanol by vortexing and centrifuged at 7000 rpm for 5 minutes at 4 °C. The residue solution was aspirated and the RNA pellet was allowed to air dry for 5 minutes. The pellet was not allowed to dry completely. RNA was dissolved by adding RNase-free water for use directly or stored at –70 °C until use. For the first strand cDNA synthesis: 1 µg of RNA sample was added into an RNase-free tube containing the following components: 1 µl Oligo (dT) (500µg/ml); 12µl RNase-free distilled water. The mixture was heated to 70 °C for 10 minutes and quickly chilled on ice. The tube was spin by a brief centrifugation, followed by adding the components: 4µl 5X First Strand Buffer, 2µl 0.1 M DTT and 1µl 10 mM dNTPs. The tube was mixed gently and incubated at 42 °C for 2 minutes. An amount 0.5µl of Superscript II (200 units, Invitrogen) was added and mixed by pipetting up and down. The tube was incubated for 50 minutes at 42 °C. The reaction was inactivated by heating at 70 °C for 15 minutes. The PCR reaction was followed the standard protocol as below: PCR was performed with forward primer of CXCR4 (F: 5'AAACATGGAGGGGATCAGTATATAC3'), reverse primer of CXCR4 (R: 5'AGCTGA GTAACAGCGGACGGGAATCCCAAA3') and first strand cDNA as template on a Pekin Elmer Gene Amp 9700 PCR machine. The PCR mixture was set up in a 50µl reaction containing 2µl of the above cDNA, as the template, 5µl 10X PCR Golden buffer (Roche); 3µl 25mM $MgCl_2$ (Roche); 1µl of 10mM dNTP mix (Invitrogen), 1µl of each 10mM forward primer and 10µM reverse primer and 1µl of Ampli Taq Golden polymerase (Roche) (5U/µl) and adjusted the volume by autoclaved distilled water. The PCR reaction was carried out at denaturation temperature at 94°C for 3 minutes. Then the amplification was performed at 94°C for 30 seconds, 55°C for 30 seconds, 72°C for 30 seconds for 30 cycles. A final extension step was given at 72°C for 7 minutes. The thermal cycling reaction was carried out in the thermal cycler (Eppendrof Matercycle gradient).

2.2.6.4 Gel Analysis of PCR Product

After the PCR amplification, 5µl of PCR product was examined by 1.5% agarose gel in presence of 0.5µg/ml ethidium bromide with 100kb marker.

2.2.6.5 Purification of PCR product

The PCR product was purified by using the High Pure™ PCR Product Purification Kit (Boehringer Mannhem) following the manufacturer's guide. Purification protocol was as mentioned in section 2.2.1.3.

2.2.6.6 Restriction enzyme digestion

The lentivirus vector Pwpxl and the PCR product were digested with appropriate restriction enzymes described as follows. Vector was digested with 0.5µl of both PmeI (20,000U/ml, NEB) and MluI (20,000U/ml, NEB), in 1X NEB buffer 4 and 1X NEB BSA in 37°C overnight. CXCR4 PCR product was digested with 0.5µl of MluI (20,000U/ml, NEB), in 1X NEB buffer 4 and 1X NEB BSA in 37°C overnight. All the reaction mixtures were then incubated in 65°C for 20 minutes for restriction enzyme inactivation.

2.2.6.7 Gene Clean

The digested vector and insert were purified by the QIAquick gel extraction kit (QIAGEN). Gene clean was conducted as mentioned in 2.2.1.5.

2.2.6.8 Ligation

The ligation was performed in 1:5 of vector to insert ratio. 10µl ligation mixture was set up: 10ng linearized expression vector, 1µl 10X T4 ligase buffer (NEB) and 50µg digested CXCR4 cDNA was mixed with 1X NEB T4 ligation buffer. 1µl of NEB T4 ligase (5U/µl) was added and incubated in 16°C overnight.

2.2.6.9 Transformation into DH5α

The ligation product was transformed into DH5α *E.coli* competent cell by heat-shocking. Frozen competent bacterial cells, DH5α, were thawed on ice for 10 minutes. 1μl of plasmid was mixed gently with 50μl thawed competent cell and incubated in ice for 10 minutes. The mixture was incubated in 42°C for 90 seconds, and then chilling in ice for 5 minutes. 200μl LB medium was added in transformed competent cells and incubated in 37°C for 1 hour with shaking at 250 rpm. 50μl of incubated product was spread on agar plate with 100μg/ml ampicillin and incubated in 37°C overnight.

2.2.6.10 Selection of positive colony

Ten different single colonies of different sets of transformation were inoculated in 1ml LB medium with 100 μl/ml ampicillin at 37°C for overnight (<16 hours) with 250 rpm shaking. 100μl of the cell was spun down at 13,000 rpm for 1 minute. Cell pellet was resuspended by autoclaved distillated water and boiled in 100°C for 2 minutes. Cell pellet was removed spun down at 13,000 rpm for 1 minute. 1μl of the supernatant was used as the template for PRC as mentioned in section 2.2.1.9. The PCR product was analyzed with 1% agarose gel.

2.2.6.11 Small scale plasmid purification

The positive clone remained culture was used on plasmid preparation by using the QIAprep Spin Miniprep kit. Experiment protocol was as mentioned in section 2.2.1.10. The extracted plasmid was stored in -20 °C. The plasmid for pWPXL with CXCR4 cDNA was named pWPXL -CXCR4. The concentration of plasmid was measured under OD_{260} 1μg of plasmid was taken for sequencing analysis by Tech Dragon Limited.

2.2.6.12 Large scale plasmid preparation by alkaline lysis and phenol/chloroform extraction.

Transfer vector pWPXL-CXCR4, packing vector psPAX2 and envelope vector pMD2G was transformed into DH5α competent cells respectively according to the

protocol mentioned before. Single clones were picked and positive clones were selected as mentioned in before. For each vector, single clone was picked and inoculated in 20 ml LB medium with 100ug/ml ampicillin in 37oC with 250rpm shaking for overnight (<16 hours). Overnight culture was centrifuged down at 5000rpm at 25°C for 15 minutes. Then large scale plasmid preparation was conducted following the protocol mentioned in section 2.2.1.11. After preparation, the plasmids were dissolved in 50µl autoclaved water for 15 minutes. The concentration of plasmids was measured under OD_{260} The plasmids were diluted to final concentration 0.5µg/µl and stored in -20°C.

2.2.7 Production of recombinant lentivirus particle

2.2.7.1 Human embryo kidney (HEK) 293T cell culture and passage

Human embryo kidney 293T cell line was purchased from ATCC. 293T cells were cultured in 100 mm^2 culture plates with Dulbecco's Modified Eagle Medium with 25mM HEPES and 10% Fetal bovine serum (FBS) (Invitrogen Cat # 10099-141), 1% of streptomycin–penicillin (Invitrogen Cat# 15140-122) was supplemented. This was the whole medium for normal keeping of cells. For every 2-3 days, the medium was removed and the cells were washed with 10 ml PBS. Then 1ml 0.25% Trypsin was added and kept for 5minutes for digestion. The cells were washed with 10 ml PBS after centrifuged at 1000rpm for 10 minutes. The cell pellet was resuspended in 1 ml DMEM medium. After counting the cells, cells were seeded at a density of 2×10^6 cells into a new culture plate with 10 ml full culture medium. The cells were incubated in a 5 % CO2 incubator at 37 °C.

2.2.7.2. Co-transfection of transfer vector, envelope vector and packing vectror

293T cells were maintained in complete culture medium in a 37°C incubator with 5% CO2. Twenty-four hours before transfection, 4×10^6 exponentially growing 293T cells were plated in 100-mm tissue culture dishes. Cell density should be approximately 80% confluent for transfection. 1 ml of calcium phosphate-DNA

suspension was prepared for each 100-mm plate of cells as follows:

Two sterile tubes were set up for transfection of one plate. The tubes were labeled 1 and 2. 0.5 ml of 2x HBS was added to Tube 1. TE 79/10 was added to Tube 2. The volume of TE 79/10 was 440µl minus the volume of the DNA solution. 20 µg transfer vector of pWPXL-CXCR4, 15µg packaging plasmid of psPAX2 and 6µg envelope plasmid of pMD2.G were added to Tube 2 and mix. 60 µl of 2 M CaCl2 solution was added to Tube 2 and was mixed gently. The contents from Tube 2 were transferred to Tube 1 dropwise with gentle mixing. The suspension was allowed to sit for 30 minutes at room temperature. Precipitate was mixed well by pipetting or vortexing. 1 ml of the suspension was added to a 100-mm plate containing cells. The suspension was added slowly, dropwise while gently swirling the medium in the plate.The plates was return to the 37°C incubator and left for 4 hours. The old medium was replaced with 6 ml of fresh culture medium. 60 µl of 0.6 M sodium butyrate was added. The cells were return to the incubator. After 48 hours of culture, the supernatant was collected and freezed at -80°C or proceeded to the concentration step(Li and Rossi, 2007)(http://www.tronolab.com/).

2.2.7.3. Concentration of the recombinant virus

The supernatant (freshly collected or thawed from the freezer) was centrifuged at 900g for 10 minutes to remove any cell debris in the supernatant. The supernatant was filtered through a 0.2µm syringe filter. The supernatant was transferred to autoclaved polyallomer tubes. The supernatant was concentrated by ultracentrifugation for 1.5 hours at 4°C in a Beckman SW 28 swinging bucket rotor at 24,500 rpm. The supernatant was removed and the pellet was resuspended in an appropriate amount of culture medium, e.g., 300 µl for 30 ml of original supernatant if a 100-fold concentration is desired. The concentrated vector was divided into 10-50µl aliquots and stored at -80°C until use(Li and Rossi, 2007) (http://www.tronolab.com/).

2.2.7.4. Titration of the Virus

5 x 10^4 293T cells pre well were seeded in a 12-well plate in complete medium and

cultured overnight in a 37°C incubator with 5% CO2. Serial diluted vector stock was and 4 µl/ml polybrene were added to the cultured cells. The cells were continuously cultured for 48 hours. The cells were trypsinized. Following centrifugation, the supernatant was removed and the pellet was resuspended in 300 µl of 3.7% formaldehyde in PBS. The percentage of EGFP-positive cells was determined by FACS analysis. The titer would be represented as transduction units (TUs) per milliliter concentrated vector (TU/ml)(Li and Rossi, 2007) (http://www.tronolab.com/).

2.2.7.5 Transduction of Lentiviral Vectors to Target Cells

2 x 10^5 cells was seeded into one well in 1 ml of culture medium into a 24-well plate. Various amounts of concentrated vector stock were added depending on cell type. For the 293T cells and Hela cells, a multiplicity of infection (moi) of 10 can achieve virtually 80% transduction. 4µg/ml polybrene was added. The cells were returned to a 37°C incubator. After overnight incubation, the cells were centrifuged. The supernatant was discarded and the cells were resuspended with fresh culture medium. The cells were return to culture hood. Transduction efficiency was determined by FACS analysis 48 hours after transduction(Li and Rossi, 2007) (http://www.tronolab.com/).

2.2.7.6 Fluorescence microscopy analysis of transducted 293T cells

The cells that seed on the flamed glass plate in the 6 well-plate were washed with 1ml PBS to remove the death cell after 24 hours post-seeding. The glass plate was mounted on the stage adaptor (Model: SA-20L/Z) with growing medium. Fluorescent imaging was carried out to monitor GFP expression. Images were collected using Leica SP5 confocal microscope.

2.2.7.7 Expressed CXCR4-GFP biological activity assay

Hela cells were cultured in 100 mm^2 culture plate with Dulbecco's Modified Eagle Medium with 25mM HEPES and 10% Fetal bovine serum (FBS) (Invitrogen Cat #

10099-141), 1% of streptomycin–penicillin (Invitrogen Cat# 15140-122) was supplemented. Seed exponentially growing cells at 10^5 cells per well in 1 ml of culture medium into 35 mm^2 glass-bottom cell culture plate 24 hours. After 24 hours, infect the cells according to the protocol mentioned in before. Three days after infection, remove the culture medium, add SDF-1α at a final concentration of 10nM. Fluorescent imaging was carried out to monitor CXCR4-GFP expression and internalization in one hour. Images were collected using Leica SP5 confocal microscope.

2.2.8 Stable cell line

2.2.8.1 Establishment of stable cell line

Exponentially growing 293T cells were seeded at 2 x 10^5 cells per well in 1 ml of culture medium into a 24-well plate. Concentrated vector stock was added with a multiplicity of infection (moi) of 10 for transduction. Polybrene was added at a final concentration of 4μg/ml. The cells were returned to a 37°C incubator. After overnight incubation, the cells were trypsined and centrifuged. The supernatant was discarded, and the cells were resuspended with fresh culture medium. The cells were returned to incubator. Transduction efficiency was determined by FACS analysis 48 hours after transduction.

Several days after transduction, cells were transferred for enlarged culture. Plate cells in 24 well plate at a concentration of 2 x 10^5 cells per well. After 24 hours, the plated cells were analyzed for CXCR4-GFP expression with fluorescence microscopy. The cells with strong green fluorescence expression were marked for further action. The marked cells were picked by clone ring for culture. After 3 rounds single clone culture, a stable cell line with highly expression of CXCR4 was established. The established cell line was continuously cultured for six months. No reduction in CXCR4 expression was observed.

2.2.8.2 Fluorescence microscopy analysis of stable cell line

The stable cells were seeded on flamed glass in 6 well culture plate. The cells were washed with 1ml PBS to remove the death cell after 24 hours post-seeding. The glass plate was mounted on the stage adaptor (Model: SA-20L/Z) with growing medium. Fluorescent imaging was carried out to monitor GFP expression. Images were collected using Leica SP5 confocal microscope.

2.2.8.3 FACS analysis of stable cell line

Cells were harvested from one 10 cm plate when grow reaches 70% confluency. Cells were washed with 5ml PBS. Then cells were digested with 0.25% trypsin for 10 minutes. Cells were resuspended in 500μl PBS after centrifuged at 1000rpm/min for 10minutes. 5 ml of cold 70% ETOH (keep at –20°C) was added immediately into the cells. Cells were mixed thoroughly. Cells were kept at 4°C for 2 hours for fixing. Cells were spun down, and washed with PBS two to three hours prior to FACS analysis. Without adding more PBS, cells were spun again for 2 min so that the residual PBS can be taken off. Cells were resuspended with 500μl PBS. Cells are transferred to FACS tubes and have them analyzed.

2.2.9 CXCR4 antagonist screening

293T stable cell line expressing CXCR4-GFP was cultured in 100 mm^2 culture plate with Dulbecco's Modified Eagle Medium with 25mM HEPES and 10% Fetal bovine serum (FBS), 1% of streptomycin–penicillin was supplemented. Exponentially growing cells were seeded into 96 well cell culture plate at 10^5 cells/well 24 hours before testing. After 24 hours, the culture medium was removed. Drug containing mediums at different concentrations were added to the culture and incubated for 15 minutes. SDF-1α was added at a final concentration of 10nM. Fluorescent imaging was carried out to monitor CXCR4-GFP expression and internalization in one hour. Images were collected using Leica DMI6000B fluorescence microscope. AMD3100 was used for positive control.

2.2.10 Molecular modeling

These compounds interrupted CXCR4 internalization. The mechanism is not clear up to now. it is hypothesized that these compounds inhibited CXCR4 internalization in the similar matter with small molecule CXCR4 antagonist-IT1t. CXCR4 crystal structure was downloaded from Protein Data Bank (PDB ID 3ODU). The structure was prepared by AutodockTools 1.5.4. for docking, including remove waters, remove additional molecules etc. The KX128, KX166, KX171 and KX180 were prepared by Chemdraw according to the structural information. IT1t and AMD3100 were downloaded from Protein Data Band and PubChem database. Gridbox was prepared according to the ligand binding information in crystal structure of CXCR4. Molecular docking was run by Autodock Vina according to the manual. Docking results were analyzed by Pymol and Ligplot.

2.2.11 HIV-1 inhibiting activities and cytotoxicity of compounds

2.2.11.1 C8166 cell culture and passage

Human T cell line C8166 was maintained in RPMI-1640 supplemented with 10% heat-inactivated newborn calf serum (Invitrogen). Evrey 3 days, the culture suspension was transferred into a snap-cap and centrifuged at 1800 rpm for 4 minutes at room temperature. The cell pellet was resuspended in 1 ml RPMI1640. After counting the cells, cells were seeded at a density of 2 x 106 cells into a new culture plate with 10 ml medium. The cells were incubated in a 5 % CO2 incubator at 37 °C. The cells used in all experiments were in log-phase growth.

2.2.11.2 HIV-1 infection titer

The laboratory-derived viruses HIV-1IIIB was obtained from MRC, AIDS Reagent Project, UK. Virus stocks were stored in aliquots at -70 °C. Virus stocks were diluted in 4 folds for 10 gradients in 96 well plate. For every gradient, 6 wells were seeded cells for repeat. 50μl (4×10^5/ ml) of C8166 cells were seeded into every well in a

final volume of 200 μl and incubated in 37℃ with 5% CO_2. In two days, add 100μl new full culture medium to every well. Cytopathic effect (CPE) caused by virus was measured by observing the syncytium in every well. The 50% HIV-1 tissue culture infectious dose (TCID50) was determined and calculated by the Reed and Muench method(Stanic, 1963).

2.2.11.3 Syncytia assay

In the presence of 100μl various concentrations of compounds, C8166 cells (4×105/ ml) were infected with virus (HIV-1IIIB) at a multiplicity of infection (M.O.I) of 0.06. The final volume per well was 200 μl. Control assays were performed without the testing compounds in HIV-1IIIB infected and uninfected cultures. AZT was included as positive control. After 3 days of culture, the cytopathic effect (CPE) was measured by counting the number of syncytia. Percentage inhibition of syncytia formation was calculated and 50% effective concentration (EC50) was calculated(Wang et al., 2004).

2.2.11.4 P24 production inhibition in acute infection

Human T cell line C8166 and HIV-1_{IIIB} were supplied by British Medical Research Council, AIDS Reagent Project. 5,000 TCID50 HIV-1_{IIIB} virus was used for inoculum for each well culturing C8166 cells for 6 hours, remove virus. Compound solutions were added to culture at 0.5 μM to 20 μM. Cells lysis was collected for ELISA assay after 3 days culture. For ELISA, anti-Fc antibody was embedded by 1μg/well at 4 ℃ for over night. Wells were blocked with 5% defatted milk powder for 2 hours at 37 ℃. 100μl mouse anti-P24 monoclonal antibody was added to each well and incubated for 1hour at 37 ℃. 100 μl Cells lysis were added to each well and incubated for 2 hour at 37℃. 100μl rabbit anti-P24 polyclonal antibody was added to each well and incubated for 1hour at 37 ℃. 100μl rabbit anti-P24 polyclonal antibody was added to each well and incubated for 1hour at 37 ℃. 100μl HRP-conjugated goat anti rabbit IgG was added to each well and incubated for 1hour at 37 ℃. OPD was used as substrate. 2M sulfuric acid was added in 10 minutes. The OD was read with Elx800ELISA at 490nm (reference wavelength was 630nm).

2.2.11.5 MTT-based cytotoxicity assay

Cellular toxicity of compounds was assessed by MTT method as described previously. Briefly, cells were seeded on a microtiter plate in the absence or presence of various concentrations of compounds in triplicate and incubated at 37 ℃ in a humid atmosphere of 5% CO2 for 3 days. Twenty microliters of MTT reagent (5 mg/ml in PBS) was added to each well, then incubated at 37 ℃ for 4 h, 100 μl of 50% DMF-20% SDS was added. After the formazan was dissolved completely, the plates were read on a Bio-Tek ELx 800 ELISA reader at 595 nm/630 nm (A595/630). The cytotoxic concentration that caused the reduction of viable cells by 50% (CC50) was calculated from dose-response curve.

Chapter 3
Characterization of HIV-1 integrase nuclear translocation for development of new class of anti- AIDS drugs

3.1 Introduction

Translocation of viral integrase (IN) into nucleus is a critical precondition of integration during the life cycle of HIV, a causative agent of Acquired Immunodeficiency Syndromes (AIDS)(Bukrinsky and Haffar, 1997). As the first discovered cellular factor to interact with IN, Lens epithelium-derived growth factor (LEDGF/p75) plays an important role in the process of integration(Cherepanov et al., 2004; Cherepanov et al., 2003). Disruption of the LEDGF/p75-IN interaction has provided a special interest for anti-HIV agent discovery(Du et al., 2008). In this work, we reported that a group of small molecular compounds, DW-IN4, DW-IN5, DW-IN6, DW-IN9, DW-IN15, DW-IN16, DW-IN17, DW-IN21 and natural product DW-IN719 could potently inhibit the IN-LEDGF/p75 interaction and affect the HIV-1 IN nuclear distribution at 1μM. Also, 6 compounds (KM7, KM8, KM30, KM37, KM14, KM79) out of more than 150 compounds from Kunming showed integrase nuclear translocation inhibiton in cell based screening platform. These compounds were further tested for HIV-1 inhibition with live virus. These compounds suppressed viral replication by measuring HIV-1 P24 antigen production and syncytia formation inhibition in HIV-1IIIB acute infected C8166 cells. These results might supply useful structural information for further anti-HIV agent discovery.

3.2 Results

3.2.1 Expression of EGFP-C-HIV-IN is localized in nucleus of the Hela cells

To construct integrase inhibitor screening platform, integrase gene from HIV-1 was cloned into pEGFP-C1, then EGFP tagged integrase gene was subcloned into pTRE2hyg. Integrase gene was confirmed by DNA sequencing. pTRE2hyg-EGFP-IN was Transiently transfected into tet off ready Hela cell line. Transfection of pTRE2hyg-EGFP was as control. Confocal microscopy imaging showed that EGFP-C-HIV-1-IN was mainly localized in nucleus while EGFP alone was localized equally in the cell (Figure 3.1).

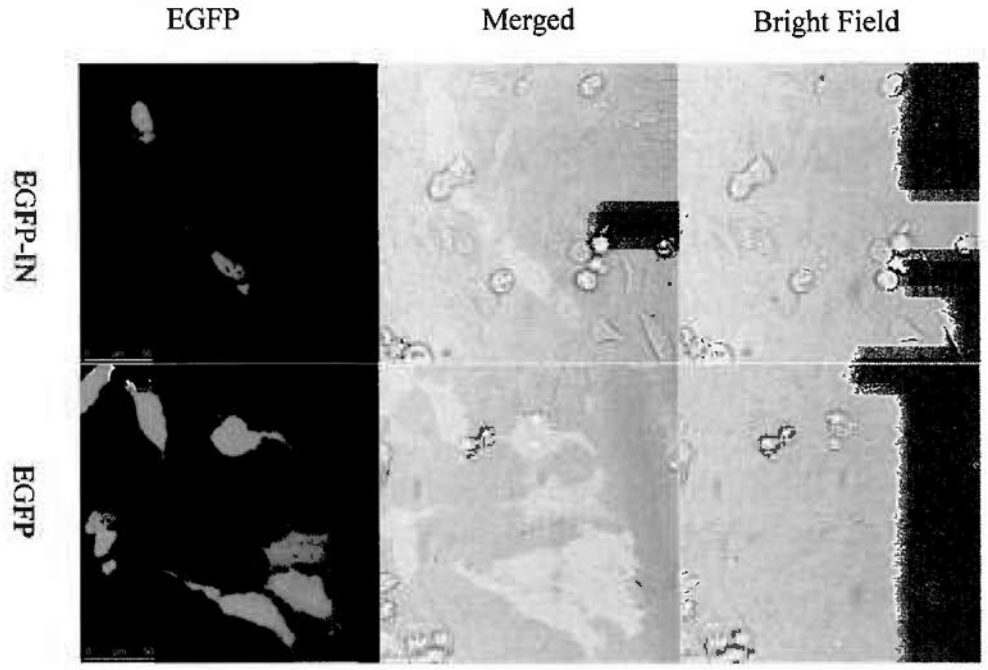

Figure 3.1 Expression of EGFP-C-HIV-IN is localized in cellular nucleus

Tet off Advanced Hela cells were transiently transfected with pTRE2hyg-EGFP-IN. Note the green fluorescence is highly localized in the nuclei of the cells. The pTRE2hyg-EGFP was used as control. EGFP was expressed in the whole cell with equal distribution.

3.2.2 Screening results of molecular docking

The crystallographic structure of HIV-integrase (2B4J) was selected from PDB. The structures were prepared by the structure editing tools PyMol and AutoDockTools. Activity binding sites were based on the 3D structural model generated in the base of the crystal structure of IN CCD in complex with IBD (PDB entry code 2B4J). For, molecular docking, a total of 23 compounds from SPECS bank with highest binding affinity to integrase resulted from virtual drug screening by Autodock 4.2 were selected for further investigation with our cell based screening platform. All these compounds possess low toxicity and suitable logP (Table 3.1). Also, seventy thousands ligands from natural product data bank ZINC were screened for integrase binding. According to the results, natural products with highest binding affinity to integrase were purchased from ChemBridge for further screening *in vitro*.

3.2.3 Eight compounds from SPECS inhibited HIV-1 integrase nuclear translocation

Using the platform we constructed, 23 compounds from SPECS with high binding affinity to HIV-1 integrase and low toxicity were screened tested on cell based platform. pTRE2hyg-EGFP-IN and pTRE2hyg-EGFP were transfected into HeLa Tet-Off Advanced Cells respectively as we mentioned above. Transfection result was analyzed with IN cell analyzer 1000 (GE Healthcare Life Sciences). Confocal imaging showed that eight compounds (DW-IN4, DW-IN5, DW-IN6, DW-IN9, DW-IN15, DW-IN16, DW-IN17, DW-IN21) were found to block integrase nuclear translocation at 1μM (Figure 3.2).Without compound, EGFP-IN was mainly localized in nucleus (Figure 3.2). Plasmid pTRE2hyg-EGFP was transfected into HeLa Tet-Off Advanced Cells as control. Expression of EGFP was distributed equally in cells. Compounds had no interaction with EGFP cellular distribution at 10 μM (Figure 3.2A). To confirm the result, eight compounds were tested for nuclear translocation inhibition at 1μM, 2μM, 4μM, 8μM. For each concentration, 100 cells were counted

Compound Number	Binding Affinity	LogP
DW-IN1	-14.23	10.3
DW-IN2	-13.7	12.9
DW-IN3	-13.6	12.4
DW-IN4	-13.4	12.1
DW-IN5	-13.4	6.37
DW-IN6	-13	10.3
DW-IN7	-13	8.06
DW-IN8	-12.8	9.83
DW-IN9	-12.8	10.5
DW-IN10	-12.6	7.93
DW-IN11	-12.6	7.29
DW-IN12	-12.5	631.7
DW-IN13	-12.5	10.4
DW-IN14	-12.4	8.27
DW-IN15	-12.3	12.8
DW-IN16	-12.2	8.51
DW-IN17	-12.2	9.14
DW-IN18	-12.1	9.63
DW-IN19	-12.1	7.81
DW-IN20	-12.1	9.28
DW-IN21	-12	9.11
DW-IN22	-12.9	5.72
DW-IN23	-12.8	7.57

Table 3.1 Screening results of molecular docking

For molecular docking, thirty thousand ligands were selected from SPECS bank. A total of 23 compounds with highest binding affinity to integrase resulted from virtual drug screening by Autodock 4.2 were selected for further investigation with our cell based screening platform. All these compounds possess low toxicity and suitable logP The logarithm of the ratio of the concentrations of the un-ionized solute in the solvents is called log *P*; the log P values is also known as a measure of lipophilicity(http://en.wikipedia.org/wiki/Partition_coefficient). Compound with higher logP is more hydrophobic.

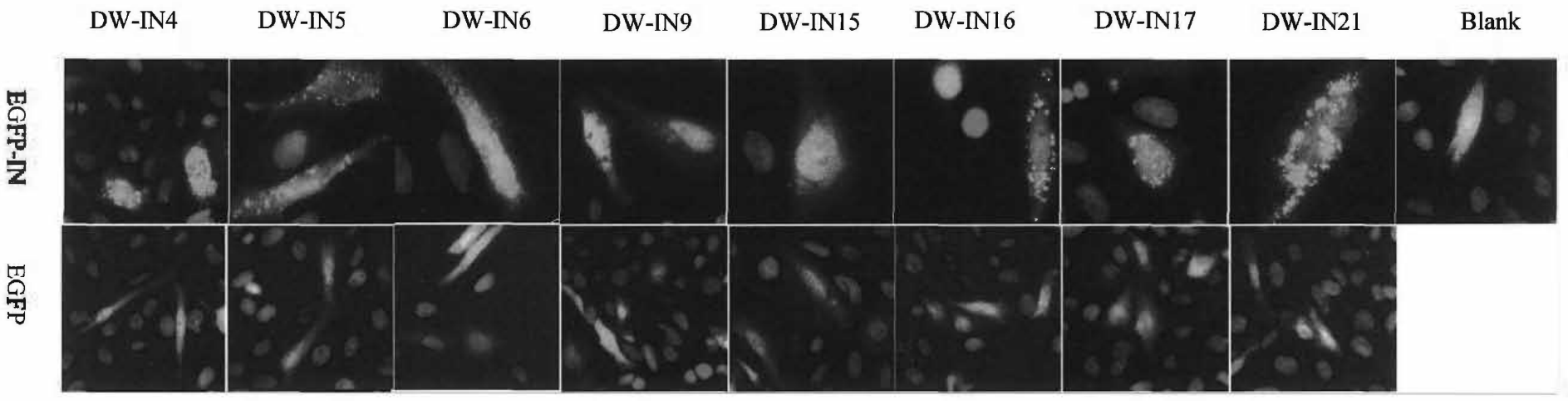

Figure 3.2A DW-IN4, DW-IN5, DW-IN6, DW-IN9, DW-IN15, DW-IN16, DW-IN17 and DW-IN21 from SPECS inhibited HIV-1 integrase nuclear translocation

Tet off Advanced Hela cells were transiently transfected with pTRE2hyg-EGFP-IN and pTRE2hyg-EGFP. Confocal imaging showed that eight compounds (DW-IN4, DW-IN5, DW-IN6, DW-IN9, DW-IN15, DW-IN16, DW-IN17, DW-IN21) were found to block integrase nuclear translocation at 1μM.Without compound, EGFP-IN was mainly localized in nucleus. Expression of EGFP was distributed equally in cells. Compounds had no interaction with EGFP cellular distribution at 10 μM.

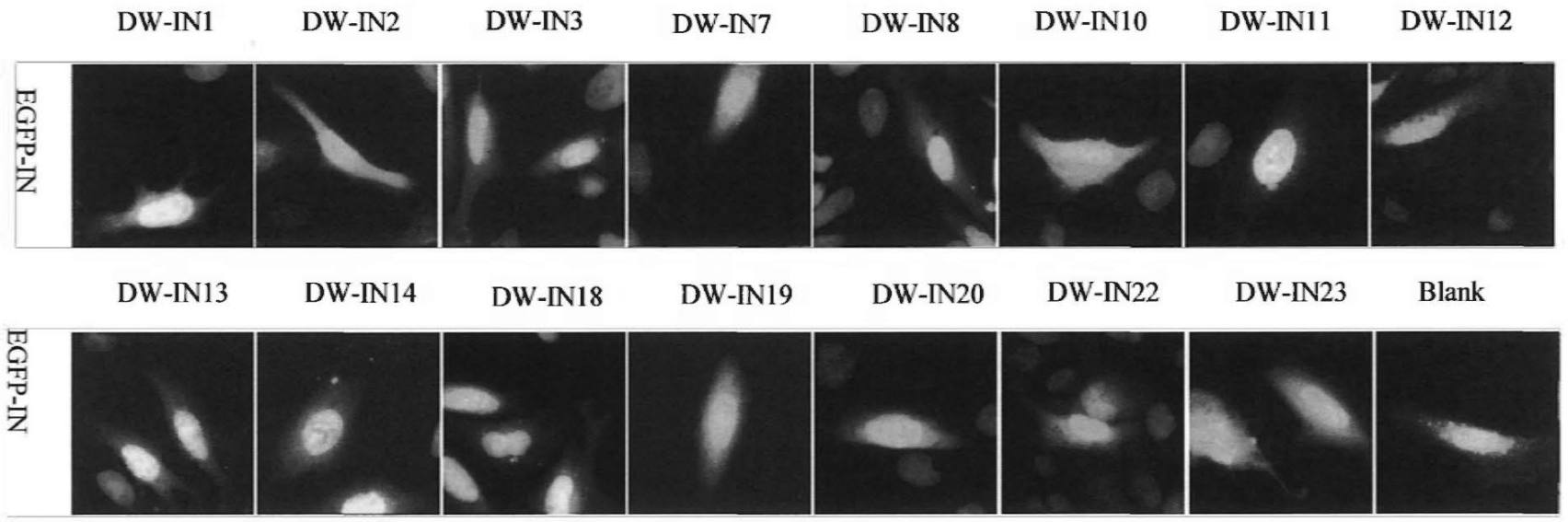

Figure 3.2B Fifteen compounds from SPECS failed to inhibit HIV-1 integrase nuclear translocation

Tet off Advanced Hela cells were transiently transfected with pTRE2hyg-EGFP-IN. Confocal imaging showed that fifteen compounds (DW-IN1, DW-IN2, DW-IN3, DW-IN7, DW-IN8, DW-IN10, DW-IN11, DW-IN12, DW-IN13, DW-IN14, DW-IN18, DW-IN19, DW-IN20 DW-IN22, DW-IN23) failed to block integrase nuclear translocation at 25μM.

for statistical analysis. Result showed that these compounds inhibited integrase nuclear translocation at a dose dependent manner (Table 3.2). Also, another fifteen compounds from SPECS failed to inhibit integrase nuclear translocation at 25μM (DW-IN1, DW-IN2, DW-IN3, DW-IN7, DW-IN8, DW-IN10, DW-IN11, DW-IN12, DW-IN13, DW-IN14, DW-IN18, DW-IN19, DW-IN20 DW-IN22, DW-IN23) (Figure 3.2B).

The interaction between these compounds with IN CCD was analyzed with molecular docking. D77 was used as control compound in molecular docking analysis(Du et al., 2008). D77 was docked into the hydrophobic pocket formed by surrounding residues of IN CCD (Figure 3.3 A). O20 of D77 formed a H-bond with OG1 of Thr125(B) with a distance of 2.90 Å. O35 of D77 formed two H-bonds with NH1 and C of Arg166(A) with distance of 2.93 Å and 3.10 Å respectively. Besides, D77 formed hydrophobic contacts with Ala129 (B), Leu102 (B), Met178 (A), Glu170 (A) and Asp167 (A) respectively (Figure 3.3 B).

DW-IN4 was docked into the hydrophobic pocket formed by surrounding residues of IN CCD (Figure 3.4 A). DW-IN4 formed hydrophobic contacts with Thr124 (B), Thr125 (B), Ala128 (B), Trp132 (B), Trp131 (B), Thr174 (A) and Gln168 (A) respectively (Figure 3.4 B).

DW-IN5 was docked into the hydrophobic pocket formed by surrounding residues of IN CCD. The hydrophobic pocket was formed by residues Gln168, Ala169, Glu 170, His171, Thr174 and Met178 in chain A and Trp132, Trp 131, Ala128, Ala129, Thr125, Leu102, Ala98 and Gln95 in Chain B (Figure 3.5).

DW-IN6 was docked into the hydrophobic pocket formed by surrounding residues of IN CCD (Figure 3.6 A). N31 of DW-IN6 formed a H-bond with N of Gln170 (A) with a distance of 3.51 Å. Besides, DW-IN6 formed hydrophobic contacts with Gln168 (A), His171 (A), Ala169 (A), Thr174 (A), Gln95 (B), Ala128 (B) and Trp131 (B) respectively (Figure 3.6 B).

DW-IN9 was docked into the hydrophobic pocket formed by surrounding residues of IN CCD (Figure 3.7 A). DW-IN9 formed hydrophobic contacts with Trp131 (B),

	1μM	2μM	4μM	8μM
DW-IN4	**52.43**	**53.41**	**60.98**	**65.63**
DW-IN5	**47.83**	**54.39**	**64.52**	**68.29**
DW-IN6	**56.36**	**59.21**	**59.26**	**67.24**
DW-IN9	**49.35**	**58.24**	**58.97**	**58.97**
DW-IN15	**45.45**	**47.06**	**65.38**	**68.62**
DW-IN16	**48.17**	**57.64**	**58.81**	**64.72**
DW-IN17	**49.25**	**58.11**	**56.82**	**67.86**
DW-IN21	**53.33**	**64**	**48.65**	**70.21**
DMSO	**25**	**34**	**19.74**	**19.69**

Table 3.2 DW-IN4, DW-IN5, DW-IN6, DW-IN9, DW-IN15, DW-IN16, DW-IN17, DW-IN21 inhibited *HIV*-1 integrase nuclear translocation in dose-dependent manner.

Eight compounds were tested for nuclear translocation inhibition at 1μM, 2μM, 4μM, 8μM. For each concentration, 100 cells were counted for statistical analysis. Result showed that these compounds inhibited integrase nuclear translocation at a dose dependent manner. The data is presented as % cells with nuclear translocation inhibition.

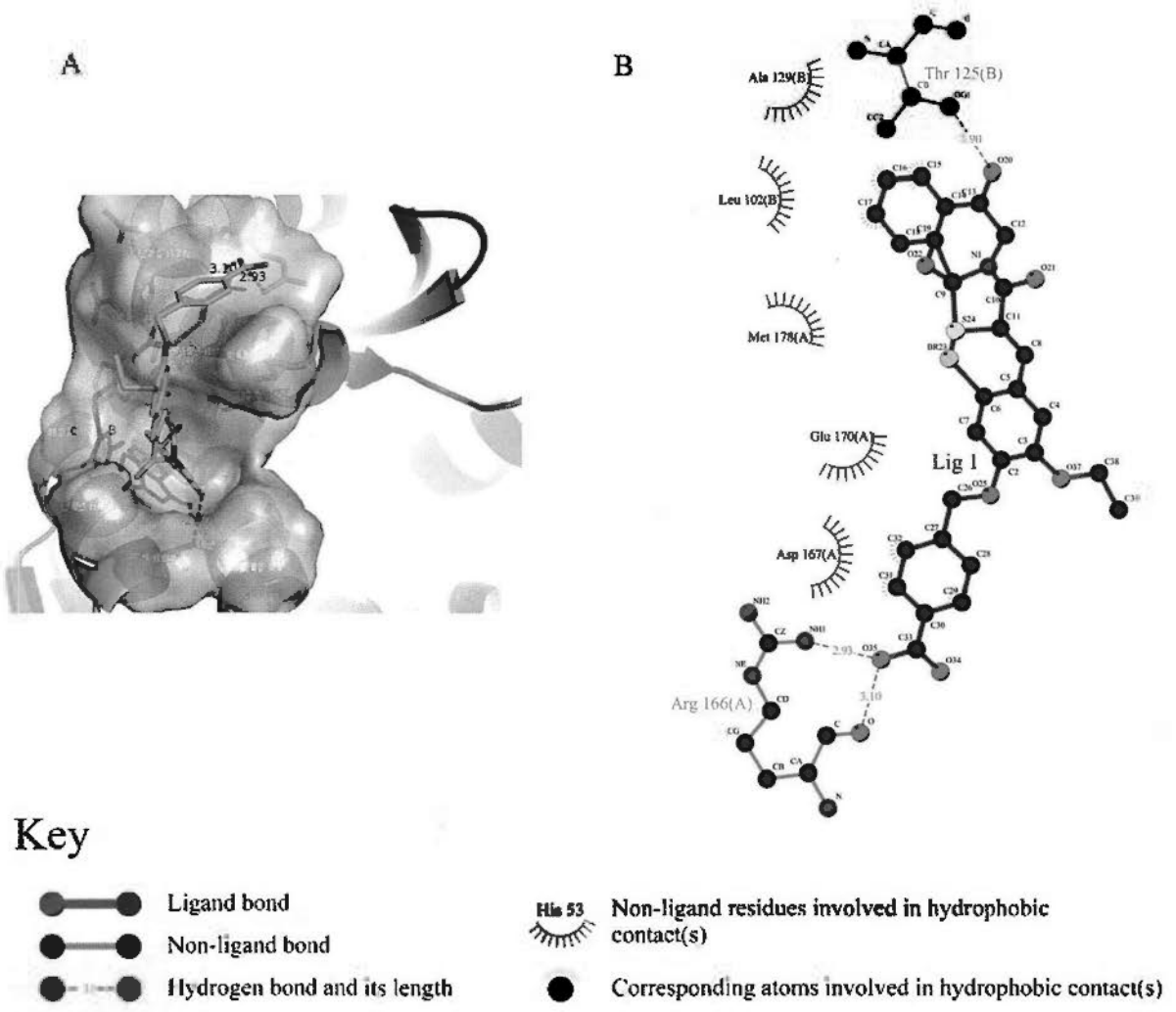

Figure 3.3 Interaction between D77 and IN CCD

A) The D77 was shown as sticks. The secondary structure of IN CCD was shown as cartoon. The H-bond was shown as red with distance label. D77 was docked into the hydrophobic pocket formed by surrounding residues of IN CCD.
B) O20 of D77 formed a H-bond with OG1 of Thr125(B) with a distance of 2.90 Å. O35 of D77 formed two H-bonds with NH1 and C of Arg166(A) with distance of 2.93 Å and 3.10 Å respectively. Besides, D77 formed hydrophobic contacts with Ala129 (B), Leu102 (B), Met178 (A), Glu170 (A) and Asp167 (A) respectively.

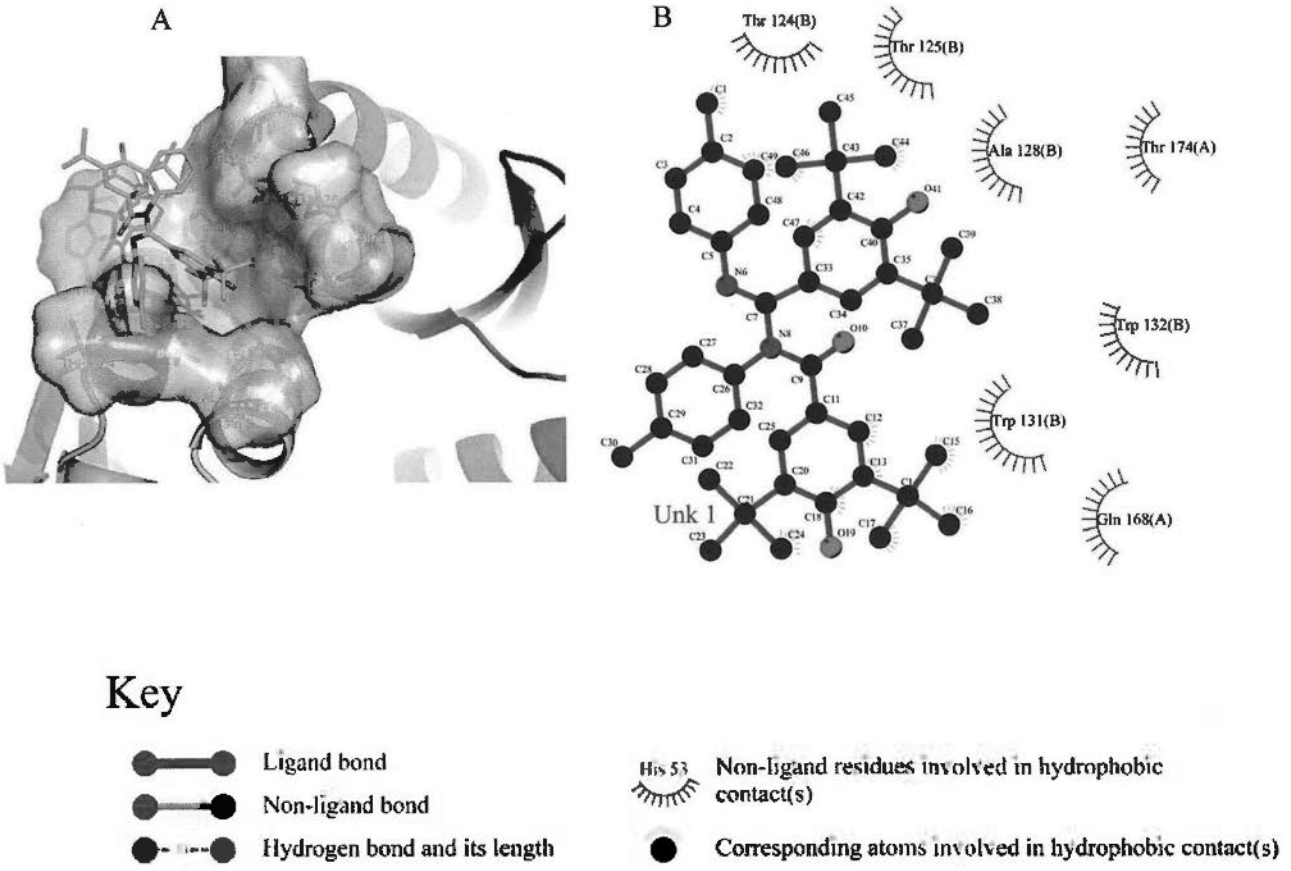

Figure 3.4 Interaction between DW-IN4 and IN CCD

A) The DW-IN4 was shown as sticks. The secondary structure of IN CCD was shown as cartoon. DW-IN4 was docked into the hydrophobic pocket formed by surrounding residues of IN CCD.
B) DW-IN4 formed hydrophobic contacts with Thr124 (B), Thr125 (B), Ala128 (B), Trp132 (B), Trp131 (B), Thr174 (A) and Gln168 (A) respectively.

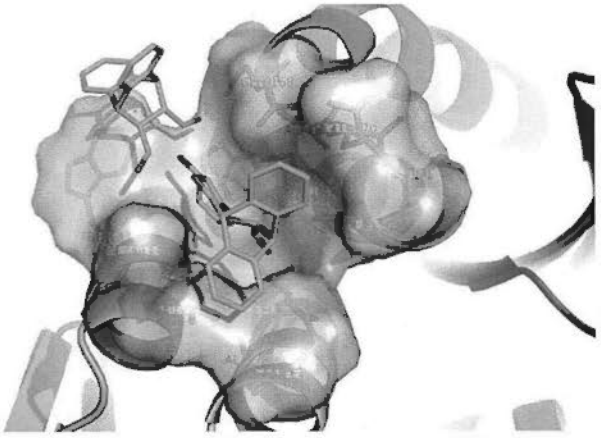

Figure 3.5 Interaction between DW-IN5 and IN CCD

A) The DW-IN5 was shown as sticks. The secondary structure of IN CCD was shown as cartoon. DW-IN5 was docked into the hydrophobic pocket formed by surrounding residues of IN CCD. The hydrophobic pocket was formed by residues Gln168, Ala169, Glu 170, His171, Thr174 and Met178 in chain A and Trp132, Trp 131, Ala128, Ala129, Thr125, Leu102, Ala98 and Gln95 in Chain B.

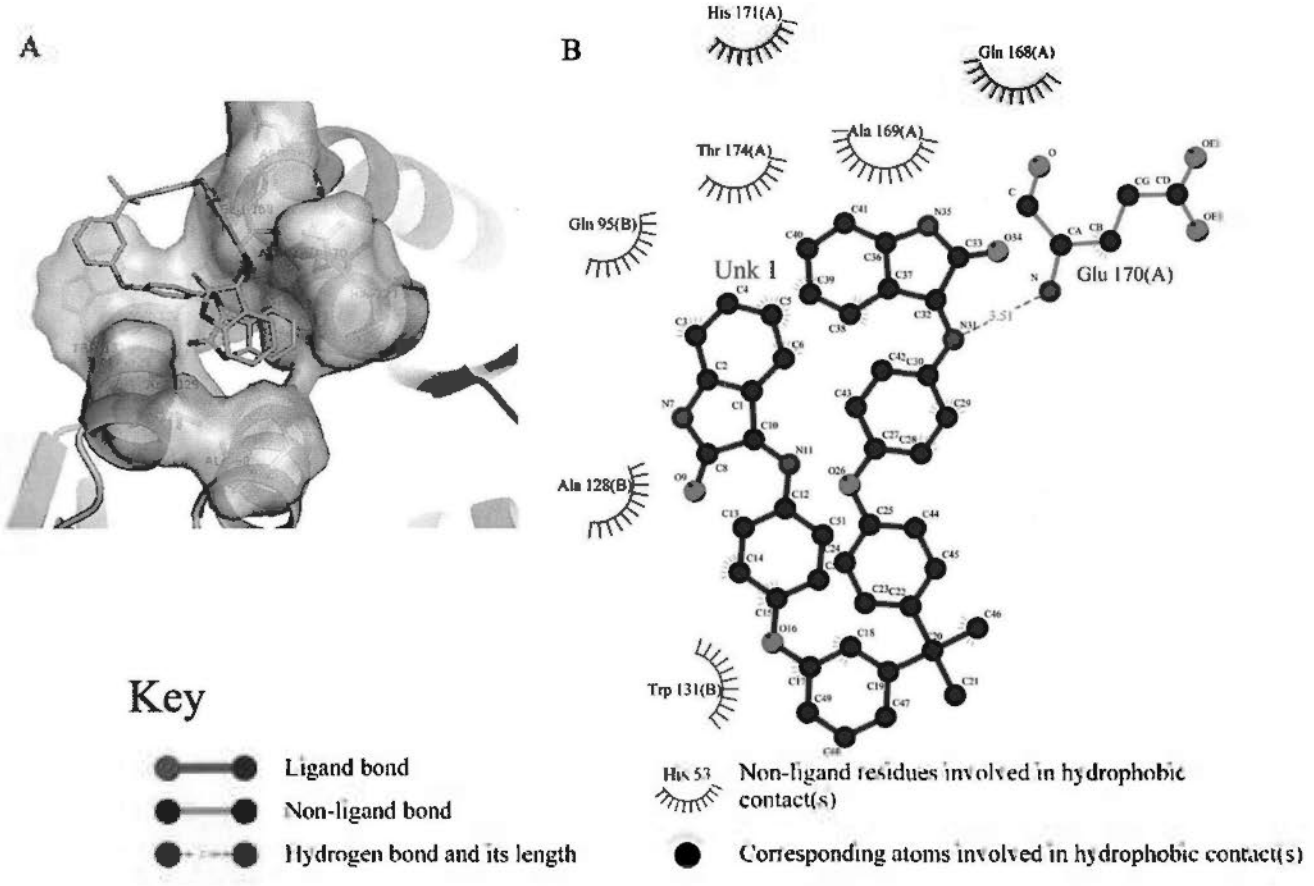

Figure 3.6 Interaction between DW-IN6 and IN CCD

A) The DW-IN6 was shown as sticks. The secondary structure of IN CCD was shown as cartoon. DW-IN6 was docked into the hydrophobic pocket formed by surrounding residues of IN CCD.
B) N31 of DW-IN6 formed a H-bond with N of Gln170 (A) with a distance of 3.51 Å. Besides, DW-IN6 formed hydrophobic contacts with Gln168 (A), His171 (A), Ala169 (A), Thr174 (A), Gln95 (B), Ala128 (B) and Trp131 (B) respectively.

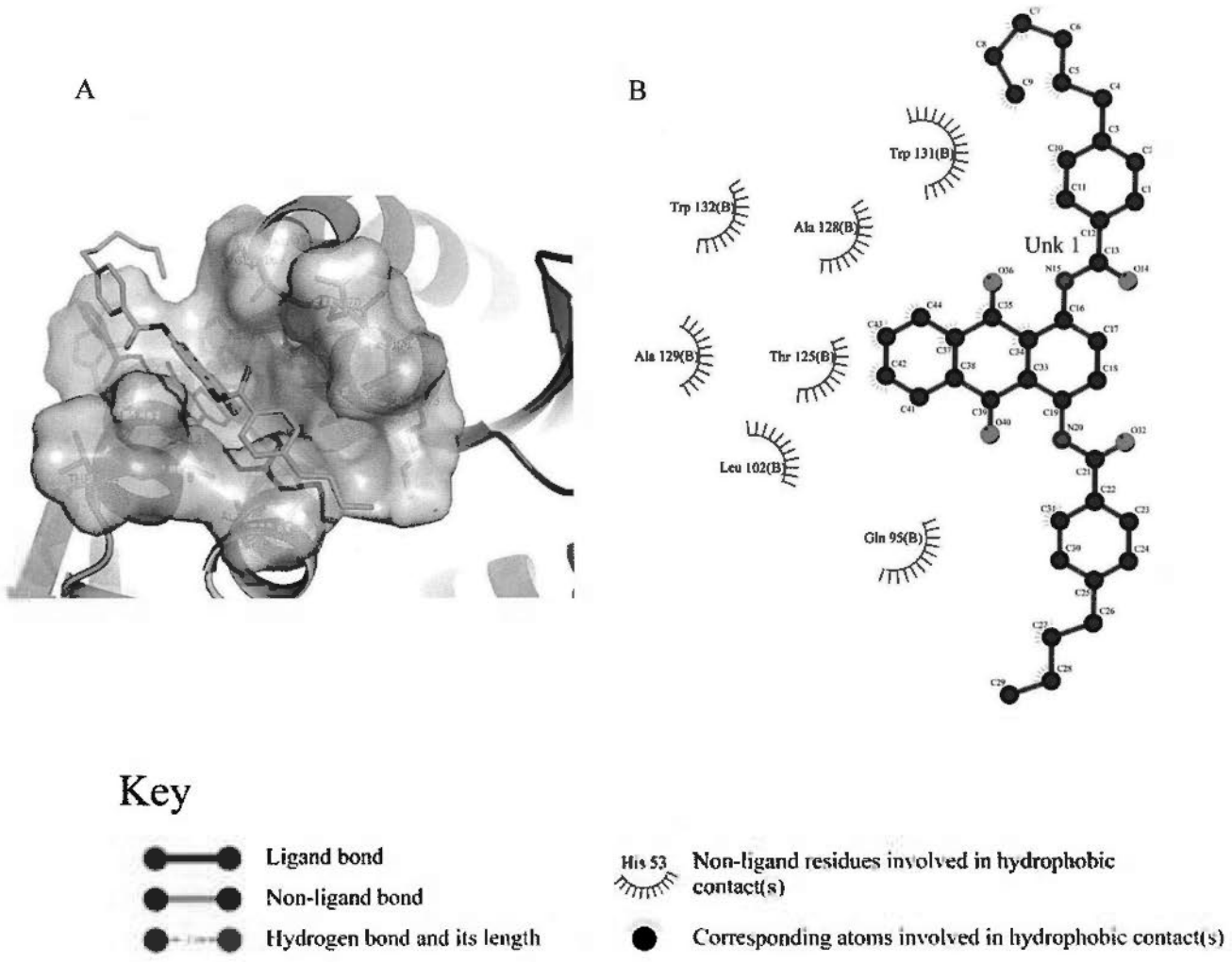

Figure 3.7 Interaction between DW-IN9 and IN CCD

A) The DW-IN9 was shown as sticks. The secondary structure of IN CCD was shown as cartoon. DW-IN9 was docked into the hydrophobic pocket formed by surrounding residues of IN CCD.
B) DW-IN9 formed hydrophobic contacts with Trp131 (B), Ala128 (B), Trp132 (B), Ala129 (B), Thr125 (B), Leu102 (B) and Gln95 (B) respectively.

Ala128 (B), Trp132 (B), Ala129 (B), Thr125 (B), Leu102 (B) and Gln95 (B) respectively (Figure 3.7 B).

DW-IN15 was docked into the hydrophobic pocket formed by surrounding residues of IN CCD (Figure 3.8 A). DW-IN15 formed hydrophobic contacts with Gln168 (A), Glu170 (A), His171 (A), Trp131 (B), Thr125 (B) and Gln95 (B) respectively (Figure 3.8 B).

DW-IN16 was docked into the hydrophobic pocket formed by surrounding residues of IN CCD (Figure 3.9 A). DW-IN16 formed hydrophobic contacts with Gln168 (A), Thr174 (A), Trp131 (B), Ala128 (B), Thr125 (B) and Gln95 (B) respectively (Figure 3.9 B).

DW-IN17 was docked into the hydrophobic pocket formed by surrounding residues of IN CCD (Figure 3.10 A). O12 of DW-IN17 formed a H-bond with O of Asp167 (A) with a distance of 2.75 Å. Besides, DW-IN17 formed hydrophobic contacts with Glu170 (A), His171 (A), Thr174 (A), Leu102 (B), Ala98 (B), Ala128 (B) and Trp131 (B) respectively (Figure 3.10 B).

DW-IN21 was docked into the hydrophobic pocket formed by surrounding residues of IN CCD (Figure 3.11 A). N16 of DW-IN21 formed a H-bond with O of Gln168 (A) with a distance of 3.08 Å. O26 of DW-IN21 formed H-bond with OE1 Gln95 (B) with distance of 2.51 Å. Besides, DW-IN21 formed hydrophobic contacts with Thr174 (A), Thr125 (B), Ala128 (B), Trp131 (B) respectively (Figure 3.11 B).

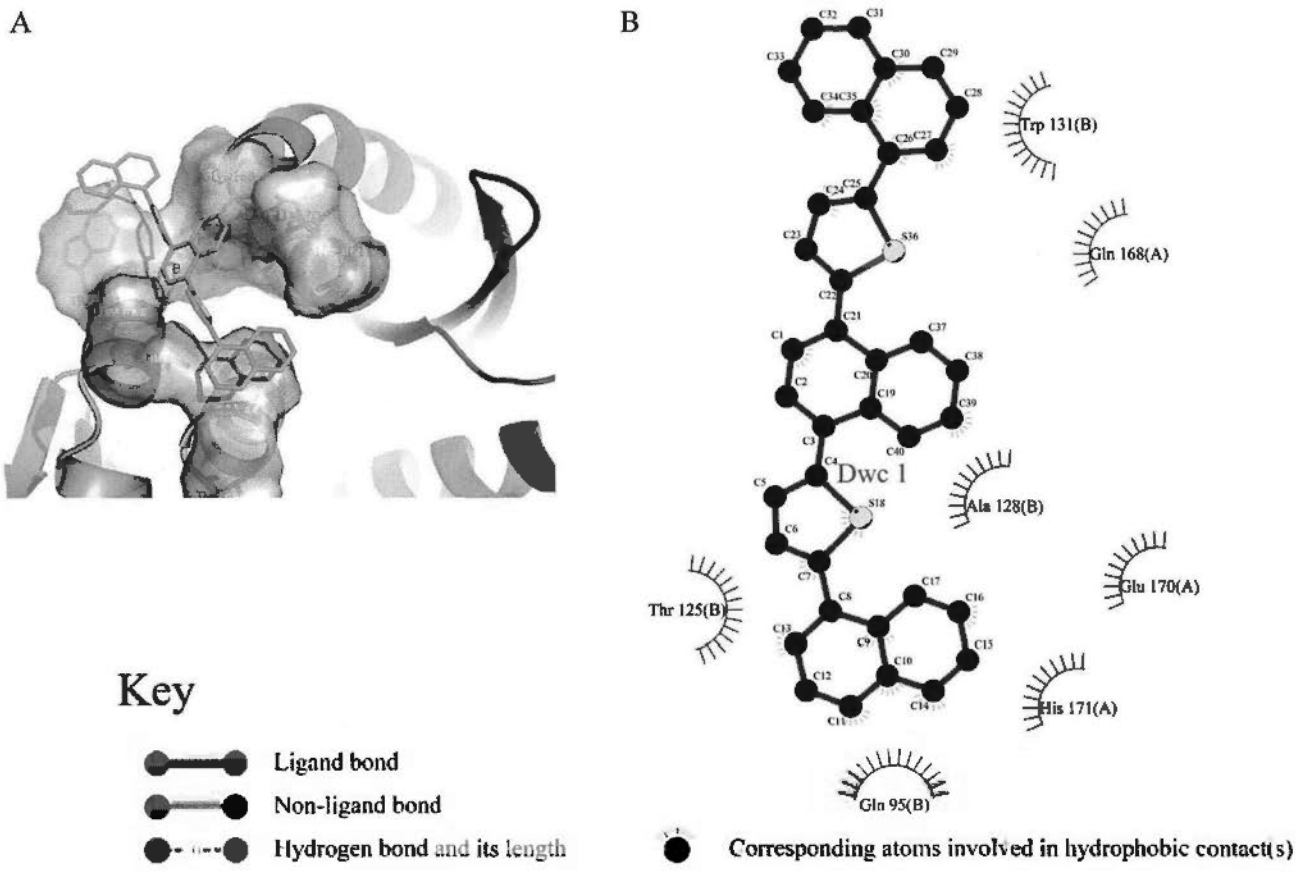

Figure 3.8 Interaction between DW-IN15 and IN CCD

A) The DW-IN15 was shown as sticks. The secondary structure of IN CCD was shown as cartoon. DW-IN15 was docked into the hydrophobic pocket formed by surrounding residues of IN CCD.
B) DW-IN15 formed hydrophobic contacts with Gln168 (A), Glu170 (A), His171 (A), Trp131 (B), Thr125 (B) and Gln95 (B) respectively.

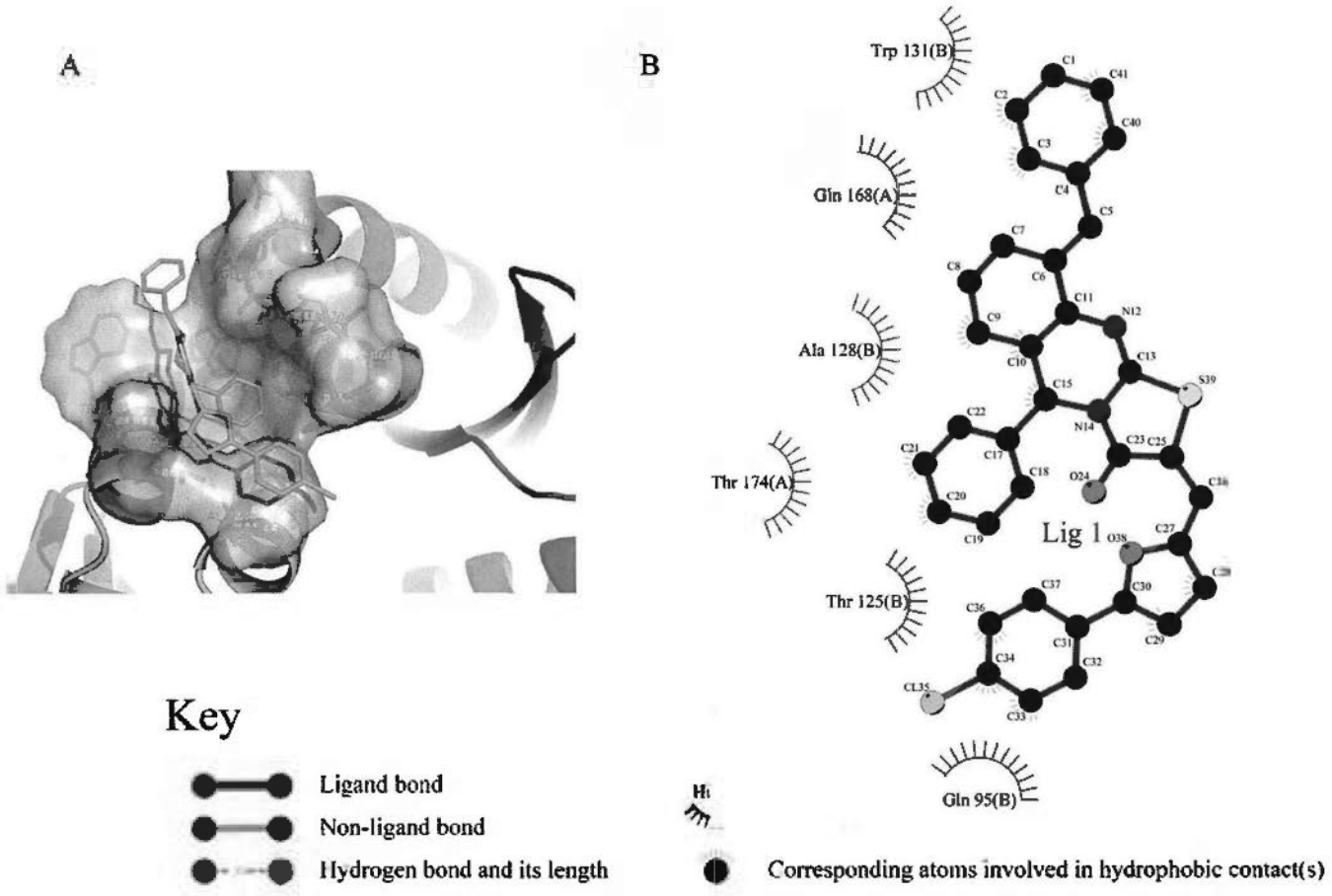

Figure 3.9 Interaction between DW-IN16 and IN CCD

A) The DW-IN16 was shown as sticks. The secondary structure of IN CCD was shown as cartoon. DW-IN16 was docked into the hydrophobic pocket formed by surrounding residues of IN CCD.
B) DW-IN16 formed hydrophobic contacts with Gln168 (A), Thr174 (A), Trp131 (B), Ala128 (B), Thr125 (B) and Gln95 (B) respectively.

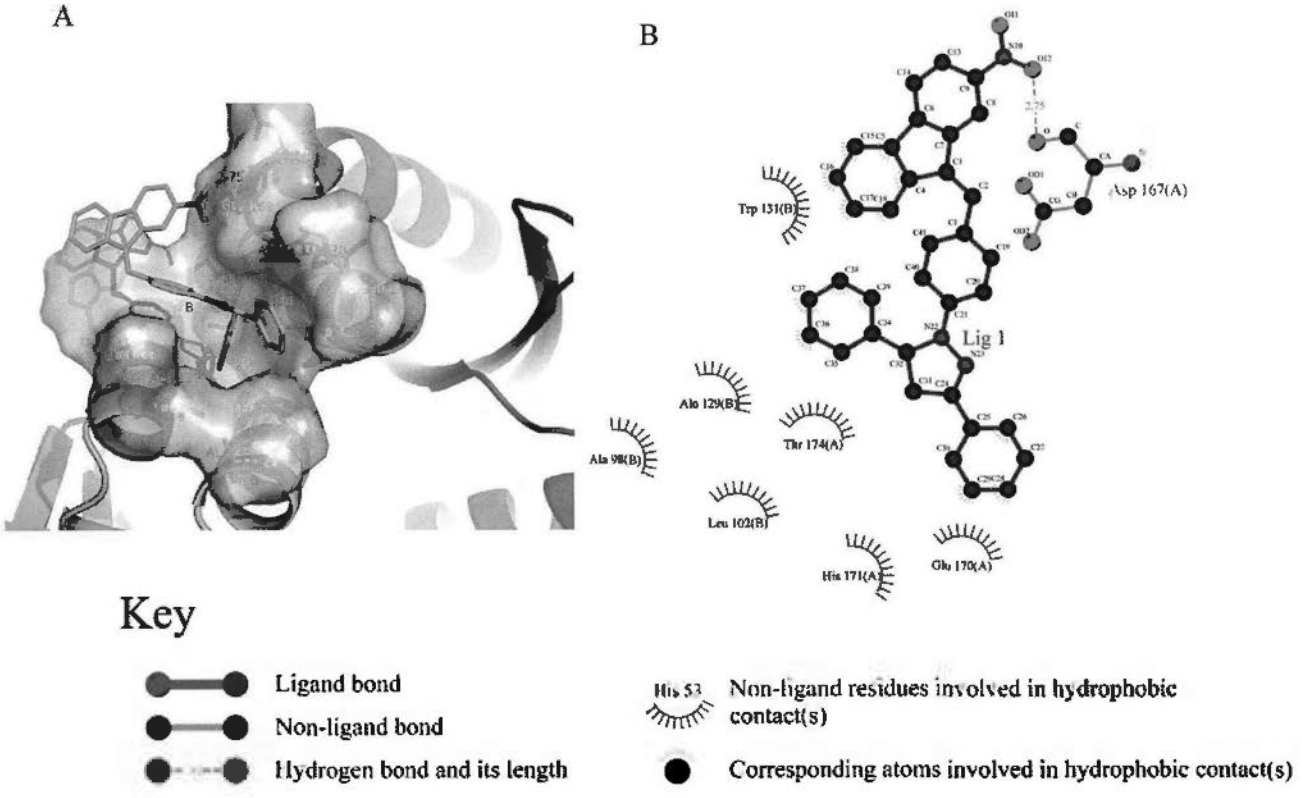

Figure 3.10 Interaction between DW-IN17 and IN CCD

A) The DW-IN17 was shown as sticks. The secondary structure of IN CCD was shown as cartoon. The H-bond was shown as red with distance label. DW-IN17 was docked into the hydrophobic pocket formed by surrounding residues of IN CCD.
B) O12 of DW-IN17 formed a H-bond with O of Asp167 (A) with a distance of 2.75 Å. Besides, DW-IN17 formed hydrophobic contacts with Glu170 (A), His171 (A), Thr174 (A), Leu102 (B), Ala98 (B), Ala128 (B) and Trp131 (B) respectively.

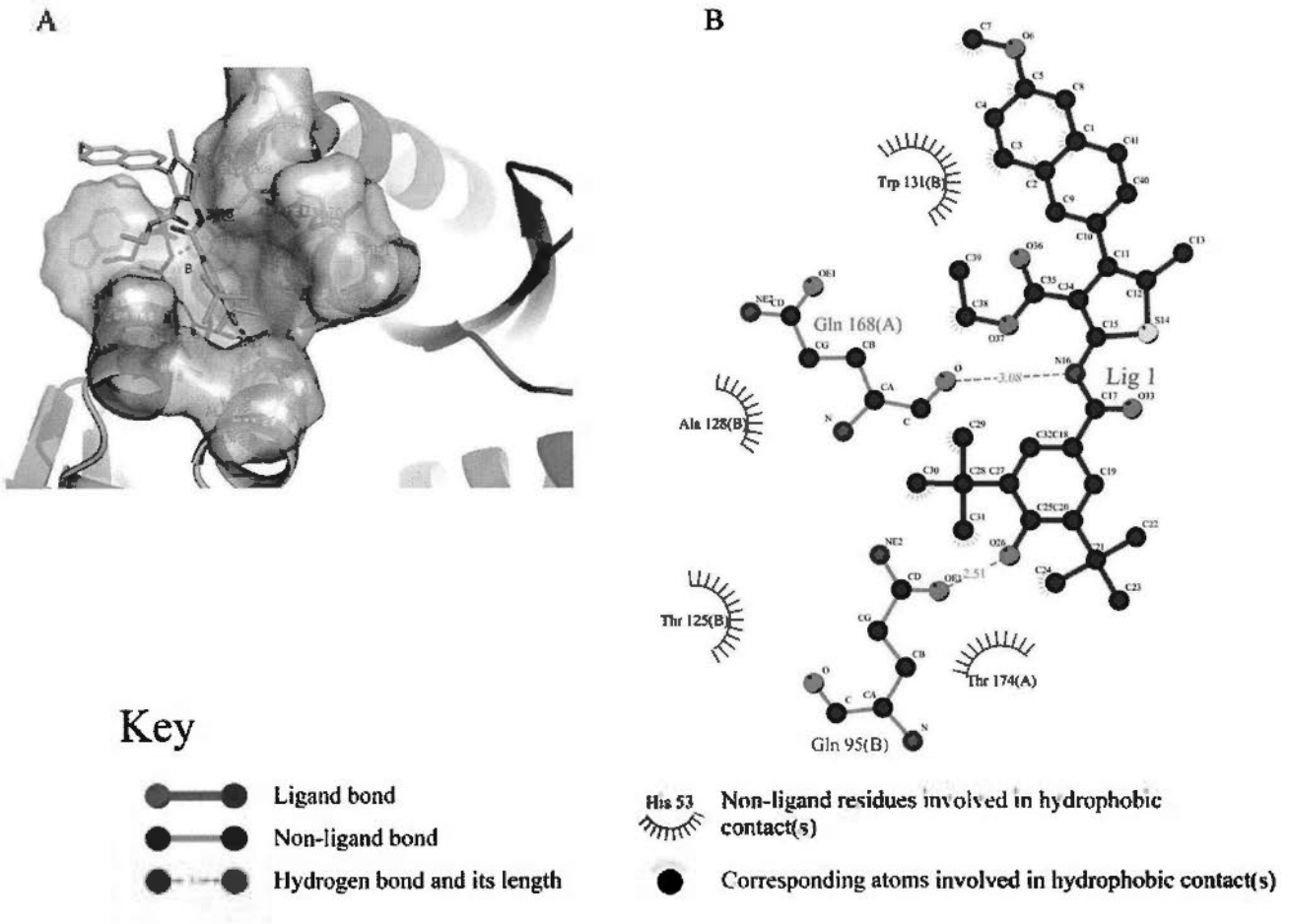

Figure 3.11 Interaction between DW-IN21 and IN CCD

A) The DW-IN21 was shown as sticks. The secondary structure of IN CCD was shown as cartoon. The H-bond was shown as red with distance label. DW-IN21 was docked into the hydrophobic pocket formed by surrounding residues of IN CCD.
B) N16 of DW-IN21 formed a H-bond with O of Gln168 (A) with a distance of 3.08 Å. O26 of DW-IN21 formed H-bond with OE1 Gln95 (B) with distance of 2.51 Å. Besides, DW-IN21 formed hydrophobic contacts with Thr174 (A), Thr125 (B), Ala128 (B), Trp131 (B) respectively.

3.2.4 Immunofluorescence

To confirm that eight compounds (DW-IN4, DW-IN5, DW-IN6, DW-IN9, DW-IN15, DW-IN16, DW-IN17, DW-IN21) blocked integrase nuclear translocation and had no interaction with EGFP, HIV-1 integrase was cloned into pcDNA6/V5-HisA (Invitrogen). Eight compounds were added at 10 μM 5 hours after transfection of pcDNA6/V5-HisA-IN into Hela cells. Immunofluorescence imaging showed that Integrase nuclear translocation was inhibited by these ompounds (Figure 3.12). Without treatment of DW-IN compounds, integrase was mainly localized in nucleus (Figure 3.12).

3.2.5 Natural product DW-IN719 inhibited HIV-1 integrase nuclear translocation

According to the docking result, three natural products with high binding affinity to HIV-1 integrase and low toxicity from ZINC were selected for further test on cell based screening platform. pTRE2hyg-EGFP-IN was transfected into HeLa Tet-Off Advanced Cells respectively as we mentioned above. Transfection result was analyzed with Leica SP5 confocal microscopy. Confocal imaging showed that DW-IN719 (Binding affinity: -8.2, LogP: 2.62) was found to block integrase nuclear translocation at 1μM (Figure 3.13).Without compound, EGFP-IN was mainly localized in nucleus (Figure 3.13).

Docking mode of DW-IN719 with integrase was showed as Figure 2.14. DW-IN719 was docked into the hydrophobic pocket formed by surrounding residues of IN CCD. Besides the H-bonds to be mentioned in Figure 2.14B, DW-IN719 formed two additional H-bonds with Thr125 (B) with a distance of 3.08 Å and Glu170 (A) with a distance of 3.09 Å (Figure 3.14A). O24 of DW-IN719 formed two H-bonds with OG1 of Thr174 (A) with a distance of 3.05 Å and N of His171 (A) with a distance of 2.94 Å. O27 of DW-IN719 formed two H-bonds with NE2 and OE1 of Gln95 (B) with distance of 3.24 Å and 2.92 Å respectively. Besides, DW-IN719 formed hydrophobic contacts with Gln168 (A), Ala128 (B), Trp131 (B), Ala129 (B) respectively (Figure 3.14B).

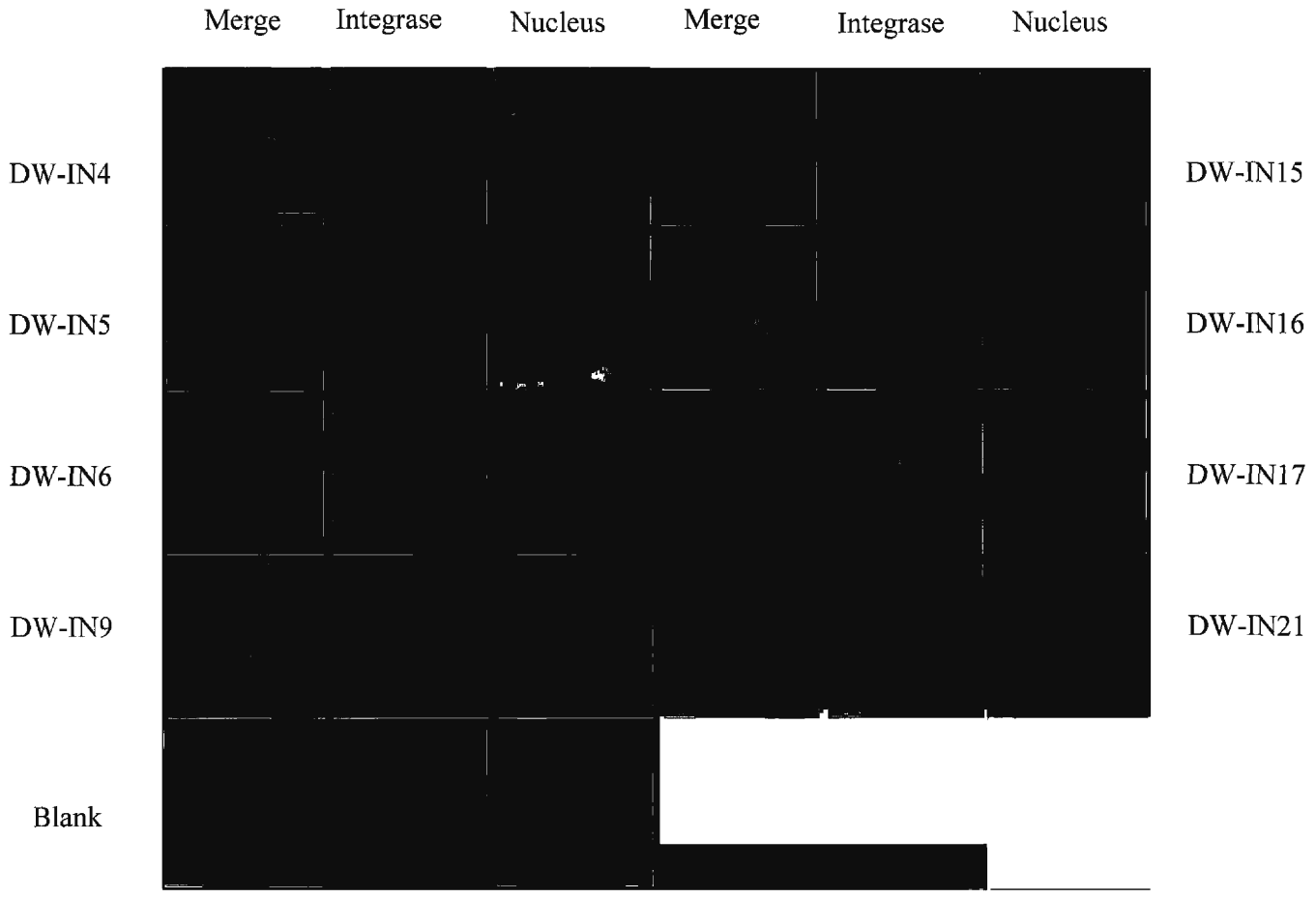

Figure 3.12 Immunofluorescence showed that DW-IN4, DW-IN5, DW-IN6, DW-IN9, DW-IN15, DW-IN16, DW-IN17 and DW-IN21 inhibited HIV-1 integrase nuclear translocation

HIV-1 integrase was cloned into pcDNA6/V5-HisA. pcDNA6/V5-HisA-IN was transfected into Hela cells, eight compounds were added at 10μM 5 hours after transfection of pcDNA6/V5-HisA-IN into Hela cells. Immunofluorescence imaging showed that Integrase nuclear translocation was inhibited by these compounds. Without treatment of DW-IN compounds, integrase was mainly localized in nucleus. Scale bar 25μm.

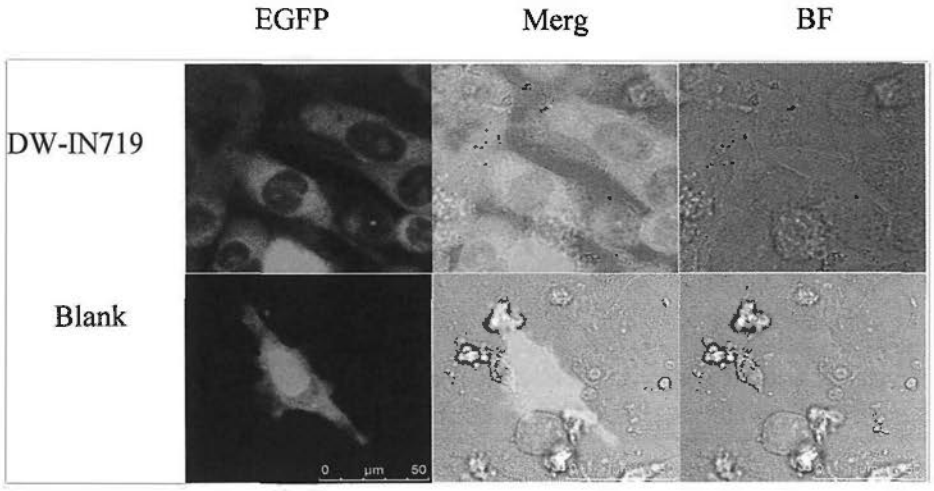

Figure 3.13 Natural product DW-IN719 inhibited integrase nuclear translocation

pTRE2hyg-EGFP-IN was transfected into HeLa Tet-Off Advanced Cells. Transfection result was analyzed with Leica SP5 confocal microscopy. Confocal imaging showed that DW-IN719 were found to block integrase nuclear translocation at 1µM.Without compound, EGFP-IN was mainly localized in nucleus Scale bar 50µm.

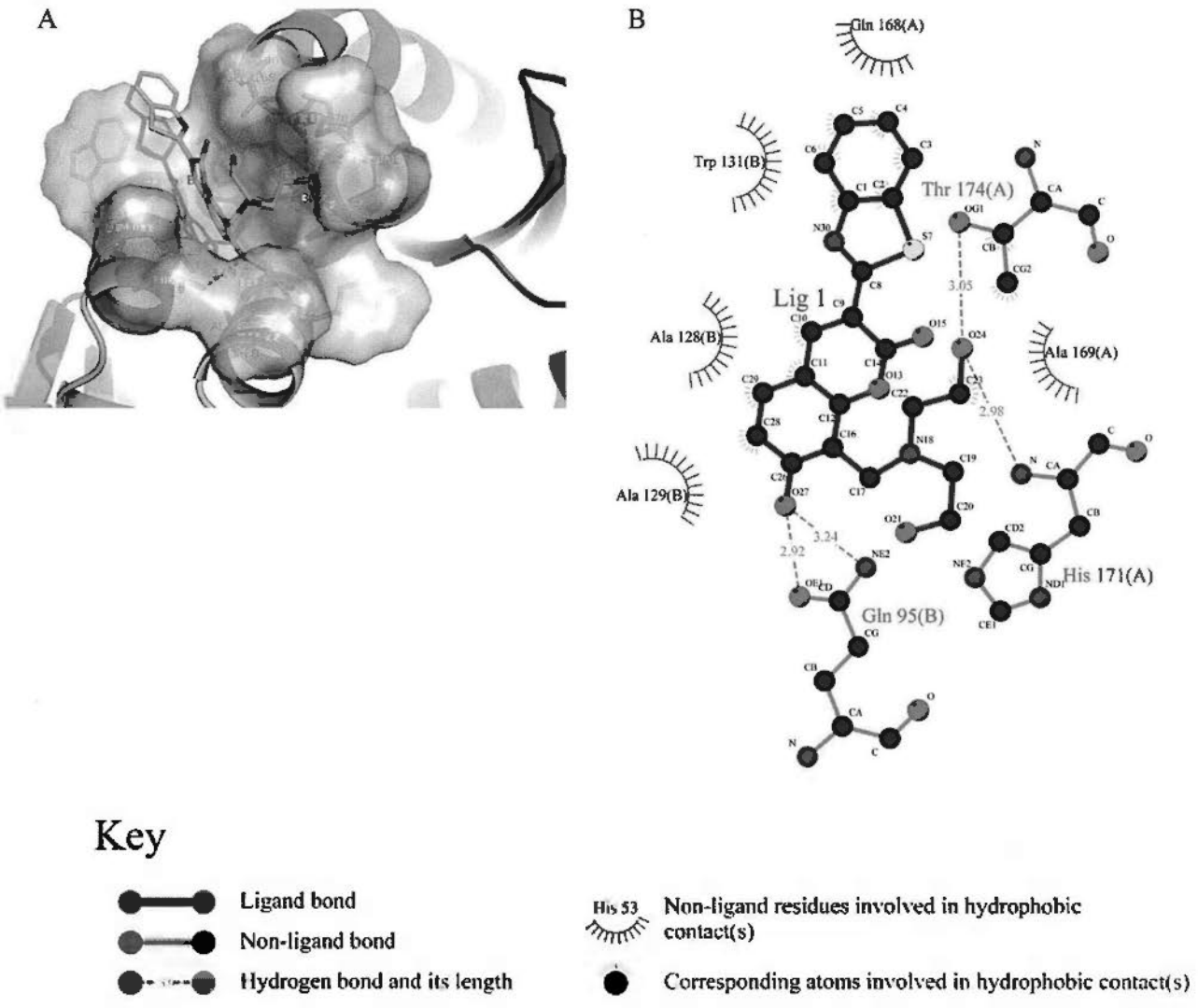

Figure 3.14 Interaction between DW-IN719 and IN CCD

A) The DW-IN719 was shown as sticks. The secondary structure of IN CCD was shown as cartoon. The H-bond was shown as red with distance label. Dw-in719 was docked into the hydrophobic pocket formed by surrounding residues of IN CCD. Besides the H-bonds to be mentioned in B), DW-IN719 formed two additional H-bonds with Thr125 (B) with a distance of 3.08 Å and Glu170 (A) with a distance of 3.09 Å.

B) O24 of DW-IN719 formed two H-bonds with OG1 of Thr174 (A) with a distance of 3.05 Å and N of His171 (A) with a distance of 2.94 Å. O27 of DW-IN719 formed two H-bonds with NE2 and OE1 of Gln95 (B) with distance of 3.24 Å and 2.92 Å respectively. Besides, DW-IN719 formed hydrophobic contacts with Gln168 (A), Ala128 (B), Trp131 (B), Ala129 (B) respectively.

3.2.6 DW-IN6 showed significant reduction of cytopathic effect (CPE)

Eight compounds (DW-IN4, DW-IN5, DW-IN6, DW-IN9, DW-IN15, DW-IN16, DW-IN17, DW-IN21) blocked integrase nuclear translocation in Fluorescence imaging experiment. To further examine the compounds' effect on HIV-1 inhibition, syncytia assay were conducted to test the reduction on cytopathic effect of these compounds. Results showed that DW-IN6 significantly reduced the cytopathic effect caused by HIV-1 infection with an EC_{50} of 3.47μM (Figure 3.15). DW-IN5 had an EC_{50} of 9.37μM while other six compounds had an EC_{50} that were larger than 10μM.

3.2.7 DW-IN6 and DW-IN719 showed significant inhibition on P24 production in acute infection

One natural product DW-IN719 and eight compounds (DW-IN4, DW-IN5, DW-IN6, DW-IN9, DW-IN15, DW-IN16, DW-IN17, DW-IN21) blocked integrase nuclear translocation in Fluorescence imaging experiment. To further assay the compounds' effect on HIV-1 replication, P24 production reduction in acute infection assay were conducted. Results showed that DW-IN6 and DW-IN719 showed significant inhibition on P24 production in acute infection of $HIV\text{-}1_{IIIB}$ with EC_{50} of 4.96μM and 4.33μM (Figure 2.16) respectively. Other seven compounds had no significant effect on P24 production inhibition in $HIV\text{-}1_{IIIB}$ acute infection (Figure 3.16).

3.2.8 MTT-based cytotoxicity assay

Cellular toxicity of natural product DW-IN719 and eight compounds (DW-IN4, DW-IN5, DW-IN6, DW-IN9, DW-IN15, DW-IN16, DW-IN17, DW-IN21) were assessed by MTT method. Results showed that most compounds had CC_{50} of around or more than 10μM (Figure 3.17).

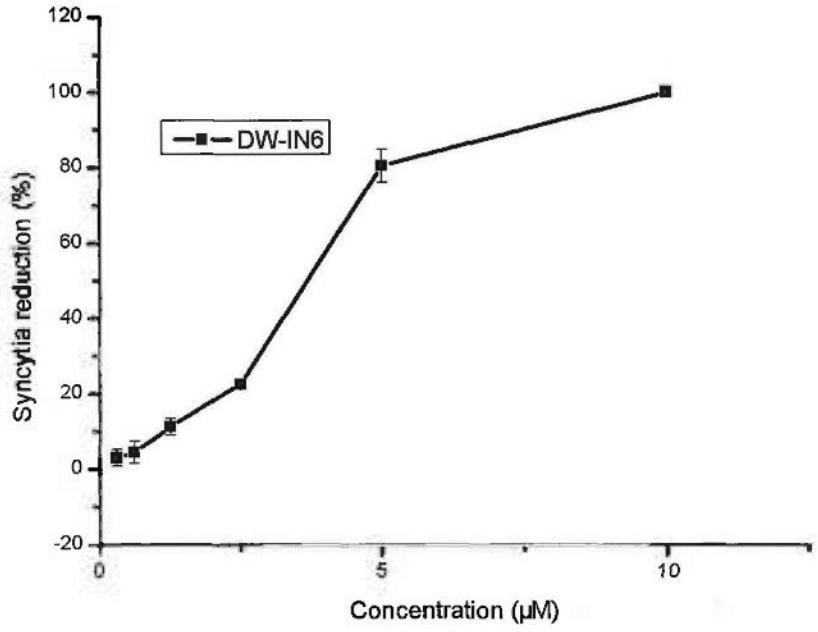

Figure 3.15 DW-IN6 showed inhibition on cytopathic effect in C8166 cells infected by HIV-1_{IIIB}

Compounds were added to cell culture with infection at a 5-fold serial dilution from the beginning of 10μM. AZT was used as positive control. Results demonstrated that DW-IN6 had significant effect on cytopathic effect reduction in C8166 cells infected by HIV-1IIIB with EC50 of 3.47μM. DW-IN5 had an EC_{50} of 9.37μM while other six compounds had an EC_{50} that were bigger than 10μM. EC50 of AZT was 1.65ng/ml. Data are shown as one test of three repeats.

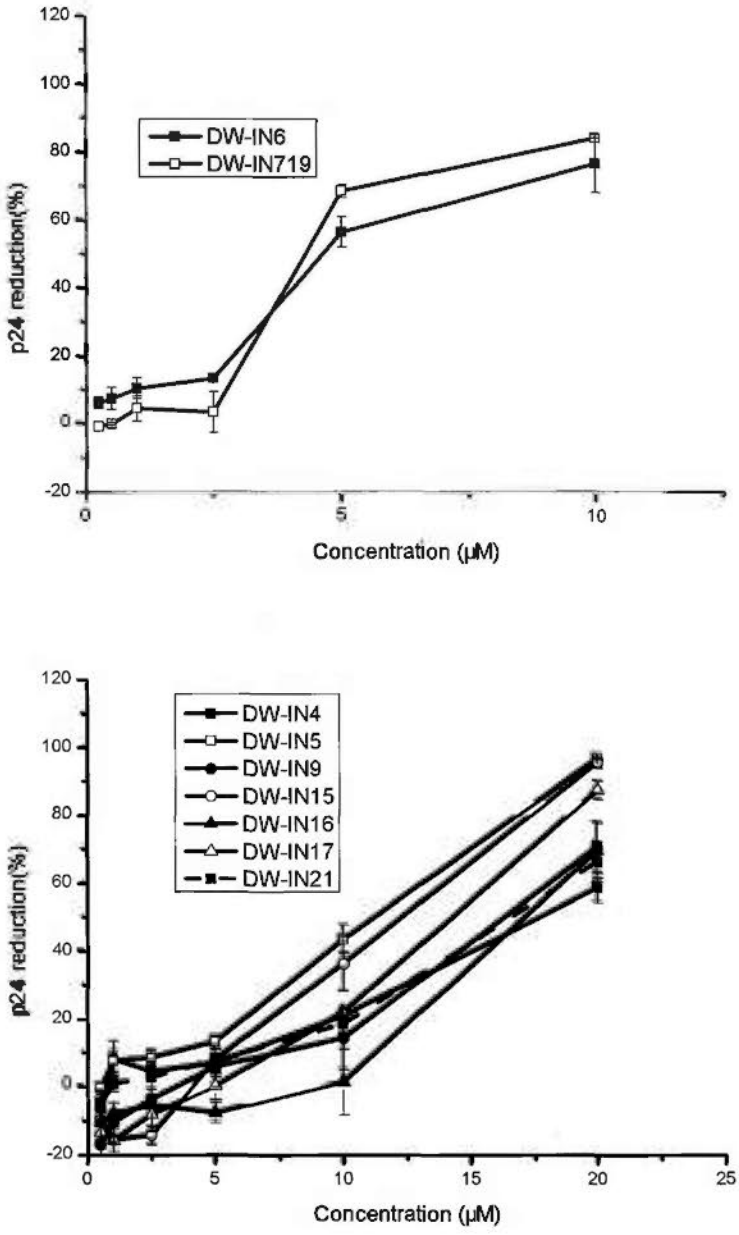

Figure 3.16 DW-IN4, DW-IN5, DW-IN6, DW-IN9, DW-IN15, DW-IN16, DW-IN17, DW-IN21 and DW-IN719 showed P24 production inhibition in acute infection

Compounds were added to cell culture with infection at a 2-fold serial dilution from the beginning of 10μM. Results showed that DW-IN719 and DW-IN6 dramatically reduced P24 production in HIV-1_{IIIB} acute infected C8166 cells with EC_{50} value of 4.33μM and 4.96μM respectively. EC50 of AZT was 1.47ng/ml. Other compounds had EC50 of 17.09μM (DW-IN4), 11.60μM (DW-IN5), 15.53μM (DW-IN9), 11.75μM (DW-IN15), 16.40μM (DW-IN16), 13.46μM (DW-IN17), 15.81μM (DW-IN21) as shown in the figure. Data are shown as one test of three repeats.

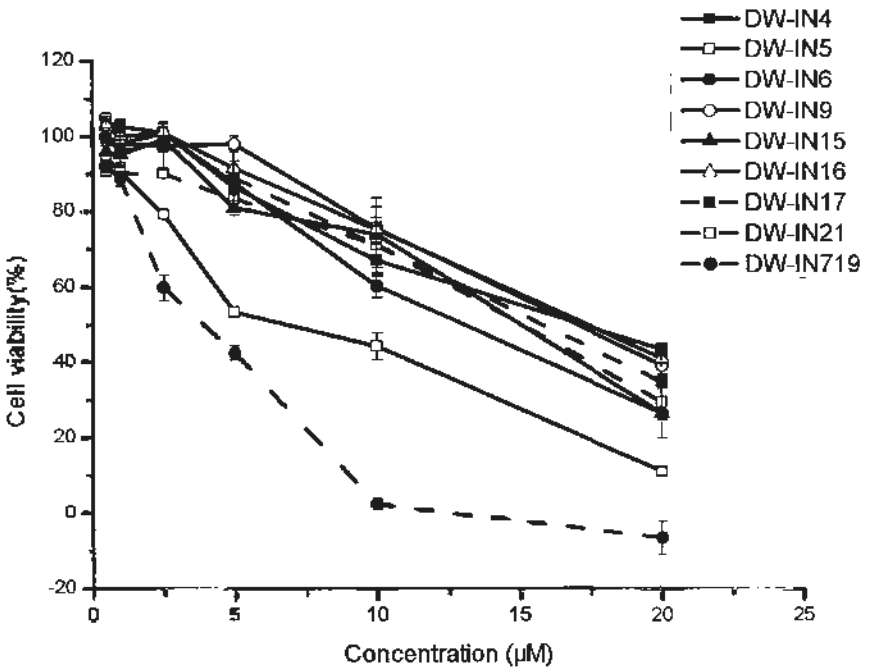

Figure 3.17 MTT-based cytotoxicity assay of DW-IN4, DW-IN5, DW-IN6, DW-IN9, DW-IN15, DW-IN16, DW-IN17, DW-IN21 and DW-IN719

Cellular toxicity of natural product DW-IN719 and eight compounds (DW-IN4, DW-IN5, DW-IN6, DW-IN9, DW-IN15, DW-IN16, DW-IN17, DW-IN21) were assessed by MTT method. Results showed that DW-IN4, DW-IN5, DW-IN6, DW-IN9, DW-IN15, DW-IN16, DW-IN17, DW-IN21 and DW-IN719 had CC_{50} of 16.36μM, 6.35μM, 14.11μM, 16.51μM, 14.51μM, 16.80μM, 14.95μM, 13.80μM and 3.33μM to human T cell line C8166 cells respectively. CC_{50} of AZT was 1010.35μg/ml. Data are shown as one test of three repeats.

3.2.9 EGFP-integrase was localized into Hela/293T cellular nucleus expressed by pEGFP-C1-IN

Transfection of pEGFP-C1-IN into Hela cells, EGFP-integrase was expressed mainly in the cellular nucleus (Figure 3.18). While in the control cells transfected with pEGFP-C1, EGFP was expressed and distributed equally in the cells (Figure 3.18). In transfected 293T cells, we got similar result (Figure 3.19). These results were consistent with the former IN expression result with pTRE2hyg-EGFP-IN in Tet off advanced Hela cells. This confirmed that our cell based integrase inhibitors screening platform was stable.

3.2.10 Six compounds from Kunming inhibited integrase nuclear translocation

Since EGFP-IN expressed well in both Hela cells and 293T cells, we repeated the transfection for more than three times. Compared the expression conditions, 293T cells were finally chosen for integrase inhibitors screening. After several rounds of screening as we described above, 6 (KM7, KM8, KM14, KM30, KM37, KM79) out of 150 compounds showed integrase inhibitive activity in cell based screening experiments (Figure 3.20). All other compounds showed negative results. Two negative results were presented as negative control (Figure 3.20).

3.2.11 Structures of KM7, KM8, KM14, KM79

Six compounds from Kunming showed integrase inhibition characters in cell based screening. The structures of KM7, KM8, KM14 and KM79 were summarized as Figure 3.21.

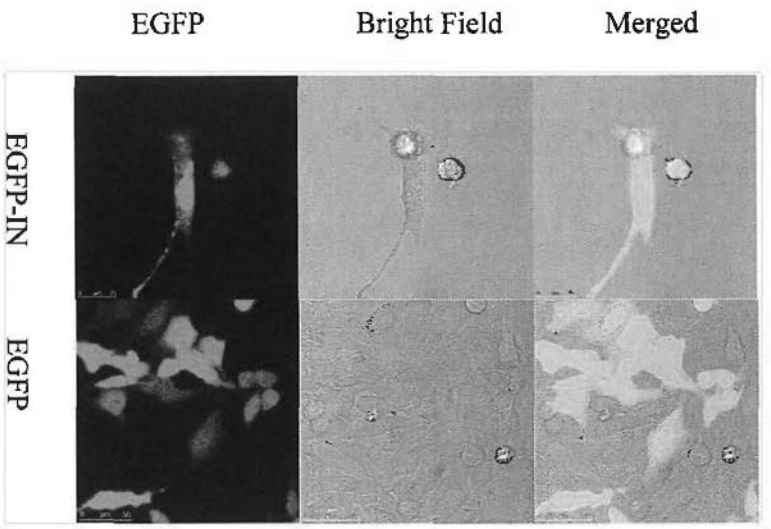

Figure 3.18 Expression of EGFP-C-IN is localized in nucleus of Hela cells

Hela cell line was transfected with pEGFP-C1-IN. EGFP-integrase was expressed mainly in the cellular nucleus. While in the control cells transfected with pEGFP, EGFP was expressed and distributed equally in the cells.

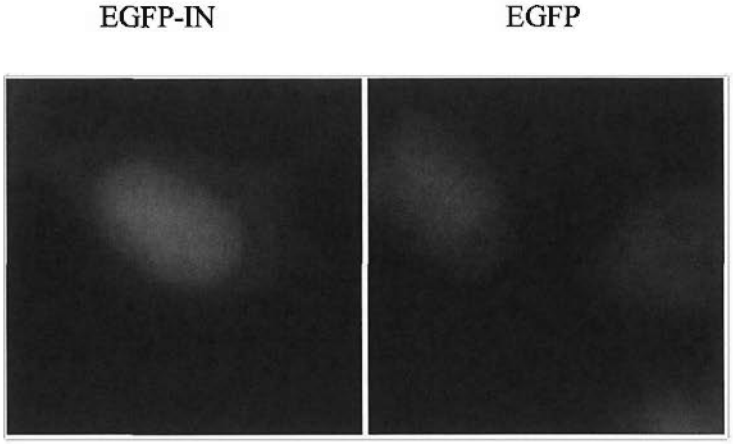

Figure 3.19 Expression of EGFP-C-IN is localized in nucleus of 293T cells

293T cell line was transfected with pEGFP-C1-IN. EGFP-integrase was expressed mainly in the cellular nucleus. While in the control cells transfected with pEGFP-C1, EGFP was expressed and distributed equally in the cells.

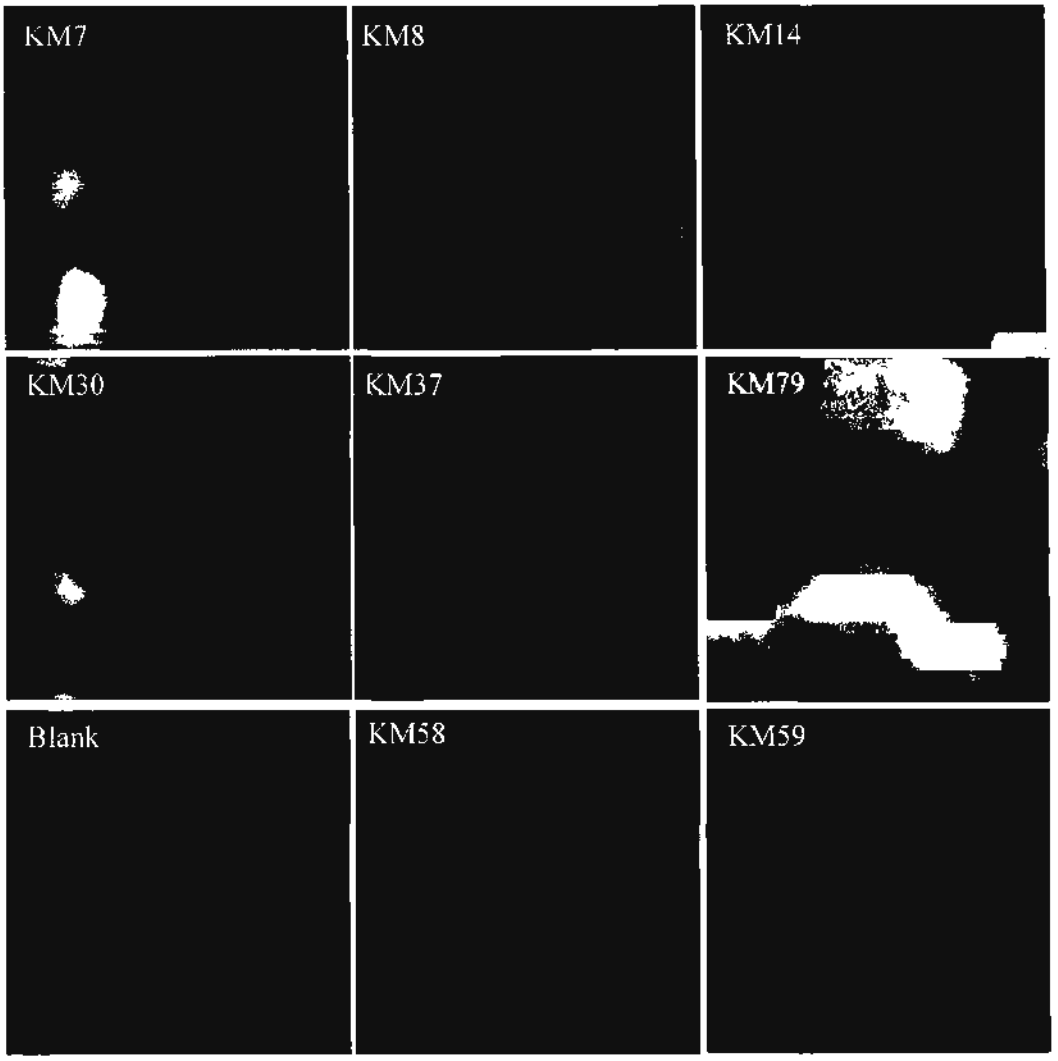

Figure 3.20 KM7, KM8, KM14, KM30, KM37 and KM79 from Kunming inhibited integrase nuclear translocation

293T cell line was transfected with pEGFP-C1-IN. Without inhibitors, EGFP-integrase was expressed mainly in the cellular nucleus. Six compounds (KM7, KM8, KM14, KM30, KM37, KM79) from Kunming showed inhibitive activity of integrase nuclear translocation at 200μg/ml. Another two compounds (KM58, KM59) that showed negative effect were presented here as negative control.

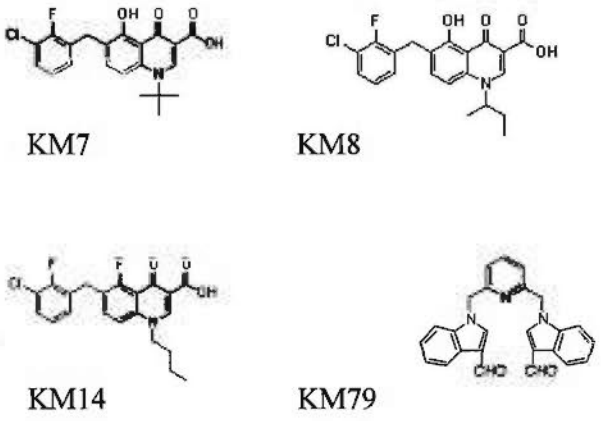

Figure 3.21 Structures of KM7, KM8, KM14, KM79

3.2.12 Molecular Docking

KM7, KM8, KM14, KM30, KM37 inhibited HIV-1 integrase nuclear translocation in cell based assay. The inhibiting mechanism was evaluated by molecular docking. Crystal structure model 2B4J was applied in the molecular docking. Ligand structures were prepared by Chemdraw. Subsequent modifications were done as former procedures. Molecular docking results showed that that these four compounds had good interaction with IN CCD.

KM7 was docked into the hydrophobic pocket formed by surrounding residues of IN CCD (Figure 3.22 A). KM7 formed two H-bonds with Gln95 (B) with distance of 2.86 Å and 3.15 Å respectively. KM7 formed H-bond with Thr174 (A) with distance of 2.70 Å. KM7 formed hydrophobic contacts with Glu170 (A), Thr174 (A), Gln168 (A), Gln95 (B), Leu102 (B), Trp132 (B), Trp131 (B) and Ala128 (B) respectively (Figure 3.22 B).

KM8 was docked into the hydrophobic pocket formed by surrounding residues of IN CCD (Figure 3.23 A). KM8 formed H-bond with Thr174 (A) with distance of 2.86 Å KM8 formed a H-bond with Gln95 (B) with a distance of 2.84 Å. KM8 formed hydrophobic contacts with Glu170 (A), Thr174 (A), Gln168 (A), Leu102 (B), Ala128 (B), Trp131 (B) and Trp132 (B) respectively (Figure 3.23 B).

KM14 was docked into the hydrophobic pocket formed by surrounding residues of IN CCD. KM14 formed H-bond with Thr174 (A) with distance of 2.7 Å KM14 formed a H-bond with Gln95 (B) with a distance of 2.8 Å (Figure 3.24 A).
KM14 formed hydrophobic contacts with Gln168 (A), Ala169 (A), Glu170 (A), Thr174 (A), Trp131 (B), Trp132 (B), Ala128 (B) and Leu102 (B) respectively (Figure 3.24 B).

Table 3.3 Ranking of KM7, KM8, KM14, KM79, D77

IN CCD dimer crystal structure was selected from PDB (PDB ID: 2B4J). The docking was run by Autodock VINA. The grid centre was set at the active-site position (-14.685, 4.189, -7.387). A gridbox of 40×40×40 was used for docking. Other parameters were set as default. The logarithm of the ratio of the concentrations of the un-ionized solute in the solvents is called log *P*; the log P values is also known as a measure of lipophilicity(http://en.wikipedia.org/wiki/Partition_coefficient). Compound with higher logP is more hydrophobic.

Compound	Affinity (kcal/mol)	LogP
KM7	**-7.8**	**4.5**
KM79	**-7.1**	**4.06**
KM8	**-7.1**	**4.77**
KM14	**-6.9**	**5.41**
D77	**-6.8**	**4.85**

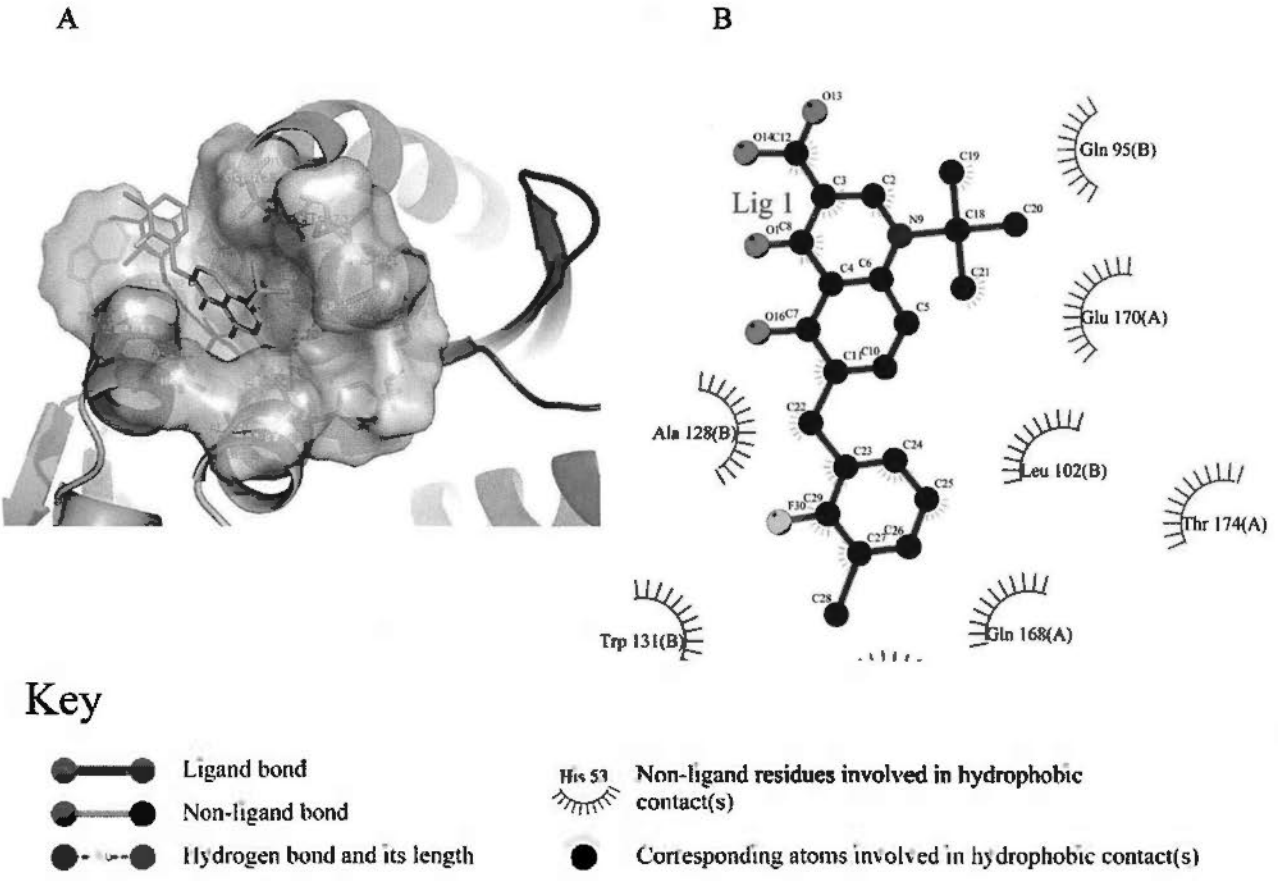

Figure 3.22 Interaction between KM7 and IN CCD

A) The KM7 was shown as sticks. The secondary structure of IN CCD was shown as cartoon. The H-bond was shown as red with distance label. KM7 was docked into the hydrophobic pocket formed by surrounding residues of IN CCD. KM7 formed two H-bonds with Gln95 (B) with distance of 2.86 Å and 3.15 Å respectively. KM7 formed H-bond with Thr174 (A) with distance of 2.70 Å
B). KM7 formed hydrophobic contacts with Glu170 (A), Thr174 (A), Gln168 (A), Gln95 (B), Leu102 (B), Trp132 (B), Trp131 (B) and Ala128 (B) respectively.

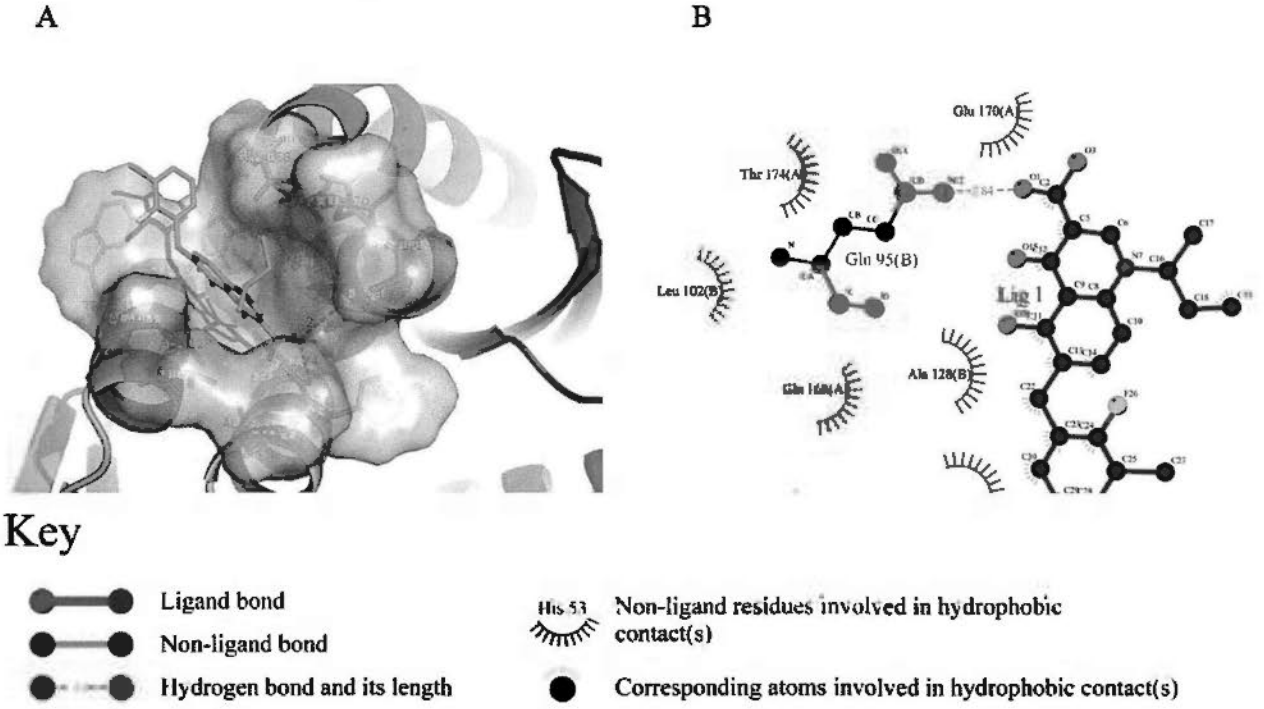

Figure 3.23 Interaction between KM8 and IN CCD

A) The KM8 was shown as sticks. The secondary structure of IN CCD was shown as cartoon. The H-bond was shown as red with distance label. KM8 was docked into the hydrophobic pocket formed by surrounding residues of IN CCD. KM8 formed H-bond with Thr174 (A) with distance of 2.86 Å KM8 formed a H-bond with Gln95 (B) with a distance of 2.84 Å.
B) KM8 formed hydrophobic contacts with Glu170 (A), Thr174 (A), Gln168 (A), Leu102 (B), Ala128 (B), Trp131 (B) and Trp132 (B) respectively.

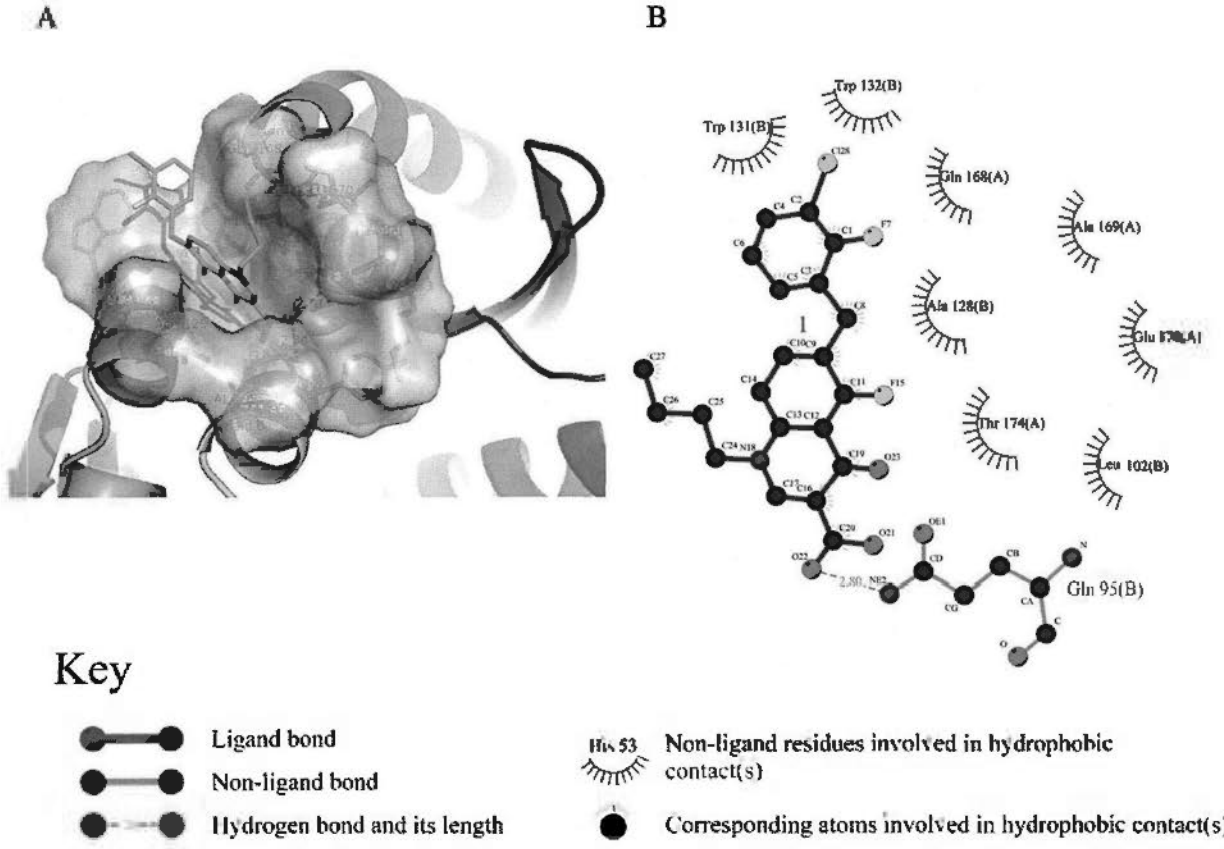

Figure 3.24 Interaction between KM14 and IN CCD

A) The KM14 was shown as sticks. The secondary structure of IN CCD was shown as cartoon. The H-bond was shown as red with distance label. KM14 was docked into the hydrophobic pocket formed by surrounding residues of IN CCD. KM14 formed H-bond with Thr174 (A) with distance of 2.7 Å KM14 formed a H-bond with Gln95 (B) with a distance of 2.8 Å.
B) KM14 formed hydrophobic contacts with Gln168 (A), Ala169 (A), Glu170 (A), Thr174 (A), Trp131 (B), Trp132 (B), Ala128 (B) and Leu102 (B) respectively.

KM79 was docked into the hydrophobic pocket formed by surrounding residues of IN CCD (Figure 3.25 A). O2 of KM79 formed a H-bond with N of Glu170 (A) with a distance of 2.90 Å. O30 of KM79 formed two H-bonds with N of Glu170 (A) with a distance of 3.04 Å and N of His171 (A) with a distance of 3.19 Å respectively. From A), an additional H-bond was found to fromed between KM79 and Thr174 (A). Besides, KM79 formed hydrophobic contacts with Met178 (A), Thr174 (A), Ala169 (A), Thr125 (B), Ala128 (B), Ala129 (B), Trp132 (B) and Leu102 (B) respectively (Figure 3.25 B).

3.2.13 KM7, KM8, KM14 showed inhibition on cytopathic effect in C8166 cells infected by HIV-1_{IIIB}

To further approach the inhibition activity of KM7, KM8, KM14 and KM79 on HIV-1 replication, syncytia assay was conducted with C8166 cells infected with virus (HIV-1IIIB) at a multiplicity of infection (M.O.I) of 0.06. The protocol was as mentioned in chapter 2. Compounds were added to cell culture with infection at a 10-fold serial dilution from the beginning of 10μg/ml. AZT was used as positive control. Results demonstrated that KM7, KM8, KM14 had significant effect on cytopathic effect reduction in C8166 cells infected by HIV-1IIIB with EC50 of 4.93μM (3.94μg/ml), 3.99μM (1.61μg/ml) and 14.33μM (5.99μg/ml). KM79 had an EC_{50} of 96.51μM (37.97μg/ml). EC50 of AZT was 15.34nM (4.10ng/ml)(Figure 3.26).

3.2.14 KM7, KM8, KM14 showed P24 production inhibition in acute infection

To further approach the inhibition activity of KM7, KM8, KM14 and KM79 on HIV-1 replication, P24 assay was conducted with C8166 cells infected with virus (HIV-1IIIB). The protocol was as mentioned in chapter 2. Compounds were added to cell culture with infection at a 10-fold serial dilution from the beginning of 100Mg/ml. Results showed that KM7, KM8 and KM14 dramatically reduced P24 production in HIV-1_{IIIB} acute infected C8166 cells with EC_{50} value of 20.54μM l(8.32μg/m), 4.88μM (1.97μg/ml) and 12.99μM (5.43μg/ml). EC50 of KM79 was 208.43μM (82.01μg/ml). EC50 of AZT was 7.07nM (1.89ng/ml) (Figure 3.27).

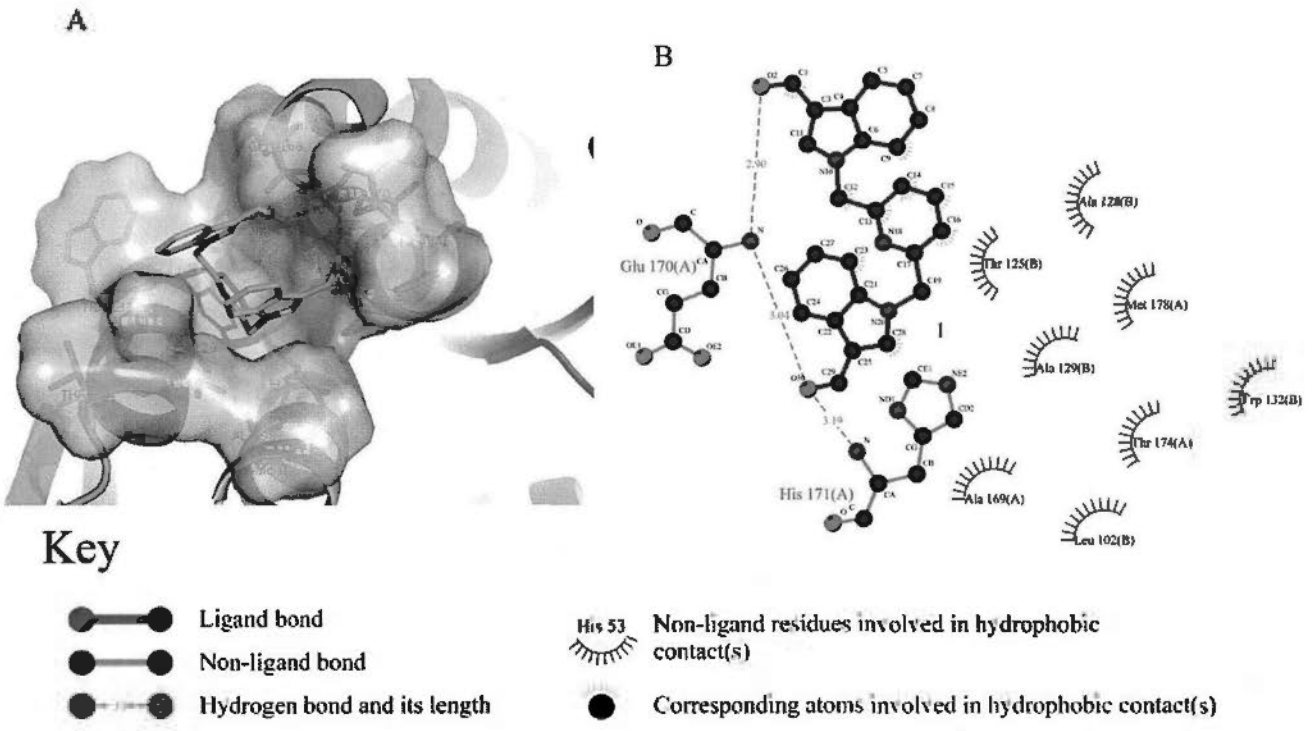

Figure 3.25 Interaction between KM79 and IN CCD

A) The KM79 was shown as sticks. The secondary structure of IN CCD was shown as cartoon. The H-bond was shown as red with distance label. KM79 was docked into the hydrophobic pocket formed by surrounding residues of IN CCD.
B) O2 of KM79 formed a H-bond with N of Glu170 (A) with a distance of 2.90 Å. O30 of KM79 formed two H-bonds with N of Glu170 (A) with a distance of 3.04 Å and N of His171 (A) with a distance of 3.19 Å respectively. From A), an additional H-bond was found to fromed between KM79 and Thr174 (A). Besides, KM79 formed hydrophobic contacts with Met178 (A), Thr174 (A), Ala169 (A), Thr125 (B), Ala128 (B), Ala129 (B), Trp132 (B) and Leu102 (B) respectively.

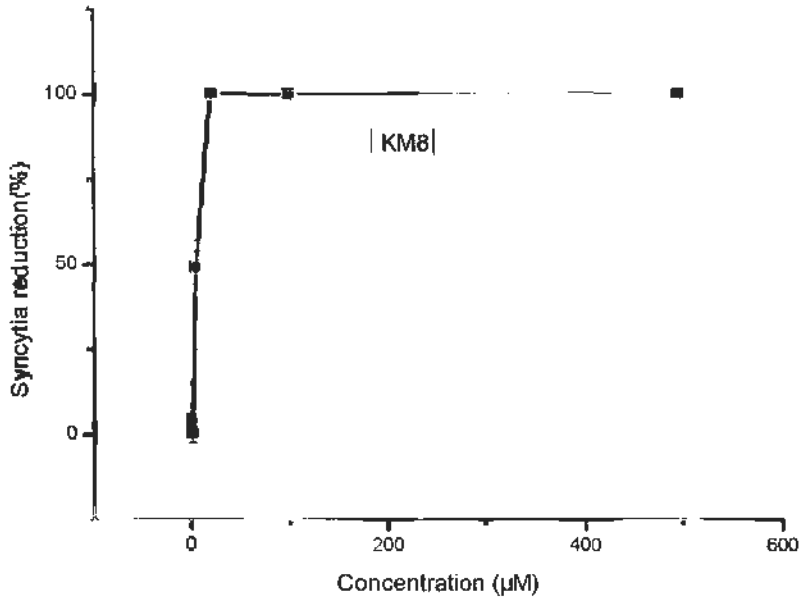
KM8
Syncytia reduction(%)
100
50
0
0
200
400
600
Concentration (μM)

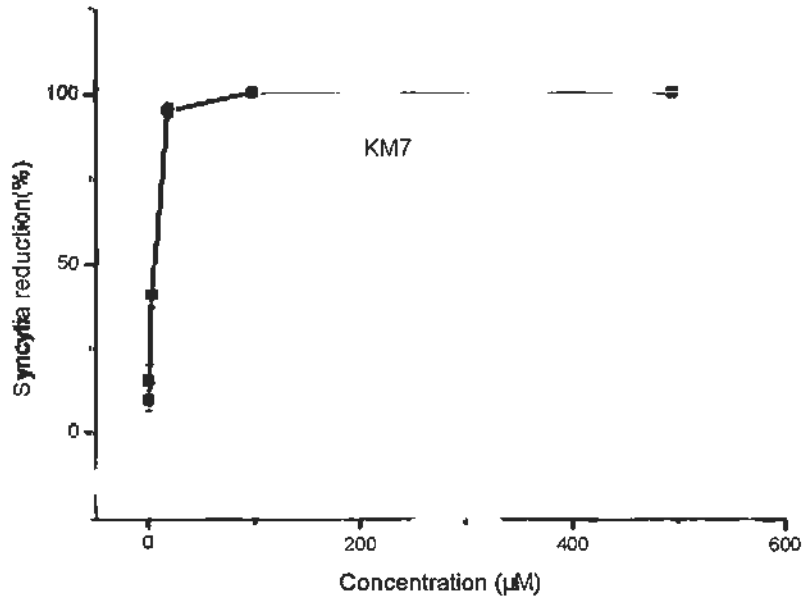
KM7
Syncytia reduction(%)
100
50
0
0
200
400
600
Concentration (μM)

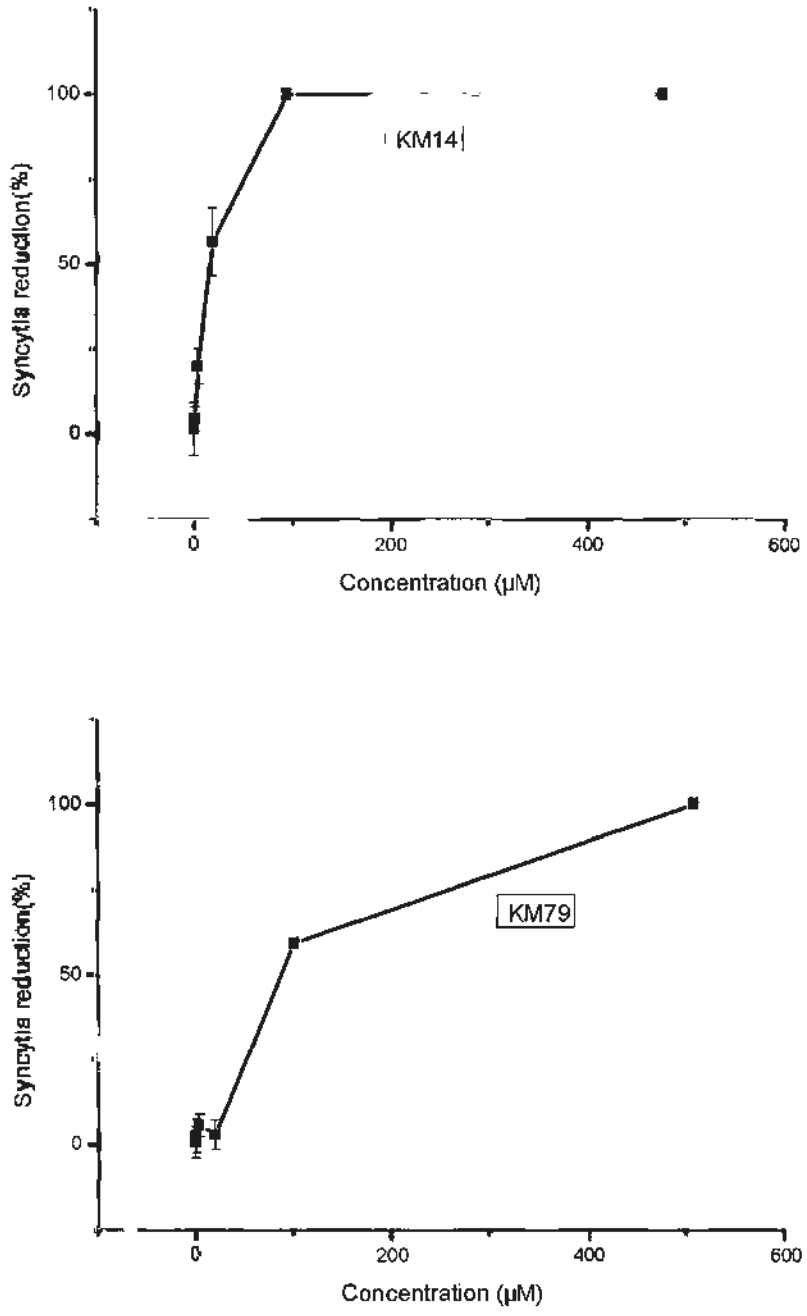

Figure 3.26 KM7, KM8, KM14 showed inhibition on cytopathic effect in C8166 cells infected by HIV-1_{IIIB}

Compounds were added to cell culture with infection at a 10-fold serial dilution from the beginning of 10μg/ml. AZT was used as positive control. Results demonstrated that KM7, KM8, KM14 had significant effect on cytopathic effect reduction in C8166 cells infected by HIV-1IIIB with EC50 of 4.93μM (3.94μg/ml), 3.99μM (1.61μg/ml) and 14.33μM (5.99μg/ml). KM79 had an EC_{50} of 96.51μM (37.97μg/ml). EC50 of AZT was 15.34nM (4.10ng/ml). Data are shown as one test of two repeats.

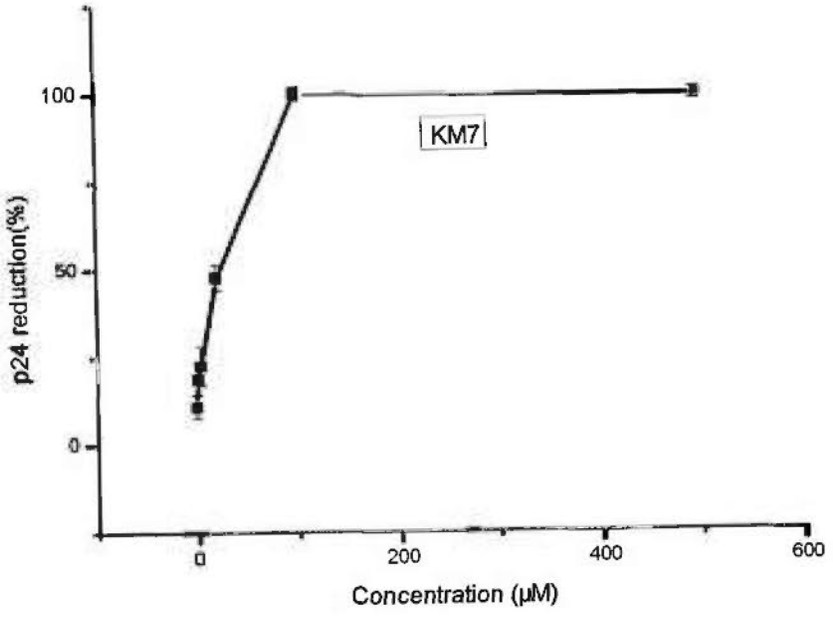
KM7
p24 reduction(%)
100
50
0
0
200
400
600
Concentration (μM)

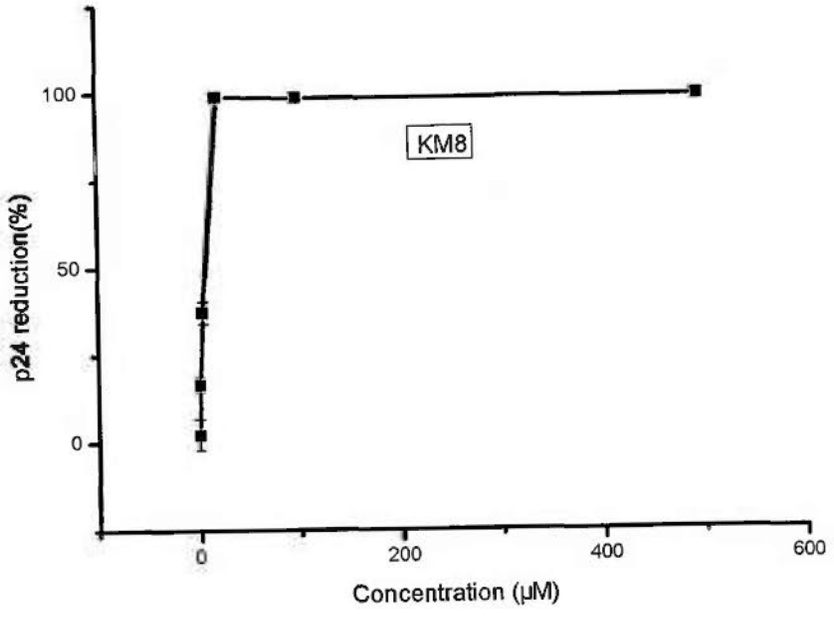
KM8
p24 reduction(%)
100
50
0
0
200
400
600
Concentration (μM)

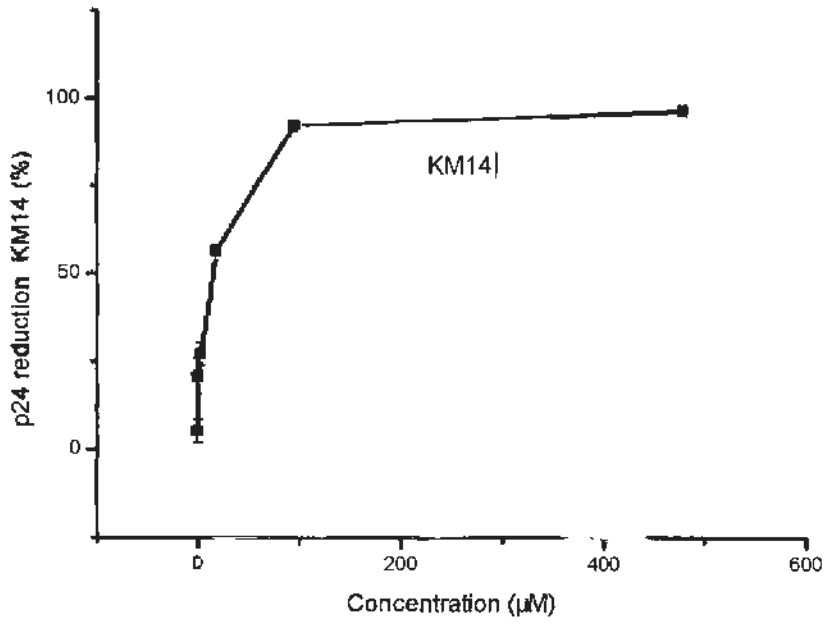

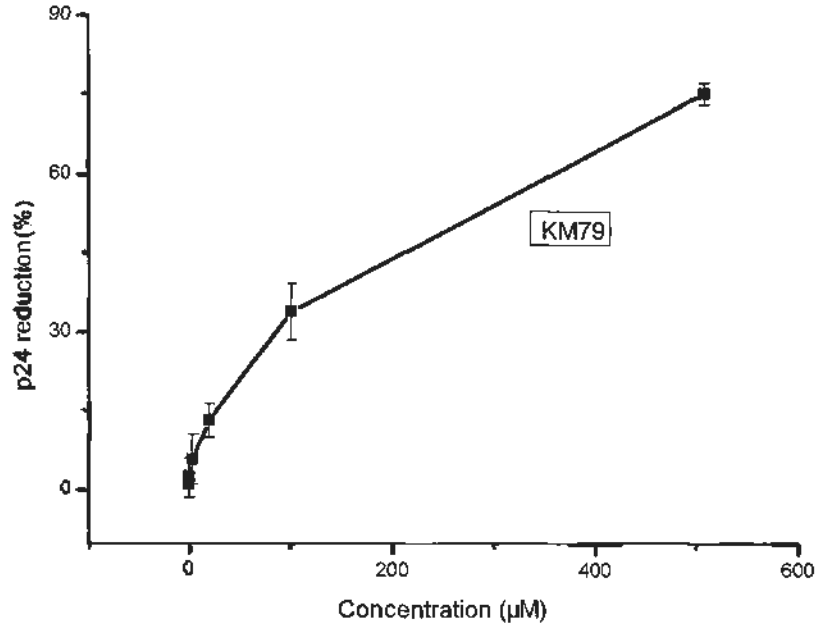

Figure 3.27 KM7, KM8, KM14 showed P24 production inhibition in acute infection

Compounds were added to cell culture with infection at a 10-fold serial dilution from the beginning of 100mg/ml. Results showed that KM7, KM8 and KM14 dramatically reduced P24 production in HIV-1_{IIIB} acute infected C8166 cells with EC_{50} value of 20.54μM l(8.32μg/m), 4.88μM (1.97μg/ml) and 12.99μM (5.43μg/ml). EC50 of KM79 was 208.43μM (82.01μg/ml). EC50 of AZT was 7.07nM (1.89ng/ml). Data are shown as one test of two repeats.

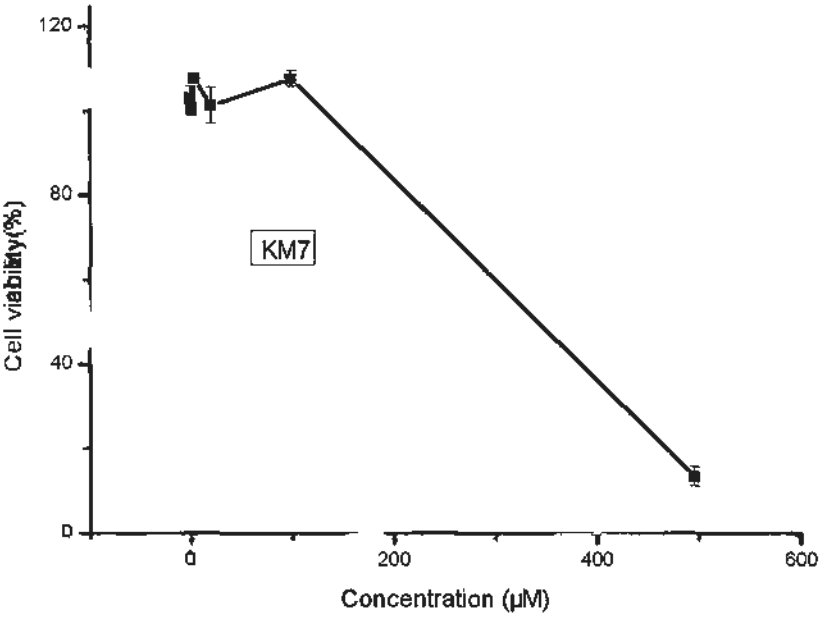
120
80
40
0
Cell viability(%)
KM7
0
200
400
600
Concentration (μM)

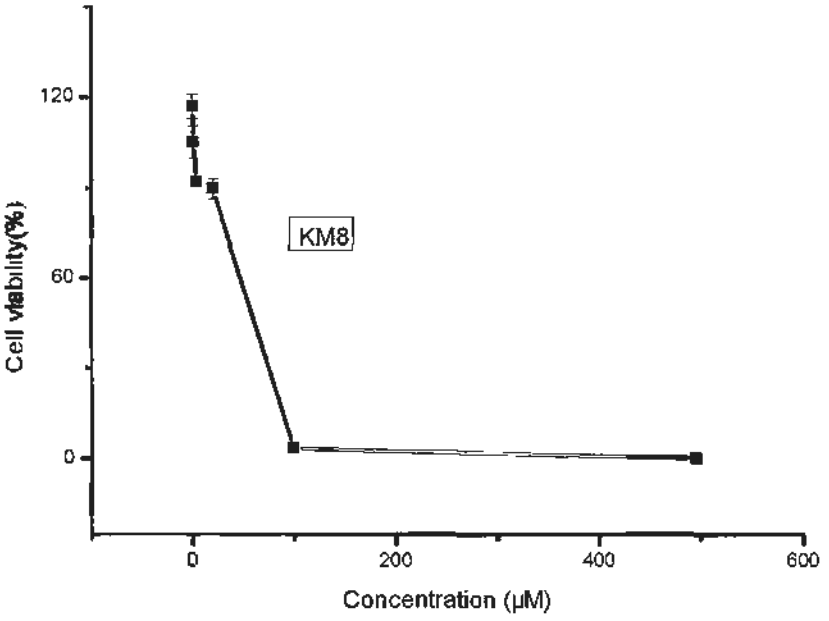
120
60
0
Cell viability(%)
KM8
0
200
400
600
Concentration (μM)

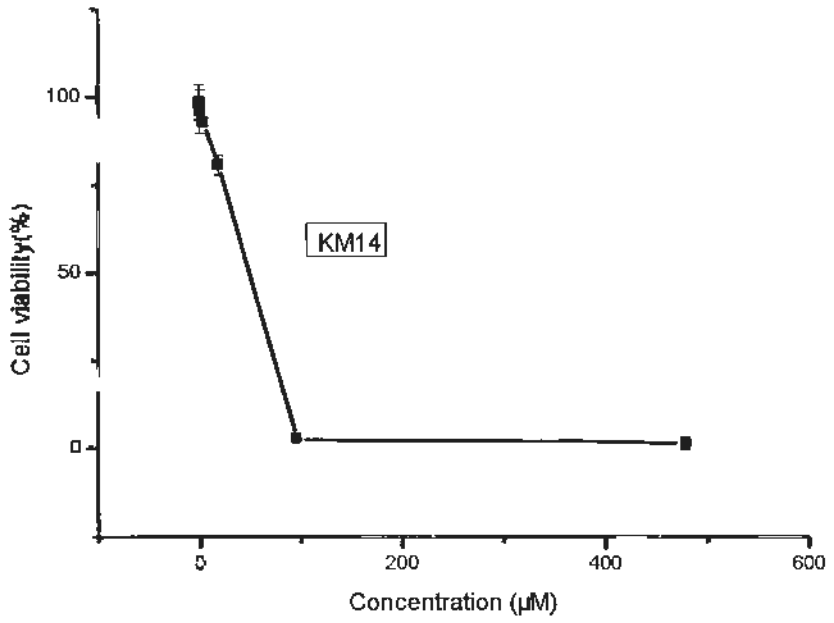

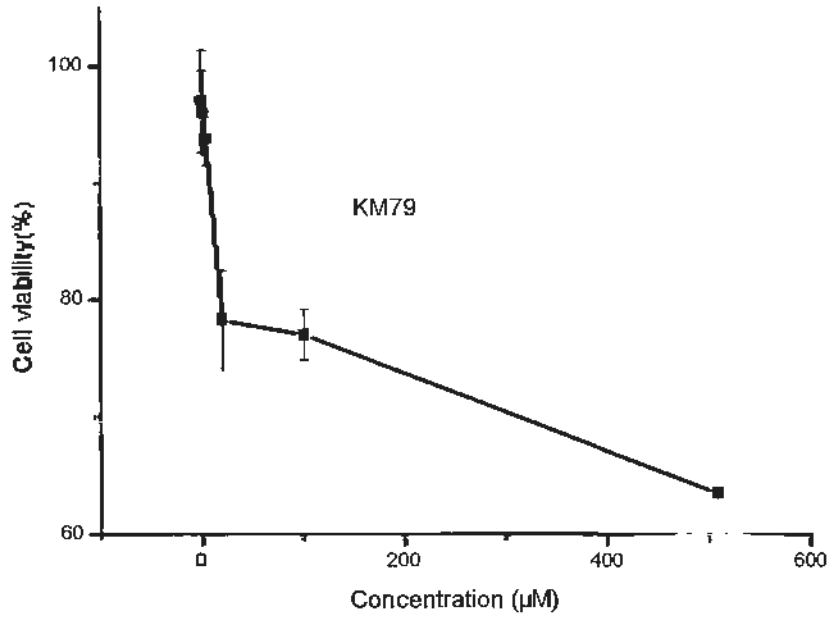

Figure 3.28 MTT-based cytotoxicity assay of KM7, KM8, KM14 and KM79

Cellular toxicity of KM compounds was assessed by MTT method. Results showed that KM7, KM8, KM14 and KM79 had CC_{50} of 436.56μM (176.3μg/ml), 36.15μM (14.62μg/ml), 29.43μM (12.39μg/ml) and >508μM (>200μg/ml), to human T cell line C8166 cells respectively. CC_{50} of AZT was 3.76mM (1007.2μg/ml). Data are shown as one test of two repeats.

3.2.15 MTT-based cytotoxicity assay

Cellular toxicity of KM compounds was assessed by MTT method. The protocol was as mentioned in chapter 2. Results showed that KM7, KM8, KM14 and KM79 had CC_{50} of 436.56μM (176.3μg/ml), 36.15μM (14.62μg/ml), 29.43μM (12.39μg/ml) and >508μM (>200μg/ml), to human T cell line C8166 cells respectively. CC_{50} of AZT was 3.76mM (1007.2μg/ml) (Figure 3.28).

3.3 Discussion

As mentioned in previous section, HIV-1 integrase was an attractive target for anti-HIV drugs development, for it has no direct cellular counterpart(Anthony, 2004). The integration was an important step in HIV replication and critical for latent infection. Targeting the strand transfer step, Raltegravir from Merck was the first HIV-1 integrase inhibitor approved by FDA in 2007(Cabrera, 2008). Raltegravir-containing regimens had potent antiretroviral activity and were well tolerated in patients in clinical trials(Cocohoba and Dong, 2008).

Preintegration complex was consisted of many known and unknown cellular cofactors(Bukrinsky and Haffar, 1997). Undoubtly, integrase is the key player in the preintegration complex. Prior to integration, the integrase has first to be translocated into the nucleus(Bukrinsky and Haffar, 1997). Lens epithelium-derived growth factor (LEDGF/p75), the first discovered cellular co-factor for integration in vivo, was implicated to play a key role in the process(Cherepanov et al., 2003). Residues 347-429 at the C-terminus of LEDGF/p75 were identified as the integrase binding domain (IBD)(Cherepanov et al., 2004).

The x-ray crystal structure suggested that when in complex with the catalytic domain of HIV-1 IN, LEDGF/p75 IBD, LEDGF/p75 acted through a tethering mechanism with the N-terminal Pro- Trp- Trp- Pro (PWWP) and A/T-hook elements binding to

chromatin, and the C-terminal integrase-binding domain (IBD) binding to integrase. Intervention of such a process could potentially be an important target for drug development(Botbol et al., 2008; Cherepanov et al., 2005; Cherepanov et al., 2004; Shun et al., 2008). D77, a benzoic acid derivative, disrupts HIV-1 integrase - LEDGF/p75 interaction as reported. D77 was the first small molecular compound discovered targeting HIV-1 integrase-LEDGF/p75 interaction(Du et al., 2008).

In this study, we constructed a cell based HIV-1 integrase inhibitors screening platform by cloning integrase fused with EGFP into eukaryotic expression system. The transfection result showed integrase was mainly localized into the human cellular nucleus both in Tet Off Advanced Hela cell line and 293T cell line. Cell imaging result demonstrated that our platform was suitable for HIV-1 integrase inhibitors screening.

For drug candidates collection, synthetic compounds and natural products were two sources usually concerned in drug screening.

SPECS, which was founded in 1987, provides chemistry and chemistry related services that are required in drug discovery. SPECS is the world's leading provider of compound management services besides being a main supplier of screening compounds and building blocks to the life science industry. SPECS database is consisting of single synthesized, well-characterized and drug-like small molecules, has been built through global acquisition programs utilizing a network of more than 2,000 academic sources worldwide(http://www.specs.net). Totally more than 30 thousands compounds were downloaded from SPECS for molecular docking in this study. This is our first source for HIV-1 integrase inhibitors screening.

ZINC is a free database of commercially-available compounds for virtual screening. ZINC is provided by the Shoichet Laboratory in the Department of Pharmaceutical Chemistry at the University of California, San Francisco (UCSF). Over thirteen million purchasable compounds were collected in ZINC database(http://zinc.docking.org/). And these compounds were usually 3D formats and prepared for docking. More than 70 thousand compounds were downloaded from ZINC natural product database. This is our second source for HIV-1 integrase inhibitors screening.

Since September of 2010, I began to collaborate with Kunming Institute of Zoology, the Chinese Academy of Sciences. The KIZ is also working on the study of antiviral research on HIV. KIZ has a collection of purified compounds extracted from Chinese herbs and synthetic compounds with a number of more than 300 hundreds. As I mentioned above, I conducted a cooperative research in KIZ for drug screening. This is our third source for HIV-1 integrase inhibitors screening.

Molecular docking have been used widely in compounds and proteins interaction approach. It is now a powerful tool in drug development and discovery. If the receptor has a clear crystal structure is available. Based on the analysis of the structure, a virtual screening can be performed. Through analyzing the virtual screening result, a ranking of the candidates can tell us which compounds are suitable for further development.

For molecular docking, the integrase structure that is used in this study is reported by Cherepanov and his coworkers. Their valuable work is the basis of our docking study. Crystal structure of intergrase catalytic core domain dimer (2B4J) was downloaded from PDB (PDB ID: 2B4J)(Cherepanov et al., 2005). LEDGF peptide was removed from IN CCD dimer. Then waters were removed from IN CCD. The receptor was then modified with Autodocktools-1.5.4 for molecular docking. Molecular docking was run between the IN CCD and ligands from SPECS and ZINC database. The

docking results guided us to select 23 compounds from SPECS and 3 from ZINC for further experiment. Finally, 8 compounds (DW-IN4, DW-IN5, DW-IN6, DWIN-9, DW-IN15, DW-IN16, DW-IN17, DW-IN21) from SPECS and 1 compound (DW-IN719) from ZINC were found to inhibit integrase nuclear translocation. This indicates that former docking results were reliable in some degree. Molecular docking improved our screening efficiency by reducing the number of compounds for cell based screening. It is time-consuming and money-consuming.

Expression of EGFP tagged HIV-1 integrase

HIV-1 integrase was cloned into pTRE2hyg to express integrase in Hela Tet off Advanced cells. Transfection of the vector into human cells was conducted by Lipofectamine 2000. This reagent has a high surrounding tolerance with the presence of FBS. But it also has comparatively higher cytotoxicity. Twenty-four hours after transfection, 5-30 percent cells died with unknown reason. Expression of integrase was usually examined twenty hours after transfection. In fact, integrase may began to express in the cells earlier than this. To reach the high transfection efficiency, we didn't disturb the cells before observing.

Expression of integrase was mainly localized into the cellular nucleus (Figure 3.1), while EGFP only expressed in the whole cell. From the cell imaging, we discovered some bright particles in the nucleus. It was the over expressed integrase that accumulated in the nucleus. Interestingly, positive cells with high expression of integrase were offen observed died faster than the negative cells. It indicates that high expression integrase may be toxic to cells.

Screening of integrase inhibitors in cell based platform

Selected compounds by molecular docking were further screened with cell based platform. Compound solutions were added to the cell culture five hours after transfection since the foreign gene may begin to express in earliest transfected cells as soon as transfection. Avoid add compound solutions to the cells during incubation

with Lipofectamine 2000, i.e in the first five hours. Because during the transfection, cell membrane were teared transiently to form small holes to let the DNA-Lipofectamine complex go into the cells. Cells were vulnerable during this time course, additional compounds may cause plenty of cell death.

The compounds were tested at 1μM, 5μM and 10μM for integrase nuclear translocation inhibition. Eight compounds (DW-IN4, DW-IN5, DW-IN6, DWIN-9, DW-IN15, DW-IN16, DW-IN17, DW-IN21) from SPECS were found to inhibit integrase nuclear translocation at 1μM (Figure 3.2). Therefore, there is approximately 35% of the selected compounds showed affinity in docking analysis showed positive results in cell based screening.

Following serial dilution assays showed that these compounds inhibited integrase nuclear translocation in a dose dependent manner (Table 3.2). These compounds showed integrase inhibition effect at 1μM indicated that these compounds were more effective than D77 which inhibited integrase nuclear translocation at 5μM.
DW-IN719, one natural product from ZINC, also showed integrase nuclear translocation inhibition at 1μM (Figure 3.13).

From more than 150 samples in KIZ, six compounds (KM7, KM8, KM14, KM30, KM37, KM79) showed inhibition activity of integrase nuclear translocation at 200μg/ml (Figure 3.20). Since these samples were either synthetic or extracted from Chinese herbs, no virtual screening were conducted before test. In fact, since the sample database is not large and not all the samples were structurally clear, virtual screening was not conducted at the beginning of the study.

Cytopathic effect reduction

To further test the compounds' effect in live virus culture, cytopathic effect reduction was conducted for the positive compounds with integrase nuclear translocation inhibition. Syncytium formation is an important biological characteristic of T tropic

HIV strains infection in cell culture. Syncytium forms in two to three days after virus infection. Although the details of the syncytium formation are not clear at present, it has been widely used in anti-HIV drug screening. HIV-1IIIB was used in the live virus assays. All the manipulations were done in Biological Safety Lab-3 in Kunming Institute of Zoology, the Chinese Academy of Sciences. Compounds were added to cell culture with infection at a 5-fold serial dilution from the beginning of 10μM. Results demonstrated that DW-IN6 had significant effect on cytopathic effect reduction in C8166 cells infected by HIV-1_{IIIB} with EC50 of 3.47μM (Figure 3.15). DW-IN5 had an EC50 of 9.37 M while other compounds had an EC50 that were > 10μM. In this study, it was found that DW-IN6 did show significant effect on the reduction of cytopathic effect.

p24 production inhibition in acute infection

P24 is the core protein in the HIV particle. It is cleaved from the P55 precursor. P24 forms the viral capsid, in which viral RNA is encapsulated. The level of anti-p24 antibody in the serum is an indicator of HIV infection progression. Testing for "heat-denatured p24 antigen" was statistically equivalent to CD4 count and viral load tests. P24 production inhibition in acute infection is key primary assay for testing the drug efficacy of HIV replication inhibition.

Compounds were added to cell culture with HIV infection at a 2-fold serial dilution from the beginning of 10μM. DW-IN719 and DW-IN6 dramatically reduced P24 production in HIV-1IIIB acute infected C8166 cells with EC50 value of 4.33μM and 4.96μM respectively. Other compounds had EC50 of 17.09μM (DW-IN4), 11.60μM (DW-IN5), 15.53μM (DW-IN9), 11.75μM (DW-IN15), 16.40μM (DW-IN16), 13.46μM (DW-IN17), 15.81 μM (DW-IN21) as shown in the figure 2.16.

Taken together, it is concluded that DW-IN6 is a promising lead compound for further drug development.

MTT-based cytotoxicity assay

Cellular toxicity of natural product DW-IN719 and eight compounds (DW-IN4, DW-IN5, DW-IN6, DW-IN9, DW-IN15, DW-IN16, DW-IN17, DW-IN21) were assessed by MTT method. Results showed that DW-IN4, DW-IN5, DW-IN6, DW-IN9, DW-IN15, DW-IN16, DW-IN17, DW-IN21 and DW-IN719 had CC_{50} of 16.36μM, 6.35μM, 14.11μM, 16.51μM, 14.51μM, 16.80μM, 14.95μM, 13.80μM and 3.33μM to human T cell line C8166 cells respectively (Figure 3.17). MTT assay showed that these compounds were toxic in some degree to human T cells. In future research, modifications could be done to reduce the cytotoxicity of these compounds in order to enhance their druggability.

Comparison of Virtual and Screening *in vitro*

In this study, both virtual screening and screening *in vitro* (cell based screening) were used in HIV-1 integrase inhibitors screening. As for virtual screening, more than 100 thousand compounds were selected from two databases (SPECS and ZINC). The virtual screening was then performed with Autodock. About 30 leading compounds with high affinity and low toxicity to integrase were selected and obtained from commercial company. Finally, 9 compounds from virtual screening showed significant integrase nuclear translocation inhibition activity in cell based screening platform.

More than 150 compounds obtained from Kunming Insititue of Zoology were selected for integrase inhibitors. After several rounds of screening, 6 compounds showed significant integrase inhibition on integrase nuclear translocation. Virtual screening has become an indispensable tool in drug screening. Compared with conventional screening method *in vitro*, virtual screening has the advantages of high efficiency, low cost, and time saving. Through virtual screening, plenty of compounds can be screened for some receptor in a short time. Virtual screening is a good complementary method to the traditional screening method *in vitro*. Compared with virtual screening, experiments are slower and time costing.

In this study, 23 compounds from SPECS with high affinity were tested on cell based platform while only 8 compounds showed integrase inhibition in cell imaging.

This shows some discrepany between the affinities calculated from docking with the efficacy of these compounds on HIV-1 IN nuclear translocation. The docking results are therefore only served as a tool for prediction of the interaction with HIV-IN and the biological response may not correlate very well with the calculated binding affinity and validation of biological efficacy has to be experimentally confirmed.

Chapter 4
Synthesis and characterization of new compounds with HIV-1 inhibitory activities

4.1 Introduction

Through virtual screening, twenty-three compounds from SPEC free database with high affinity and low toxicity to HIV-1 integrase were selected. These twenty-three compounds were purchased from SPECS. On cell based integrase inhibitors screening platform, eight out of twenty-three compounds showed significant inhibition on HIV-1 integrase nuclear translocation. These compounds also showed inhibitory effect on HIV-1 replication in live virus assays such as P24 antigen production in acute infection and syncytia assay. While these compounds also showed cytotoxicity in MTT assay performed with Human T cell line C8166. Based on these findings, we hypothesize that if some new compounds with better effect on HIV-1 replication inhibition as well as lower cytotoxicity to human cell and human body could be synthesized, then these compounds would be good new anti-HIV drug candidates. This would be beneficial to anti-HIV drug development and contribution to present HARRT treatment of HIV-1 infection. In this part, three out of eight compounds from SPECS which showed significant inhibition on HIV-1 integrase nuclear translocation were selected for derivative synthesis candidates. These compounds were analyzed by NMR for purity and structure confirmation. NMR result showed that these compounds were with high purity with the right structure as provided by SPECS. Based on the NMR information, one compound DW-IN16, was selected as study candidate. First, one derivative of DW-IN16 was synthesized, named INNE-1. The structure of INNE-1 was confirmed by NMR. Subsequently, INNE-1 inhibited HIV-1 integrase nuclear translocation at 10μM. This encouraged us to design and synthesize more compounds. Based on the structural information and cell imaging results of both DW-IN16 and INNE-1, another five compounds named INNE-2, INNE-3, INNE-4, INNE-5, INNE-6 were synthesized. All the derivatives were analyzed for structure confirmation by NMR. Cell imaging results showed that INNE-1 and INNE-2 showed inhibitory effect on HIV-1 integrase nuclear translocation. Four compounds, INNE-1, INNE-2, INNE-3, INNE-4 showed HIV-1 replication inhibition effect with live virus infection.

4.2 Results

4.2.1 NMR analysis of DW-IN6, DW-IN15 and DW-IN-16

Three compounds DW-IN6, DW-IN15 and DW-IN-16 were analyzed by NMR (Figure 4.1a, b, c). NMR results confirmed the structures as provided by SPECS. These certified that previous results were credible and these compounds were suitable for further modification.

4.2.2 Synthesis of INNE-1 and NMR analysis

The synthesis of INNE compounds were made in collaboration with Dr. Joseph Chan, According to the structural information of DW-IN6, DW-IN15 and DW-IN-16 provided by NMR analysis, first derivative was design mainly based on the structure of DW-IN-16 aiming to reinforce the inhibitory effective on HIV-1 and reduce the cytotoxicity to human cells and human body. The first synthesized derivative was named INNE-1. After synthesis, INNE-1 was dissolved in DMSO-D6, and analyzed with NMR. NMR result showed that INNE-1 was synthesized with the right structure as designed.

4.2.3 INNE-1 showed inhibition on HIV-1 integrase nuclear translocation

After confirmation of the structure, INNE was dissolved in DMSO. Integrase nuclear translocation assay was conducted with HeLa Tet-Off Advanced cells transfected with EGFP-C-IN expression vector by Lipofectamine according to the manufacturer's instruction. EGFP expression vector was transfected as control. Cell imaging results showed that INNE-1 inhibited HIV-1 integrase nuclear translocation at 10μM (Figure 4.2).

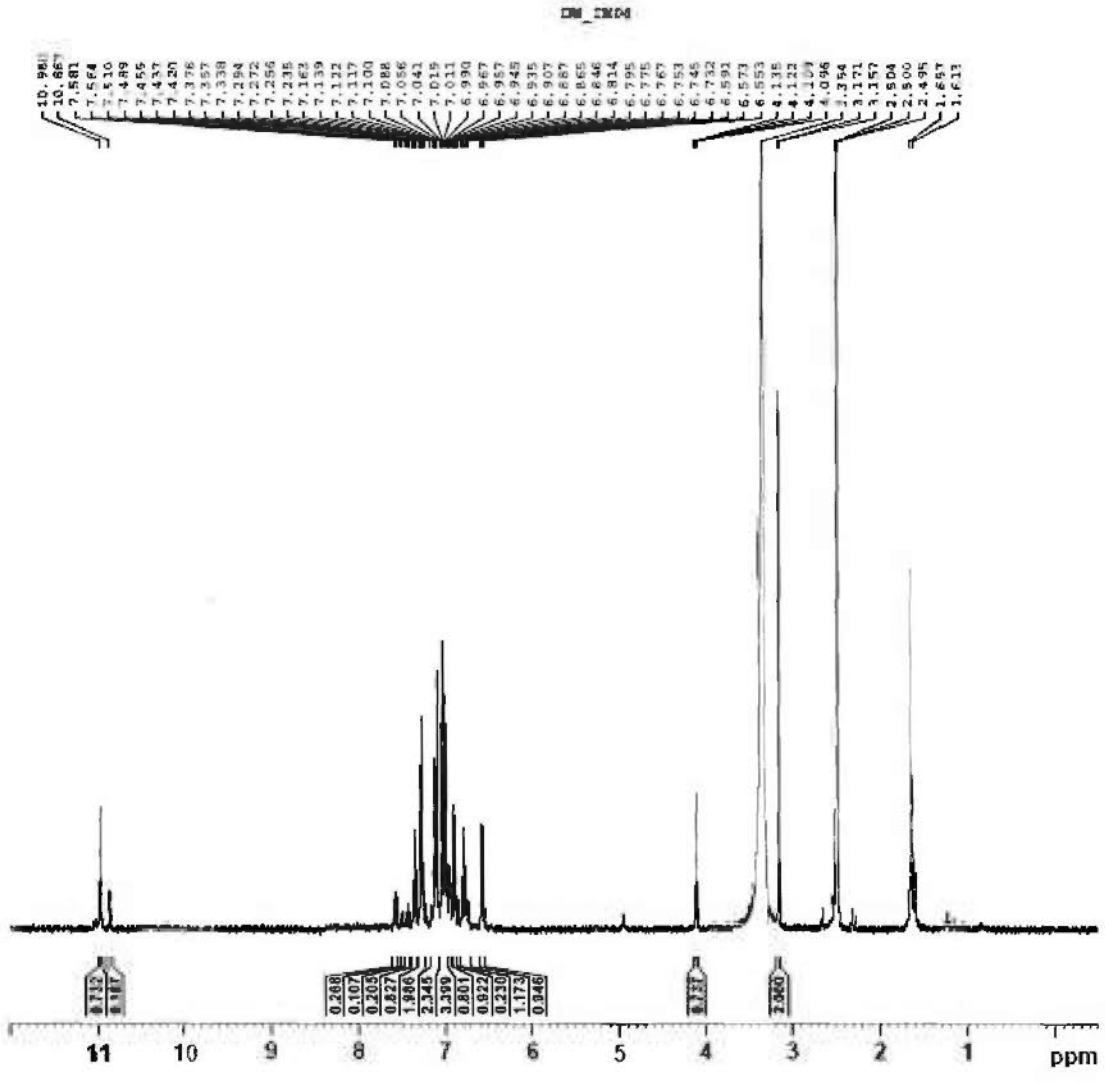

Figure 4.1a NMR analysis of DW-IN6.

Compound DW-IN6 was analyzed by NMR. NMR result showed that the compound's structure was identical with the structure provided by SPECS.

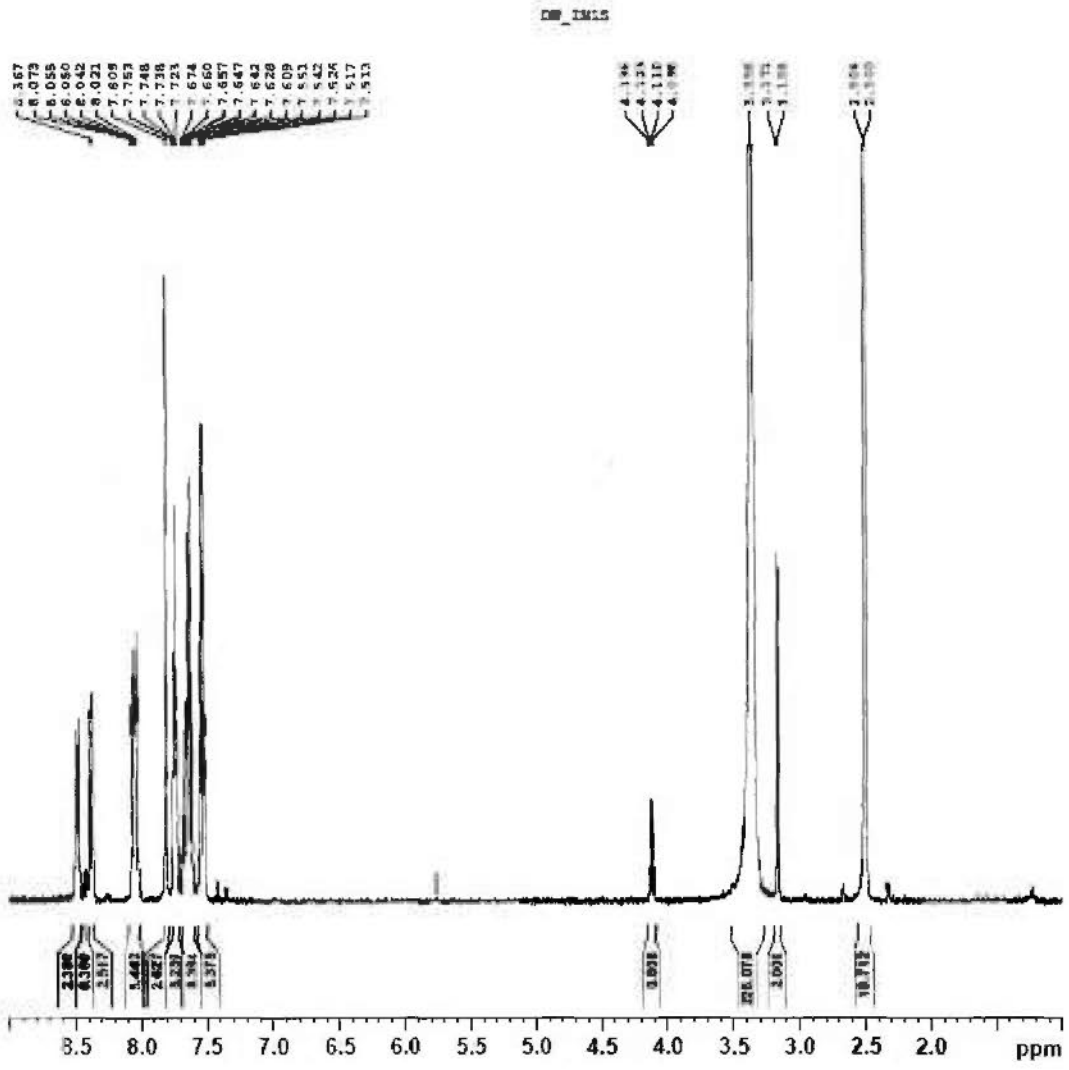

Figure 4.1b NMR analysis of DW-IN15.

Compound DW-IN15 was analyzed by NMR. NMR result showed that the compound's structure was identical with the structure provided by SPECS.

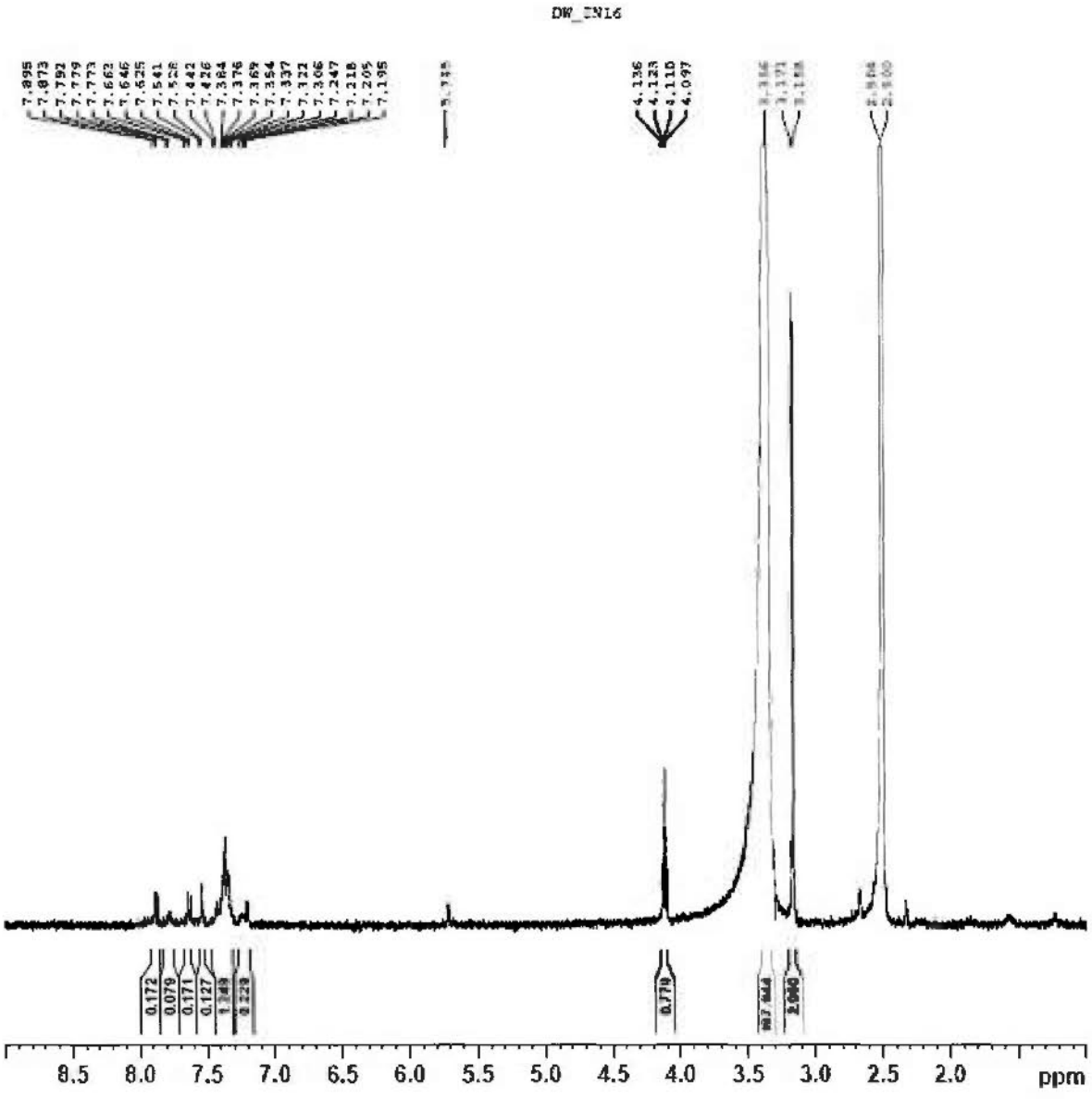

Figure 4.1c NMR analysis of DW-IN16.

Compound DW-IN16 was analyzed by NMR. NMR result showed that the compound's structure was identical with the structure provided by SPECS.

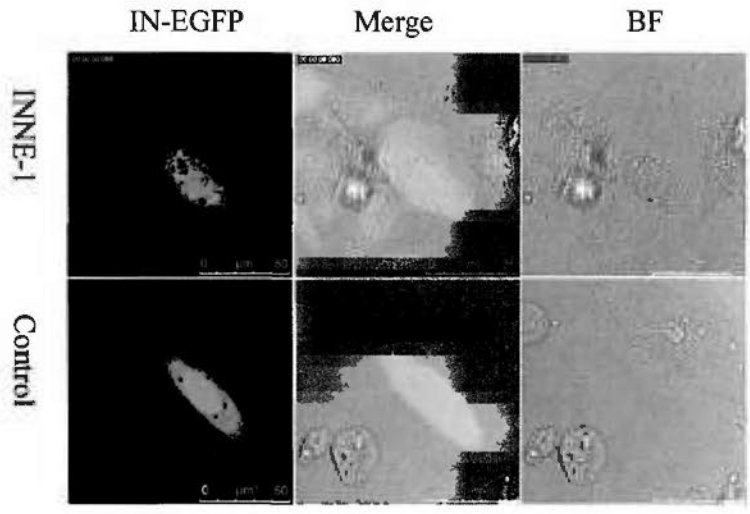

Figure 4.2 INNE-1 inhibited HIV-1 integrase nuclear translocation

INNE-1 was synthesized based on the structure information of DW-IN16. Cell imaging showed that INNE-1 inhibited IN nuclear translocation at 10 μM.

4.2.4 Synthesis of INNE-2, INNE-3, INNE-4, INNE-5, INNE-6 and NMR analysis

The first derivative, INNE-1, inhibited HIV-1 integrase nuclear translocation at 10μM. This result demonstrated that the design trend of new derivative is in the right direction. According to the structure and synthesis route of INNE-1, more modifications were designed to DW-IN16 and INNE-1. Subsequently, another five derivatives were synthesized named INNE-2, INNE-3, INNE-4, INNE-5 and INNE-6. NMR analysis showed that the five derivatives were with the correct structure as designed.

4.2.5 INNE-2 showed inhibition on HIV-1 integrase nuclear translocation

Integrase nuclear translocation assay was conducted to test the inhibition effect of the synthesized compounds. INNE-1 and DW-IN17 were tested under the same condition as positive controls. Cell imaging results showed that INNE-2, INNE-1 and DW-IN17 inhibited HIV-1 integrase nuclear translocation at 15μM (Figure 4.3).

4.2.6 INNE-1, INNE-2, INNE-3, INNE-4 showed inhibition on cytopathic effect in C8166 cells infected by HIV-1_{IIIB}

The derivatives of DW-IN16 were further studied for anti-HIV-1 activity. Syncytia assay were conducted to test whether these compounds could reduce cytopathic effect in T cell line C8166 infected by HIV-1_{IIIB}. Compounds were added to cell culture with infection at a 5-fold serial dilution from the beginning of 10μM. AZT was used as positive control. Results demonstrated that INNE-1, INNE-2, INNE-3, INNE-4 had significant effect on cytopathic effect reduction in C8166 cells infected by HIV-1IIIB with EC50 of 3.94μM, 4.90μM, 4.11 μM and 5.54μM respectively (Figure 4.4).

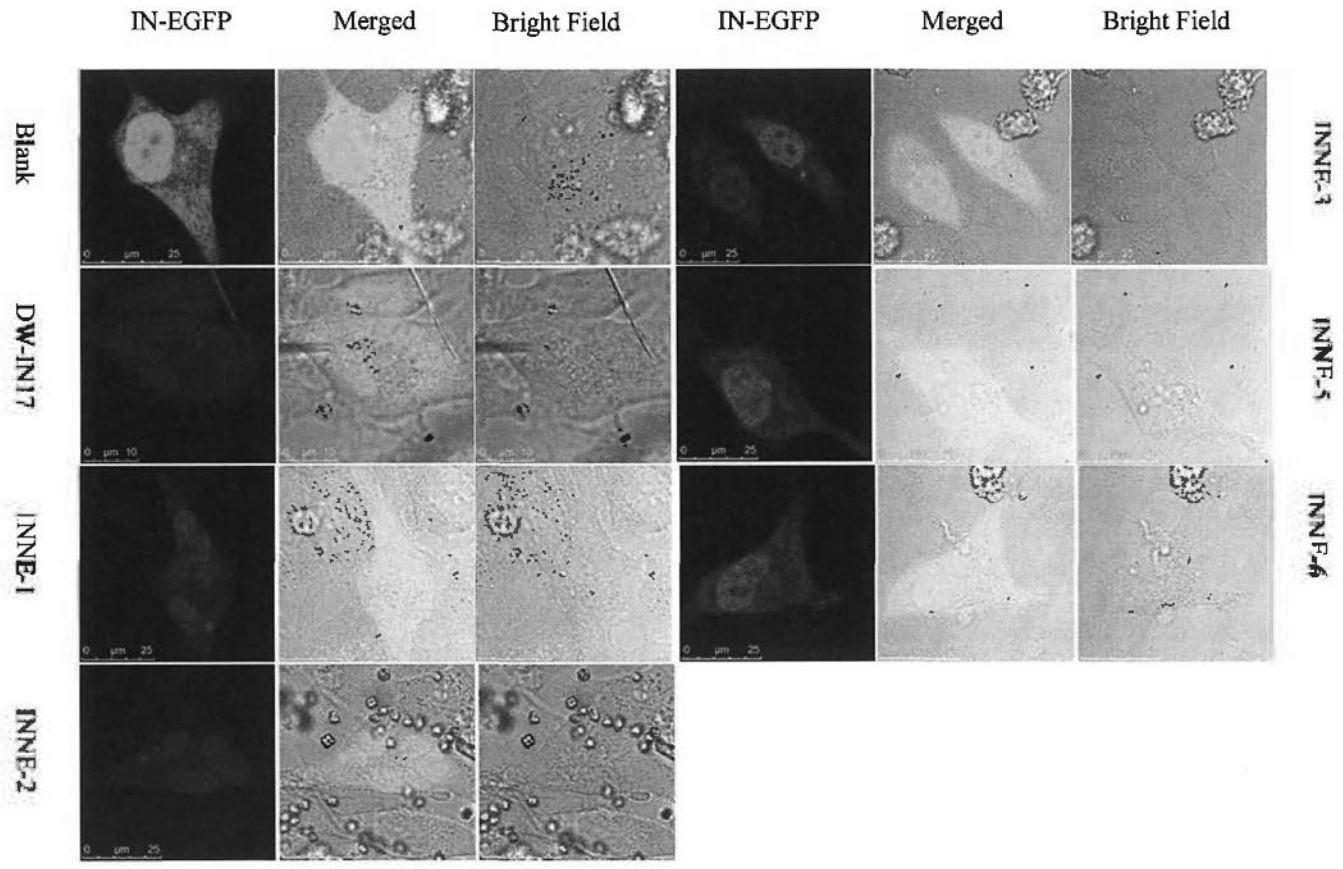

Figure 4.3 INNE-2 inhibited HIV-1 integrase nuclear translocation

Integrase nuclear translocation assay was conducted to test new derivatives' inhibition effect on HIV-1 integrase nuclear translocation. INNE-1 and DW-IN16 were tested under the same condition as positive controls. Cell imaging results showed that INNE-2, INNE-1 and DW-IN17 inhibited HIV-1 integrase nuclear translocation at 15μM. While INN-3, INN-5 and INN-6 failed to inhibit HIV-1 integrase nuclear translocation.

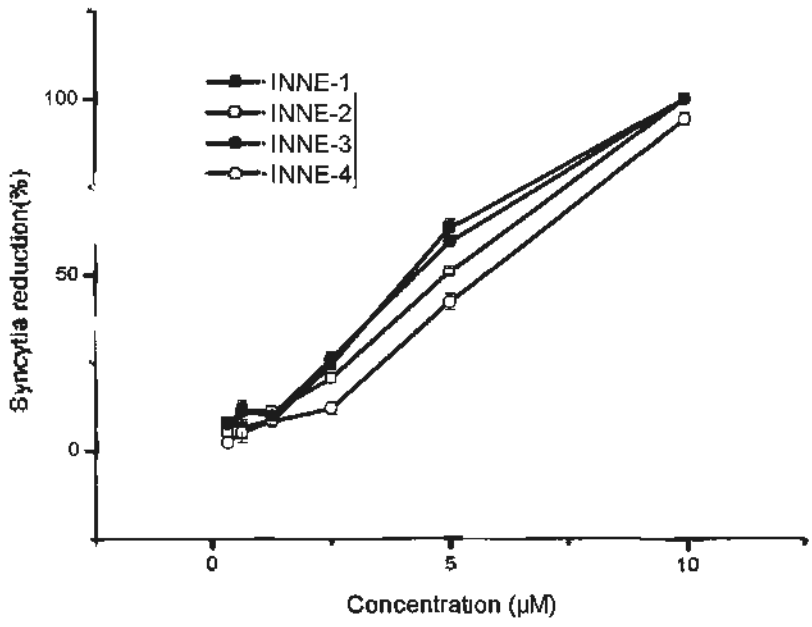

Figure 4.4 INNE-1, INNE-2, INNE-3, INNE-4 showed inhibition on cytopathic effect in C8166 cells infected by HIV-1_{IIIB}

Compounds were added to cell culture with infection at a 5-fold serial dilution from the beginning of 10μM. AZT was used as positive control. Results demonstrated that INNE-1, INNE-2, INNE-3, INNE-4 had significant effect on cytopathic effect reduction in C8166 cells infected by HIV-1IIIB with EC50 of 3.94μM, 4.90μM, 4.11μM and 5.54μM respectively. Data are shown as one test of three repeats.

4.2.7 P24 production inhibition in acute infection

Suppression of the synthesized compounds on viral replication was also assessed by measuring expression of HIV-1 P24 antigen. Compounds were added to cell culture with HIV-1_{IIIB} infection at a 2-fold serial dilution from the beginning of 10μM. Results showed that INNE-1, INNE-2, INNE-3 and INNE-4 dramatically reduced P24 production in HIV-1_{IIIB} acute infected C8166 cells with EC_{50} value of 4.51μM, 5.98μM, 5.62μM and 6.97μM respectively (Figure 4.5).

4.2.8 MTT-based cytotoxicity assay

To reduce the cytotoxicity to human cells was one of the important concerns in designing and synthesizing of derivatives. Cellular toxicity of synthesized compounds was assessed by MTT method. Compounds were added to cell culture at a 2-fold serial dilution from the beginning of 20μM. Results showed that INNE-1, INNE-2, INNE-3 and INNE-4 had CC_{50} of 14.75μM, 7.93μM, 5.77μM and 6.34μM to human T cell line C8166 cells respectively (Figure 4.6).

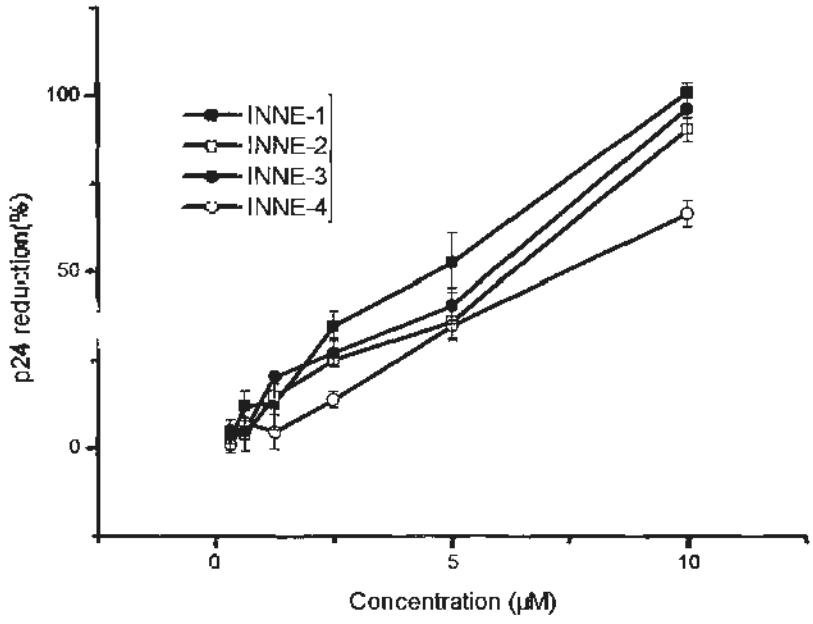

Figure 4.5 INNE-1, INNE-2, INNE-3, INNE-4 showed P24 production inhibition in acute infection

Compounds were added to cell culture with infection at a 2-fold serial dilution from the beginning of 10μM. Results showed that INNE-1, INNE-2, INNE-3 and INNE-4 dramatically reduced P24 production in HIV-1_{IIIB} acute infected C8166 cells with EC_{50} value of 4.51μM, 5.98μM, 5.62μM and 6.97μM respectively. EC50 of AZT was 1.47ng/ml. Data are shown as one test of three repeats.

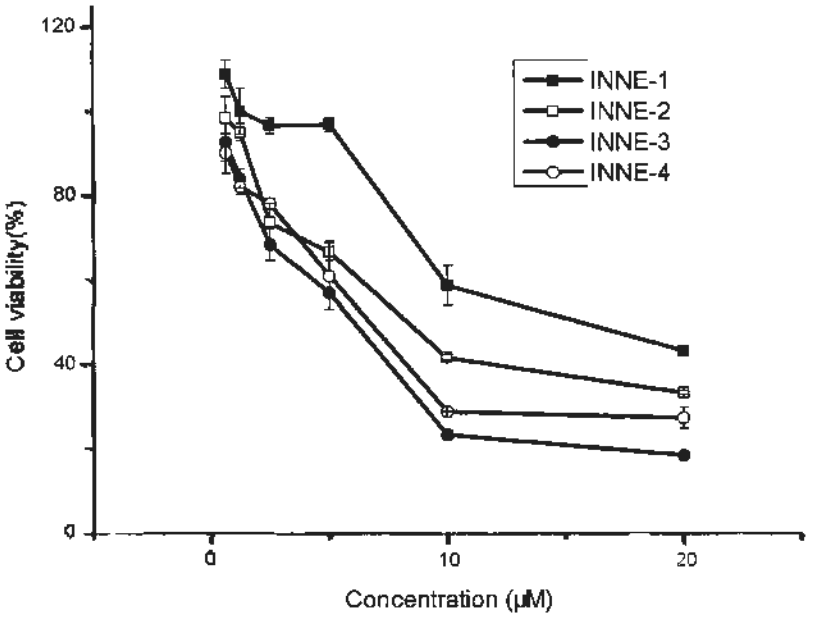

Figure 4.6 MTT-based cytotoxicity assay of INNE-1, INNE-2, INNE-3 and INNE-4

Cellular toxicity of synthesized compounds was assessed by MTT method. Compounds were added to cell culture at a 2-fold serial dilution from the beginning of 20μM. Results showed that INNE-1, INNE-2, INNE-3 and INNE-4 had CC_{50} of 14.75μM, 7.93μM, 5.77μM and 6.34μM to human T cell line C8166 cells respectively. Data are shown as one test of three repeats.

4.3 Discussion

Based on the structural interaction analysis of of HIV-1 integrase and it interaction with LEDGF (Cherepanov et al., 2005), virtual screening with the crystal structure of HIV-IN (PDB 1D:2B4J) on two chemical databases in public domain was conducted. It is hypothesized that small molecules that are of high affinity to disrupt the LEDGF-IN interaction so as to inhibitor integrase nuclear translocation. Such intearation-interation inhibiton may have resulted in the blockage of HIV-1 integrase to enter the nucleus and thereby to inibit HIV-1 integration and replication.

A structure-based virtual screening was performed by using the advanced docking program AutoDock 4.2, by starting with the crystal structure of dimeric catalytic core domain of HIV-1 IN complexed to the IN-binding domain of LEDGF(PDB ID:2B4J)(Cherepanov et al., 2005). The principal structural features of IN that are recognized by the host factor are the backbone conformation of residues 168–171 from one monomer and a hydrophobic patch that is primarily comprised of α-helices 1 and 3 of the second IN monomer. For molecular docking, the hydrophobic pocket enclosed by Chain A and Chain B including the LEDGF/p75 binding site in HIV-1 IN CCD dimer interface was used for virtual screening. In this work, a SPECS (http://www.specs.net/) library that contains 30000 drug-like molecules was screened. Small compounds were docked into the LEDGF/p75 -binding site of IN CCD dimer to obtain their docking modes, and they were ranked according to their calculated binding free energies. On the basis of virtual screening and commercial availability, a total of 23 candidates were selected for further study to provide experimental evidence of HIV-1 IN inhibition.

As shown in Chapter 3, only 8 of the 23 compounds, designated as, DW-IN4, DW-IN5, DW-IN6, DW-IN9, DW-IN15, DW-IN16, DW-IN17, DW-IN21 were found to inhibit the IN-LEDGF/p75 interaction and affect the HIV-1 IN nuclear

distribution at 1μM. These compounds suppressed viral replication by measuring HIV-1 P24 antigen production in HIV-1IIIB acute infected C8166 cells. These results provide useful structural information for further anti-HIV agent discovery. Cellular toxicity of eight compounds (DW-IN4, DW-IN5, DW-IN6, DW-IN9, DW-IN15, DW-IN16, DW-IN17, DW-IN21) were assessed by MTT method. Results showed that most compounds had CC_{50} of around or more than 10μM, indicating the compounds have modest toxicity to the cells.

During the course of the study, a separate natural product database (ZINC) was also used in the search for HIV-1 integrase inhibitors. Another way is to design and synthesize new compounds based on computational chemistry or existing HIV-1 inhibitors structural information. Several trials have been made in synthesis of new anti-HIV inhibitors.

New drugs are designed based on the structure information on the target proteins and existing drugs. After synthesis, newly synthesized drug candidates are tested for biological activity.. This will return useful structural information for understanding and interpreting of the effective structure and interaction between the drug and target protein. This feedback will assist scientists to design and synthesize more effective drugs.

Small molecules are more promising as drug candidates in anti-HIV treatment. But peptides discovery with anti-HIV character can provide us with some useful information on drug binding site and drug-virus interaction so as to assist further drug design and development.

In this study, several of small molecules from SPECS and ZINC with distinct structural diversity showed excellent binding affinity to integrase using the virual screeing analysis. These compounds were purchased from the vendors and were selected for screening on cell based imaging platform on integrase nuclear

translocation and immunofluorescence experiments. Among the 23 potential candidates, only eight of them showed predicted in vtiro inhibition of HIV-1 IN nuclear translocation. They are designated as compounds from SPECS (DW-IN4, DW-IN5, DW-IN6, DW-IN9, DW-IN15, DW-IN16, DW-IN17, DW-IN21) and one compound from ZINC (DW-IN719) as novel anti-HIV inhibitors targeting the interaction between integrase and cellular lens epithelium-derived growth factor LEDGF. These compounds suppressed viral replication by measuring HIV-1 P24 antigen production in HIV-1IIIB acute infected C8166 cells. These results might supply useful structural information for further anti-HIV agent discovery. Cellular toxicity of eight compounds (DW-IN4, DW-IN5, DW-IN6, DW-IN9, DW-IN15, DW-IN16, DW-IN17, DW-IN21) were assessed by MTT method. Results showed that most compounds had CC_{50} of around or more than 10μM.

On the basis of these findings, we hypothesize that if some new compounds with better effect on HIV-1 replication inhibition as well as lower cytotoxicity to human cell and human body could be synthesized, then these compounds would be good novel anti-HIV drug candidates. This would be beneficial to anti-HIV drug development and do contribution to the present HARRT treatment of HIV-1 infection.

Subsequently, three out of eight compounds from SPEC which showed significant inhibition on HIV-1 integrase nuclear translocation were selected for derivative synthesis candidates. These compounds were analyzed by NMR for purity and structure confirmation. NMR result showed that these compounds were with high purity with the right structure as provided by SPECS.

Based on the NMR information, one compound DW-IN16, was selected as study candidate. First, one derivative of DW-IN16 was synthesized, named INNE-1. The structure of INNE-1 was confirmed by NMR. INNE-1 inhibited HIV-1 integrase nuclear translocation at 10μM. This encouraged us to design and synthesize more compounds.

Based on the structural information and cell imaging results of both DW-IN16 and INNE-1, another five compounds named INNE-2, INNE-3, INNE-4, INNE-5, INNE-6 were synthesized. All the derivatives were analyzed for structure confirmation by NMR. Cell imaging results showed that INNE-1 and INNE-2 showed inhibitive effect on HIV-1 integrase nuclear translocation. Four compounds, INNE-1, INNE-2, INNE-3, INNE-4 showed HIV-1 inhibition effect with live virus infection. We demonstrated that INNE-1, INNE-2, INNE-3, INNE-4 had significant effect on cytopathic effect reduction in C8166 cells infected by HIV-1IIIB with EC50 of 3.94μM, 4.90μM, 4.11 μM and 5.54μM respectively. Experiment results showed that INNE-1, INNE-2, INNE-3 and INNE-4 dramatically reduced P24 production in HIV-1_{IIIB} acute infected C8166 cells with EC_{50} value of 4.51μM, 5.98μM, 5.62μM and 6.97μM respectively. Cellular toxicity of synthesized compounds was assessed by MTT method. Results showed that INNE-1, INNE-2, INNE-3 and INNE-4 had CC_{50} of 14.75μM, 7.93μM, 5.77μM and 6.34μM to human T cell line C8166 cells respectively. Compared with SPECS compounds, most of newly synthesized compounds have lower cytotoxicity.

The above data showed that the synthesis of new anti-HIV compounds are consistent with the structure activity prediction. Promising compounds have been synthesized such as INNE-1 and INNE-2, which showed inhibitory effect both in cell imaging and live virus assays. The next step may be to design more compounds that are the derivaties of these core structures. Compounds with stronger effect and lower toxicity would be achieved.

Chapter 5
Characterization of CXCR4 chemokine receptor internalization for development of new class of anti- AIDS drugs

5.1 Introduction

In this study, a platform on anti-AIDS drugs screening by expressing CXCR4-GFP on 293T cell line with lentivirus expression system was developed. Using cell imaging techniques, the GFP-tagged chemokine receptor CXCR4 using the lentivirus expression system was generated for live cell fluorescence imaging experiment. CXCR4 receptor is a critical co-receptor in CD4 positive lymphocytes mediating the fusion of HIV into the CD4 positive cells. CXCR4-C-GFP was over-expressed in 293T cells and the results showed that GFP-CXCR4 receptor is expressed at the plasma membrane of the cells. These cells will be used to monitor the blockage of CXCR4 receptor internalization as potential platform for drug development. It is hypothesized that antagonists to CXCR4 internalization may be potential candidates for development of new drugs that can block HIV-1 fusion into cells.

A library containing more than 150 drug like compounds and natural products extracted from herbs were screened for CXCR4 antagonists. After several rounds of screening, four compounds (KX128, KX166, KX171 and KX180) inhibited SDF-1 induced CXCR4 internalizaiton in cell based assay. These four compounds were further tested for HIV-1 inhibition through live virus asssays such as P24 produciton inhibition and syncytia formation inhibition assay in acute HIV infection. Results showed that KX128 inhibited HIV-1 replication significantly. The binding mode of these four compounds to CXCR4 was also analyzed by molecular docking.

5.2 Results

5.2.1 Expression of CXCR4-GFP fusion protein in 293T cells

Human CXCR4 gene (genebank ID: AY242129) was amplified by RT-PCR from the total RNA extracted from human T lymphoblasts (H9 cell line). The primer sequences are forward primer 5'-AAACATGGAGGGGATCAGTATATAC-3', reverse primer 5'-AGCTGAGTAACAGCGGACGGGAATCCCAAA-3'. After confirmation of its identity by DNA sequencing, CXCR4 cDNA was subcloned into lentivirus vector-pWPXL. The recombinant plasmid was confirmed by PCR with CXCR4 specific primers and by restriction enzyme digestion reaction with PmeI (20,000U/ml, NEB) and MluI (20,000U/ml, NEB), in 1X NEB buffer 4 and 1X NEB BSA in 37 °C overnight. Then transfer vector pWPXL-CXCR4, packing vector psPAX2 and envelope vector pMD2G were transformed into DH5α competent cells respectively. After single positive clones were selected for three vectors, clones were cultured in 20ml LB medium respectively with gentle shaking for overnight. The three vectors were extracted from the bacterial cultures according to the lentivirus production protocol as mentioned in section 2.2.7.2.

Lentivirus was produced by co-transfection of transfer vector pWPXL-CXCR4, packing vector psPAX2 and envelope vector pMD2G into Human embryo kidney (HEK) 293T cell line (Figure 5.1). Since the first generation of recombinant virus was with low infect efficiency, no obvious phenotypic changes were observed from the morphology of the cells. The infection was repeated for three times in 293T cells to get a high infective recombinant virus. After three rounds of infection, the infectivity of virus reached 40-50% percent. Then the recombinant virus liquid was concentrated with the protocol mentioned in 2.2.7.3. After concentration, the infectivity of the recombinant virus can reach up to 80-90%. After infection, the CXCR4-GFP was expressed mainly on 293T cell plasma membrane while GFP was expressed in the whole cell in 293T cells infected with control virus without foreign gene (Figure 5.2).

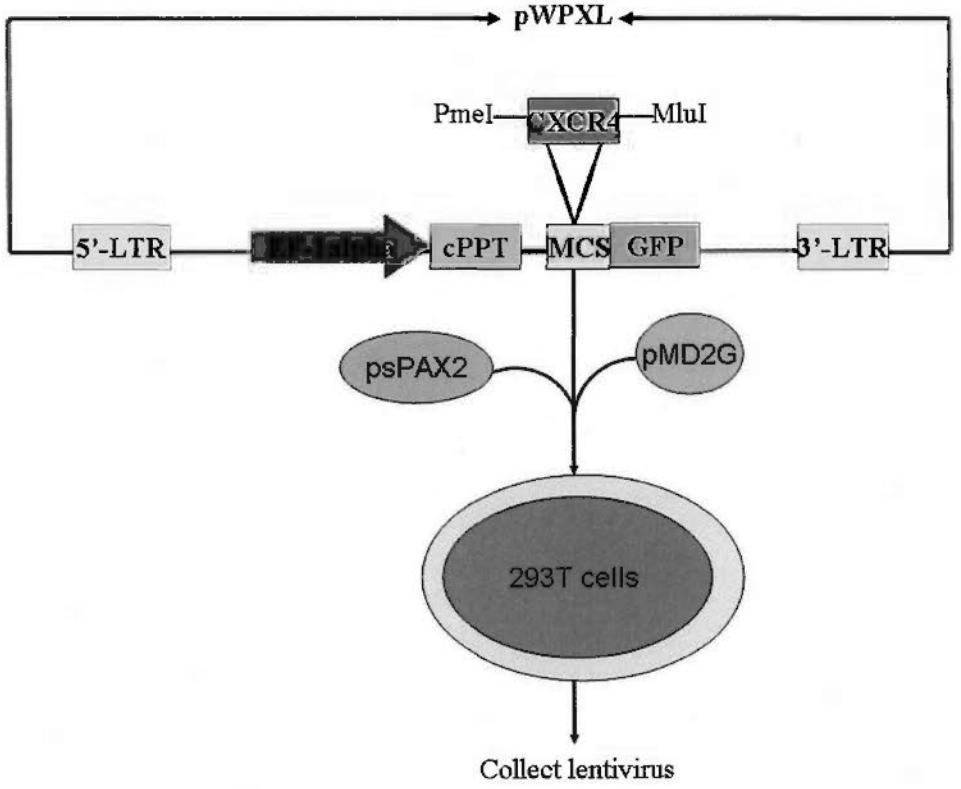

Figure 5.1 Production of CXCR4 expressing lentivirus

CXCR4 gene was cloned into the lentivirus expression vector pWPXL. Restriction enzyme sites used for CXCR4 cloning were PmeI and MluI. Expression of CXCR4 was fused with GFP. This made CXCR4 trackable in fluorescence microscopy. EF-1alpha (human elongation factor alpha) promoter leads to high expression of CXCR4-GFP fusion protein. cPPT (central polypurine tract) was introduced into the lentivirus expression vector to improve the efficiency of transduction(Park and Kay, 2001). Co-transfection of pWPXL-CXCR4-GFP, psPAX2 and pMD2G into 293T cells to produce recombinant viruses.

5.2.2 SDF1 induced CXCR4 internalization

Hela cells were infected with CXCR4 expressing lentivirus. Fourty-hours after infection, fluorescence analysis was performed with Leica SP5 confocal microscopy. Similar to infection of 293T cells, CXCR4-GFP was mainly expressed on the cell membrane of Hela cells (Figure 5.3). With the induction of an endogenous CXCR4 receptor agonist SDF-1α at 10 nM, the CXCR4 began to internalize in 15 minutes (Figure 5.3). More than 85% of plasma membrane expressed CXCR4 was internalized by 10 nM SDF-1α in 1 hour (Figure 5.4).

5.2.3 Stable cell line expressing CXCR4-GFP in 293T

The 293T cells stably transfected with high infective CXCR4-GFP expressing recombinant virus was established in this study. Forty-eight hours after infection, the percentage of infected cells was examined by fluorescence with Leica SP5 confocal microscopy. Green fluorescence expressed on the 293T cell membrane showed that infection was successful. By counting of fluorescence expressing cells, more than 50 percent of cells were infected successfully while the expression levels were different in all the infected cells. It was observed that although lentivirus has a character of integration of viral genes into host genome, not all the infected cells could live for a long time with foreign gene expression and many of the infected cells eventually died. Clonal selection was necessary to select clones with high degree of viability. After three rounds of clone selection, a stable cell line expressing CXCR4-GFP was established. To check the stability of the established cell line, the cells were cultured for more than 6 months continuously without evident change of CXCR4 expressing level (Figure 5.5). The positive cell percentage remained the similar to the cells at early passages. The stable cell line was stored in aliquot in liquid nitrogen for later use

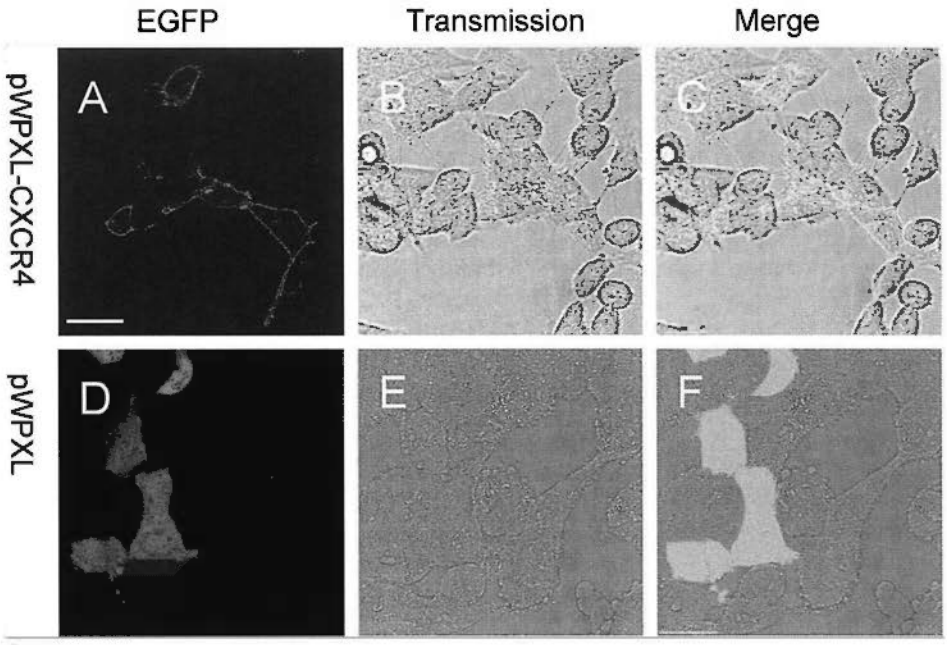

Figure 5.2 Expression of GFP-CXCR4 was localized on cellular membrane

293T cells were transiently infected with CXCR4 expressing lentivirus. Note the green fluorescence is highly localized on the membrane of the cells. The blank lentivirus without foreign gene was used as control. GFP expressed in the whole cell with equal distribution. Scale bar = 25μm.

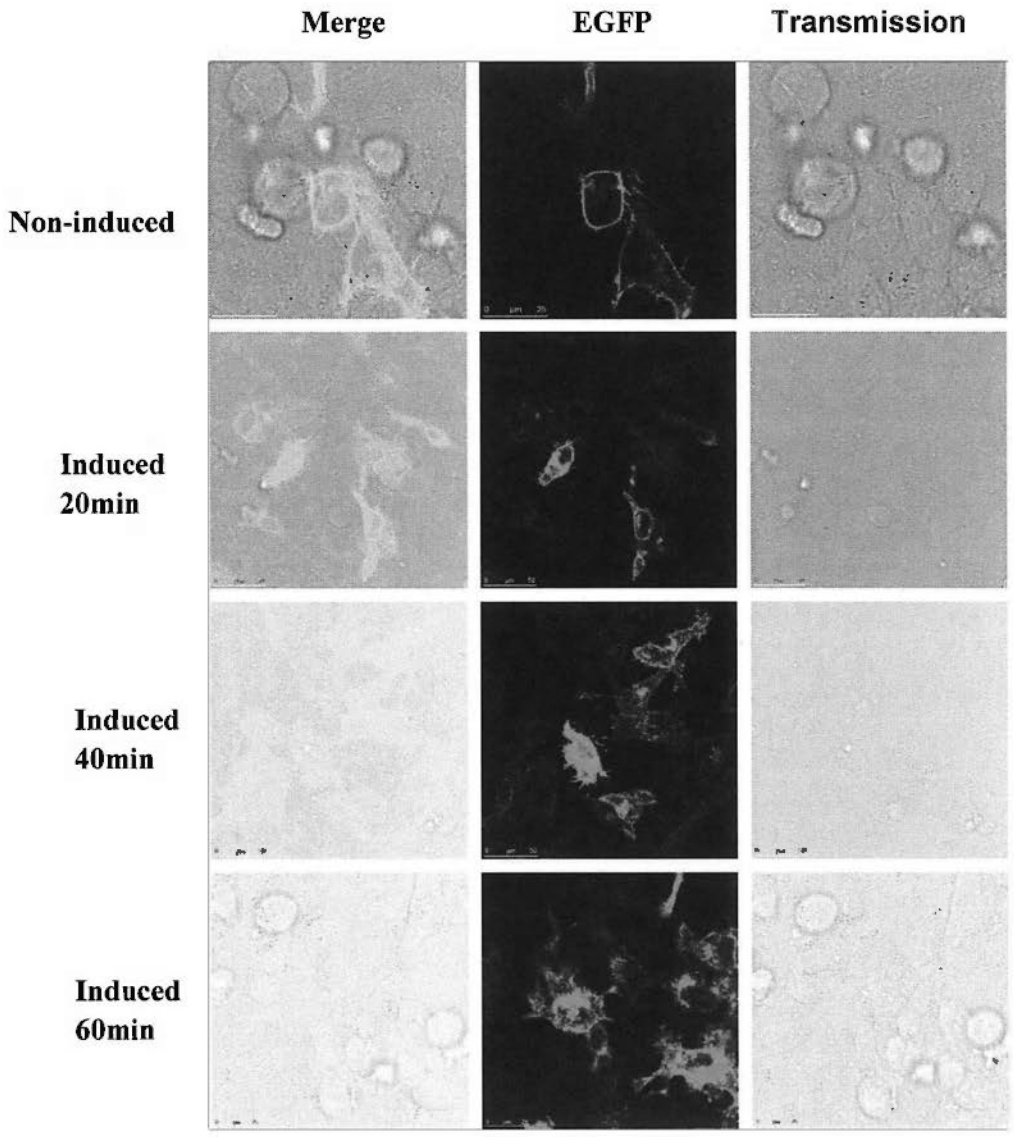

Figure 5.3 SDF1 induced CXCR4 internalization

Hela cells were infected with CXCR4 expressing lentivirus. CXCR4-GFP was mainly expressed on the cell membrane of Hela cells. Induced with SDF-1α at 10 nM, the CXCR4 began to internalize in 15 minutes. More than 85 percent of plasma membrane expressed CXCR4 was internalized by 10 nM SDF-1α in 1 hour.

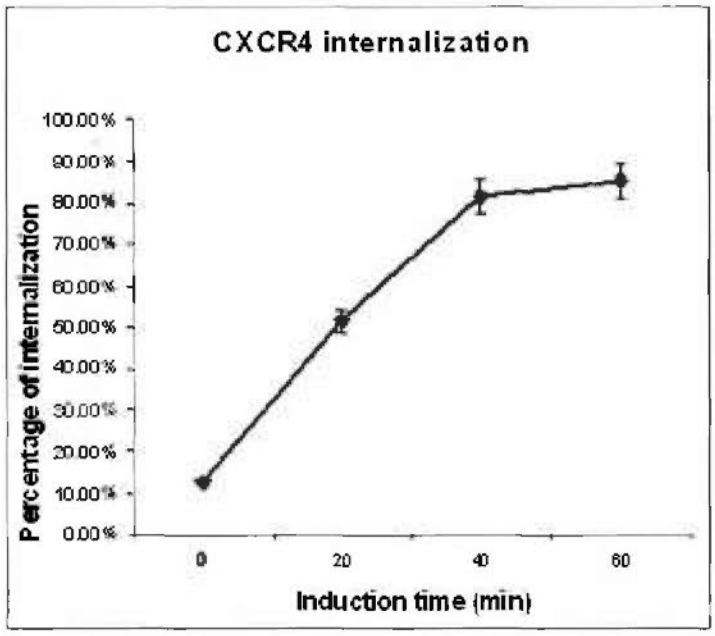

Figure 5.4 SDF1 induced CXCR4 internalization was time dependent

5.2.4 Fluorescence percentage of stable cell line measured by Flow Cytometry

After the CXCR4-GFP expressing stable cell line was constructed, the positive cells percentage was measured by flow cytometry. Fluorescence positive cells counting showed that 90.45% cells were expressing CXCR4-GFP fusion protein (Figure 5.6).

5.2.5 Screening of CXCR4 antagonist

In collaboration with Prof. YT Zheng of Kunming Institute of Zoology, compounds that have the antagonist activity against CXCR4 in stably tranfected cells, were screened. After several rounds of screening using the cell imaging experiment as described in section 2.2.4, four compounds (KX128, KX166, KX171, KX180) out of more than 150 showed CXCR4 internalization inhibition activity in cell based screening experiments (Figure 5.7). The structures of KX128, KX166, KX171 and KX180 were summarized showed in figure 5.8.

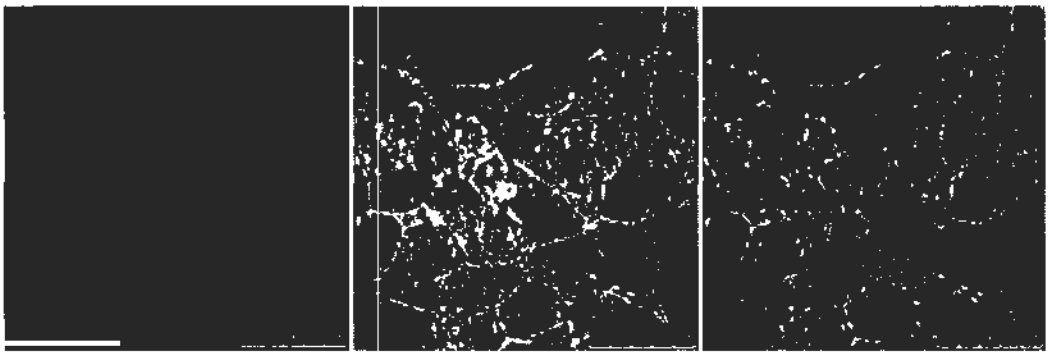

Figure 5.5 Stable 293T cell line expressing CXCR4-GFP.

Note that CXCR4 is preferentially expressed in the plasma membrane of the cells.

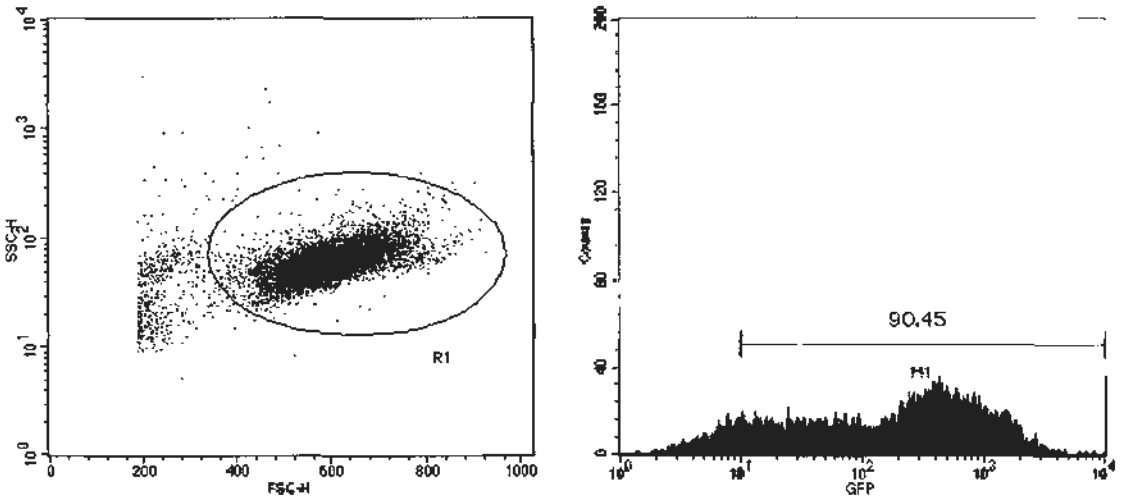

Figure 5.6 Flow cytometry analysis of stable cell line expressing CXCR4-GFP in 293T

Fluorescence cells percentage was measured by flow cytometry. Fluorescence positive cells counting showed that 90.45% cells were expressing CXCR4-GFP fusion protein

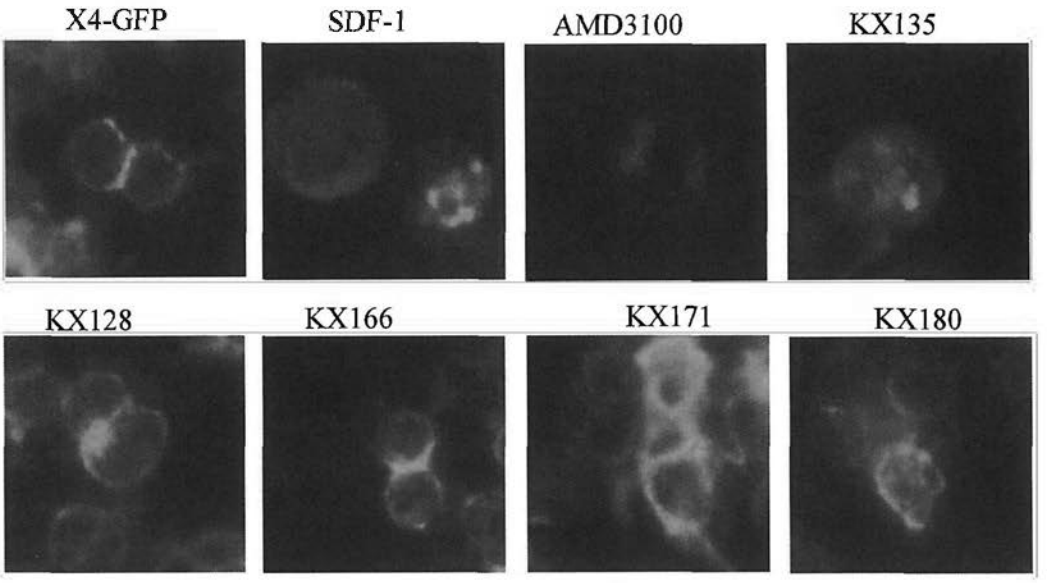

Figure 5.7 Screening results of CXCR4 antagonist

After several rounds of screening, four (KX128, KX166, KX171, KX180) out of more than 150 compounds showed CXCR4 internalization inhibitive activity in cell based screening experiments. CXCR4-expressing cells were pre-incubated with 200 μg/ml (KX128: 475.95μM, KX166: 254.78μM, KX171: 402.73μM, KX180: 323.25μM) compounds or 50μg/ml (62.95μM) AMD3100 for 15 minutes. Then SDF-1α was added to the culture at final concentration of 20nM. After induction of 45 minutes, cells were fixed with 4% paraformaldehyde in PBS for 15 min at room temperature. One negative result KX135 is shown as control.

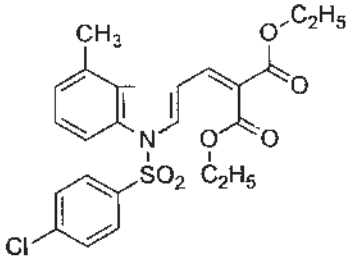

KX128

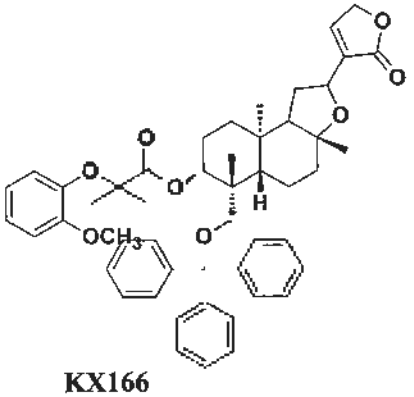

KX166

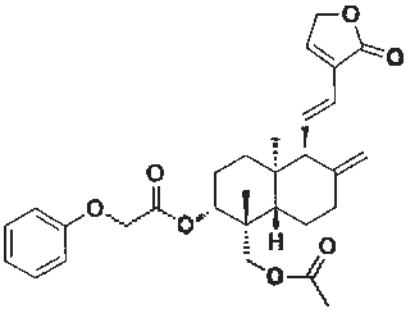

KX171

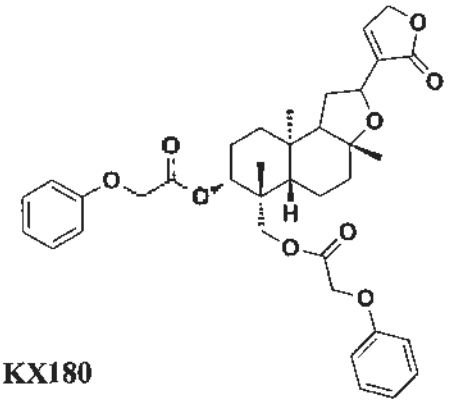

KX180

Figure 5.8 Structures of KX compounds

5.2.6 Molecular docking

Previous studies from other research groups have reported that two chemicals, designated as of IT1t and AMD3100 had CXCR4 antagonist activity(Donzella et al., 1998; Thoma et al., 2008). The structures of IT1t and AMD3100 were showed in figure 5.9. Molecular docking was run by Autodock Vina. The binding sites were referred to the ligand binding pocket reported in crystal structure of CXCR4 together with IT1t (PDB ID: 3ODU) (citation). A girdbox of 40×40×40 was applied in the docking. Others parameters were set as default. To compare KX compounds' binding affinity to CXCR4, KX128, KX166, KX171 and KX180 were docked in comparison to those of IT1t and AMD3100. These six compounds were ranked according to the binding affinity to CXCR4 in molecular docking (Table 5.1). KX166 showed the highest binding affinity to CXCR4. KX180 and KX128 had the similar binding affinity following KX166. AMD3100, KX171 and IT1t had similar binding affinity.

The interaction of these compounds with CRCR4 was analyzed by Pymol and Ligplot (http://www.pymol.org, http://www.ebi.ac.uk/thornton-srv/software/LIGPLOT/). The docking results showed that KX128, KX166, KX171, KX180 and AMD3100 were docked into the hydrophobic pocket formed by surrounding residues of CXCR4.

AMD3100 formed four H-bonds with CXCR4. OD1 of Asp97 formed two H-bonds with N3 and N7 of AMD3100 with distances of 2.80 Å and 3.22 Å respectively. N5 of AMD3100 formed H-bond with O of Cys186 with a distance of 2.88 Å. N4 of AMD3100 formed H-bond with OE1 of Gln200 with a distance of 3.00 Å. Besides, AMD3100 formed hydrophobic contacts with His113, Ala98, Asp187, Phe199, Tyr190, Trp94 and Arg188 respectively (Figure 5.10).

KX128 formed three H-bonds with CXCR4. O19 of KX128 formed a H-bond with OH of Tyr116 with a distance of 2.96 Å. O20 of KX128 formed two H-bonds with NH1 and NH2 of Arg188 with distance of 3.04 Å and 3.04 Å respectively. Besides,

KX128 formed hydrophobic contacts with Trp102, His113, Trp94, Leu41, Ile284 and Ile259 respectively (Figure 5.11).

KX166 formed four H-bonds with CXCR4. KX166 formed three H-bonds with His281 with a distance of 2.99 Å, with His113 with a distance of 3.18 Å, with Cys186 with a distance of 3.16 Å respectively. O56 of KX166 formed a H-bond with NH1of Arg30 with a distance of 2.99 Å. Besides, KX166 formed hydrophobic contacts with His113, Glu32, Ala98, Ile185, Trp94, Tyr45, Tyr116, Val112, Asp97, Ile284 and His281 respectively (Figure 5.12).

AMD3100

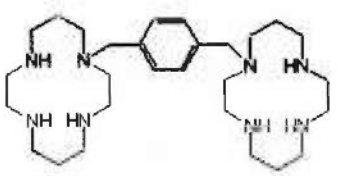

IT1t

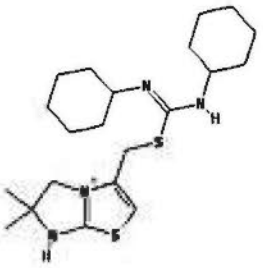

Figure 5.9 Structures of AMD3100 and IT1t.

Table 5.1 Ranking of KX128, KX166, KX171, KX180, AMD3100 and IT1t

CXCR4 crystal structure was selected from PDB (PDB ID: 3ODU). The binding sites were referred to the ligand binding pocket reported in crystal structure of CXCR4 together with IT1t (PDB ID: 3ODU).The docking was run by Autodock VINA. A gridbox of 40×40×40 was used for docking. Other parameters were set as default. The logarithm of the ratio of the concentrations of the un-ionized solute in the solvents is called log *P*; the log P values is also known as a measure of lipophilicity (http://en.wikipedia.org/wiki/Partition_coefficient). Compound with higher logP is more hydrophobic.

Compound	Affinity (kcal/mol)	LogP
KX166	**-10.7**	**21.247**
KX180	**-9.9**	**5.04**
KX128	**-9.7**	**4.59**
AMD3100	**-9.4**	**-2.80**
KX171	**-9.1**	**4.54**
IT1t	**-8.0**	**5.62**

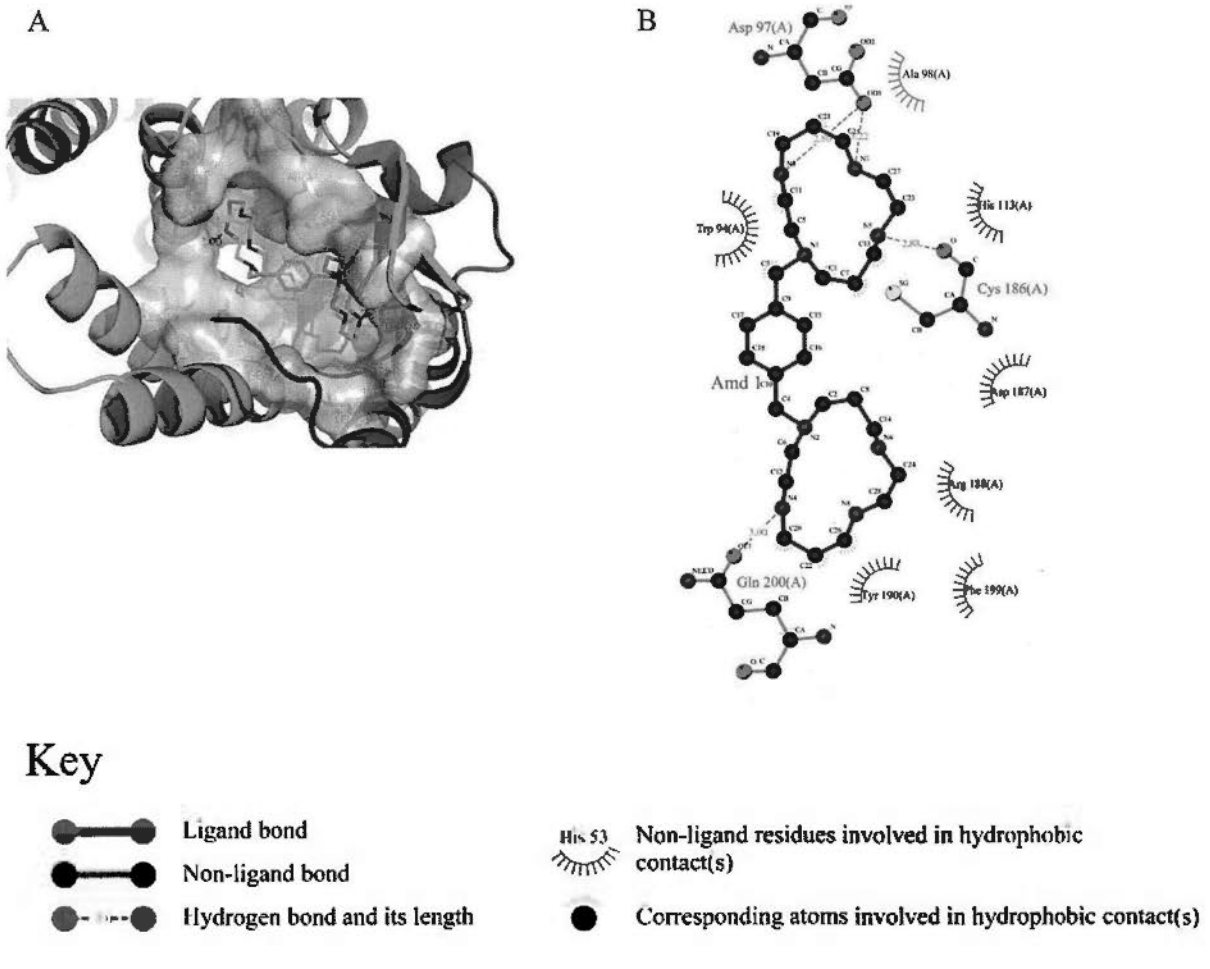

Figure 5.10 Interaction analysis between AMD3100 and CXCR4

A) The AMD3100 was shown as sticks. The secondary structure of CXCR4 was shown as cartoon. The H-bond was shown as red with distance label. AMD3100 was docked into the hydrophobic pocket formed by surrounding residues of CXCR4.
B) OD1 of Asp97 formed two H-bonds with N3 and N7 of AMD3100 with distances of 2.80 Å and 3.22 Å respectively. N5 of AMD3100 formed H-bond with O of Cys186 with a distance of 2.88 Å. N4 of AMD3100 formed H-bond with OE1 of Gln200 with a distance of 3.00 Å. Besides, AMD3100 formed hydrophobic contacts with His113, Ala98, Asp187, Phe199, Tyr190, Trp94 and Arg188 respectively.

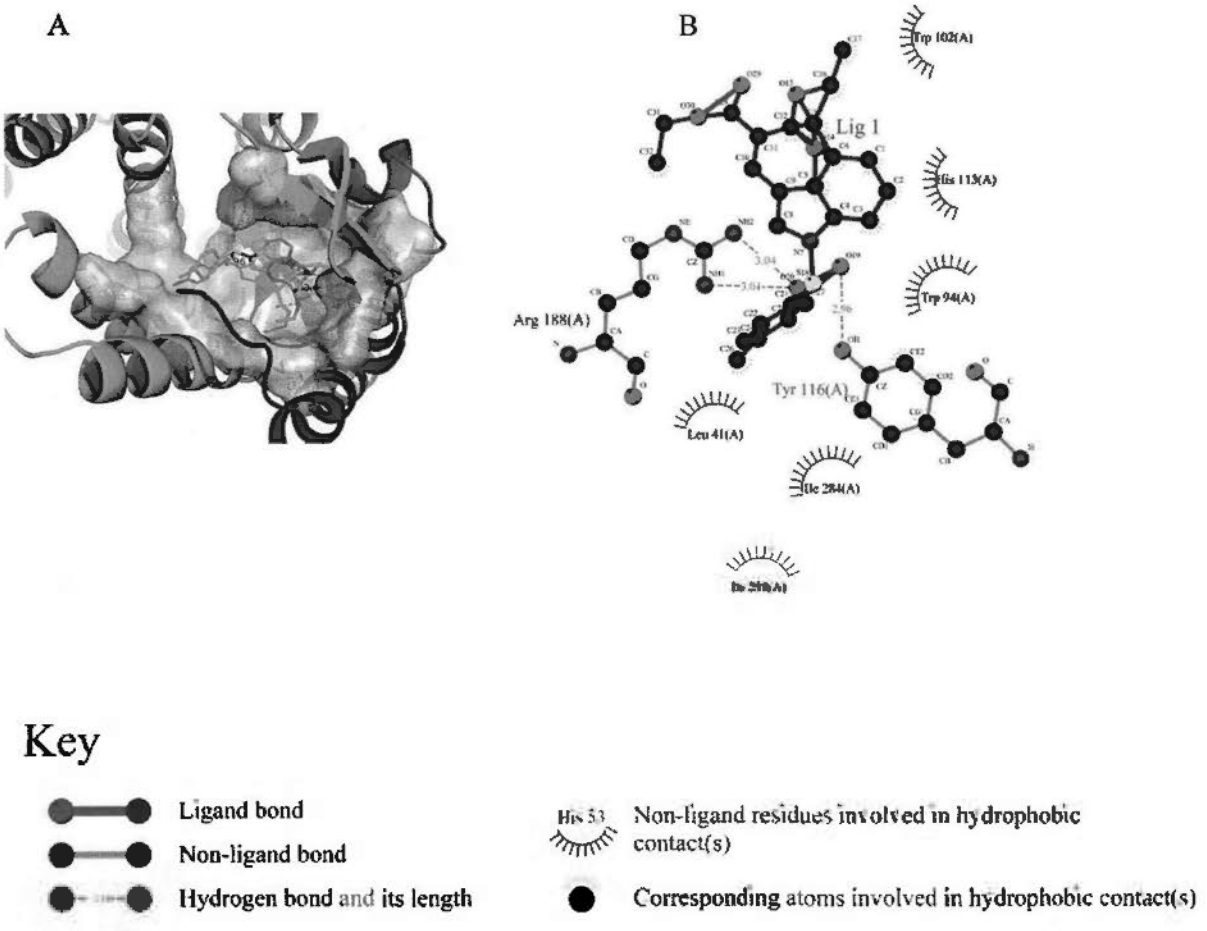

Figure 5.11 Interaction analysis between KX128 and CXCR4

A) The KX128 was shown as sticks. The secondary structure of CXCR4(PDB ID 3ODU) was shown as cartoon. The H-bond was shown as red with distance label. KX128 was docked into the hydrophobic pocket formed by surrounding residues of CXCR4.

B) O19 of KX128 formed a H-bond with OH of Tyr116 with a distance of 2.96 Å. O20 of KX128 formed two H-bonds with NH1 and NH2 of Arg188 with distance of 3.04 Å and 3.04 Å respectively. Besides, KX128 formed hydrophobic contacts with Trp102, His113, Trp94, Leu41, Ile284 and Ile259 respectively.

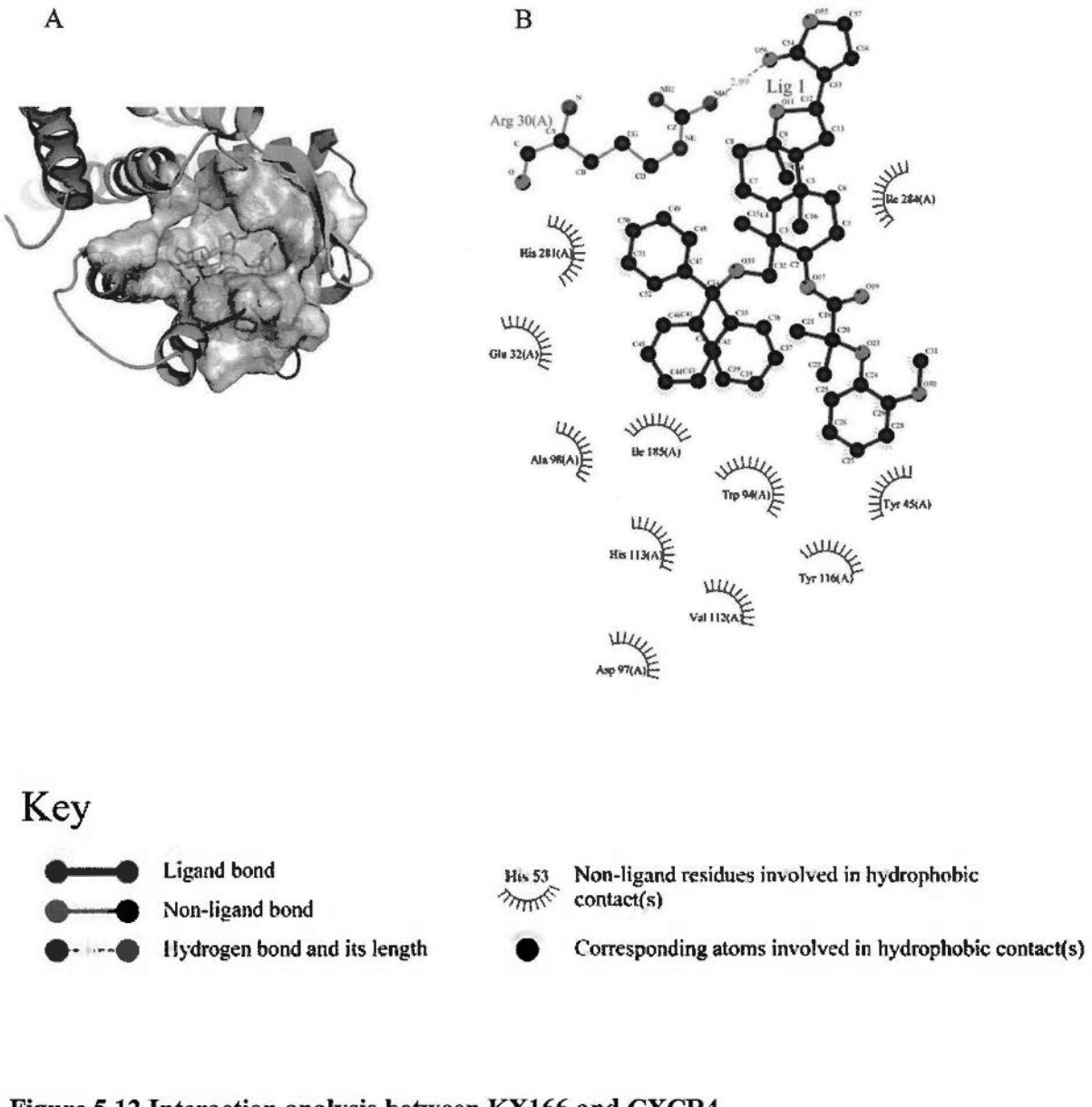

Figure 5.12 Interaction analysis between KX166 and CXCR4

A) The KX166 was shown as sticks. The secondary structure of CXCR4 was shown as cartoon. The H-bond was shown as red with distance label. KX166 was docked into the hydrophobic pocket formed by surrounding residues of CXCR4. KX166 formed three H-bonds with His281 with a distance of 2.99 Å, with His113 with a distance of 3.18 Å, with Cys186 with a distance of 3.16 Å respectively.
B) O56 of KX166 formed a H-bond with NH1of Arg30 with a distance of 2.99 Å. Besides, KX166 formed hydrophobic contacts with His113, Glu32, Ala98, Ile185, Trp94, Tyr45, Tyr116, Val112, Asp97, Ile284 and His281 respectively.

KX171 formed three H-bonds with CXCR4. O17 of KX171 formed H-bond with NE2 of Gln200 with a distance of 2.92 Å. O17 of KX171 also formed H-bond with OH of Tyr255 with a distance of 2.77 Å. O28 of KX171 formed H-bond with NH1 of Arg188 with a distance of 3.27 Å. Besides, KX166 formed hydrophobic contacts with His203, Leu120, Phe199, Glu288, Leu41, Trp94 and Ile204 respectively (Figure 5.13).

KX180 formed three H-bonds with CXCR4. KX180 formed H-bond with His113 with a distance of 3.15 Å. KX180 formed two H-bonds with Arg188 with distances of 3.05 Å and 3.20 Å respectively. KX180 formed hydrophobic contacts with Tyr116, Trp94 Val112, Tyr190 and Val196 respectively (Figure 5.14).

5.2.7 Syncytia assay

The compounds (KX128, KX166, KX171, KX180) that inhibited SDF-1 induced CXCR4 internalization were further analyzed in syncytia assay. Results demonstrated that KX128 had significant effect on cytopathic effect reduction in C8166 cells infected by HIV-1IIIB with EC50 of 1.13μM (0.54μg/ml). KX171 also had significant effect with an EC_{50} of23.16μM (11.52μg/ml). KX166 and KX180 had EC_{50} of 59.75μM (46.93μg/ml) and 29.58μM (18.39μg/ml) respectively. EC50 of AZT was 6.77nM (1.81ng/ml) (Figure 5.15).

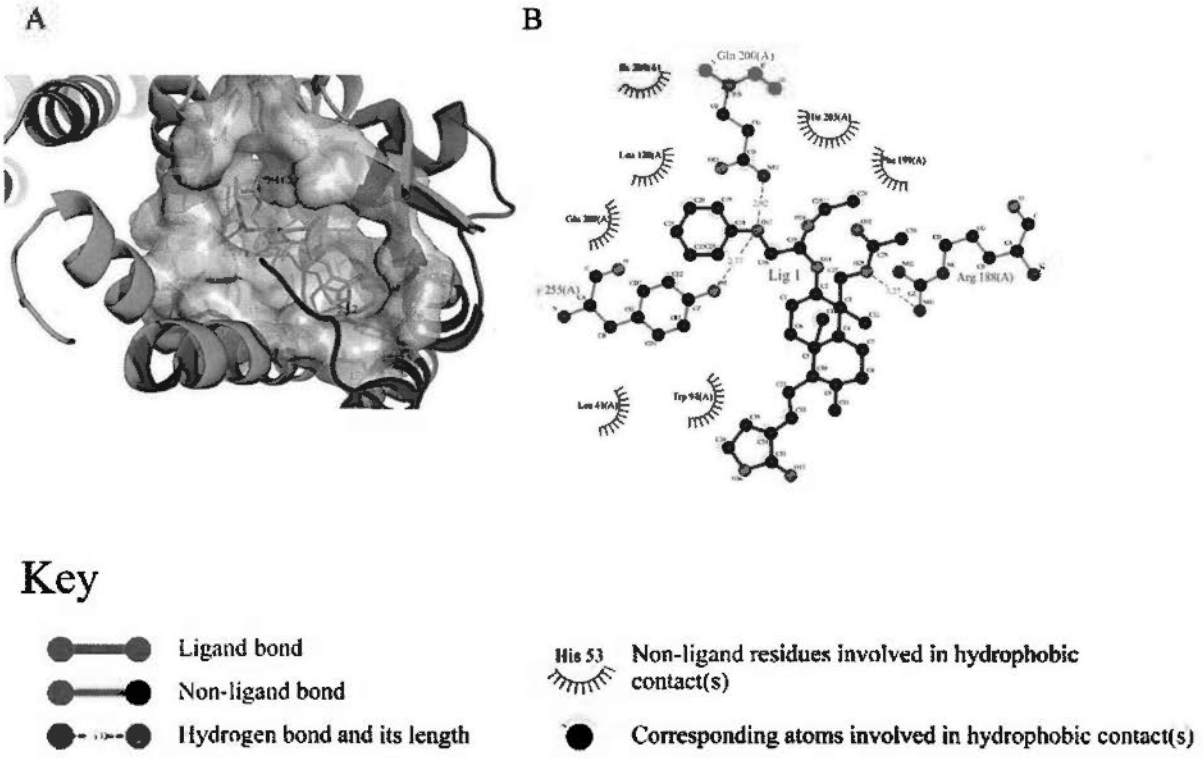

Figure 5.13 Interaction analysis between KX171 and CXCR4

A) The KX171 was shown as sticks. The secondary structure of CXCR4 was shown as cartoon. The H-bond was shown as red with distance label. KX171 was docked into the hydrophobic pocket formed by surrounding residues of CXCR4.
B) O17 of KX171 formed H-bond with NE2 of Gln200 with a distance of 2.92 Å. O17 of KX171 also formed H-bond with OH of Tyr255 with a distance of 2.77 Å. O28 of KX171 formed H-bond with NH1 of Arg188 with a distance of 3.27 Å. Besides, KX166 formed hydrophobic contacts with His203, Leu120, Phe199, Glu288, Leu41, Trp94 and Ile204 respectively.

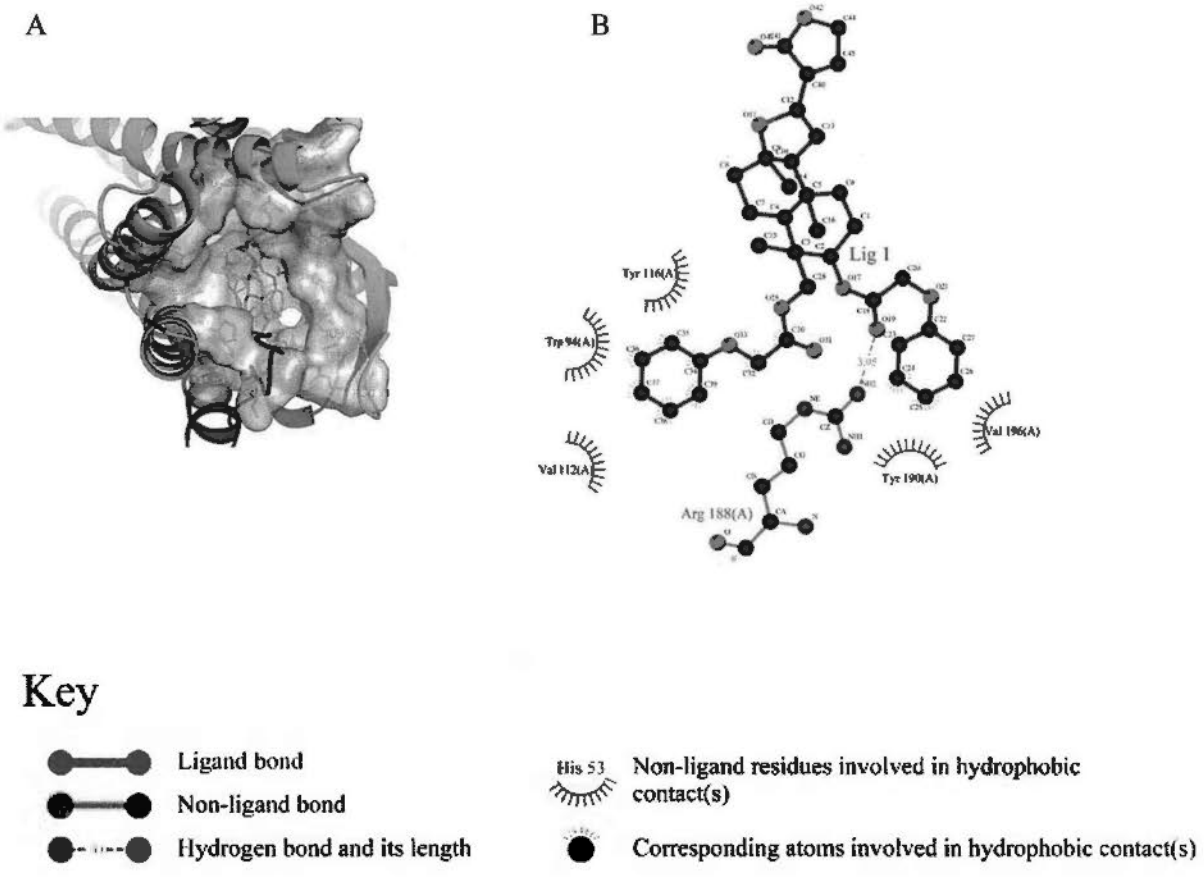

Figure 5.14 Interaction analysis between KX180 and CXCR4

A) The KX180 was shown as sticks. The secondary structure of CXCR4 was shown as cartoon. The H-bond was shown as red with distance label. KX180 was docked into the hydrophobic pocket formed by surrounding residues of CXCR4. KX180 formed H-bond with His113 with a distance of 3.15 Å. KX180 formed two H-bonds with Arg188 with distances of 3.05 Å and 3.20 Å respectively.
B) KX180 formed hydrophobic contacts with Tyr116, Trp94 Val112, Tyr190 and Val196 respectively.

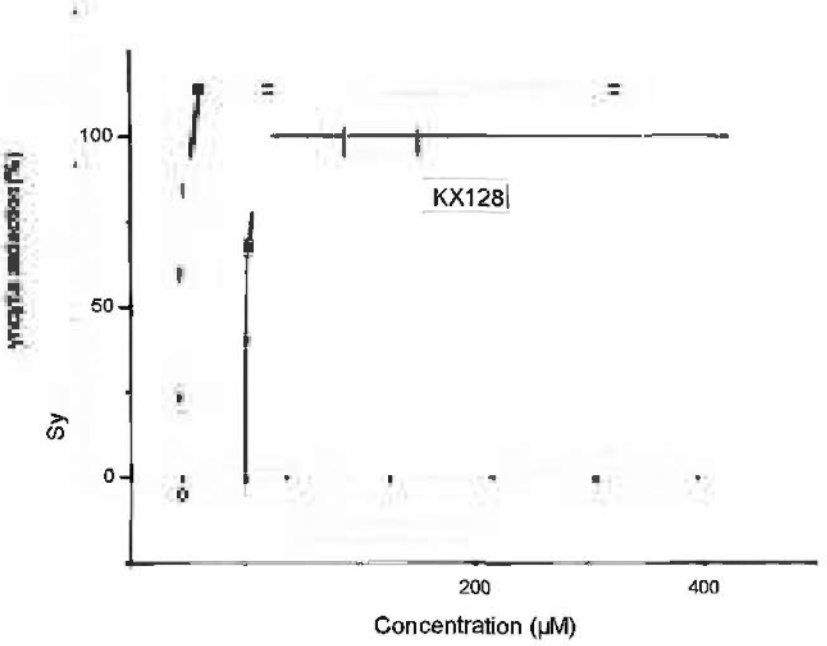
100
50
0
Sy
KX128
200
400
Concentration (μM)

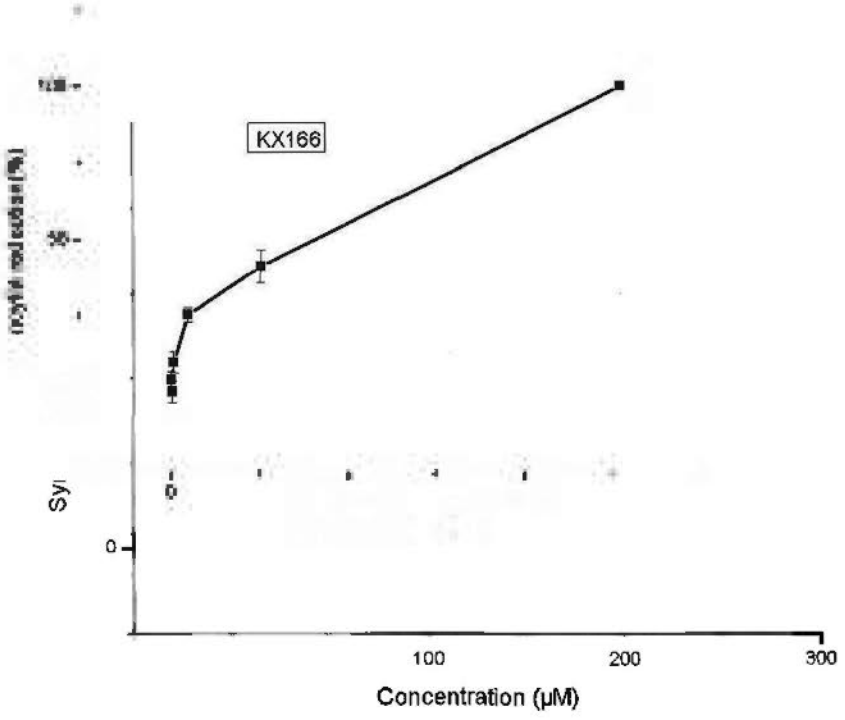
KX166
0
100
200
300
Concentration (μM)

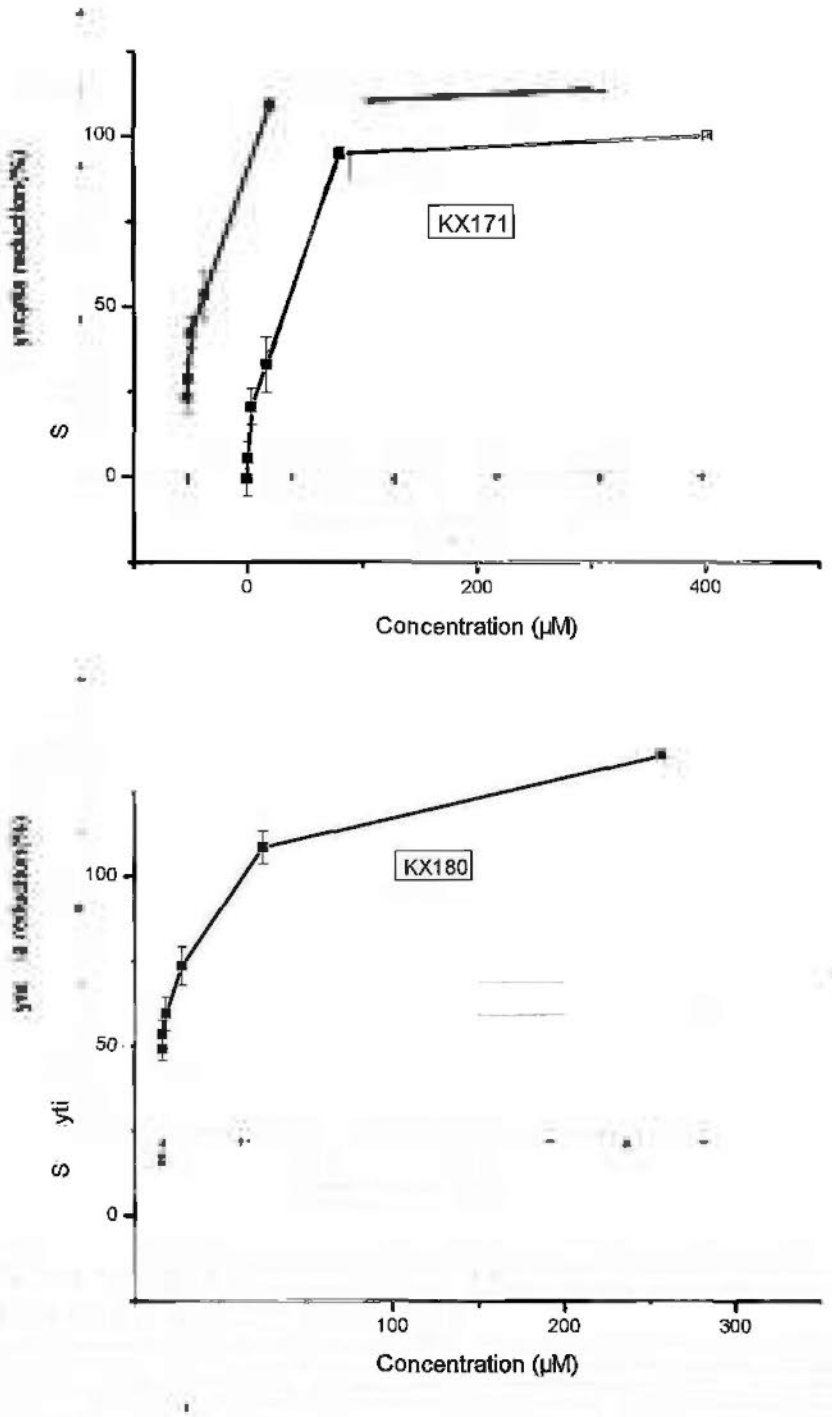

Figure 5.15 KX128, KX166, KX171 and KX180 showed inhibition on cytopathic effect in C8166 cells infected by HIV-1_{IIIB}

Compounds were added to cell culture with infection at a 10-fold serial dilution from the beginning of 100μg/ml. AZT was used as positive control. Results demonstrated that KX128 had significant effect on cytopathic effect reduction in C8166 cells infected by HIV-1IIIB with EC50 of 1.13μM (0.54μg/ml). KX171 also had significant effect with an EC_{50} of 23.16μM (11.52μg/ml). KX166 and KX180 had EC_{50} of 59.75μM (46.93μg/ml) and 29.58μM (18.39μg/ml) respectively.EC50 of AZT was 6.77nM (1.81ng/ml). Data are shown as one test of two repeats.

5.2.8 P24 production in acute infection assay of KX compounds

Four compounds (KX128, KX166, KX171, KX180) out of more than 150 compounds showed CXCR4 internalization inhibitive activity in cell based screening experiments. To further assay the compounds' effect on HIV-1 replication, P24 production reduction in acute infection assay were conducted. KX128 showed significant inhibition on P24 production in acute infection of HIV-1_{IIIB} with EC_{50} of 3.57μM (1.70μg/ml) and respectively. KX166, KX180 and KX171 had EC_{50} of 51.08μM (40.17μg/ml), 27.47μM (17.07μg/ml) and 38.46μM (19.1μg/ml) respectively (Figure 5.16). EC50 of AZT was 7.07μM (1.89ng/ml).

5.2.9 MTT-based cytotoxicity assay

Cellular toxicity of four KX compounds (KX128, KX166, KX171, KX180) were assessed by MTT method. Results showed that KX128, KX166, KX171, KX180 had CC_{50} of 2.68μg/ml(5.63μM), 187.63μg/ml(239.02μM), 33.78μg/ml(67.86μM) and 50.10μg/ml(80.97μM) respectively. CC_{50} of AZT was 1007.22μg/ml (3.76mM). (Figure 5.17).

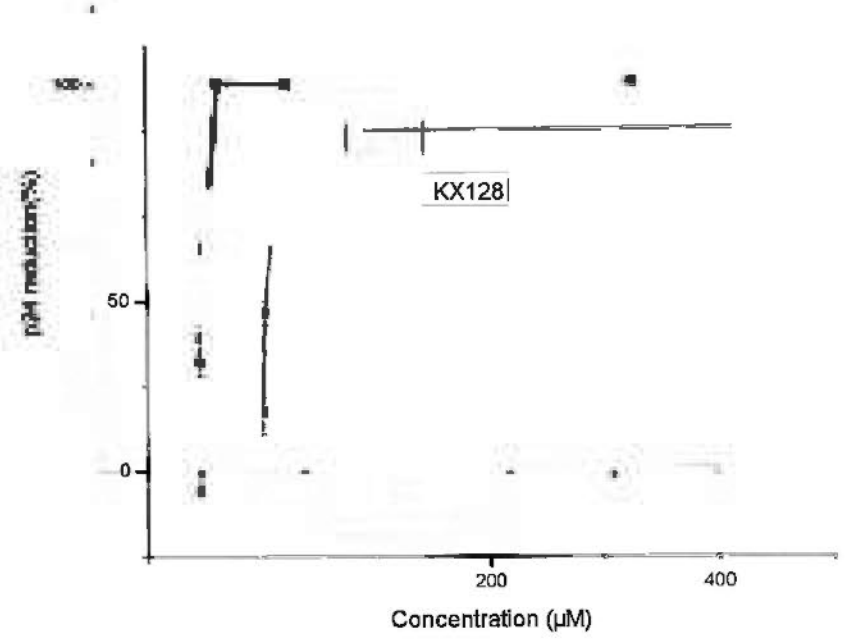
KX128
50
0
200
400
Concentration (μM)

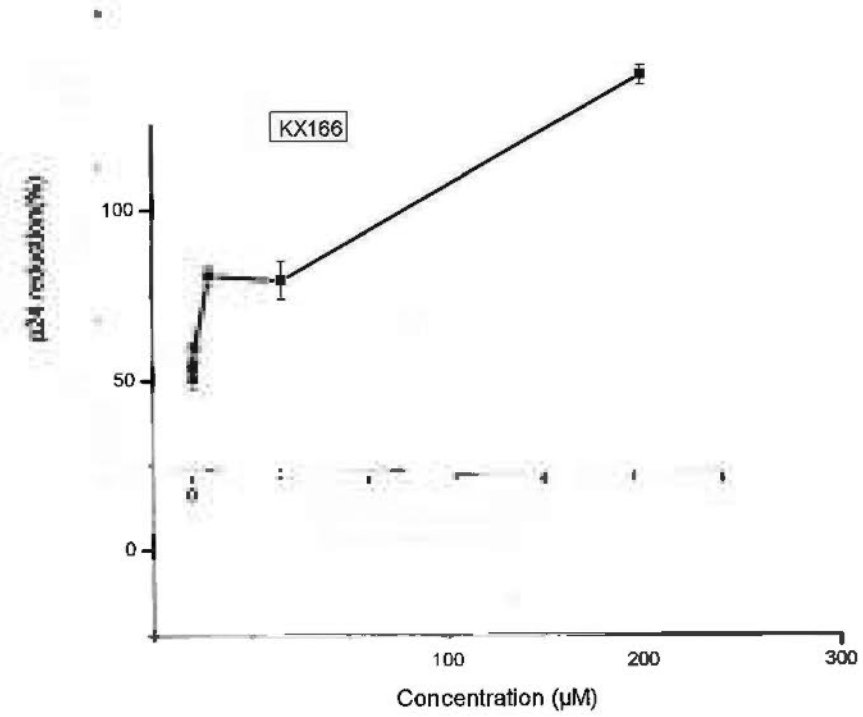
KX166
100
50
0
100
200
300
Concentration (μM)

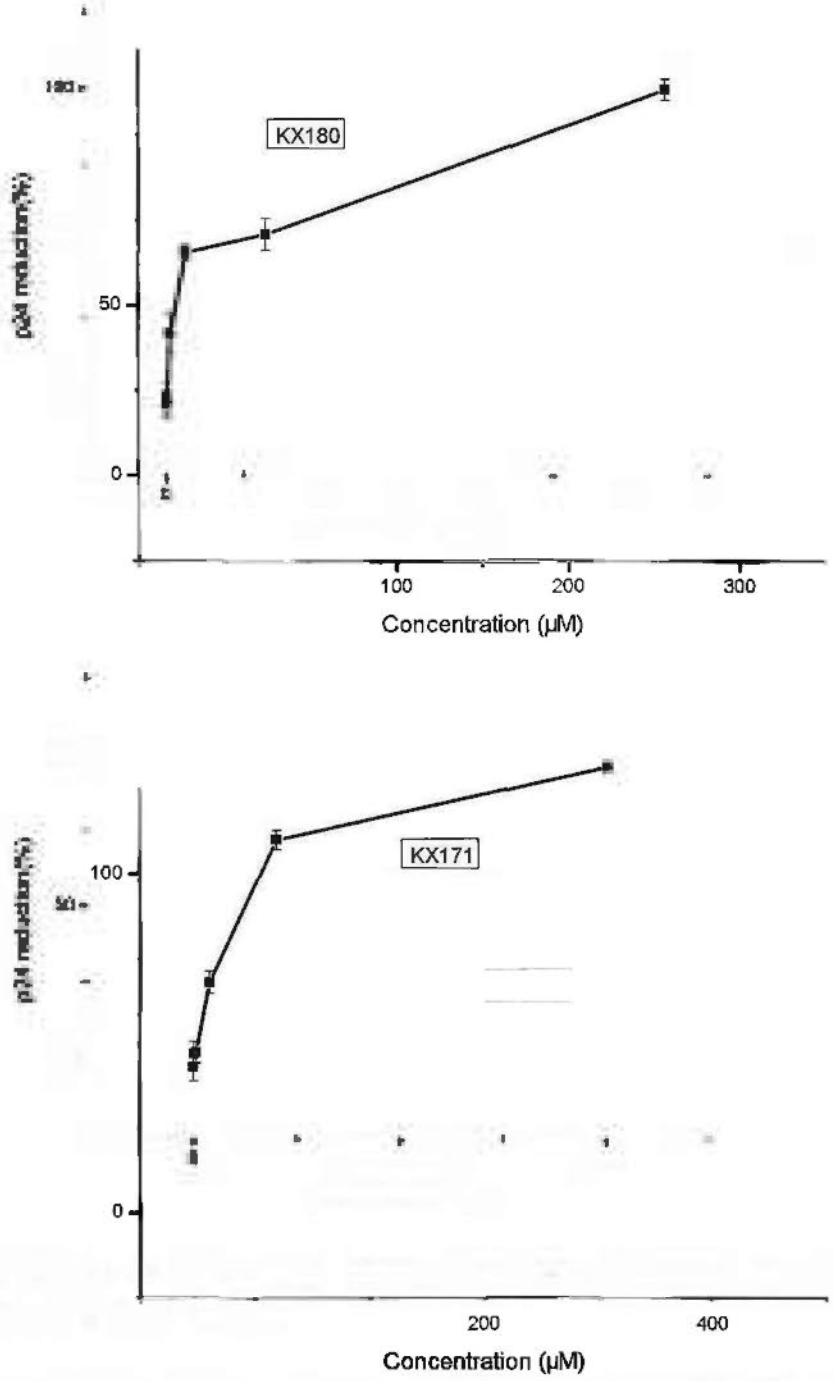

Figure 5.16 KX128, KX166, KX171 and KX180 showed P24 production inhibition in acute infection

Compounds were added to cell culture with infection at a 10-fold serial dilution from the beginning of 100μg/ml. KX128 showed significant inhibition on P24 production in acute infection of HIV-1_{IIIB} with EC_{50} of 3.57μM (1.70μg/ml) and respectively. KX166, KX180 and KX171 had EC_{50} of 51.08μM (40.17μg/ml), 27.47μM (17.07μg/ml) and 38.46μM (19.1μg/ml) respectively. EC50 of AZT was 7.07μM (1.89ng/ml). Data are shown as one test of two repeats.

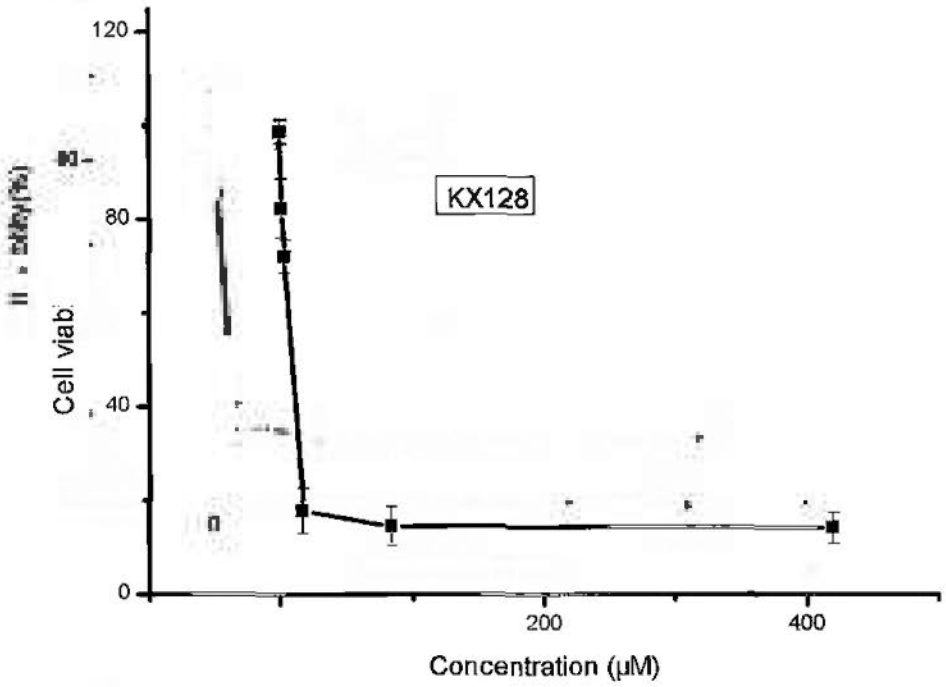
120
80
40
0
KX128
200
400
Concentration (μM)

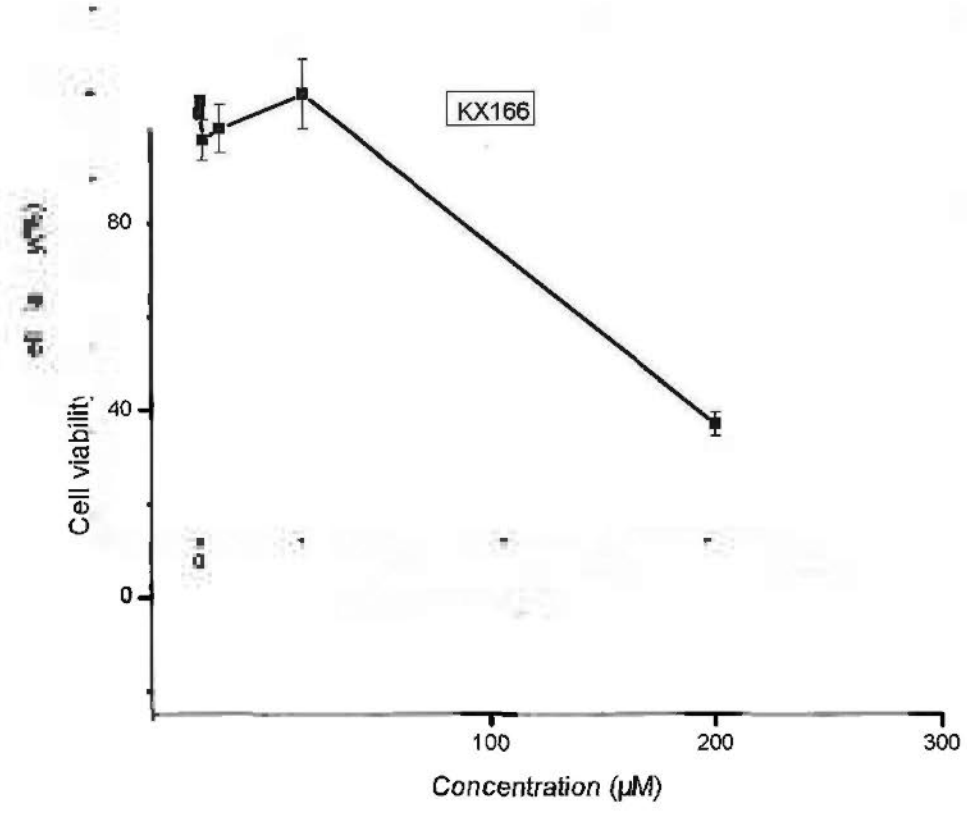
80
40
0
KX166
100
200
300
Concentration (μM)

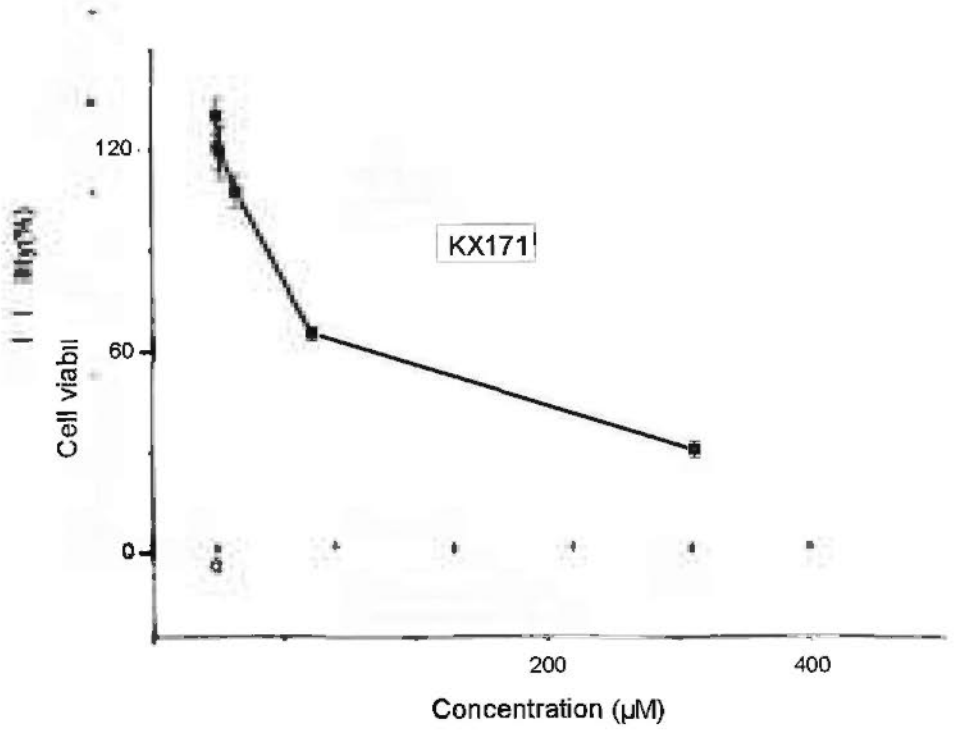

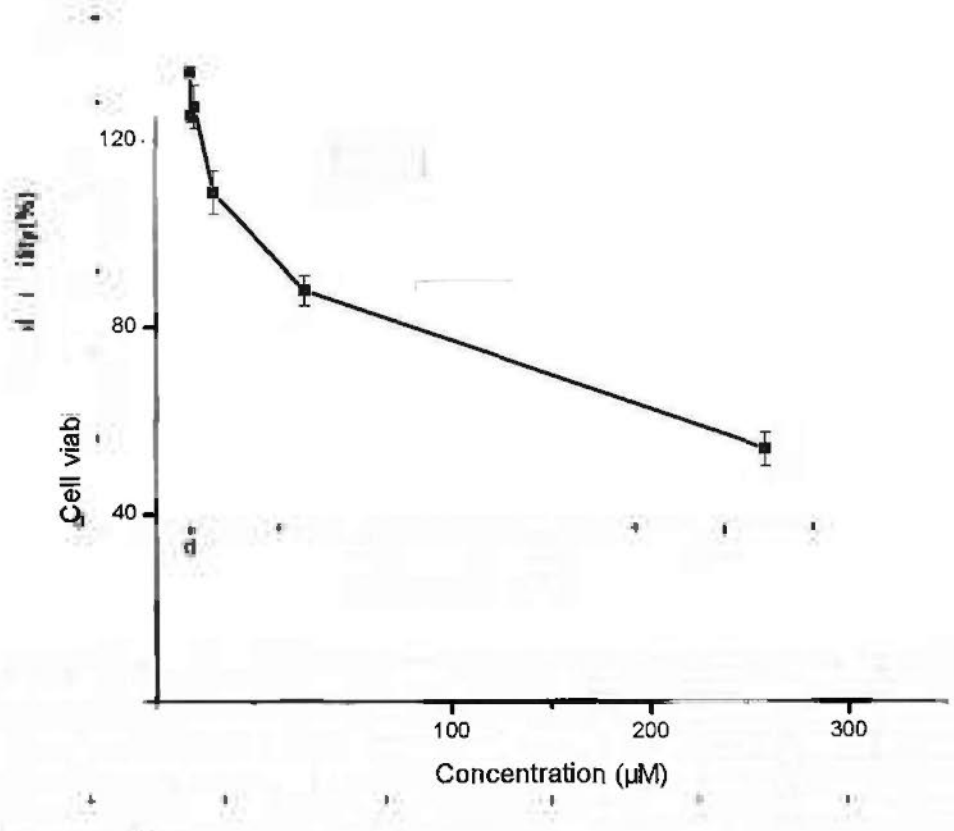

Figure 5.17 MTT-based cytotoxicity assay of KX128, KX166, KX171 and KX180
Cellular toxicity of four KX compounds (KX128, KX166, KX171, KX180) were assessed by MTT method. Results showed that KX128, KX166, KX171, KX180 had CC_{50} of 2.68μg/ml(5.63μM), 187.63μg/ml(239.02μM), 33.78μg/ml(67.86μM) and 50.10μg/ml(80.97μM) respectively. CC_{50} of AZT was 1007.22μg/ml(3.76mM). Data are shown as one test of two repeats.

5.3 Discussion

CXCR4, a known HIV-1 corecepto, is an attractive target for anti-HIV drug development. In this study, CXCR4 gene was amplified from total RNA extracted from human lymphoblasts (H9 cell line) by RT-PCR and cloned into lentivirus expresson vector. Lentivirus expressing system includes three vectors: transfer vector pWPXL, packing vector psPAX2 and envelop vector psMD2G (www.tronolab.com). Co-transfection of three vectors into 293T cells produces recombinant lentivirus. After DNA sequencing confirmation, CXCR4 was subcloned into lentivirus vector-pWPXL. Lentivirus was produced by co-transfection of transfer vector pWPXL-CXCR4, packing vector psPAX2 and envelope vector pMD2G into 293T cell line. By co-transfecting these 3 vectors into 293T cell line, CXCR4-expressing lentivirus particles were collected from culture medium. The first generation of recombinant virus was infective but with comparable low infectivity. To improve the infect efficiency, two methods are usually feasible. One is to concentrate the virus liquid by centrifuge. The other is to infect 293T cells with recombinant virus for several rounds until highly infective virus particles were achieved. Both methods were tried in this study. The second method showed better result in recombinant lentivirus production.

293T cells were infected with recombinant viruses. CXCR4 was expressed mainly on 293T cell plasma membrane. Some small bright spots were also observed in the intracellular space of infected cells. This showed that CXCR4 were accumulated in some part in the cell plasma in normal biological process. In fact, CXCR4 expression is a dynamic recycling process between cell membrane and intracellular space in normal cells (Wagener et al., 2009).

Similar to CXCR4 expression in 293T cells, CXCR4 was mainly expressed on the cell membrane of Hela cells. The expression level is also similar. With the induction of SDF-1α, the CXCR4 began to internalize in 15 minutes. More than 85 percent of

plasma membrane expressed CXCR4 was internalized by 10 nM SDF-1α in 1 hour. This demonstrated that the expressed CXCR4 was physiologically functional and was suitable for antagonist screening. The GFP tag made the CXCR4 bright green in real time fluorescence microscopy imaging. By monitoring the fluorescence imaging, CXCR4 antagonists screening was conducted.

The SDF-1 induced CXCR4 internalization demonstrated good biological activity of expressed CXCR4. When the infectivity efficiency of recombinant virus reaches 50-80%, establishment of stable cell line becomes easily obtained. Serial dilution and cloning ring were used in stable cell line establishing. Since CXCR4 were fused expression with GFP tag, pick out single positive cell became feasible under fluorescence microscopy observation.

A common problem in stable cell line establishment is the stability of the cell line. Since 100 percent positive cells were almost impossible to get in current culture, sometimes stable cell line lost foreign gene expression after a long period of culture. In this study, the stable line was cultured continuously for half a year without obvious decrease of CXCR4 expression was observed by fluorescence microscopy and flow cytometry analysis.

To predict the bound confirmations and the binding affinity, structures of receptor and ligand must be obtained. The protein structures are usually got from crystal study or NMR data. Since there was no enough and accurate structural information available before the screening of CXCR4 antagonists in this study, a cell based imaging screening platform was constructed as we described above.

Based on the drug data bank in Kunming Institute of Zoology (CAS), after several rounds of screening as we described above, four (KX166, KX180, KX171, KX128) out of more than 150 compounds showed CXCR4 internalization inhibitive activity in cell based screening experiments. Then the HIV inhibition activities were tested by

live virus in P3 lab. Results showed that these drugs had HIV inhibitory effect in some degree.

KX166, KX171 and KX180 have similar structures. They are derivatives isolated from the herb of andrographolide

[293H)-Furanone, 3-[2-[decahydro-6-hydroxy-5- (hydroxy-methyl)-5, 8a-dimethyl-2-methylene-1-naphthalenyl] ethylidene]dihydro-4-hydroxy-)].

Andrographolide was studied for potential clinical purpose as early as in 1981(Lu et al., 1981). Andrographolide was reported to inhibit growth of acute promyelocytic leukaemia cells by inducing retinoic acid receptor-independent cell differentiation and apoptosis(Manikam and Stanslas, 2009). Since andrographolide showed important clinical potential, a number of derivatives were synthesized. In 2007, four andrographolide derivatives, 3,19-isopropylideneandrographolide (2), 14-acetyl-3,19-isopropylideneandrographolide (3) and 14-acetylandrographolide (4) was synthesized and reported to have in vitro antitumour activities against a 2-cell line panel consisting of MCF-7 (breast cancer cell line) and HCT-116 (colon cancer cell line) (Jada et al., 2007). Benzylidene derivatives of andrographolide were found to inhibit growth of breast and colon cancer cells in vitro by inducing G(1) arrest and apoptosis(Jada et al., 2008). The above studies showed that andrographolide and its derivatives are important in anti-cancer research. While other studies showed that andrographolide and its derivatives also play important role in anti-virus research. Andrographolide and its derivatives were also reported to have activity against influenza virus in vivo and in vitro(Chen et al., 2009). Recent studies have showed that andrographolide has potential activity in anti-HIV research. A series of andrographolide derivatives were synthesized and demonstrated anti-HIV characteristics , including KX166, KX171 and KX180(Wang et al., 2010). In this study, these three andrographolide derivatives were discovered to inhibit SDF-1 inducing CXCR4 internalization. The possible binding modes of these derivatives to CXCR4 were built and several important residues were identified. These findings will provide assistance for further study of andrographolide, in the anti-HIV research

But since the compounds we screened are from different sources. Some are synthetic, some are derivatives (such as KX128, KX166 and KX180). Some samples were extraction from herbs without detailed information on structures and other chemical characters. It remains unclear exactly how these compounds inhibit CXCR4 internalization induced by SDF-1. It is proposed that new compounds should be synthesized based on these compounds. Through structural based modifications, it is hoped that better compounds could be found in which CXCR4 internalization inhibition could be demonstrated as drugs to combat HIV infection.

By analyzing the CXCR4 crystal structure, it was hypothesized that the IT1t interaction pocket is very suitable for ligand binding. The KX compounds' binding mode to CXCR4 was analyzed based on the IT1t-CXCR4 interaction information by Autodock Vina(Trott and Olson, 2010).

From the published data, IT1t formed hydrophobic contacts with CXCR4 through Arg183, Asp97, Asp187, Glu288, Ile185, Cys186, Trp102, Trp94, Val112 and Tyr116. Peptide CVX15 formed eight H-bonds with CXCR4 through Asp193, Asp 262, Asp 171, Asp 187, Tyr190 and Arg188.

AMD3100 was used as control in CXCR4 antagonist screening. Here we also analyzed the binding mode of AMD3100 to CXCR4. AMD3100 was docked into the hydrophobic pocket formed by surrounding residues of CXCR4. AMD3100 formed four H-bonds with CXCR4. OD1 of Asp97 formed two H-bonds with N3 and N7 of AMD3100 with distances of 2.80 Å and 3.22 Å respectively. N5 of AMD3100 formed H-bond with O of Cys186 with a distance of 2.88 Å. N4 of AMD3100 formed H-bond with OE1 of Gln200 with a distance of 3.00 Å. Besides, AMD3100 formed hydrophobic contacts with His113, Ala98, Asp187, Phe199, Tyr190, Trp94 and Arg188 respectively (Figure 5.14).

KX128, KX166, KX171 and KX180 were docked into the hydrophobic pocket formed by surrounding residues of CXCR4. KX128 formed three H-bonds with CXCR4: O19 of KX128 formed a H-bond with OH of Tyr116 with a distance of 2.96 Å. O20 of KX128 formed two H-bonds with NH1 and NH2 of Arg188 with distance of 3.04 Å and 3.04 Å respectively. Besides, KX128 formed hydrophobic contacts with Trp102, His113, Trp94, Leu41, Ile284 and Ile259 respectively (Figure 5.10). KX166 formed four H-bonds with CXCR4 totally. KX166 formed three H-bonds with His281 with a distance of 2.99 Å, with His113 with a distance of 3.18 Å, with Cys186 with a distance of 3.16 Å respectively. O56 of KX166 formed one H-bond with NH1of Arg30 with a distance of 2.99 Å. Besides, KX166 formed hydrophobic contacts with His113, Glu32, Ala98, Ile185, Trp94, Tyr45, Tyr116, Val112, Asp97, Ile284 and His281 respectively (Figure 5.11). KX171 formed three H-bonds with CXCR4. O17 of KX171 formed H-bond with NE2 of Gln200 with a distance of 2.92 Å. O17 of KX171 also formed H-bond with OH of Tyr255 with a distance of 2.77 Å. O28 of KX171 formed H-bond with NH1 of Arg188 with a distance of 3.27 Å. Besides, KX166 formed hydrophobic contacts with His203, Leu120, Phe199, Glu288, Leu41, Trp94 and Ile204 respectively (Figure 5.12). KX180 formed three H-bonds with CXCR4. KX180 formed H-bond with His113 with a distance of 3.15 Å. KX180 formed two H-bonds with Arg188 with distances of 3.05 Å and 3.20 Å respectively. KX180 formed hydrophobic contacts with Tyr116, Trp94 Val112, Tyr190 and Val196 respectively (Figure 5.13).

According to the ranking of affinity to CXCR4 in molecular docking, KX166 showed the highest binding affinity to CXCR4. KX180 and KX128 had the similar binding affinity following KX166. AMD3100, KX171 and IT1t had similar binding affinity.

From the binding mode, AMD3100 shares two amino acids with IT1t in interaction with CXCR4, the two amino acids are Asp97 and Cys186. AMD3100 shared four amino acids with CVX15 in interaction with CXCR4, they are Asp187, Tyr190, Trp94 and Arg188. KX128 shares two amino acids with IT1t, the two amino acids are

Trp102 and Trp94. KX166 shares four amino acids with IT1t, the four amino acids are Ile185, Trp94 and Tyr116, Val112. KX171 shares two amino acids with IT1t, the two amino acids are Glu288 and Trp94. KX171 also shares Arg188 with CVX15 in interaction with CXCR4. KX180 shares two amino acids with IT1t in interaction with CXCR4, they are Trp94 and Val112. Besides, KX180 shares Tyr190 with CVX15 in interaction with CXCR4. In comparison these KX compounds with AMD3100 in interaction with CXCR4, we find that: KX128 shares three amino acids with AMD3100 in interaction with CXCR4, the three amino acids are Arg188, His113 and Trp94. KX166 shares three amino acids with AMD3100 in interaction with CXCR4, the three amino acids are His113, Ala98 and Trp94. KX171 shares three amino acids with AMD3100 in interaction with CXCR4, the three amino acids are Arg188, Phe199 and Trp94. KX180 shares four amino acids with AMD3100 in interaction with CXCR4, the four amino acids are His113, Arg188, Trp94 and Tyr190.

It is therefore concluded that the following amino acid residues of CXCR4 are important for ligands interaction with CXCR4: His113, Arg188, Trp94, Asp187, Tyr190, Asp97, Val112. These amino acids are shared by three or more ligands in interaction with CXCR4. Among them, His113 (shared by four ligands), Arg188 (shared by five ligands), Trp94 (shared by six ligands) are key amino acids in interaction of ligand with CXCR4.

In our study, not only a cell based screening were conducted for new CXCR4 antagonists searching, the drug candidates which showed good inhibition of CXCR4 internalization in cell imaging were also further tested by live virus assays. KX128 significantly reduced the cytopathic effect caused by HIV-1 infection with an EC_{50} of 0.60μg/ml. KX171 also had significant effect with an EC_{50} of 6.33μg/ml. P24 production in acute infection assay result showed that KX128 and KX171 had significant inhibition on P24 production in acute infection of HIV-1_{IIIB} with EC_{50} of 1.36μg/ml and 7.00μg/ml respectively. From the above results, it is concluded KX128 and KX171 could serve as core lead compounds for further drug development First,

KX128 and KX171 inhibited CXCR4 internalization induced by SDF-1 (it was presumed that inhibition of SDF-1 induced CXCR4 internalization would disrupt HIV-1 entry), and then resulted in inhibition on HIV-1 replication. Cellular toxicity of four KX compounds (KX128, KX166, KX171, KX180) were assessed by MTT method. Results showed that KX128, KX166, KX171, KX180 had CC_{50} of 2.68μg/ml(5.63μM), 187.63μg/ml(239.02μM), 33.78μg/ml(67.86μM) and 50.10μg/ml(80.97μM) respectively. CC_{50} of AZT was 1007.22μg/ml(3.76mM).

KX128 showed best effect on HIV-1 inhibition as well as higher cytotoxicity. This implies that KX128 is promising but need to be modified in order to reduce the cytotoxicity in further study. While KX171 also showed significant inhibition on HIV-1 replication but with much lower cytotoxicity.

In summary, we had screened more than 150 drug candidates for CXCR4 antagonist. Finally, four (KX2, KX8, KX17, KX128) compounds showed CXCR4 internalization inhibitive activity in cell based screening experiments. Binding mode analysis showed that these compounds had good binding affinity to CXCR4 ligand-binding pocket through H-bond and hydrophobic contacts. The bioinformatics analysis provides us important information on ligand binding sites to CXCR4. This would assist CXCR4 antagonist design and screening. Subsequent live virus assays further demonstrated that these compounds had HIV-1 replication inhibition activity with some cytotoxicity. Through molecular docking, amino acid residues which are important for ligands-CXCR4 interaction are identified. These amino acids are His113, Arg188, Trp94, Asp187, Tyr190, Asp97, Val112. Three key amino acids are identified as His113, Arg188 and Trp94. These sites provide us important information on CXCR4 antagonists design and development. They are also important for the structure and activity study of CXCR4.

Chapter 6
General discussion

Since there is no effective vaccine for the prevention and treatment of HIV infection, the HAART is still the most effective way in AIDS treatment. HAART requires a combination of different drugs targeting different steps in virus infection. Although more than 20 drugs have been approved in the past 2 decades, there is still a constant need for more drugs targeting on different mechanism of HIV replication.

The present FDA approved drugs are mainly targeting the reverse transcriptase and protease of HIV. Besides, many drugs have been developed aiming several steps in virus infection, including the drugs directly or indirectly targeting the HIV envelope, the drugs targeting the fusion of virus and the cell membrane, the drugs targeting the HIV integration, the drugs targeting the virus proteins synthesis and transportation, finally the drugs targeting the virus budding.

Because of the urgent need for more anti-HIV drugs targeting different and new steps in HIV infection, this work was focused on two novel targets of HIV replication. They are the targeted towards the process of HIV-1 integrase/LEDGF interaction and HIV entry through CXCR4 internalization. For drug development, convenient and high-throughput screening platforms are preferred. To achieve our goal, two platforms are constructed based on cell imaging techniques.

Firstly, a cell based HIV-1 integrase inhibitors screening platform by cloning integrase fused with EGFP into eukaryotic expression system was constructed. Any drugs that can inhibit the translocation process are novel class of drugs for AIDS treatment. Through virtual screening and cell imaging, eight compounds (DW-IN4, DW-IN5, DW-IN6, DW-IN9, DW-IN15, DW-IN16, DW-IN17, DW-IN21) were found to block integrase nuclear translocation at 1μM.

Then the binding mode of these compounds was analyzed by molecular docking. Docking results showed that these compounds were docked into the hydrophobic pocket of integrase dimer. Though the residues involved in different compounds'

interaction with integrase are not totally identical, all the compounds "bind" tightly to integrase. Hydrogen bond and hydrophobic contact are two major connections involved in the compound-integrase interaction. In drug development, cell based screening is a convenient way compared than live virus assays in cells or animals.

HIV-1 inhibition assays were conducted with HIV-1_{IIIB} infection. Results showed that DW-IN6 and DW-IN719 showed significant inhibition on P24 production in acute infection of HIV-1_{IIIB} with EC_{50} of 4.96μM and 4.33μM respectively. Since the integrase nuclear translocation is a step far from P24 production in HIV-1 life cycle, not all these compounds showed significant inhibition on P24 production in acute infection. In fact, even the compound can inhibit integrase nuclear translocation entirely, it may be not effective in reduction of P24 inhibition. But P24 is an important antigen and structural protein of HIV, it is also a widely acknowledged factor for HIV replication assay.

The screening results and live virus assays results are encouraging to us. By analyzing the structures of these compounds, it is feasible to synthesize new compounds aiming improving the activities of these compounds with lower toxicity. In searching for new drug candidates, screening from the existing synthetic compound database is one way. Another way is to design and synthesize new compounds based on computational chemistry or existing HIV-1 inhibitors structural information. Modification of parent compounds may lead to discovery of drugs suitable for clinical use.

Based on the structural information of DW-IN-16 provided by NMR, six new compounds were designed and synthesized. The principle concerns of new compounds were to reinforce the anti-HIV activity as well as to reduce the cytotoxicity to human cells and human body. Four compounds, INNE-1, INNE-2, INNE-3, INNE-4 showed HIV-1 inhibition effect with live virus infection. This result is encouraging to us. Because it tells that we are on the right way. Since these compounds are novel anti-HIV-1 drug candidates. Though they are toxic to cells in

some degree, further modification of these compounds to reduce cytotoxicity but retain anti-HIV activity is necessary.

In collaboration with Prof. YT Zheng from Kunming Institute of Zoology (The Chinese Academy of Sciences), four novel CXCR4 antagonists were screened. These compounds showed HIV-1 replication inhibition in virus infection assays. To predict the binding mode of KX compounds to CXCR4. The interaction of KX compounds with CXCR4 was analyzed by molecular docking. The binding mode of AMD3100 to CXCR4 was compared and the following amino acids are found important for ligands in interaction with CXCR4: His113, Arg188, Trp94, Asp187, Tyr190, Asp97, Val112. These amino acids are shared by three or more ligands in interaction with CXCR4. Among them, His113 (shared by four ligands), Arg188 (shared by five ligands), Trp94 ((shared by six ligands) are key amino acids in interaction of ligand with CXCR4. These cores should serve as critical spots for further drug development.

Comparing the binding affinity of newly screened CXCR4 antagonists with AMD3100 and IT1t, All six compounds were analyzed and ranked by molecular docking. According to the ranking of affinity to CXCR4 in molecular docking, KX166 showed the highest binding affinity to CXCR4. KX180 and KX128 had the similar binding affinity following KX166. AMD3100, KX171 and IT1t had similar binding affinity. This shows that our CXCR4 antagonist candidates are promising. KX128 showed significant HIV-1 inhibition activity. First, KX128 inhibited CXCR4 internalization induced by SDF-1 (it was presumed that inhibition of SDF-1 induced CXCR4 internalization would disrupt HIV-1 entry), and then resulted in inhibition on HIV-1 replication.

Since CXCR4 is involved in many normal biological process in human body. For example, PBSF/SDF-1 and CXCR4 were reported to define a new signaling system for organ vascularization(Tachibana et al., 1998). Also, CXCR4-SDF-1 ligand pair was found to involved in directed migration of cancer cells to sites of metastasis so as to improve survival of cancer cells(Balkwill, 2004). CXCR4-SDF-1 ligand pair was

also reported to involve in tumor progression, angiogenesis, metastasis, and survival(Teicher and Fricker, 2010).

Although the CXCR4 antagonist candidates are demonstrated to inhibit HIV-1 replication in live virus assays. They may also play roles in other CXCR4 involving physiological process. Since CXCR4 is important in cancer research, inhibition of CXCR4 internalization induced by SDF-1, thus may stop the downstream cell signaling. Subsequently, the cancer cells survival, tumor progression, angiogenesis, metastasis, and survival may also been influenced. It is interesting to determine that candidate may be used as anti-cancer agents.

In conclusion, eight compounds (DW-IN4, DW-IN5, DW-IN6, DW-IN9, DW-IN15, *DW-IN16, DW-IN17* and *DW-IN21*) from SPECS, one natural product (*DW-IN719*) from ZINC, six compounds (KM7, KM8, KM14, KM79, KM30, KM37) are identified as integrase inhibitors candidates. Four compounds (KX128, KX166, *KX171, KX180*) are identified as CXCR4 antagonists candidates.

The emerging of drug resistant viruses to current antiretroviral drugs makes it urgent to development of new drugs with novel targets. The continuously transmission of drug- resistant viruses enhances this urgent demand. Though more and more researchers are focusing on the anti-HIV drug discovery and development and a number of inhibitors to emerging targets are in preclinical and clinical trials, the dilemma of lacking suitable HAART regimen for some treatment experienced patients is not solved. The first consideration of HAART is likely to combine inhibitors that target multiple stages of the viral life cycle in order to provide better prospects for enhanced containment of viral replication. Novel HIV inhibitors with good tolerability, low potential for drug--drug interactions, effective to current drug-resistant HIV strains are in high demand in HIV infection and AIDS treatment.

References:

Allan, J. S., Coligan, J. E., Lee, T. H., Barin, F., Kanki, P. J., M'Boup, S., McLane, M. F., Groopman, J. E. and Essex, M. (1987). Immunogenic nature of a Pol gene product of HTLV-III/LAV. *Blood* **69**, 331-3.

Allaway, G. P., Davis-Bruno, K. L., Beaudry, G. A., Garcia, E. B., Wong, E. L., Ryder, A. M., Hasel, K. W., Gauduin, M. C., Koup, R. A., McDougal, J. S. et al. (1995). Expression and characterization of CD4-IgG2, a novel heterotetramer that neutralizes primary HIV type 1 isolates. *AIDS Res Hum Retroviruses* **11**, 533-9.

Anker, M. and Corales, R. B. (2008). Raltegravir (MK-0518): a novel integrase inhibitor for the treatment of HIV infection. *Expert Opin Investig Drugs* **17**, 97-103.

Anthony, N. J. (2004). HIV-1 integrase: a target for new AIDS chemotherapeutics. *Curr Top Med Chem* **4**, 979-90.

Arnold, E., Jacobo-Molina, A., Nanni, R. G., Williams, R. L., Lu, X., Ding, J., Clark, A. D., Jr., Zhang, A., Ferris, A. L., Clark, P. et al. (1992). Structure of HIV-1 reverse transcriptase/DNA complex at 7 A resolution showing active site locations. *Nature* **357**, 85-9.

Baldwin, C. E., Sanders, R. W., Deng, Y., Jurriaans, S., Lange, J. M., Lu, M. and Berkhout, B. (2004). Emergence of a drug-dependent human immunodeficiency virus type 1 variant during therapy with the T20 fusion inhibitor. *J Virol* **78**, 12428-37.

Balkwill, F. (2004). The significance of cancer cell expression of the chemokine receptor CXCR4. *Semin Cancer Biol* **14**, 171-9.

Barklis, E., McDermott, J., Wilkens, S., Fuller, S. and Thompson, D. (1998). Organization of HIV-1 capsid proteins on a lipid monolayer. *J Biol Chem* **273**, 7177-80.

Barre-Sinoussi, F., Chermann, J. C., Rey, F., Nugeyre, M. T., Chamaret, S., Gruest, J., Dauguet, C., Axler-Blin, C., Vezinet-Brun, F., Rouzioux, C. et al. (1983). Isolation of a T-lymphotropic retrovirus from a patient at risk for acquired immune deficiency syndrome (AIDS). *Science* **220**, 868-71.

Barrientos, L. G., Louis, J. M., Botos, I., Mori, T., Han, Z., O'Keefe, B. R., Boyd, M. R., Wlodawer, A. and Gronenborn, A. M. (2002). The domain-swapped dimer of cyanovirin-N is in a metastable folded state: reconciliation of X-ray and NMR structures. *Structure* **10**, 673-86.

Berger, E. A., Murphy, P. M. and Farber, J. M. (1999). Chemokine receptors as HIV-1 coreceptors: roles in viral entry, tropism, and disease. *Annu Rev Immunol* **17**, 657-700.

Bleul, C. C., Farzan, M., Choe, H., Parolin, C., Clark-Lewis, I., Sodroski, J. and Springer, T. A. (1996). The lymphocyte chemoattractant SDF-1 is a ligand for LESTR/fusin and blocks HIV-1 entry. *Nature* **382**, 829-33.

Botbol, Y., Raghavendra, N. K., Rahman, S., Engelman, A. and Lavigne, M. (2008). Chromatinized templates reveal the requirement for the LEDGF/p75 PWWP domain during HIV-1 integration in vitro. *Nucleic Acids Res* **36**, 1237-46.

Botos, I., Mori, T., Cartner, L. K., Boyd, M. R. and Wlodawer, A. (2002). Domain-swapped structure of a mutant of cyanovirin-N. *Biochem Biophys Res Commun* **294**, 184-90.

Bouyac-Bertoia, M., Dvorin, J. D., Fouchier, R. A., Jenkins, Y., Meyer, B. E., Wu, L. I., Emerman, M. and Malim, M. H. (2001). HIV-1 infection requires a functional integrase NLS. *Mol Cell* **7**, 1025-35.

Bowersox, J. (1996). Nevirapine approved by FDA. Food and Drug Administration. *NIAID AIDS Agenda*, 10.

Boyle, N. A., Rajwanshi, V. K., Prhavc, M., Wang, G., Fagan, P., Chen, F., Ewing, G. J., Brooks, J. L., Hurd, T., Leeds, J. M. et al. (2005). Synthesis of 2',3'-dideoxynucleoside 5'-alpha-P-borano-beta,gamma-(difluoromethylene)triphosphates and their inhibition of HIV-1 reverse transcriptase. *J Med Chem* **48**, 2695-700.

Broder, S. (1990). Pharmacodynamics of 2',3'-dideoxycytidine: an inhibitor of human immunodeficiency virus. *Am J Med* **88**, 2S-7S.

Brown, A. J., Lobidel, D., Wade, C. M., Rebus, S., Phillips, A. N., Brettle, R. P., France, A. J., Leen, C. S., McMenamin, J., McMillan, A. et al. (1997). The molecular epidemiology of human immunodeficiency virus type 1 in six cities in Britain and Ireland. *Virology* **235**, 166-77.

Bruce, C., Clegg, C., Featherstone, A., Smith, J. and Oram, J. (1993). Sequence analysis of the gp120 region of the env gene of Ugandan human immunodeficiency proviruses from a single individual. *AIDS Res Hum Retroviruses* **9**, 357-63.

Bukrinsky, M. I. and Haffar, O. K. (1997). HIV-1 nuclear import: in search of a leader. *Front Biosci* **2**, d578-87.

Bukrinsky, M. I., Sharova, N., McDonald, T. L., Pushkarskaya, T., Tarpley, W. G. and Stevenson, M. (1993). Association of integrase, matrix, and reverse transcriptase antigens of human immunodeficiency virus type 1 with viral nucleic acids following acute infection. *Proc Natl Acad Sci U S A* **90**, 6125-9.

Busschots, K., Vercammen, J., Emiliani, S., Benarous, R., Engelborghs, Y., Christ, F. and Debyser, Z. (2005). The interaction of LEDGF/p75 with integrase is lentivirus-specific and promotes DNA binding. *J Biol Chem* **280**, 17841-7.

Busti, A. J., Hall, R. G. and Margolis, D. M. (2004). Atazanavir for the treatment of human immunodeficiency virus infection. *Pharmacotherapy* **24**, 1732-47.

Buzon, M. J., Marfil, S., Puertas, M. C., Garcia, E., Clotet, B., Ruiz, L., Blanco, J., Martinez-Picado, J. and Cabrera, C. (2008). Raltegravir susceptibility and fitness progression of HIV type-1 integrase in patients on long-term antiretroviral therapy. *Antivir Ther* **13**, 881-93.

Cabrera, C. (2008). Raltegravir, an HIV-1 integrase inhibitor for HIV infection. *Curr Opin Investig Drugs* **9**, 885-98.

Callahan, L. N., Phelan, M., Mallinson, M. and Norcross, M. A. (1991). Dextran sulfate blocks antibody binding to the principal neutralizing domain of

human immunodeficiency virus type 1 without interfering with gp120-CD4 interactions. *J Virol* **65**, 1543-50.

Candotti, D., Chappey, C., Rosenheim, M., M'Pele, P., Huraux, J. M. and Agut, H. (1994). High variability of the gag/pol transframe region among HIV-1 isolates. *C R Acad Sci III* **317**, 183-9.

Carr, J. M., Davis, A. J., Coolen, C., Cheney, K., Burrell, C. J. and Li, P. (2006). Vif-deficient HIV reverse transcription complexes (RTCs) are subject to structural changes and mutation of RTC-associated reverse transcription products. *Virology* **351**, 80-91.

Casals, A., Ovalle, A., Toledo, M. and Northland, R. (1991). [AIDS and pregnancy. The clinical management of 2 cases of HIV infection]. *Rev Chil Obstet Ginecol* **56**, 446-52.

Caumont, A. B., Jamieson, G. A., Pichuantes, S., Nguyen, A. T., Litvak, S. and Dupont, C. (1996). Expression of functional HIV-1 integrase in the yeast Saccharomyces cerevisiae leads to the emergence of a lethal phenotype: potential use for inhibitor screening. *Curr Genet* **29**, 503-10.

Champagne, K., Shishido, A. and Root, M. J. (2009). Interactions of HIV-1 inhibitory peptide T20 with the gp41 N-HR coiled coil. *J Biol Chem* **284**, 3619-27.

Chan, D. C., Fass, D., Berger, J. M. and Kim, P. S. (1997). Core structure of gp41 from the HIV envelope glycoprotein. *Cell* **89**, 263-73.

Charles-Nino, C., Pedroza-Roldan, C., Viveros, M., Gevorkian, G. and Manoutcharian, K. (2011). Variable epitope libraries: New vaccine immunogens capable of inducing broad human immunodeficiency virus type 1-neutralizing antibody response. *Vaccine*.

Chen, J. X., Xue, H. J., Ye, W. C., Fang, B. H., Liu, Y. H., Yuan, S. H., Yu, P. and Wang, Y. Q. (2009). Activity of andrographolide and its derivatives against influenza virus in vivo and in vitro. *Biol Pharm Bull* **32**, 1385-91.

Cheng, B. (1995). Advances in protease inhibitors. *PI Perspect*, 8-9.

Cherepanov, P., Ambrosio, A. L., Rahman, S., Ellenberger, T. and Engelman, A. (2005). Structural basis for the recognition between HIV-1 integrase and transcriptional coactivator p75. *Proc Natl Acad Sci U S A* **102**, 17308-13.

Cherepanov, P., Devroe, E., Silver, P. A. and Engelman, A. (2004). Identification of an evolutionarily conserved domain in human lens epithelium-derived growth factor/transcriptional co-activator p75 (LEDGF/p75) that binds HIV-1 integrase. *J Biol Chem* **279**, 48883-92.

Cherepanov, P., Maertens, G., Proost, P., Devreese, B., Van Beeumen, J., Engelborghs, Y., De Clercq, E. and Debyser, Z. (2003). HIV-1 integrase forms stable tetramers and associates with LEDGF/p75 protein in human cells. *J Biol Chem* **278**, 372-81.

Christ, F., Voet, A., Marchand, A., Nicolet, S., Desimmie, B. A., Marchand, D., Bardiot, D., Van der Veken, N. J., Van Remoortel, B., Strelkov, S. V. et al. (2010). Rational design of small-molecule inhibitors of the LEDGF/p75-integrase interaction and HIV replication. *Nat Chem Biol* **6**, 442-8.

Clavel, F., Brun-Vezinet, F., Guetard, D., Chamaret, S., Laurent, A., Rouzioux, C., Rey, M., Katlama, C., Rey, F., Champelinaud, J. L. et al. (1986). [LAV type II: a second retrovirus associated with AIDS in West Africa]. *C R Acad Sci III* **302**, 485-8.

Cleary, P. D., Rogers, T. F., Singer, E., Avorn, J., van Devanter, N., Perry, S. and Pindyck, J. (1986). Health education about AIDS among seropositive blood donors. *Health Educ Q* **13**, 317-29.

Cocohoba, J. and Dong, B. J. (2008). Raltegravir: the first HIV integrase inhibitor. *Clin Ther* **30**, 1747-65.

Curran, J. W., Morgan, W. M., Starcher, E. T., Hardy, A. M. and Jaffe, H. W. (1985). Epidemiological trends of AIDS in the United States. *Cancer Res* **45**, 4602s-4604s.

Dayam, R. and Neamati, N. (2003). Small-molecule HIV-1 integrase inhibitors: the 2001-2002 update. *Curr Pharm Des* **9**, 1789-802.

Dayam, R., Sanchez, T., Clement, O., Shoemaker, R., Sei, S. and Neamati, N. (2005). Beta-diketo acid pharmacophore hypothesis. 1. Discovery of a novel class of HIV-1 integrase inhibitors. *J Med Chem* **48**, 111-20.

De Clercq, E. (2009). Anti-HIV drugs: 25 compounds approved within 25 years after the discovery of HIV. *Int J Antimicrob Agents* **33**, 307-20.

De Clercq, E., Yamamoto, N., Pauwels, R., Balzarini, J., Witvrouw, M., De Vreese, K., Debyser, Z., Rosenwirth, B., Peichl, P., Datema, R. et al. (1994). Highly potent and selective inhibition of human immunodeficiency virus by the bicyclam derivative JM3100. *Antimicrob Agents Chemother* **38**, 668-74.

De Luca, L., Ferro, S., Gitto, R., Barreca, M. L., Agnello, S., Christ, F., Debyser, Z. and Chimirri, A. (2010). Small molecules targeting the interaction between HIV-1 integrase and LEDGF/p75 cofactor. *Bioorg Med Chem* **18**, 7515-21.

Deng, H., Liu, R., Ellmeier, W., Choe, S., Unutmaz, D., Burkhart, M., Di Marzio, P., Marmon, S., Sutton, R. E., Hill, C. M. et al. (1996). Identification of a major co-receptor for primary isolates of HIV-1. *Nature* **381**, 661-6.

Desfarges, S., Salin, B., Calmels, C., Andreola, M. L., Parissi, V. and Fournier, M. (2009). HIV-1 integrase trafficking in S. cerevisiae: a useful model to dissect the microtubule network involvement of viral protein nuclear import. *Yeast* **26**, 39-54.

Desjobert, C., de Soultrait, V. R., Faure, A., Parissi, V., Litvak, S., Tarrago-Litvak, L. and Fournier, M. (2004). Identification by phage display selection of a short peptide able to inhibit only the strand transfer reaction catalyzed by human immunodeficiency virus type 1 integrase. *Biochemistry* **43**, 13097-105.

Ding, J., Das, K., Tantillo, C., Zhang, W., Clark, A. D., Jr., Jessen, S., Lu, X., Hsiou, Y., Jacobo-Molina, A., Andries, K. et al. (1995). Structure of HIV-1 reverse transcriptase in a complex with the non-nucleoside inhibitor alpha-APA R 95845 at 2.8 A resolution. *Structure* **3**, 365-79.

Doms, R. W. (2001). Chemokine receptors and HIV entry. *Aids* **15 Suppl 1**, S34-5.

Doms, R. W. and Peiper, S. C. (1997). Unwelcomed guests with master keys: how HIV uses chemokine receptors for cellular entry. *Virology* **235**, 179-90.

Dong, B. J. (1998). Efavirenz DuPont Pharmaceuticals Co. *IDrugs* **1**, 700-11.

Donzella, G. A., Schols, D., Lin, S. W., Este, J. A., Nagashima, K. A., Maddon, P. J., Allaway, G. P., Sakmar, T. P., Henson, G., De Clercq, E. et al. (1998). AMD3100, a small molecule inhibitor of HIV-1 entry via the CXCR4 co-receptor. *Nat Med* **4**, 72-7.

Du, L., Zhao, Y., Chen, J., Yang, L., Zheng, Y., Tang, Y., Shen, X. and Jiang, H. (2008). D77, one benzoic acid derivative, functions as a novel anti-HIV-1 inhibitor targeting the interaction between integrase and cellular LEDGF/p75. *Biochem Biophys Res Commun* **375**, 139-44.

Elhaggar, S. (1993). Treatment / control of HIV infection. *Arch AIDS Res* **7**, 120-1.

Emiliani, S., Mousnier, A., Busschots, K., Maroun, M., Van Maele, B., Tempe, D., Vandekerckhove, L., Moisant, F., Ben-Slama, L., Witvrouw, M. et al. (2005). Integrase mutants defective for interaction with LEDGF/p75 are impaired in chromosome tethering and HIV-1 replication. *J Biol Chem* **280**, 25517-23.

Endres, M. J., Clapham, P. R., Marsh, M., Ahuja, M., Turner, J. D., McKnight, A., Thomas, J. F., Stoebenau-Haggarty, B., Choe, S., Vance, P. J. et al. (1996). CD4-independent infection by HIV-2 is mediated by fusin/CXCR4. *Cell* **87**, 745-56.

Engelman, A. (2009). Mechanistic and pharmacological analyses of HIV-1 integration. *Methods* **47**, 225-8.

Engelman, A., Oztop, I., Vandegraaff, N. and Raghavendra, N. K. (2009). Quantitative analysis of HIV-1 preintegration complexes. *Methods*.

Esser, M. T., Mori, T., Mondor, I., Sattentau, Q. J., Dey, B., Berger, E. A., Boyd, M. R. and Lifson, J. D. (1999). Cyanovirin-N binds to gp120 to interfere with CD4-dependent human immunodeficiency virus type 1 virion binding, fusion, and infectivity but does not affect the CD4 binding site on gp120 or soluble CD4-induced conformational changes in gp120. *J Virol* **73**, 4360-71.

Este, J. A., Cabrera, C., Schols, D., Cherepanov, P., Gutierrez, A., Witvrouw, M., Pannecouque, C., Debyser, Z., Rando, R. F., Clotet, B. et al. (1998). Human immunodeficiency virus glycoprotein gp120 as the primary target for the antiviral action of AR177 (Zintevir). *Mol Pharmacol* **53**, 340-5.

Eugen-Olsen, J., Iversen, A. K., Garred, P., Koppelhus, U., Pedersen, C., Benfield, T. L., Sorensen, A. M., Katzenstein, T., Dickmeiss, E., Gerstoft, J. et al. (1997). Heterozygosity for a deletion in the CKR-5 gene leads to prolonged AIDS-free survival and slower CD4 T-cell decline in a cohort of HIV-seropositive individuals. *Aids* **11**, 305-10.

Fanales-Belasio, E., Raimondo, M., Suligoi, B. and Butto, S. (2010). HIV virology and pathogenetic mechanisms of infection: a brief overview. *Ann Ist Super Sanita* **46**, 5-14.

Fassati, A. and Goff, S. P. (2001). Characterization of intracellular reverse transcription complexes of human immunodeficiency virus type 1. *J Virol* **75**, 3626-35.

Fouret, P. J., Touboul, J. L., Mayaud, C. M., Akoun, G. M. and Roland, J. (1987). Pulmonary Kaposi's sarcoma in patients with acquired immune deficiency syndrome: a clinicopathological study. *Thorax* **42**, 262-8.

Gao, W. Y., Johns, D. G. and Mitsuya, H. (1994). Anti-human immunodeficiency virus type 1 activity of hydroxyurea in combination with 2',3'-dideoxynucleosides. *Mol Pharmacol* **46**, 767-72.

Garza, H. H., Jr. and Carr, D. J. (1995). Interactions of human immunodeficiency virus type 1 transactivator of transcription protein with signal transduction pathways. *Adv Neuroimmunol* **5**, 321-5.

Gelderblom, H. R., Hausmann, E. H., Ozel, M., Pauli, G. and Koch, M. A. (1987). Fine structure of human immunodeficiency virus (HIV) and immunolocalization of structural proteins. *Virology* **156**, 171-6.

Ghani, A. C., Donnelly, C. A. and Anderson, R. M. (2003). Patterns of antiretroviral use in the United States of America: analysis of three observational databases. *HIV Med* **4**, 24-32.

Goldgur, Y., Craigie, R., Cohen, G. H., Fujiwara, T., Yoshinaga, T., Fujishita, T., Sugimoto, H., Endo, T., Murai, H. and Davies, D. R. (1999). Structure of the HIV-1 integrase catalytic domain complexed with an inhibitor: a platform for antiviral drug design. *Proc Natl Acad Sci U S A* **96**, 13040-3.

Gonda, M. A. (1988). Molecular genetics and structure of the human immunodeficiency virus. *J Electron Microsc Tech* **8**, 17-40.

Gostin, L. O. (1990). The AIDS Litigation Project. A national review of court and human rights commission decisions, Part I: The social impact of AIDS. *Jama* **263**, 1961-70.

Gottlinger, H. G., Dorfman, T., Sodroski, J. G. and Haseltine, W. A. (1991). Effect of mutations affecting the p6 gag protein on human immunodeficiency virus particle release. *Proc Natl Acad Sci U S A* **88**, 3195-9.

Graeble, M. A., Churcher, M. J., Lowe, A. D., Gait, M. J. and Karn, J. (1993). Human immunodeficiency virus type 1 transactivator protein, tat, stimulates transcriptional read-through of distal terminator sequences in vitro. *Proc Natl Acad Sci U S A* **90**, 6184-8.

Greenberg, M., Cammack, N., Salgo, M. and Smiley, L. (2004). HIV fusion and its inhibition in antiretroviral therapy. *Rev Med Virol* **14**, 321-37.

Hayouka, Z., Hurevich, M., Levin, A., Benyamini, H., Iosub, A., Maes, M., Shalev, D. E., Loyter, A., Gilon, C. and Friedler, A. (2010a). Cyclic peptide inhibitors of HIV-1 integrase derived from the LEDGF/p75 protein. *Bioorg Med Chem* **18**, 8388-95.

Hayouka, Z., Levin, A., Maes, M., Hadas, E., Shalev, D. E., Volsky, D. J., Loyter, A. and Friedler, A. (2010b). Mechanism of action of the HIV-1 integrase inhibitory peptide LEDGF 361-370. *Biochem Biophys Res Commun* **394**, 260-5.

Hayouka, Z., Rosenbluh, J., Levin, A., Loya, S., Lebendiker, M., Veprintsev, D., Kotler, M., Hizi, A., Loyter, A. and Friedler, A. (2007). Inhibiting HIV-1 integrase by shifting its oligomerization equilibrium. *Proc Natl Acad Sci U S A* **104**, 8316-21.

Hayouka, Z., Rosenbluh, J., Levin, A., Maes, M., Loyter, A. and Friedler, A. (2008). Peptides derived from HIV-1 Rev inhibit HIV-1 integrase in a shiftide mechanism. *Biopolymers* **90**, 481-7.

He, J., Chen, Y., Farzan, M., Choe, H., Ohagen, A., Gartner, S., Busciglio, J., Yang, X., Hofmann, W., Newman, W. et al. (1997). CCR3 and CCR5 are co-receptors for HIV-1 infection of microglia. *Nature* **385**, 645-9.

Heeney, J. L., Dalgleish, A. G. and Weiss, R. A. (2006). Origins of HIV and the evolution of resistance to AIDS. *Science* **313**, 462-6.

Hendrix, C. W., Flexner, C., MacFarland, R. T., Giandomenico, C., Fuchs, E. J., Redpath, E., Bridger, G. and Henson, G. W. (2000). Pharmacokinetics and safety of AMD-3100, a novel antagonist of the CXCR-4 chemokine receptor, in human volunteers. *Antimicrob Agents Chemother* **44**, 1667-73.

Herzyk, P., Beveridge, A. and Neidle, S. (1987). Conformational properties of 3'-azido-3'deoxy-thymidine (AZT), an inhibitor of HIV reverse transcriptase. *Biochem Biophys Res Commun* **145**, 1356-61.

Hirschel, B. and Francioli, P. (1998). Progress and problems in the fight against AIDS. *N Engl J Med* **338**, 906-8.

Holler, T. P., Foltin, S. K., Ye, Q. Z. and Hupe, D. J. (1993). HIV1 integrase expressed in Escherichia coli from a synthetic gene. *Gene* **136**, 323-8.

Huang, M., Orenstein, J. M., Martin, M. A. and Freed, E. O. (1995a). p6Gag is required for particle production from full-length human immunodeficiency virus type 1 molecular clones expressing protease. *J Virol* **69**, 6810-8.

Huang, Y., Zhang, L. and Ho, D. D. (1995b). Characterization of nef sequences in long-term survivors of human immunodeficiency virus type 1 infection. *J Virol* **69**, 93-100.

Husain, S., Goila, R., Shahi, S. and Banerjea, A. (1998). First report of a healthy Indian heterozygous for delta 32 mutant of HIV-1 co-receptor-CCR5 gene. *Gene* **207**, 141-7.

Ingold, F. R. and Ingold, S. (1989). The effects of the liberalization of syringe sales on the behaviour of intravenous drug users in France. *Bull Narc* **41**, 67-81.

Jada, S. R., Matthews, C., Saad, M. S., Hamzah, A. S., Lajis, N. H., Stevens, M. F. and Stanslas, J. (2008). Benzylidene derivatives of andrographolide inhibit growth of breast and colon cancer cells in vitro by inducing G(1) arrest and apoptosis. *Br J Pharmacol* **155**, 641-54.

Jada, S. R., Subur, G. S., Matthews, C., Hamzah, A. S., Lajis, N. H., Saad, M. S., Stevens, M. F. and Stanslas, J. (2007). Semisynthesis and in vitro anticancer activities of andrographolide analogues. *Phytochemistry* **68**, 904-12.

James, J. S. (1995). Agouron protease inhibitor AG1343: activity reported. *AIDS Treat News*, 6.

Jenkinson, S., Thomson, M., McCoy, D., Edelstein, M., Danehower, S., Lawrence, W., Wheelan, P., Spaltenstein, A. and Gudmundsson, K. (2010). Blockade of X4-tropic HIV-1 cellular entry by GSK812397, a potent noncompetitive CXCR4 receptor antagonist. *Antimicrob Agents Chemother* **54**, 817-24.

Jones, J., Taylor, B., Wilkin, T. J. and Hammer, S. M. (2007). Advances in antiretroviral therapy. *Top HIV Med* **15**, 48-82.

Justice, A. C., Feinstein, A. R. and Wells, C. K. (1989). A new prognostic staging system for the acquired immunodeficiency syndrome. *N Engl J Med* **320**, 1388-93.

Kaplan, G., Ziza, J. M., Prier, A., Chamaret, S., Piette, J. C. and Godeau, P. (1989). [Inflammatory arthropathies in patients with human immunodeficiency virus infection]. *Presse Med* **18**, 525-8.

Kashanchi, F., Shibata, R., Ross, E. K., Brady, J. N. and Martin, M. A. (1994). Second-site long terminal repeat (LTR) revertants of replication-defective human immunodeficiency virus: effects of revertant TATA box motifs on virus infectivity, LTR-directed expression, in vitro RNA synthesis, and binding of basal transcription factors TFIID and TFIIA. *J Virol* **68**, 3298-307.

Kelly, T. A., McNeil, D. W., Rose, J. M., David, E., Shih, C. K. and Grob, P. M. (1997). Novel non-nucleoside inhibitors of human immunodeficiency virus type 1 reverse transcriptase. 6. 2-Indol-3-yl- and 2-azaindol-3-yl-dipyridodiazepinones. *J Med Chem* **40**, 2430-3.

Kitchen, C. M., Nuno, M., Kitchen, S. G. and Krogstad, P. (2008). Enfuvirtide antiretroviral therapy in HIV-1 infection. *Ther Clin Risk Manag* **4**, 433-9.

Kong, R., Wang, C., Ma, X., Liu, J. and Chen, W. (2005). Peptides design based on the interfacial helix of integrase dimer. *Conf Proc IEEE Eng Med Biol Soc* **5**, 4743-6.

Korber, B., Muldoon, M., Theiler, J., Gao, F., Gupta, R., Lapedes, A., Hahn, B. H., Wolinsky, S. and Bhattacharya, T. (2000). Timing the ancestor of the HIV-1 pandemic strains. *Science* **288**, 1789-96.

Lalezari, J. P., Henry, K., O'Hearn, M., Montaner, J. S., Piliero, P. J., Trottier, B., Walmsley, S., Cohen, C., Kuritzkes, D. R., Eron, J. J., Jr. et al. (2003). Enfuvirtide, an HIV-1 fusion inhibitor, for drug-resistant HIV infection in North and South America. *N Engl J Med* **348**, 2175-85.

Ledesma-lujan, F. X., Chi-chan, J., Rayas, Y. R. J. A., Ortiz-contreras, F. and Campero-rosas, A. (1989). [AIDS in the newborn. Case report]. *Perinatol Reprod Hum* **3**, 164-70.

Lee, W. Y. (1993). [AIDS. The etiologic agent for acquired immunodeficiency syndrome]. *Kanhohak Tamgu* **2**, 138-50.

Lemey, P., Pybus, O. G., Rambaut, A., Drummond, A. J., Robertson, D. L., Roques, P., Worobey, M. and Vandamme, A. M. (2004). The molecular population genetics of HIV-1 group O. *Genetics* **167**, 1059-68.

Li, M. and Craigie, R. (2009). Nucleoprotein complex intermediates in HIV-1 integration. *Methods*.

Li, M. J. and Rossi, J. J. (2007). Lentivirus transduction of hematopoietic cells. *CSH Protoc* **2007**, pdb prot4755.

Little, J. and Rhodus, N. L. (2007). HIV and AIDs: update for dentistry. *Gen Dent* **55**, 184-96.

Llano, M., Saenz, D. T., Meehan, A., Wongthida, P., Peretz, M., Walker, W. H., Teo, W. and Poeschla, E. M. (2006). An essential role for LEDGF/p75 in HIV integration. *Science* **314**, 461-4.

Lu, D., Sham, Y. Y. and Vince, R. (2010). Design, asymmetric synthesis, and evaluation of pseudosymmetric sulfoximine inhibitors against HIV-1 protease. *Bioorg Med Chem* **18**, 2037-48.

Lu, X. L., Zhang, S. L. and Wang, Z. S. (1981). [Analysis of andrographolide compounds. I. Ion pair high performance liquid chromatographic analysis of andrographolide derivatives (author's transl)]. *Yao Xue Xue Bao* **16**, 182-9.

Lyons, M. (1994). Sexually transmitted diseases in the history of Uganda. *Genitourin Med* **70**, 138-45.

Maertens, G., Cherepanov, P., Pluymers, W., Busschots, K., De Clercq, E., Debyser, Z. and Engelborghs, Y. (2003). LEDGF/p75 is essential for nuclear and chromosomal targeting of HIV-1 integrase in human cells. *J Biol Chem* **278**, 33528-39.

Manikam, S. D. and Stanslas, J. (2009). Andrographolide inhibits growth of acute promyelocytic leukaemia cells by inducing retinoic acid receptor-independent cell differentiation and apoptosis. *J Pharm Pharmacol* **61**, 69-78.

Marchand, C., Maddali, K., Metifiot, M. and Pommier, Y. (2009). HIV-1 IN inhibitors: 2010 update and perspectives. *Curr Top Med Chem* **9**, 1016-37.

Martin, M. P., Carrington, M., Dean, M., O'Brien, S. J., Sheppard, H. W., Wegner, S. A. and Michael, N. L. (1998). CXCR4 polymorphisms and HIV-1 pathogenesis. *J Acquir Immune Defic Syndr Hum Retrovirol* **19**, 430.

Meyer, L., Magierowska, M., Hubert, J. B., Rouzioux, C., Deveau, C., Sanson, F., Debre, P., Delfraissy, J. F. and Theodorou, I. (1997). Early protective effect of CCR-5 delta 32 heterozygosity on HIV-1 disease progression: relationship with viral load. The SEROCO Study Group. *Aids* **11**, F73-8.

Mhalu, F. S. (1990). Inter-relationships between HIV infection and other sexually transmitted diseases. *East Afr Med J* **67**, 512-7.

Michael, N. L., Chang, G., d'Arcy, L. A., Tseng, C. J., Birx, D. L. and Sheppard, H. W. (1995). Functional characterization of human immunodeficiency virus type 1 nef genes in patients with divergent rates of disease progression. *J Virol* **69**, 6758-69.

Minoli, L. and Grossi, P. (1994). [AIDS: biological aspects]. *Radiol Med* **87**, 5-12.

Montagnier, L. (1988). Origin and evolution of HIVs and their role in AIDS pathogenesis. *J Acquir Immune Defic Syndr* **1**, 517-20.

Nair, V., Chi, G., Ptak, R. and Neamati, N. (2006). HIV integrase inhibitors with nucleobase scaffolds: discovery of a highly potent anti-HIV agent. *J Med Chem* **49**, 445-7.

Ndirangu, J., Bland, R., Barnighausen, T. and Newell, M. L. (2011). Validating child vaccination status in a demographic surveillance system using data from a clinical cohort study: evidence from rural South Africa. *BMC Public Health* **11**, 372.

Netzer, K. O., Schliephake, A., Maurer, B., Watanabe, R., Aguzzi, A. and Rethwilm, A. (1993). Identification of pol-related gene products of human foamy virus. *Virology* **192**, 336-8.

Ng, H. (2000). AIDS in Africa: a regional overview. *Harv AIDS Rev*, 2-5.

Nishitsuji, H., Tamura, Y., Fuse, T., Habu, Y., Miyano-Kurosaki, N. and Takaku, H. (2001). Inhibition of HIV-1 replication by 5'LTR decoy RNA. *Nucleic Acids Res Suppl*, 141-2.

O'Brien, W. A., Koyanagi, Y., Namazie, A., Zhao, J. Q., Diagne, A., Idler, K., Zack, J. A. and Chen, I. S. (1990). HIV-1 tropism for mononuclear phagocytes can be determined by regions of gp120 outside the CD4-binding domain. *Nature* **348**, 69-73.

Ondoa, P., Davis, D., Kestens, L., Vereecken, C., Garcia Ribas, S., Fransen, K., Heeney, J. and van der Groen, G. (2002). In vitro susceptibility to infection with SIVcpz and HIV-1 is lower in chimpanzee than in human peripheral blood mononuclear cells. *J Med Virol* **67**, 301-11.

Ondoa, P., Vereecken, C., Fransen, K., Colebunders, R., van der Groen, G., Heeney, J. L. and Kestens, L. (2003). Human and simian immunodeficiency virus-infected chimpanzees do not have increased intracellular levels of beta-chemokines in contrast to infected humans. *J Med Virol* **69**, 297-305.

Park, F. and Kay, M. A. (2001). Modified HIV-1 based lentiviral vectors have an effect on viral transduction efficiency and gene expression in vitro and in vivo. *Mol Ther* **4**, 164-73.

Partaledis, J. A., Yamaguchi, K., Tisdale, M., Blair, E. E., Falcione, C., Maschera, B., Myers, R. E., Pazhanisamy, S., Futer, O., Cullinan, A. B. et al. (1995). In vitro selection and characterization of human immunodeficiency virus type 1 (HIV-1) isolates with reduced sensitivity to hydroxyethylamino sulfonamide inhibitors of HIV-1 aspartyl protease. *J Virol* **69**, 5228-35.

Pinheiro Edos, S., Antunes, O. A. and Fortunak, J. M. (2008). A survey of the syntheses of active pharmaceutical ingredients for antiretroviral drug combinations critical to access in emerging nations. *Antiviral Res* **79**, 143-65.

Pivel, L., Di Piramoll, S. and Betancor, E. (1987). [Human acquired immunodeficiency syndrome (AIDS)]. *Odontol Postgrado* **1**, 51-80.

Raghavendra, N. K., Shkriabai, N., Graham, R., Hess, S., Kvaratskhelia, M. and Wu, L. (2010). Identification of host proteins associated with HIV-1 preintegration complexes isolated from infected CD4+ cells. *Retrovirology* **7**, 66.

Reed-Inderbitzin, E. and Maury, W. (2003). Cellular specificity of HIV-1 replication can be controlled by LTR sequences. *Virology* **314**, 680-95.

Reeves, J. D., Lee, F. H., Miamidian, J. L., Jabara, C. B., Juntilla, M. M. and Doms, R. W. (2005). Enfuvirtide resistance mutations: impact on human

immunodeficiency virus envelope function, entry inhibitor sensitivity, and virus neutralization. *J Virol* **79**, 4991-9.

Reimann, K. A., Lin, W., Bixler, S., Browning, B., Ehrenfels, B. N., Lucci, J., Miatkowski, K., Olson, D., Parish, T. H., Rosa, M. D. et al. (1997). A humanized form of a CD4-specific monoclonal antibody exhibits decreased antigenicity and prolonged plasma half-life in rhesus monkeys while retaining its unique biological and antiviral properties. *AIDS Res Hum Retroviruses* **13**, 933-43.

Rerks-Ngarm, S., Pitisuttithum, P., Nitayaphan, S., Kaewkungwal, J., Chiu, J., Paris, R., Premsri, N., Namwat, C., de Souza, M., Adams, E. et al. (2009). Vaccination with ALVAC and AIDSVAX to prevent HIV-1 infection in Thailand. *N Engl J Med* **361**, 2209-20.

Reynolds, L., Ullman, C., Moore, M., Isalan, M., West, M. J., Clapham, P., Klug, A. and Choo, Y. (2003). Repression of the HIV-1 5' LTR promoter and inhibition of HIV-1 replication by using engineered zinc-finger transcription factors. *Proc Natl Acad Sci U S A* **100**, 1615-20.

Rinaldi, M., Tintori, C., Franchi, L., Vignaroli, G., Innitzer, A., Massa, S., Este, J. A., Gonzalo, E., Christ, F., Debyser, Z. et al. (2011). A versatile and practical synthesis toward the development of novel HIV-1 integrase inhibitors. *ChemMedChem* **6**, 343-52.

Rodriguez-Barrios, F. and Gago, F. (2004). HIV protease inhibition: limited recent progress and advances in understanding current pitfalls. *Curr Top Med Chem* **4**, 991-1007.

Rosenberg, Z. F. and Fauci, A. S. (1989). Immunopathogenic mechanisms of HIV infection. *Clin Immunol Immunopathol* **50**, S149-56.

Ross, E. K., Buckler-White, A. J., Rabson, A. B., Englund, G. and Martin, M. A. (1991). Contribution of NF-kappa B and Sp1 binding motifs to the replicative capacity of human immunodeficiency virus type 1: distinct patterns of viral growth are determined by T-cell types. *J Virol* **65**, 4350-8.

Rusconi, S., Moonis, M., Merrill, D. P., Pallai, P. V., Neidhardt, E. A., Singh, S. K., Willis, K. J., Osburne, M. S., Profy, A. T., Jenson, J. C. et al. (1996). Naphthalene sulfonate polymers with CD4-blocking and anti-human immunodeficiency virus type 1 activities. *Antimicrob Agents Chemother* **40**, 234-6.

Saag, M. S. (1994). Evolving understanding of the immunopathogenesis of HIV. *AIDS Res Hum Retroviruses* **10**, 887-92.

Salemi, M., Strimmer, K., Hall, W. W., Duffy, M., Delaporte, E., Mboup, S., Peeters, M. and Vandamme, A. M. (2001). Dating the common ancestor of SIVcpz and HIV-1 group M and the origin of HIV-1 subtypes using a new method to uncover clock-like molecular evolution. *Faseb J* **15**, 276-8.

Sarker, M. S., Rahman, M., Yirrell, D., Campbell, E., Rahman, A. S., Islam, L. N. and Azim, T. (2008). Molecular evidence for polyphyletic origin of human immunodeficiency virus type 1 subtype C in Bangladesh. *Virus Res* **135**, 89-94.

Sarrami-Forooshani, R., Das, S. R., Sabahi, F., Adeli, A., Esmaeili, R., Wahren, B., Mohraz, M., Haji-Abdolbaghi, M., Rasoolinejad, M., Jameel, S. et al.

(2006). Molecular analysis and phylogenetic characterization of HIV in Iran. *J Med Virol* **78**, 853-63.

Saxinger, C., Alter, H. J., Eichberg, J. W., Fauci, A. S., Robey, W. G. and Gallo, R. C. (1987). Stages in the progression of HIV infection in chimpanzees. *AIDS Res Hum Retroviruses* **3**, 375-85.

Schneider, K., Kerr, C. C., Hoare, A. and Wilson, D. P. (2011). Expected epidemiological impacts of introducing an HIV vaccine in Thailand: A model-based analysis. *Vaccine*.

Schols, D. (2004). HIV co-receptors as targets for antiviral therapy. *Curr Top Med Chem* **4**, 883-93.

Schols D, C. S., Hatse S, et al. (2003). Anti-HIV activity profile of AMD070, an orally bioavailable CXCR4 antagonist H. *10th Conference on Retroviruses and Opportunistic Infections*.

Schols, D., Este, J. A., Henson, G. and De Clercq, E. (1997a). Bicyclams, a class of potent anti-HIV agents, are targeted at the HIV coreceptor fusin/CXCR-4. *Antiviral Res* **35**, 147-56.

Schols, D., Struyf, S., Van Damme, J., Este, J. A., Henson, G. and De Clercq, E. (1997b). Inhibition of T-tropic HIV strains by selective antagonization of the chemokine receptor CXCR4. *J Exp Med* **186**, 1383-8.

Seligmann, M. (1990). Immunological features of human immunodeficiency virus disease. *Baillieres Clin Haematol* **3**, 37-63.

Shun, M. C., Botbol, Y., Li, X., Di Nunzio, F., Daigle, J. E., Yan, N., Lieberman, J., Lavigne, M. and Engelman, A. (2008). Identification and characterization of PWWP domain residues critical for LEDGF/p75 chromatin binding and human immunodeficiency virus type 1 infectivity. *J Virol* **82**, 11555-67.

Smith, A. J. and Walker, D. M. (1992). The origins of the human immunodeficiency viruses: an update. *J Oral Pathol Med* **21**, 145-9.

Solomon, M. Z. and DeJong, W. (1986). Recent sexually transmitted disease prevention efforts and their implications for AIDS health education. *Health Educ Q* **13**, 301-16.

Song, C. Z., Loewenstein, P. M., Toth, K. and Green, M. (1995). Transcription factor TFIID is a direct functional target of the adenovirus E1A transcription-repression domain. *Proc Natl Acad Sci U S A* **92**, 10330-3.

Sousa, J. D. d. (2009). Pandemic HIV-1: Its Old Origin and Overlooked Mysteries. *AIDS Rev* **11**, 52-52.

St Clair, M. H., Richards, C. A., Spector, T., Weinhold, K. J., Miller, W. H., Langlois, A. J. and Furman, P. A. (1987). 3'-Azido-3'-deoxythymidine triphosphate as an inhibitor and substrate of purified human immunodeficiency virus reverse transcriptase. *Antimicrob Agents Chemother* **31**, 1972-7.

Stanic, M. (1963). [A simplification of the estimation of the 50 percent endpoints according to the Reed and Muench method]. *Pathol Microbiol (Basel)* **26**, 298-302.

Strebel, K., Daugherty, D., Clouse, K., Cohen, D., Folks, T. and Martin, M. A. (1987). The HIV 'A' (sor) gene product is essential for virus infectivity. *Nature* **328**, 728-30.

Tachibana, K., Hirota, S., Iizasa, H., Yoshida, H., Kawabata, K., Kataoka, Y., Kitamura, Y., Matsushima, K., Yoshida, N., Nishikawa, S. et al. (1998). The chemokine receptor CXCR4 is essential for vascularization of the gastrointestinal tract. *Nature* **393**, 591-4.

Takamatsu, J. (1997). [HIV infection and acquired immunodeficiency syndrome]. *Rinsho Byori* **45**, 409-14.

Tasara, T., Amacker, M. and Hubscher, U. (1999). Intramolecular chimeras of the p51 subunit between HIV-1 and FIV reverse transcriptases suggest a stabilizing function for the p66 subunit in the heterodimeric enzyme. *Biochemistry* **38**, 1633-42.

Taube, S. and Goldberg, M. (1983). The science base underlying research on acquired immune deficiency syndrome. *Public Health Rep* **98**, 559-65.

Teasdale, C. A., Marais, B. J. and Abrams, E. J. (2011). HIV: prevention of mother-to-child transmission. *Clin Evid (Online)* **2011**.

Teicher, B. A. and Fricker, S. P. (2010). CXCL12 (SDF-1)/CXCR4 pathway in cancer. *Clin Cancer Res* **16**, 2927-31.

Thoma, G., Streiff, M. B., Kovarik, J., Glickman, F., Wagner, T., Beerli, C. and Zerwes, H. G. (2008). Orally bioavailable isothioureas block function of the chemokine receptor CXCR4 in vitro and in vivo. *J Med Chem* **51**, 7915-20.

Tindall, B., Evans, L., Cunningham, P., McQueen, P., Hurren, L., Vasak, E., Mooney, J. and Cooper, D. A. (1992). Identification of HIV-1 in semen following primary HIV-1 infection. *Aids* **6**, 949-52.

Titti, F., Lazzarin, A., Costigliola, P., Oliva, C., Nicoletti, L., Negri, C., Ricchi, E., Donati, G., Uberti-Foppa, C., Re, M. C. et al. (1987). Human immunodeficiency virus (HIV) seropositivity in intravenous (i.v.) drug abusers in three cities of Italy: possible natural history of HIV infection in i.v. drug addicts in Italy. *J Med Virol* **23**, 241-8.

Tramontano, E., Onidi, L., Esposito, F., Badas, R. and La Colla, P. (2004). The use of a new in vitro reaction substrate reproducing both U3 and U5 regions of the HIV-1 3'-ends increases the correlation between the in vitro and in vivo effects of the HIV-1 integrase inhibitors. *Biochem Pharmacol* **67**, 1751-61.

Trott, O. and Olson, A. J. (2010). AutoDock Vina: improving the speed and accuracy of docking with a new scoring function, efficient optimization, and multithreading. *J Comput Chem* **31**, 455-61.

Unutmaz, D., KewalRamani, V. N. and Littman, D. R. (1998). G protein-coupled receptors in HIV and SIV entry: new perspectives on lentivirus-host interactions and on the utility of animal models. *Semin Immunol* **10**, 225-36.

Vacca, J. P., Dorsey, B. D., Schleif, W. A., Levin, R. B., McDaniel, S. L., Darke, P. L., Zugay, J., Quintero, J. C., Blahy, O. M., Roth, E. et al. (1994). L-735,524: an orally bioavailable human immunodeficiency virus type 1 protease inhibitor. *Proc Natl Acad Sci U S A* **91**, 4096-100.

Van Maele, B. and Debyser, Z. (2005). HIV-1 integration: an interplay between HIV-1 integrase, cellular and viral proteins. *AIDS Rev* **7**, 26-43.

van Rij, R. P., Portegies, P., Hallaby, T., Lange, J. M., Visser, J., de Roda Husman, A. M., van 't Wout, A. B. and Schuitemaker, H. (1999). Reduced

prevalence of the CCR5 delta32 heterozygous genotype in human immunodeficiency virus-infected individuals with AIDS dementia complex. *J Infect Dis* **180**, 854-7.

Varin, A., Manna, S. K., Quivy, V., Decrion, A. Z., Van Lint, C., Herbein, G. and Aggarwal, B. B. (2003). Exogenous Nef protein activates NF-kappa B, AP-1, and c-Jun N-terminal kinase and stimulates HIV transcription in promonocytic cells. Role in AIDS pathogenesis. *J Biol Chem* **278**, 2219-27.

Vazquez, E. (1997). DMP 266 on the horizon. *Posit Aware* **8**, 25.

Venet, A., Tourani, J. M., Beldjord, K., Eme, D., Even, P. and Andrieu, J. M. (1990). Actuarial rate of clinical and biological progression in a cohort of 250 HIV-1-seropositive subjects. Laennec HIV Study Group. *Clin Exp Immunol* **80**, 151-5.

Vermeire, K., Bell, T. W., Choi, H. J., Jin, Q., Samala, M. F., Sodoma, A., De Clercq, E. and Schols, D. (2003). The Anti-HIV potency of cyclotriazadisulfonamide analogs is directly correlated with their ability to down-modulate the CD4 receptor. *Mol Pharmacol* **63**, 203-10.

Vermeire, K. and Schols, D. (2003). Specific CD4 down-modulating compounds with potent anti-HIV activity. *J Leukoc Biol* **74**, 667-75.

Vermeire, K., Zhang, Y., Princen, K., Hatse, S., Samala, M. F., Dey, K., Choi, H. J., Ahn, Y., Sodoma, A., Snoeck, R. et al. (2002). CADA inhibits human immunodeficiency virus and human herpesvirus 7 replication by down-modulation of the cellular CD4 receptor. *Virology* **302**, 342-53.

Volsky, D. J., Wu, Y. T., Sinangil, F. and Goldsmith, J. C. (1986). HTLV-III/LAV antibodies and virus in hemophilia patients in Nebraska: survey and initiation of a prospective study. *AIDS Res* **2**, 51-61.

Vrang, L., Bazin, H., Remaud, G., Chattopadhyaya, J. and Oberg, B. (1987). Inhibition of the reverse transcriptase from HIV by 3'-azido-3'-deoxythymidine triphosphate and its threo analogue. *Antiviral Res* **7**, 139-49.

Wagener, B. M., Marjon, N. A., Revankar, C. M. and Prossnitz, E. R. (2009). Adaptor protein-2 interaction with arrestin regulates GPCR recycling and apoptosis. *Traffic* **10**, 1286-300.

Wain-Hobson, S., Vartanian, J. P., Henry, M., Chenciner, N., Cheynier, R., Delassus, S., Martins, L. P., Sala, M., Nugeyre, M. T., Guetard, D. et al. (1991). LAV revisited: origins of the early HIV-1 isolates from Institut Pasteur. *Science* **252**, 961-5.

Wang, B., Ge, L., Huang, W., Zhang, H., Qian, H., Li, J. and Zheng, Y. (2010). Synthesis and preliminary anti-HIV activities of andrographolide derivatives. *Med Chem* **6**, 252-8.

Wang, Q., Ding, Z. H., Liu, J. K. and Zheng, Y. T. (2004). Xanthohumol, a novel anti-HIV-1 agent purified from Hops Humulus lupulus. *Antiviral Res* **64**, 189-94.

Waskin, H., Smith, K. J., Simon, T. L., Gribble, T. J. and Mertz, G. J. (1986). Prevalence of HTLV-III antibody among New Mexico residents with hemophilia. *West J Med* **145**, 477-80.

Weissenhorn, W., Dessen, A., Harrison, S. C., Skehel, J. J. and Wiley, D. C. (1997). Atomic structure of the ectodomain from HIV-1 gp41. *Nature* **387**, 426-30.

Weissenhorn, W., Wharton, S. A., Calder, L. J., Earl, P. L., Moss, B., Aliprandis, E., Skehel, J. J. and Wiley, D. C. (1996). The ectodomain of HIV-1 env subunit gp41 forms a soluble, alpha-helical, rod-like oligomer in the absence of gp120 and the N-terminal fusion peptide. *Embo J* **15**, 1507-14.

Wiese, E. (1997). [Nevirapine--the first non-nucleoside inhibitor of reverse transcriptase in the battle against AIDS]. *Pharm Unserer Zeit* **26**, 99-100.

Williams, A. B. (1997). New horizons: antiretroviral therapy in 1997. *J Assoc Nurses AIDS Care* **8**, 26-38.

Woloschak, G. E., Panozzo, J., Schreck, S. and Libertin, C. R. (1995). Salicylic acid inhibits ultraviolet- and cis-platinum-induced human immunodeficiency virus expression. *Cancer Res* **55**, 1696-700.

Wu, B., Chien, E. Y., Mol, C. D., Fenalti, G., Liu, W., Katritch, V., Abagyan, R., Brooun, A., Wells, P., Bi, F. C. et al. (2010). Structures of the CXCR4 chemokine GPCR with small-molecule and cyclic peptide antagonists. *Science* **330**, 1066-71.

Yang, L., Xu, X., Huang, Y., Zhang, B., Zeng, C., He, H., Wang, C. and Hu, L. (2010). Synthesis of polyhydroxylated aromatics having amidation of piperazine nitrogen as HIV-1 integrase inhibitor. *Bioorg Med Chem Lett* **20**, 5469-71.

Zhu, T., Korber, B. T., Nahmias, A. J., Hooper, E., Sharp, P. M. and Ho, D. D. (1998). An African HIV-1 sequence from 1959 and implications for the origin of the epidemic. *Nature* **391**, 594-7.

Zou, Y. R., Kottmann, A. H., Kuroda, M., Taniuchi, I. and Littman, D. R. (1998). Function of the chemokine receptor CXCR4 in haematopoiesis and in cerebellar development. *Nature* **393**, 595-9.